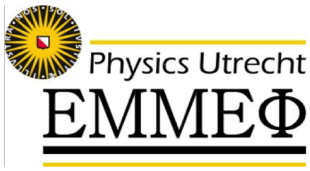

Dirac Superconductors:
Superconductivity in Artificial Graphene

Flore K. Kunst

March 29, 2015

Master's Thesis

Under Supervision of:

Prof. Dr. Cristiane Morais Smith and Dr. Vladimir Juričić

Utrecht University

Faculty of Science - Institute for Theoretical Phyiscs

Abstract

In this Master's thesis, I investigate the possibility to build a Dirac superconductor under supervision of Prof. Dr. Cristiane Morais Smith and Dr. Vladimir Juričić. By arranging nanocrystals that are known to be superconducting in honeycomb superlattices, we combine the physics of graphene with that of superconductivity. In this research, the focus is on CdSe nanocrystals in a honeycomb configuration. It is assumed there is one effective phonon per site that couples to on-site and nearest-neighbor electrons. Using a path-integral approach, the phonons are integrated out such that effective Hubbard U and V terms are derived. Order parameters for the on-site Cooper pairs and Cooper pairs of nearest-neighbor electrons were defined. For the latter, the competition between the hidden order, which renormalizes Fermi velocity instead of opening a gap, and the Kekule order, which opens a gap, is considered. Using the order parameters, the electron densities in the Hubbard terms are decoupled via mean-field theory. BCS theory is used to recover the gap equations and critical temperature. I find that the Kekule order is preferred over the hidden order provided nearest-neighbor coupling is favored over on-site coupling.

Contents

Chapter 1

Introduction

Since its isolation, graphene has enjoyed much attention from the scientific world [1]. The monolayer of carbon atoms arranged in a honeycomb configuration is light, transparent, flexible, strong and conductive. This combination of properties is extraordinary and has attracted much interest from both within and outside the scientific community. However, besides the numerous industrial applications that are envisioned for this wondrous material, it also possesses some features that are of interest purely from a scientific point of view. The low-energy excitations in the system are massless Dirac fermions, which were believed to only be realizable in accelerators. The existence of these particles in a condensed matter system is of fundamental importance because phenomena that were predicted to occur in high-energy systems, such as the Klein paradox and Zitterbewegung [2], can now be measured.

Superconductivity is not a property that occurs naturally in graphene. This is unfortunate because the relativistic quantum mechanics that govern the system have interesting consequences for the physics of superconductivity that are worthwhile investigating. A clear example in this regard is how Andreev reflection[1] is manifested in graphene as compared to normal metals: instead of the expected retroreflection, graphene exhibits specular reflection [3]. This shows that exploring the interplay between superconductivity and relativistic quantum dynamics leads to novel insights. To that end, the superconducting properties of graphene have been studied on a theoretical basis. This resulted in researching the possibilities of plasmon-mediated superconductivity [4], the Kekule superconductor [5], the effect of a repulsive Hubbard model on an anisotropic honeycomb lattice [6], chiral superconductivity due to repulsive interactions [7], $d + id$ superconductivity near the Van Hove singularity due to the competition between many-body instabilities [8], chiral d-wave superconductivity [9], quantum critical behavior at the semimetal superconductor quantum phase transition [10], and the effect of straining, which results in a superconductor with a time-reversal symmetry breaking $f + is$ order parameter [11]. Superconductivity in Dirac-like systems was also investigated in ultracold atoms with a staggered flux in square lattices [12, 13].

Not only theorists are interested in studying superconductivity in graphene. Experimentalists have devised set-ups in which they can probe a superconducting state in the material. Their endeavors have proved to be fruitful and superconductivity was induced via the proximity effect as well as via doping. It was shown that building a Josephson junction [14], which is

[1] Andreev reflection is a scattering process that occurs at interfaces between a superconducting and a normal metal, and facilitates the conversion from an electron into a hole induced by the superconducting pair potential.

based on the proximity effect, out of graphene led to the observation of a supercurrent [15], which shows that Cooper pairs can propagate through the material coherently [4]. In another, more recent experiment based on the proximity effect, graphene was grown on rhenium and superconductivity was successfully induced [16]. Another way of inducing superconductivity is by doping the surface with atoms. Phonon-mediated superconductivity was observed for graphene sheets doped with calcium and lithium [17].

The fact that superconductivity is not an intrinsic property of graphene has led to the idea to look for the Dirac superconductor in materials with graphene-like properties. This has inspired the investigation of superconductivity in artificial graphene samples. These samples are made of nanocrystals with a truncated cubic shape that self-assemble into a honeycomb superlattice. The motivation to build these materials was to study the electronic bandstructures that emerge when gapped, semi-conducting systems are combined with the physics of graphene, which is strictly a gapless system, by arranging the nanocrystals in a honeycomb structure. These materials have been experimentally realized for lead selenide (PbSe) and cadmium selenide (CdSe) nanocrystals [18]. The electronic band structure has been described theoretically for PbSe, CdSe, and mercury telluride (HgTe) semiconducting nanocrystals in a honeycomb superlattice [19, 20]. It has been predicted that they exhibit properties from both the gapped system and graphene: at high energy there are Dirac cones in the energy spectrum but at zero energy the spectrum is gapped [19].

In this Master's thesis, I have investigated superconductivity in artificial graphene samples made of CdSe nanocrystals. The same model can be used for studying superconductivity in materials composed of PbSe nanocrystals. The system is described through an effective model where one nanocrystal is modeled as a superatom. The effective phonon of a single CdSe nanocrystal is the longitudinal optical one [21], and therefore, it is assumed that there is one Einstein phonon per superatom site. Only the effective s-like electrons close to the lowest Dirac point are considered and they are described by a tight-binding Hamiltonian, which includes the chemical potential, nearest-neighbor hopping, and Hubbard terms for electron-pairing on-site and between nearest neighbors. A path-integral approach is used to integrate out the phonons to obtain the effective interaction. An estimate for this effective interaction was obtained based on the numerical analysis performed in the group of Prof. C. Delerue (Lille, France). Order parameters for the on-site Cooper pairs and Cooper pairs between nearest-neighbor sites were defined. For the latter, the competition between the hidden order [4], which renormalizes the Fermi velocity instead of opening a gap, and the Kekule order [5], which opens a gap, was considered. Then, by employing a mean-field approximation, the ground-state energy, gap equations at zero and finite temperature, and the critical temperature were obtained. As a result from this analysis, the phase diagrams were compiled. It is found that the Kekule order is preferred over the hidden order, provided that nearest-neighbor coupling is favored over on-site coupling.

This thesis is organized as follows. To give a brief survey of the phenomenon of superconductivity, Chapter 2 is devoted to BCS theory, which is named after its discoverers Bardeen, Cooper and Schrieffer. The theory describes conventional superconductivity in which the pair formation is driven by electron-phonon interaction. Some techniques introduced in this Chapter will be used later when considering superconductivity in artificial graphene samples. In the following Chapter, graphene is discussed. Among other subjects, the lattice structure, tight-binding model and effective Dirac Hamiltonian are addressed. In Chapter 4, superconductivity

in artificial graphene is analyzed. The effective electron-electron interaction is derived and the aforementioned competition between the Kekule and hidden order is studied extensively. This will be followed by the conclusion in Chapter 5.

Chapter 2

BCS Theory

Superconductivity was discovered in 1911 by the Dutch physicist Kamerlingh Onnes. He found that some metals have the peculiar feature of a complete absence of electric resistance when the material is cooled below a certain temperature, the so-called critical temperature T_c. Such materials are called superconductors. More research into superconducting materials revealed that they are also perfectly diamagnetic, which means that any magnetic field is expelled from the superconductor when the material is in the superconducting state. This phenomenon is known as the Meissner effect, and was discovered by Meissner and Ochsenfeld in 1933. The way in which superconductors behave when they are subjected to an external magnetic field can be divided into two categories. When the magnetic field increases, there is a point at which the superconductor is no longer able to produce a counteracting magnetic field and the external field will penetrate the superconductor. A type I superconductor experiences an abrupt penetration of the external magnetic field. In type II superconductors, on the other hand, there is an intermediary state in which the external field penetrates the superconductor in the shape of vortices, which form a lattice. Inside the vortex there is no superconducting state, whereas outside the vortex there is. Upon increasing the external magnetic field even more, the vortex lattice melts and the material becomes normal.

Theoretically, superconductivity is understood to result from electron pair creation. As the critical temperature is reached, it is energetically favorable for the superconductor to support attractive phonon-mediated electron-electron interaction leading to the creation of pairs. The idea is then that the electron pairs do not experience any resistivity from other electrons when they travel through the superconductor, and thus form a supercurrent without any decay in strength. These electron pairs are called Cooper pairs, named after their discoverer.

In 1957, Bardeen, Cooper and Schrieffer (BCS) proposed a theory, afterwards called BCS theory, that describes conventional superconductivity [22]. Due to their important work, Bardeen, Cooper and Schrieffer got awarded the Nobel Prize in Physics in 1972. BCS theory was revolutionary in its time because it uses a microscopic approach to describe superconductivity unlike all other theories proposed before that revolved around superfluidity. In the theory, a superconducting state is treated as a condensate of electron pairs. The existence of such pairs was discovered by Cooper a year earlier in 1956 [23]. A Cooper pair exists out of two electrons that are connected via time-reversal symmetry, which means that they have opposite momentum and opposite spin. The phase transition of a Fermi liquid to the superconducting phase can be interpreted as a condensation due to weak attraction between electrons. This phe-

nomenon can be seen in metals when the motion of the ions around their equilibrium positions is taken into account. The transition of the Fermi liquid to the superconducting states carries similarities with Bose-Einstein condensation. For an ideal Bose gas, it is energetically favorable for all bosons to occupy the lowest quantum state when the temperature is lowered below the transition temperature T_c. The transition of the Fermi liquid to the superconducting state undergoes a similar process. However, there is a fundamental difference between how bosons and fermions condense. Bosons obey Bose-Einstein statistics whereas fermions satisfy the more restrictive Fermi-Dirac statistics. The latter impose the Pauli exclusion principle on fermions, which dictates that two fermions identical to each other cannot occupy the same quantum state. This has a fundamental impact on how the electrons condense into the superconducting phase. BCS theory shows that for this process to take place, pair formation is crucial. It turns out that below a critical temperature T_c, it is energetically favorable for such Cooper pairs to exist. The formation of these pairs gives rise to a new ground state when many electrons are considered. One of the most important features of BCS theory is that it allows for the determination of the energy gap that characterizes a superconductor. The energy gap equation can be found by evaluating the thermodynamic properties of the system.

The discovery of superconductors and the Meissner effect are discussed in Section 2.1. Section 2.2 provides a physical picture of attractive electron-electron interaction, and it is shown with the help of the effective action that the interaction can indeed be attractive. The Cooper problem is discussed in Section 2.3, and the BCS wavefunction in Section 2.4. Lastly, in Section 2.5 the gap equation is derived.

2.1 The Phenomenon of Superconductivity

Kamerlingh Onnes was led to the discovery of superconductivity by the observation that some metals, such as Hg and Pb, have a completely vanishing electrical resistance below a critical temperature T_c. Experiments have shown that currents running through such materials below T_c do not decrease in strength. In fact, a change in the field or current is not expected to be seen for at least $10^{10^{10}}$ years [24]. Therefore, one of the fundamental properties of a superconducting material is the absence of electrical resistivity.

In 1933, Meissner and Ochsenfeld found that superconducting materials are also perfectly diamagnetic [25]; when an external magnetic field is present, the superconductor will produce a magnetic field counteracting this external field. Effectively this means that a magnetic field cannot enter a superconductor and that any magnetic field present in the original sample is expelled when the sample is cooled below T_c. This is known as the Meissner effect. Physically, this effect can be explained by realizing that in the presence of a magnetic field the Cooper pair[1] amplitude becomes an incoherent phase-dependent object such that in the absence of any disturbance, the Cooper pair amplitude at position $\mathbf{r}$ looks like

$$\langle \mathbf{r}, \mathbf{r} | \mathbf{k} \uparrow, -\mathbf{k} \downarrow \rangle \sim \mathrm{e}^{-i\mathbf{k}\cdot\mathbf{r}} \mathrm{e}^{+i\mathbf{k}\cdot\mathbf{r}} = \text{constant},$$

as opposed to the shape of the amplitude in the presence of a magnetic field

$$\langle \mathbf{r}, \mathbf{r} | \mathbf{k} \uparrow, -\mathbf{k} \downarrow \rangle \sim \mathrm{e}^{-i\int \mathrm{d}\mathbf{r}(\mathbf{k}-e\mathbf{A})} \mathrm{e}^{-i\int \mathrm{d}\mathbf{r}(-\mathbf{k}-e\mathbf{A})} \sim \mathrm{e}^{2ie\mathbf{A}\cdot\mathbf{r}},$$

[1] As mentioned before, the Cooper pair exists of two electrons with opposite momentum and opposite spin, i.e. $(\mathbf{k}, \uparrow)$ and $(-\mathbf{k}, \downarrow)$. This configuration is explained elaborately in Section 2.3.

where $\mathbf{A}$ is the vector potential which is related to the magnetic field $\mathbf{B} = \mathrm{rot}(\mathbf{A})$ and is assumed to vary slowly [14]. The magnetic field creates an instability in the amplitude which makes its presence undesirable, and the superconductor will attempt to expel it. However, if the magnetic field is strong enough, it will be able to penetrate the superconductor. This works as follows. When there is a magnetic field present, there is a competition between superconductive ordering and the magnetic field energy. This can be explained by considering the phenomenological Ginzburg-Landau action

$$S_{GL}\left[\Delta, \bar{\Delta}\right] \sim \int \mathrm{d}^d r \left[\frac{r}{2}\left|\Delta\right|^2 + \frac{c}{2}\left|\left(\nabla - 2i\mathbf{A}\right)\Delta\right|^2 + g\left|\Delta\right|^4\right], \tag{2.1}$$

where $\mathbf{A}$ is the aforementioned vector potential, $r \sim (T - T_c)$, $c \sim (v_F/T)^2$ with the Fermi velocity v_F and Δ is the superconducting order parameter, which is non-zero when the system is in the superconducting phase (see Section 2.5) [26]. Minimizing this action with respect to Δ^* yields

$$\left[r + c\left(-i\nabla - 2\mathbf{A}\right)^2 + 4g\left|\Delta\right|^2\right]\Delta = 0. \tag{2.2}$$

It is assumed that the temperature is below T_c such that r is smaller than zero and Δ is a constant. The last term in Eq. (2.2) is positive, which means that in order to solve this equation, the first two terms must add up to a net negative contribution [14]. Due to these requirements, a finite pairing amplitude can only be found if

$$B < B_2 \equiv \frac{|r|}{2c}. \tag{2.3}$$

If the magnetic field exceeds this value, the energy that is needed to expel the magnetic field is larger than the energy gained by condensating into a superconducting state and the latter state will break down [14]. Superconductors that exhibit diamagnetic behavior for $B < B_2$ and that are penetrated for values of the magnetic field greater than this critical field are called type I superconductors.

However, not all superconductors behave in this manner. There exist superconductors that show an intermediate state between complete expulsion of, and penetration by the magnetic field. They are called type II superconductors. In this case, Δ is assumed to be spatially dependent. What happens is that when $B_1 < B < B_2$ where B_1 is the critical field strength, the magnetic field penetrates the superconducting state in the form of vortex tubes of quantized flux [14]. These vortices are named after Abrikosov, who discovered them in 1957. Inside a vortex the superconducting state no longer exists, whereas outside the vortex it does.

The difference between the type I and type II superconductors can be described in terms of the so-called Ginzburg-Landau parameter

$$\kappa = \frac{\lambda}{\xi}, \tag{2.4}$$

named after Ginzburg and Landau who realized that the value of this parameter determines the type of superconductor.[2] In this relation, ξ is the correlation length characterizing the distance over which the wavefunction of the condensate can vary without increasing the energy, and λ is the magnetic penetration depth. For type I superconductors, $\lambda \ll \xi$ such that $\kappa \ll 1$ and

[2]This paragraph is based on Ref. [24].

the magnetic field is expelled as long as $B < B_2$. For type II superconductors, $\xi \ll \lambda$, implying that κ is large and the magnetic field penetrates the superconductor in the form of vortices, when $B_1 < B < B_2$. When B exceeds the critical field B_2, the magnetic field will penetrate the type II material completely.

2.2 Electron-Electron Attraction

The mechanism behind superconductivity is electron pair formation. Below T_c, it is energetically favorable for electrons to condense into so-called Cooper pairs that are related via time-reversal symmetry. Electrons are usually repulsive so it is interesting to understand how an attractive interaction between two electrons can arise in a many electron system. Such an effective interaction is a consequence of phonon exchange. To yield an attractive net interaction, the phonon-mediated interaction should be stronger than the Coulomb interaction [27]. The latter can be calculated. The assumption is made that the N-electron system has a two-body potential $V(\mathbf{q})$

$$V(\mathbf{q}) = V(\mathbf{k} - \mathbf{k}') = \frac{1}{\hat{\Omega}} \int \mathrm{d}^3 r \, \mathrm{e}^{i\mathbf{q}\cdot\mathbf{r}} \, V(\mathbf{r}),$$

where $V(\mathbf{r})$ is the Coulomb interaction $e^2/|\mathbf{r}|$, and $\hat{\Omega}$ is the volume taken to be unity [24]. Computing the integral yields

$$V(\mathbf{q}) = \frac{4\pi e^2}{\hat{\Omega}\mathbf{q^2}} = \frac{4\pi e^2}{\mathbf{q^2}}.$$

One can see immediately that $V(\mathbf{q})$ is always positive and as such yields repulsive behavior.

The motion of ions plays an important role in generating an attractive potential. The physical picture which considers the interaction between the electrons and the lattice is as follows: when an electron moves through a metal, it yields a dynamical distortion in the ionic crystal.[3] An electron needs a time $\sim E_F^{-1}$ to navigate close to a lattice ion and disturb this ion's equilibrium position into a new state which is energetically favorable for both the particles. By doing this, the electron polarizes the medium [24]. The excited ion lives on another time scale. It needs a time of order $(\hbar\omega_D)^{-1} \gg E_F^{-1}$ to decay back to its equilibrium, where ω_D is the Debye frequency, which characterizes phonon excitations. This time difference allows for another electron to be attracted by the excited ion before it decays. Therefore, there is a net attractive interaction between the two electrons and pair creation occurs [24]. When the attractive potential between electrons is stronger than the repulsive Coulomb interaction, the Fermi liquid will experience a phase transition to the superconducting state. This physical picture is confirmed by the existence of the isotope effect, which says that the critical temperature T_c and the critical field H_c are proportional to $A^{-1/2}$ where A is the atomic number, i.e. the ionic mass [27]. This means that in the presence of different isotopes in the same superconductor, the energy scales of the superconducting system described by the critical temperature T_c and the critical field H_c vary with the isotope mass in the same fashion as phonon frequencies [27]. The maximum energy scale of ionic excitation is of the range $\hbar\omega_D$. Therefore, for the interaction between two electrons to be attractive, the energy difference may not exceed this value; if the difference is larger, the interaction becomes repulsive [24]. This can be shown explicitly.

[3]The description in this paragraph is based on p. 266 in Ref. [14] unless indicated otherwise.

Consider the phonon Hamiltonian

$$H_{\text{ph}} = \sum_{\mathbf{q},j} \hbar\omega_q c^\dagger_{\mathbf{q},j} c_{\mathbf{q},j} + \text{const.},$$

where ω_q is the phonon dispersion, $c^\dagger_{\mathbf{q},j}$ ($c_{\mathbf{q},j}$) the boson creation (annihilation) operators of a phonon with momentum $\mathbf{q}$ on site j, and the index $j = 1, 2, 3$ accounts for the three dimensions in space in which the phonon can oscillate. The electron-phonon Hamiltonian is derived in App. 6.1.1 and reads

$$H_{\text{el-ph}} = \hbar\gamma \sum_{\mathbf{q},j} \frac{iq_j}{(2M\omega_q)^{1/2}} \hat{n}_{\mathbf{q}} \left(c^\dagger_{-\mathbf{c},j} + c_{\mathbf{q},j} \right),$$

where $\hat{n}_{\mathbf{q}} = \sum_{\mathbf{k}} a^\dagger_{\mathbf{k}+\mathbf{q}} a_{\mathbf{k}}$ is the electron density with $a^\dagger_{\mathbf{k}}$ ($a_{\mathbf{k}}$) the fermion creation (annihilation) operator of an electron with momentum $\mathbf{k}$, and spin is neglected for simplicity. To be able to show that there is an attractive electron-electron interaction, one should derive the effective action of this system. To find the corresponding actions, the operators need to be replaced by fields

$$\begin{aligned} a_{\mathbf{q}} &\rightarrow \psi_{\mathbf{q}}(\tau) = \frac{1}{\sqrt{\hbar\beta}} \sum_{\hat{\omega}_n} \psi_{\mathbf{q},n} \mathrm{e}^{-i\omega_n \tau}, \\ c_{\mathbf{q},j} &\rightarrow \phi_{\mathbf{q},j}(\tau) = \frac{1}{\sqrt{\hbar\beta}} \sum_{\omega_n} \phi_{\mathbf{q},j,n} \mathrm{e}^{-i\hat{\omega}_n \tau}, \end{aligned}$$

where $\omega_n = (2n+1)\pi/(\hbar\beta)$ and $\hat{\omega}_n = 2n\pi/(\hbar\beta)$ for $n \in \mathbb{Z}$ are the Matsubara frequencies for fermions and bosons, respectively, and $\phi^\dagger$ ($\psi^\dagger$) and ϕ (ψ) obey the boson (fermion) (anti)commutation relations. In App. 6.1.2, it is shown how this leads to the actions S_{ph} and $S_{\text{el-ph}}$. The result reads

$$\begin{aligned} S_{\text{ph}}\left[\phi^\dagger, \phi\right] &= \sum_{q,j} \phi^\dagger_{q,j} \left(-i\hat{\omega}_n + \omega_q\right) \phi_{q,j}, \\ S_{\text{el-ph}}\left[\psi^\dagger, \psi, \phi^\dagger, \phi\right] &= \frac{\gamma}{\sqrt{\hbar\beta}} \sum_{\mathbf{k},\mathbf{q},j} \sum_{n,n'} \frac{iq_j}{(2M\omega_q)^{1/2}} \psi^\dagger_{\mathbf{k}+\mathbf{q},n} \psi_{\mathbf{k},n'} \left(\phi^\dagger_{-\mathbf{q},j,n'-n} + \phi_{\mathbf{q},j,n-n'} \right). \end{aligned}$$

Using the partition function

$$\mathcal{Z} = \int D\left[\psi^\dagger, \psi\right] \int D\left[\phi^\dagger, \phi\right] \mathrm{e}^{-\left(S_{\text{el}}\left[\psi^\dagger,\psi\right] + S_{\text{ph}}\left[\phi^\dagger,\phi\right] + S_{\text{el-ph}}\left[\psi^\dagger,\psi,\phi^\dagger,\phi\right]\right)/\hbar},$$

the effective action S_{eff} can be obtained by integrating out the phonon fields. This derivation can be found in App. 6.1.3 and the result reads

$$S_{\text{eff}}\left[\psi^\dagger, \psi\right] = S_{\text{el}}\left[\psi^\dagger, \psi\right] - \frac{\gamma^2}{2M} \sum_q \frac{q^2}{\hat{\omega}_n^2 + \omega_q^2} \rho_q \rho_{-q}, \tag{2.5}$$

where $q = (n, \mathbf{q})$ and $\rho_q = \rho_{\mathbf{q},n} = (1/\sqrt{\hbar\beta}) \sum_{\mathbf{k},m} \psi^\dagger_{\mathbf{k}+\mathbf{q},m} \psi_{\mathbf{k},m+n}$. For there to be an attractive interaction, the relative sign between the first and second term should be a minus. As all terms in the second term are positive, this is indeed the case and there is an attractive electron-electron interaction.

2.3 The Cooper Problem

Cooper showed in 1956 how attractive interaction between electrons can give rise to electron pair formation using the Pauli exclusion principle [23]. He proved that in the presence of this interaction between two electrons, it is energetically favorable for the Fermi liquid that these two electrons form a pair, the so-called Cooper pair. He even alluded to how this can be related to the emerging superconducting properties of metals at low temperatures. To see how this works, an interacting pair of electrons that occupy the states above the Fermi level, or in other words above a filled Fermi sea, will be considered. These electrons can form a bound pair if there is a net attraction. Cooper simplified the problem of describing such an interaction by realizing that the superconducting transition is comparable in different metals and that it is therefore reasonable to assume that the structure of these metals does not affect the superconducting state. The band and lattice structure of the metals is thus neglected. Instead, an electron is considered as moving freely in a box of volume $\hat{\Omega}$. It is assumed that the electrons are only subjected to Coulomb repulsions or lattice vibrations (phonons) [23].

The first step is to write down a two-particle wavefunction. The lowest-energy state has zero total momentum which means that the two electrons must have opposite momenta [24]. Furthermore, the electron pair is assumed to be in a spin-singlet state yielding a rotationally symmetric wavefunction. Considering the Pauli exclusion principle, the wavefunction will be constructed from the states above the Fermi level [27]. The wavefuntion has the following form

$$|\psi\left(\mathbf{r_1}, \mathbf{r_2}\right)\rangle = \left(|\uparrow\rangle_1 |\downarrow\rangle_2 - |\downarrow\rangle_1 |\uparrow\rangle_2\right) \sum_{|\mathbf{k}|>k_F} g_{\mathbf{k}} \mathrm{e}^{i\mathbf{k}\cdot(\mathbf{r_1}-\mathbf{r_2})}, \tag{2.6}$$

where the index on the arrows refers to either electron 1 or 2 and, $g_{\mathbf{k}}$ can be determined by requiring that this wavefunction is a solution to the Schrödinger equation [27], such that

$$H\,|\psi\rangle = E\,|\psi\rangle\,,$$

where E is the energy of the pair and H is the Hamiltonian

$$H = 2\sum_{|\mathbf{k}|>k_F} \epsilon_{\mathbf{k}} + \sum_{1\neq 2} V\left(\mathbf{r_1} - \mathbf{r_2}\right),$$

with the electron dispersion $\epsilon_{\mathbf{k}} = \hbar^2 k^2/2m$ and where the factor of two for the electron dispersion relation comes from the fact that there are two electrons. The Schrödinger equation reads

$$\sum_{|\mathbf{k}|>k_F} g_{\mathbf{k}} \mathrm{e}^{i\mathbf{k}\cdot(\mathbf{r_1}-\mathbf{r_2})} V\left(\mathbf{r_1} - \mathbf{r_2}\right) = \sum_{|\mathbf{k}|>k_F} \left(E - 2\epsilon_{\mathbf{k}}\right) g_{\mathbf{k}} \mathrm{e}^{i\mathbf{k}\cdot(\mathbf{r_1}-\mathbf{r_2})}.$$

The following operator will be applied to both sides of the Schrödinger equation

$$\frac{1}{\hat{\Omega}} \int \mathrm{d}^d\left(\mathbf{r_1} - \mathbf{r_2}\right) \mathrm{e}^{-i\mathbf{q}\cdot(\mathbf{r_1}-\mathbf{r_2})},$$

which leads to

$$\frac{1}{\hat{\Omega}} \sum_{|\mathbf{k}|>k_F} g_{\mathbf{k}} V_{\mathbf{k}-\mathbf{q}} = \left(E - 2\epsilon_{\mathbf{q}}\right) g_{\mathbf{q}},$$

where $\hat{\Omega}$ is the volume of the system [27]. The potential is assumed to be constant and attractive in the phonon-energy range in accordance with what was found in the previous Section,

$$V(q) = \begin{cases} -V & \text{for } |\xi_k| \leq \hbar\omega_D, \\ 0 & \text{otherwise,} \end{cases}$$

with $\xi_{\mathbf{k}} = \epsilon_{\mathbf{k}} - \mu$ where $\epsilon_{\mathbf{k}} = \hbar^2\mathbf{k}^2/2m$, such that

$$\frac{V}{\hat{\Omega}} \sum_{|\mathbf{k}|>k_F} g_{\mathbf{k}} = (2\epsilon_{\mathbf{q}} - E)\, g_{\mathbf{q}},$$

where the sum on the left hand side is restricted to states only within the interval of energy equal to $\hbar\omega_D$ around the Fermi level, which is a consequence of plugging in the approximation for the potential $V(q)$ [27]. Rewriting the solution

$$\frac{1}{\hat{\Omega}} \sum_{\epsilon=E_F}^{\epsilon=E_F+\hbar\omega_D} \frac{1}{2\epsilon - E} = \frac{1}{V},$$

and replacing the sum with an integral, results in

$$\int_{E_F}^{E_F+\hbar\omega_D} \mathrm{d}\epsilon\, \frac{\rho}{2\epsilon - E} = \frac{\rho}{2} \ln\left[\frac{2\,(E_F + \hbar\omega_D) - E}{2E_F - E}\right] = \frac{1}{V},$$

with ρ the density of states [27]. The weak-coupling approximation, valid for $\rho\, V \ll 1$, can be used to find a solution for E at the Fermi level [24]. This method is justified because for most classical superconductors $\rho\, V < 0.3$ [24]. The binding energy E' is

$$E' = 2E_F - E \approx 2\hbar\omega_D \mathrm{e}^{-2/\rho V}. \tag{2.7}$$

This solution shows that there exists a bound state with negative energy with respect to the Fermi surface which consists solely of two electrons with $k > k_F$ meaning that there is an excess of kinetic energy with respect to the Fermi energy [24]. However, the energy of the attractive potential contributes more than the surplus of kinetic energy, such that binding occurs for any strength of V, or similarly, regardless of how weak the interaction is [24]. Note that the solution cannot be expanded in powers of V meaning that it could not have been found using perturbation theory.

2.4 The BCS Wavefunction

In the previous Sections, it was discussed that the formation of a Cooper pair creates instability in the Fermi liquid and that it is favorable for the formed pairs to condense into a new ground state, which represents the superconducting state. This process will take place until it reaches an equilibrium point. At this point, the system has changed so much from the initial Fermi sea that the binding energy for additional pairs has gone to zero [24]. The complexity of this system makes it difficult to work with were it not for the introduction of the BCS wavefunction.

Upon constructing this wavefunction, it is important to realize that when one wants to write down a wavefunction for more than two electrons, it is troublesome to write it in the form of

Eq. (2.6) due to the difficulty that is involved when one wants to include the anti-symmetry in a similar fashion [24]. Instead, it is more convenient to use the $N \times N$ Slater determinants.[4] In the language of second quantization, the Slater determinants can be written in terms of creation operators $a^\dagger_{\mathbf{k}\uparrow}$ which create an electron of momentum $\mathbf{k}$ and spin up. The annihilation operators $a_{\mathbf{k}\uparrow}$ annihilate the corresponding electron. The spin-singlet wavefunction is

$$|\psi_0\rangle = \sum_{\mathbf{k}>k_F} f_{\mathbf{k}} a^\dagger_{\mathbf{k}\uparrow} a^\dagger_{-\mathbf{k}\downarrow} |\mathbf{F}\rangle$$

where $|\mathbf{F}\rangle$ is the Fermi sea with all states filled up to k_F [24]. From this equation, it is immediatly clear that pairs of time-reversed states are always occupied simultaneously because when time is reversed, i.e. $t \to -t$, the sign of the momentum changes $\mathbf{k} \to -\mathbf{k}$ and the spin flips. Electrons must obey Fermi-Dirac statistics, so the creation and annihilation operators must satisfy the following anti-commutation relations

$$\left\{a_{\mathbf{k}\sigma}, a^\dagger_{\mathbf{k}'\sigma'}\right\} = \delta_{\mathbf{k}\mathbf{k}'}\delta_{\sigma\sigma'}, \qquad \{a_{\mathbf{k}\sigma}, a_{\mathbf{k}'\sigma'}\} = \left\{a^\dagger_{\mathbf{k}\sigma}, a^\dagger_{\mathbf{k}'\sigma'}\right\} = 0,$$

where σ is the spin index.

A general expression for the BCS wavefunction for an N-electron system is

$$|\psi_N\rangle = \sum f(\mathbf{k}_i, \ldots, \mathbf{k}_l)\, a^\dagger_{\mathbf{k}_i\uparrow} a^\dagger_{-\mathbf{k}_i\downarrow} \ldots a^\dagger_{\mathbf{k}_l\uparrow} a^\dagger_{-\mathbf{k}_l\downarrow} |0\rangle\,,$$

where $|0\rangle$ is the vacuum state, $\mathbf{k}_i$ and $\mathbf{k}_l$ are the first and last of the $\mathbf{k}$ values in the band, which are occupied in a given term in the sum, and f is the weight with which the product of the $N/2$ pairs of creation operators appears [24]. The sum runs over all $\mathbf{k}$ values in the band leading to an incredibly large number of possibilities to choose the $N/2$ states for pair occupancy. Therefore, Bardeen, Cooper and Schrieffer decided to use a Hartree self-consistent field or mean-field approach, where the occupancy of each state $\mathbf{k}$ is taken to depend only on the average occupancy of other states [24]. This relieves the constraint on the total number of particles being N because now the occupancies are treated only statistically. This is analogous to statistical mechanics when going from the canonical to the grand canonical distributions [27].

Taking all of the previous into consideration, the BCS wavefunction acquirs the following form

$$|\psi_{BCS}\rangle = \prod_{\mathbf{k}} \left(u_{\mathbf{k}} + v_{\mathbf{k}} a^\dagger_{\mathbf{k}\uparrow} a^\dagger_{-\mathbf{k}\downarrow}\right) |0\rangle\,, \tag{2.8}$$

where $|u_{\mathbf{k}}|^2 + |v_{\mathbf{k}}|^2 = 1$ and the probability of the pair $(\mathbf{k}\uparrow, -\mathbf{k}\downarrow)$ being occupied is $|v_{\mathbf{k}}|^2$ such that the probability that it is not occupied is $|u_{\mathbf{k}}|^2 = 1 - |v_{\mathbf{k}}|^2$ [24].

Depending on the choice of $v_{\mathbf{k}}$, a variety of states can be described by a wavefunction of the form of Eq. (2.8). For a filled Fermi sea, $v_{\mathbf{k}} = 1$ for $\mathbf{k}$ inside the Fermi surface and $v_{\mathbf{k}} = 0$ outside. In a state with many Cooper pairs, it is expected that $v_{\mathbf{k}}$ varies smoothly between 1 and 0 across the range of $\hbar\omega_D$ around the Fermi energy [27]. $v_{\mathbf{k}}$ can be found using a variational approach or a mean-field treatment of the Hamiltonian.

[4] Slater determinants describe the wavefunction of a multi-fermionic system and are particularly useful because they satisfy the Pauli exclusion principle by including anti-symmetry requirements.

2.5 The Gap Equation

So far it was assumed that the attractive interaction between two electrons leads to the creation of a pair. However, the interaction is not strong enough for the formation of a true local pair. In fact, the distance between two electrons that are coupled is larger than the average distance between pairs. This means that a theory describing such interactions should take both pairing and condensation into account. Moreover, the electron pairs also interact with all other pairs, which makes mean-field theory suitable for treating this problem.

BCS theory uses a microscopic approach by considering a system of N electrons. This N-electron system has a two-body interaction described by the following Hamiltonian

$$H = -\frac{\hbar^2}{2m}\sum_{j=1}^{N}\nabla_j^2 + \frac{1}{2}\sum_{i\neq j}^{N} V\left(\mathbf{r_i} - \mathbf{r_j}\right).$$

The first term is the kinetic term and the second is the present Coulomb repulsion between two electrons. $\mathbf{k}$ is the wave vector and $\sigma = \pm\frac{1}{2}$ are the spin states.

From the previous sections, it has become clear that BCS based their theory on two assumptions. Firstly, there are only single-particle states arranged in pairs, namely $(\mathbf{k},\uparrow)$ and $(-\mathbf{k},\downarrow)$, which are simultaneously occupied or empty such that they form a spin singlet. As the phenomenon of superconductivity originates from the interaction between electrons mediated by phonons, the energy is restricted to $|\xi_k| \leq \hbar\omega_D$, where ω_D is the maximal frequency of a phonon.[5] The second assumption is that the electron-phonon interaction is constant in this energy range, i.e. $V(q) = -V$, and zero otherwise as defined in Section 2.3. Using these assumptions, second quantization can be used to rewrite the Hamiltonian

$$H - \mu N = \sum_{\mathbf{k}\sigma}\xi_{\mathbf{k}} a^\dagger_{\mathbf{k}\sigma} a_{\mathbf{k}\sigma} - \frac{V}{L^3}\sum_{\mathbf{k}\mathbf{k}'} a^\dagger_{\mathbf{k}\uparrow} a^\dagger_{-\mathbf{k}\downarrow} a_{-\mathbf{k}'\downarrow} a_{\mathbf{k}'\uparrow}, \tag{2.9}$$

with $\xi_{\mathbf{k}} = \epsilon_{\mathbf{k}} - \mu$ where $\epsilon_{\mathbf{k}} = \hbar^2\mathbf{k}^2/2m$ [28]. The parameter μ is called the chemical potential and can be found through minimizing the free energy. For a Fermi liquid at zero temperature, the chemical potential is equal to the Fermi energy E_F. In fact, if the kinetic energy of a superconducting state is small enough, the chemical potential can be approximated to be equal to the Fermi energy. Therefore, in the first approximation μ is equal to E_F [28]. This Hamiltonian explains the physics of a thin shell of states of width of the order $\hbar\omega_D$ around the Fermi surface shown in Fig. 2.1.

To find the gap equation, the thermodynamic properties should be evaluated.[6] The free energy is defined as

$$\Omega = -\frac{1}{\hbar\beta}\log(Z),$$

with $\beta = 1/k_BT$ and the partition function

$$Z = \mathrm{Tr}\left[\mathrm{e}^{-\hbar\beta(H-\mu N)}\right].$$

[5] This can be recognized as the quantized energy of the electron that goes with $n\,\hbar\omega_D$. This energy is restricted to the limit where $n = -1, 0, 1$ because if the energy were higher, the system can no longer be considered as a lattice.

[6] This entire derivation is based on Ref. [28] unless indicated otherwise.

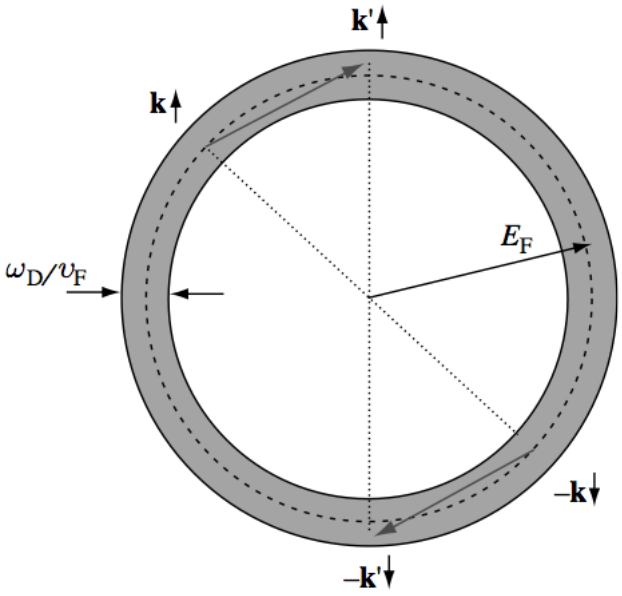

Figure 2.1: A thin shell of width $\sim \omega_D$ around the Fermi surface. Figure from Ref. [14].

Unfortunately, the Hamiltonian is not exactly solvable, which necessitates the use of the Bogoliubov inequality, which introduces the molecular field Hamiltonian H_m and its free energy Ω_m

$$\Omega \leq \Omega_m + \langle H - H_m \rangle_m \equiv \tilde{\Omega}. \tag{2.10}$$

The new quantity $\tilde{\Omega}$ can be calculated exactly. To determine H_m, it is convenient to use a mean-field approximation

$$a_{-\mathbf{k},\downarrow} a_{\mathbf{k},\uparrow} = \langle a_{-\mathbf{k},\downarrow} a_{\mathbf{k},\uparrow} \rangle + \delta \left(a_{-\mathbf{k},\downarrow} a_{\mathbf{k},\uparrow} \right) = \Delta + \delta \left(a_{-\mathbf{k},\downarrow} a_{\mathbf{k},\uparrow} \right).$$

This transformation makes the Hamiltonian bilinear in the electron operators by eliminating the interacting term and in return introduces a new auxiliary field, $\Delta = \langle a_{-\mathbf{k},\downarrow} a_{\mathbf{k},\uparrow} \rangle$. Δ is chosen to be real, i.e. $\Delta^* = \Delta$. The excitation spectrum is the part of interest such that the term quadratic in Δ is neglected here because it only contributes to the energy of the condensate. Applying the mean-field approximation to Eq. (2.9) yields

$$H_m - \mu N = \sum_{\mathbf{k}} \left[\xi_k \left(a^\dagger_{\mathbf{k}\uparrow} a_{\mathbf{k}\uparrow} + 1 - a_{-\mathbf{k}\downarrow} a^\dagger_{-\mathbf{k}\downarrow} \right) - \Delta \left(a^\dagger_{\mathbf{k}\uparrow} a^\dagger_{-\mathbf{k}\downarrow} + a_{-\mathbf{k}\downarrow} a_{\mathbf{k}\uparrow} \right) \right]. \tag{2.11}$$

The first term is diagonal, but the second term is not. It is diagonalized using the canonical Bogoliubov transformation

$$a_{\mathbf{k}\uparrow} = \cos(\theta_{\mathbf{k}}) \alpha_{\mathbf{k}\uparrow} + \sin(\theta_{\mathbf{k}}) \alpha^\dagger_{-\mathbf{k}\downarrow}, \qquad a^\dagger_{-\mathbf{k}\downarrow} = -\sin(\theta_{\mathbf{k}}) \alpha_{\mathbf{k}\uparrow} + \cos(\theta_{\mathbf{k}}) \alpha^\dagger_{-\mathbf{k}\downarrow}.$$

Using the anti-commutation relations for fermions defined in the previous Section leads to

$$\left\{ \alpha_{\mathbf{k}\sigma}, \alpha^\dagger_{\mathbf{k}'\sigma'} \right\} = \delta_{\mathbf{k}\mathbf{k}'} \delta_{\sigma\sigma'}, \qquad \{ \alpha_{\mathbf{k}\sigma}, \alpha_{\mathbf{k}'\sigma'} \} = \left\{ \alpha^\dagger_{\mathbf{k}\sigma}, \alpha^\dagger_{\mathbf{k}'\sigma'} \right\} = 0.$$

Plugging in this transformation, the Hamiltonian reads

$$\begin{aligned} H_m - \mu N &= \sum_{\mathbf{k}} \Big\{ \xi_{\mathbf{k}} + [\xi_{\mathbf{k}} \cos(2\theta_{\mathbf{k}}) + \Delta \sin(2\theta_{\mathbf{k}})] \left(a^\dagger_{\mathbf{k}\uparrow} a_{\mathbf{k}\uparrow} - a_{-\mathbf{k}\downarrow} a^\dagger_{-\mathbf{k}\downarrow} \right) \\ &\quad + [\xi_{\mathbf{k}} \sin(2\theta_{\mathbf{k}}) - \Delta \cos(2\theta_{\mathbf{k}})] \left(a^\dagger_{\mathbf{k}\uparrow} a^\dagger_{-\mathbf{k}\downarrow} + a_{-\mathbf{k}\downarrow} a_{\mathbf{k}\uparrow} \right) \Big\}. \end{aligned}$$

By choosing

$$\tan 2\theta_{\mathbf{k}} = \frac{\Delta}{\xi_{\mathbf{k}}},$$

the last term in the Hamiltonian vanishes and the entire expression is rendered diagonal. The tangent is $\pi/2$-periodic, so $\theta_{\mathbf{k}}$ has the range $-\pi/4 \leq \theta_{\mathbf{k}} \leq \pi/4$. This leads to

$$\begin{aligned} \cos 2\theta_{\mathbf{k}} &= \frac{1}{\sqrt{1 + \tan^2 2\theta_{\mathbf{k}}}} = \frac{|\xi_{\mathbf{k}}|}{\sqrt{\xi^2_{\mathbf{k}} + \Delta^2}}, \\ \sin 2\theta_{\mathbf{k}} &= \tan 2\theta_{\mathbf{k}} \cos 2\theta_{\mathbf{k}} = \mathrm{sgn}\,(\xi_{\mathbf{k}}) \frac{\Delta}{\sqrt{\xi^2_{\mathbf{k}} + \Delta^2}}. \end{aligned}$$

Using these relations, the Hamiltonian can be written more compactly

$$H_m - \mu N = \sum_{\mathbf{k}} \left[(\xi_k - E_k) + \sum_\sigma E_k \alpha^\dagger_{k\sigma} \alpha_{k\sigma} \right], \tag{2.12}$$

where

$$E_k = \mathrm{sgn}\,(\xi_k) \sqrt{\xi^2_k + \Delta^2}. \tag{2.13}$$

Here, Δ represents the superconducting gap and describes the energy gap between the lowest and first excited energy states. The gap is $E_g = 2|\Delta|$. This gap prevents elementary excitations at low temperature making the ground state rigid [14]. Using these equations, the partition partition function Z_m and the free energy Ω_m can be computed. $\langle H - H_m \rangle_m$ needs to be determined to obtain $\tilde{\Omega}$. Substituting all results in Eq. (2.10) yields

$$\tilde{\Omega} = \sum_{\mathbf{k}} \left[\xi_k - E_k - \frac{2}{\beta} \log\left(1 + e^{-\beta E_k}\right) + \frac{\Delta^2}{E_k} \tanh \frac{\beta E_k}{2} \right] - \frac{V}{L^3} \left[\frac{1}{2} \sum_k \frac{\Delta}{E_k} \tanh \frac{\beta E_k}{2} \right]^2. \tag{2.14}$$

Minimizing this equation with respect to Δ leads to

$$\frac{d\tilde{\Omega}}{d\Delta} = \left[\Delta - \frac{V}{2L^3} \Delta f(\Delta) \right] [f(\Delta) + \Delta f'(\Delta)] = 0,$$

with

$$f(\Delta) \equiv \sum_k \frac{\tanh(\beta E_k/2)}{E_k},$$

such that the gap equation reads

$$\Delta = \frac{V}{2L^3} \sum_k \frac{\Delta}{E_k} \tanh \frac{\beta E_k}{2}, \tag{2.15}$$

where Δ is assumed to be constant. This non-linear equation can be solved numerically. A solution is $\Delta = 0$ which corresponds to normal metal. For $\Delta \neq 0$ the solutions can be found by dividing out Δ on both sides of Eq. (2.15) such that one finds

$$1 = \frac{V}{2} \int \frac{\mathrm{d}^3 k}{(2\pi)^3} \frac{1}{E_k} \tanh \frac{\beta E_k}{2}. \tag{2.16}$$

Substituting the solution for $E_{\mathbf{k}}$ in Eq. (2.13) and rewriting the integral in terms of the density of states leads to

$$2 \approx V\rho \int_0^{\hbar\omega_D} \mathrm{d}\xi \frac{1}{\sqrt{\xi^2 + \Delta^2}} \tanh\left(\frac{\beta}{2}\sqrt{\xi^2 + \Delta^2}\right), \tag{2.17}$$

where the density of states is taken to be constant in the energy range $\xi \leq \hbar\omega_D$

$$\rho = \frac{1}{2\pi^2} k^2 \left.\frac{\mathrm{d}k}{\mathrm{d}\xi}\right|_{\xi=0}. \tag{2.18}$$

The term on the right hand side of Eq. (2.17) decreases in function of the temperature and the superconducting gap such that the gap becomes smaller for increasing temperature until the critical temperature is reached at which the superconducting gap vanishes as shown in Fig. 2.2. This property of Δ makes its value a defining measure for the phase of the material. Therefore, Δ is called the order parameter of the superconducting transition.

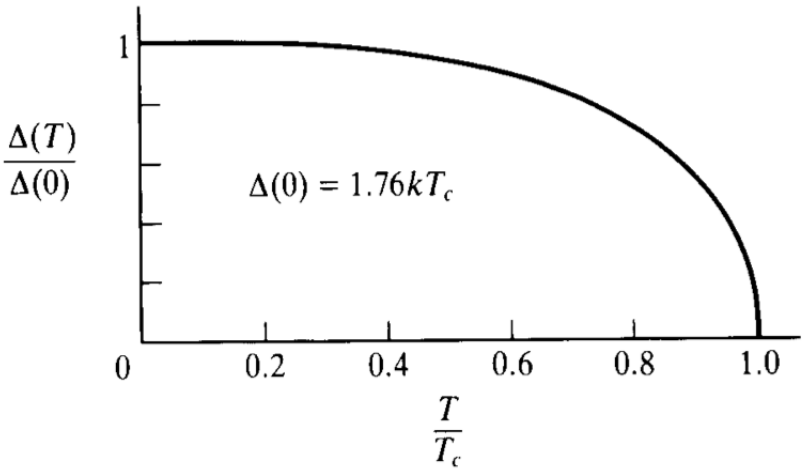

Figure 2.2: The relation between temperature and the energy gap in BCS theory. Figure from Ref. [24].

Sending β to infinity in Eq. (2.17), allows one to consider the superconducting gap at zero temperature. This yields

$$2 \approx V\rho \int_0^{\hbar\omega_D} \mathrm{d}\xi \frac{1}{\sqrt{\xi^2 + \Delta^2}},$$

such that a solution for $\Delta(0)$ can be found upon solving the integral

$$\Delta(0) = \frac{\hbar\omega_D}{\sinh\left[2/V\rho\right]}.$$

In the weak-coupling limit, $V\rho \ll 1$, the zero-temperature gap reads

$$\Delta(0) = 2\hbar\omega_D \mathrm{e}^{-2/V\rho}, \tag{2.19}$$

which coincides with the binding energy in Eq. (2.7).

The superconducting gap vanishes at the critical temperature. This yields the following for Eq. (2.17)

$$2 = V\rho \int_0^{\hbar\omega_D} \mathrm{d}\xi \frac{\tanh\left(\beta_c \xi/2\right)}{\xi}.$$

This integral can be solved using integration by parts

$$\frac{2}{V\rho} = \log(y)\tanh(y)|_0^z - \int_0^\infty \mathrm{d}y \log(y)\,\mathrm{sech}^2(y),$$

with $z = \hbar\omega_D\beta_c/2$. Taking the limit $z \to \infty$ results in

$$\frac{2}{V\rho} = \log\left(\beta_c \frac{\hbar\omega_D}{2}\right) + \log\left(4\frac{\mathrm{e}^\gamma}{\pi}\right),$$

where $\gamma = 0.577$ is the Euler constant. Rearranging the right hand side leads to the following result

$$k_B T_c \approx 2\frac{\mathrm{e}^\gamma}{\pi}\hbar\omega_D \mathrm{e}^{-2/V\rho}, \tag{2.20}$$

which can be rewritten in terms of the earlier result for zero-temperature superconducting gap $\Delta(0)$ as

$$k_B T_c \approx \Delta(0)\frac{\mathrm{e}^\gamma}{\pi}. \tag{2.21}$$

Plugging in the values for γ and π leads to the universal result

$$\frac{2\Delta(0)}{k_B T_c} = 3.53, \tag{2.22}$$

which agrees with experiment.

Chapter 3

Graphene

Ever since its isolation in 2004, graphene and graphene-related topics have been the main object of research for many scientists. Being only one-atom thick, it is considered to be the thinnest material ever produced. It is light, transparent, flexible, strong, conducts electricity, and it is made out of the main ingredient of life itself, carbon. This collection of characteristics has not only spurred the interest of the scientific world, but also of the industry where applications are envisioned, such as for instance using graphene to make smartphones [30]. The existence of graphene was postulated in the late 1800s when it was realized to be the fundamental building block of graphite. Graphite is made of stacked layers of graphene and has been a well-known material since the 1500s because it makes up the core of a pencil. The theory of graphene was first written down by Wallace in 1947 [31], the results of which are still quoted today. Even though the existence of graphene was known for a long time, futile attempts to isolate it led to the believe that it could not exist as a free state. However, in 2003, Andre Geim and Kostya Novoselov developed a method to isolate the material by the use of Scotch tape. Sticking a piece of tape on graphite and pealing it off leaves a residue on the tape, which consists of some layers of graphene. Upon repeating this procedure, more and more layers of graphene will be peeled off, until one layer is left. This is exactly what Geim and Novoselov did and they published their results in 2004 [1]. For this simple and yet groundbreaking discovery, they won the Noble Prize for Physics in 2010.

Graphene consists of carbon atoms arranged in a honeycomb structure, which can be interpreted as a configuration of benzene rings without hydrogen atoms connected in a lattice. Graphene is one-atom thick, and as such is treated as a two-dimensional object. The honeycomb lattice is not translationally invariant because it consists of two inequivalent atom sites. Its structure is described as two interpenetrating triangular lattices, hence the basis of a unit cell is formed by two atoms.

Carbon contains four valence electrons described by s, p_x, p_y, and p_z orbital functions. One carbon atom is connected with three other carbon atoms in the honeycomb-lattice structure forming a two-dimensional object in the x and y direction.[1] The s, p_x and p_y orbitals are invariant under reflection over the z-axis. Together they hybridize to form an sp^2 bond, also called σ bond, that binds the carbon atoms together. σ bonds are the strongest type of covalent bonds because they are formed by direct overlap between the orbitals. These bonds are responsible for the robustness of the lattice [32]. The remaining p_z orbital is perpendicular to the plane

[1] The plane can be chosen in any direction without changing the physics.

and antisymmetric under reflection over the z-axis. It can form π-bonds through covalent binding with neighboring atoms. The overlap between the p_z orbitals facilitates electron hopping between carbon sites.

The hopping of electrons between carbon atoms is described using a tight-binding model. In this chapter, only nearest-neighbor and next-nearest-neighbor hopping is included. Hopping to more remote sites is not considered because the overlap between the orbitals is negligible. Upon calculating the energy bands of the model, a linear dispersion relation is found at zero energy near the K and K' points of the Brillouin zone. This means that there are Dirac cones located at these points and the conductance of electricity is possible. Moreover, from the linearity of the dispersion it can be concluded that the low-energy excitations in the system are massless Dirac fermions described by the two-dimensional Dirac equation. This means that phenomena such as the Klein paradox[2] and Zitterbewegung[3] that only occur for Dirac fermions and were only known to exist in high-energy systems, can now be measured.

This chapter is set up as follows. In the first Section, the lattice structure of graphene will be discussed. The next Section will briefly recapture orbitals and explain their relevance to graphene. This will be followed by a description of the tight-binding model used to study graphene and a derivation of the linear-dispersion relation around the K (K') points in Section 3.3. In Section 3.4, the cyclotron mass will be introduced, which is a measurable quantity that can be used to derive other quantities. The density of states is derived in Section 3.5, and Section 3.6 contains a discussion about the effective Dirac Hamiltonian.

3.1 Lattice Structure

Graphene is build up from carbon atoms arranged in a honeycomb lattice, as shown in Fig. 3.1(a), where the carbon sites are represented by blue and yellow dots. The color difference indicates the geometrical inequivalence between sites A (blue) and sites B (yellow); all A sites have a bond north-west, south-west and east, whereas all B sites have a bond north-east, south-east and west. This inequivalence between neighboring sites means that the honeycomb lattice is not a Bravais lattice. A reciprocal lattice vector (indicated in Fig. 3.1(b) by $\mathbf{b}_i$) can connect all sites A and all sites B together forming two triangular Bravais lattices with a basis formed by two atoms, sites A and B.

The lattice vectors $\mathbf{a}_i$, indicated in Fig. 3.1(a), span the triangular Bravais lattice. They are

$$\mathbf{a}_1 = \frac{a}{2}\left(3, \sqrt{3}\right), \quad \mathbf{a}_2 = \frac{a}{2}\left(3, -\sqrt{3}\right), \tag{3.1}$$

with the spacing between the atoms A and B in the unit cell, called lattice spacing, $a \approx 1.42$ Å. The spacing between the atoms in the triangular lattice is equal to the modulus of the lattice vectors $|\mathbf{a}_1| = |\mathbf{a}_2| = \sqrt{3}a \approx 2.4$ Å. The area of the unit cell is $\mathcal{A} = 3\sqrt{3}a^2/2 = 0.051\,\mathrm{nm}^2$ [35]. There are two atoms in the unit cell, hence the density of carbon atoms is $n_C = 2/\mathcal{A} = 39\,\mathrm{nm}^{-2} = 3.9 \times 10^{15}\,\mathrm{cm}^{-2}$. Per carbon atom, there is one π electron, therefore, the density of valence electrons equals the density of carbon atoms $n_\pi = n_C = 3.9 \times 10^{15}\,\mathrm{cm}^{-2}$. The three

[2]The Klein paradox is the phenomenon where regardless of the height of the potential barrier, this barrier will always be transparent for Dirac fermions coming in with normal incidence.

[3]When confining Dirac fermions, these fermions exhibit jittery motion, also called Zitterbewegung.

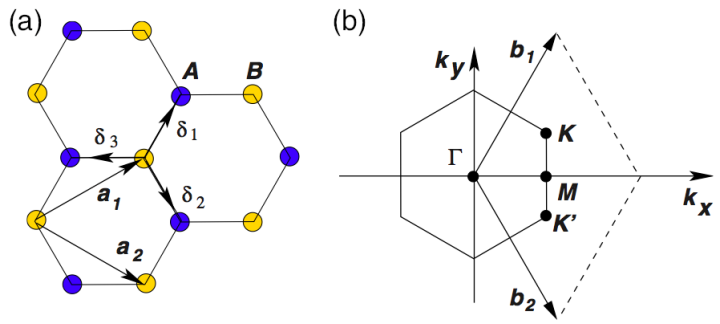

Figure 3.1: Graphene honeycomb lattice and its Brillouin zone. (a) Lattice of graphene with $\mathbf{a}_1$ and $\mathbf{a}_2$ denoting lattice vectors, and $\boldsymbol{\delta}_1$, $\boldsymbol{\delta}_2$ and $\boldsymbol{\delta}_3$ the nearest-neighbor vectors. (b) Brillouin zone of graphene, with the reciprocal-lattice vectors $\mathbf{b}_1$ and $\mathbf{b}_2$ and the high-symmetry points K and K' where the dispersion is Dirac-like. Figure from Ref. [32].

nearest-neighbor vectors are

$$\boldsymbol{\delta}_1 = \frac{a}{2}\left(1, \sqrt{3}\right), \quad \boldsymbol{\delta}_2 = \frac{a}{2}\left(1, -\sqrt{3}\right), \quad \boldsymbol{\delta}_3 = -a\left(1, 0\right), \tag{3.2}$$

and the next-nearest neighbors are

$$\boldsymbol{\delta}'_1 = \pm\mathbf{a}_1, \quad \boldsymbol{\delta}'_2 = \pm\mathbf{a}_2, \quad \boldsymbol{\delta}'_3 = \pm\left(\mathbf{a}_2 - \mathbf{a}_1\right). \tag{3.3}$$

Performing a Fourier transform allows one to define reciprocal-lattice vectors that span the reciprocal space. The primitive cell in this space is called the Brillouin zone, shown in Fig. 3.1(b). The reciprocal-lattice vectors $\mathbf{b}_i$ are related to the lattice vectors $\mathbf{a}_i$ via $\mathbf{a}_i \cdot \mathbf{b}_j = 2\pi\delta_{ij}$. They are given by

$$\mathbf{b}_1 = \frac{2\pi}{3a}\left(1, \sqrt{3}\right), \quad \mathbf{b}_2 = \frac{2\pi}{3a}\left(1, -\sqrt{3}\right). \tag{3.4}$$

The K and K' points in Fig. 3.1(b) are the corners of the Brillouin zone, called Dirac points.[4] In momentum space, they are located at

$$\mathbf{K} = \left(\frac{2\pi}{3a}, \frac{2\pi}{3\sqrt{3}a}\right), \quad \mathbf{K}' = \left(\frac{2\pi}{3a}, -\frac{2\pi}{3\sqrt{3}a}\right). \tag{3.5}$$

All K and K' points can be connected via the reciprocal-lattice vectors. The low-energy excitations in graphene are located around these two points, as will be discussed in Section 3.3. It is important to realize at this point that the inequivalence between the K and K' points is unrelated to the inequivalence between the A and B lattice sites [35]. The Bravais lattice determines the form of the Brillouin zone, irrespective of whether there is more than one atom present in the unit cell.

3.2 Orbitals

In the introduction, it was mentioned that the four valence electrons in carbon correspond to s, p_x, p_y and p_z orbital functions. In this Section, this nomenclature will be made more explicit.

[4]The reason for this name will be explained soon.

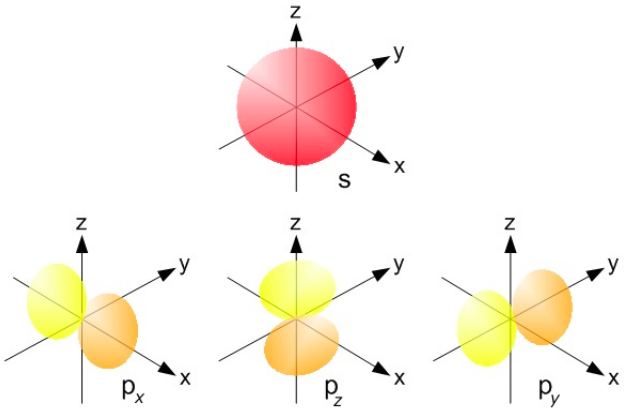

Figure 3.2: s, p_x, p_y and p_z orbitals. Figure from Ref. [34].

Electrons in an atom are bound to shells denoted by n, where $n = 1$ is the first shell around the nucleus, $n = 2$ the second, and so on. With a higher shell number n, the electron is further away from the nucleus. The number of electrons in a shell is dictated by the Pauli principle. The degrees of freedom increase upon increasing shell-number, so that the number of electrons increases with increasing shell-number. Away from the nucleus, the wavefunctions describing these electrons look like plane waves [33]. However, upon closer inspection, they are described by atomic orbitals. The shape of the orbital of an electron depends on the angular momentum quantum number l according to $0 \leq l \leq n-1$, where l is an integer. These orbitals are called s, p, d and so on, corresponding to $l = 0, 1, 2...$, respectively. The number l corresponds to the number of nodes of the orbital. The magnetic quantum number determines the number of orbitals according to $-l \leq m \leq l$ with m an integer. For example, the p orbital has three different magnetic moment quantum numbers, $m = -1, 0, 1$. The three orbitals, p_{-1}, p_0, and p_{+1} can be combined to p_x, p_y and p_z. The s and p orbitals are shown in Fig. 3.2.

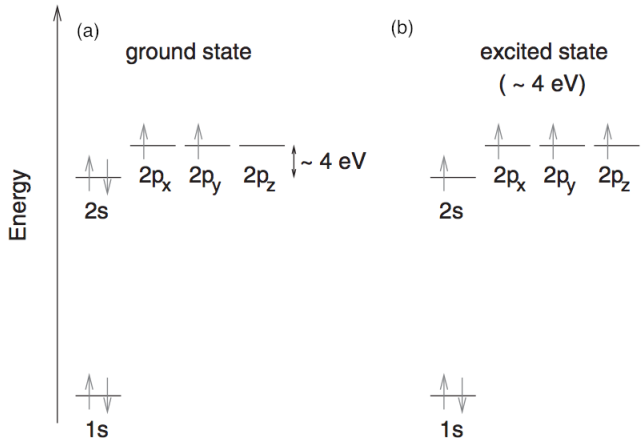

Figure 3.3: Configurations of electrons in a carbon atom. (a) Electrons in the ground state. (b) One electron excited from the $2s$ orbital to the available $2p$ orbitals. Figure from Ref. [35].

Carbon contains six electrons; two are in the first orbit ($n = 1$) around the nucleus and four are in the second ($n = 2$). These four are the valence electrons which means that one carbon

atom can form four bands with other atoms. The core electrons are so close to the nucleus of the atom that they are deemed irrelevant for the chemical reactions and they are neglected when developing the theory of graphene [35]. In carbon, the groundstate configuration of the electrons is $1s^2\,2s^2\,2p^2$. This configuration is energetically most favorable because the $2p$ orbitals are 4 eV higher in energy than the $2s$ orbitals [35]. However, in graphene this configuration of electrons is not the preferred state. In the presence of other carbon atoms, it is energetically most favorable to excite one electron from the $2s$ orbital into the third available $2p$ orbital, as shown in Fig. 3.3, so that covalent bonds between carbon atoms can be formed [35]. Now, the electron configuration is $1s^2\,2s^1\,2p^3$.

Graphene is two dimensional in the x and y direction. The plane is invariant under reflection over the z-axis, a symmetry also exhibited by the s, p_x and p_y orbitals. A superposition of these states $|2s\rangle$, $|2p_x\rangle$ and $|2p_y\rangle$ is called sp^2 hybridization [35]. The three sp^2 orbitals are oriented in the x and y direction with an angle $2\pi/3$ between them, as shown in Fig. 3.4. The sp^2 bond, also called σ bond, binds the carbon atoms together in the honeycomb lattice. σ bonds are formed by direct overlap of the orbitals, which makes them the strongest among different types of covalent bonds. Therefore, they are responsible for making the lattice robust [32]. The remaining orbital p_z is perpendicular to the plane and can form π-bonds through covalent binding with neighboring atoms. It is this orbital that is responsible for the electronic properties of graphene.

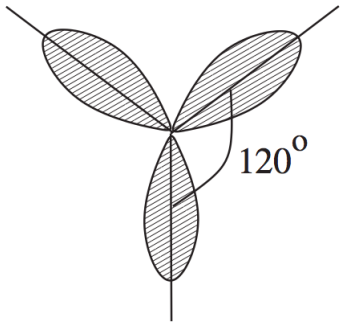

Figure 3.4: sp^2 hybridized orbitals at an angle $2\pi/3$ apart. Figure from Ref. [35].

3.3 Tight-Binding Model

The energy bands of a crystal contain information about the electrons in the system. In the case of graphene, the linear behavior of the dispersion reveals that the electronic excitations are Dirac fermions. A convenient way to retrieve the energy bands is by using a tight-binding model. In this Section, the model will be briefly sketched and it will be justified why this approximation can be used to find the energy bands of graphene. After a short introduction, the model will be applied to graphene.

3.3.1 A Brief Introduction

By assuming that atoms in a solid are far apart from each other, the solid can be described by treating these atoms as if they are isolated. Upon decreasing the spacing, the atoms will be

brought closer to each other and the orbital functions of the electrons of the different atoms will start to overlap. The tight-binding model is capable of describing the corrections provided by this overlap to the picture of isolated orbitals.

In this model, it is assumed that near the lattice point the Hamiltonian can be approximated by the Hamiltonian H_{at} of the single atom at that lattice point [36]. It is also assumed that the bound levels of the Hamiltonian are well localized, which means that if ψ_n is a bound level of H, then $\psi_n(\mathbf{r})$ is very small when $\mathbf{r}$ exceeds a distance of the order of the lattice spacing [36]. Such a bound level satisfies the atomic Schrödinger equation

$$H_{\text{at}}\psi_n = E_n\psi_n.$$

The Hamiltonian of the entire crystal H can be written as

$$H = H_{\text{at}} + \Delta U(\mathbf{r}),$$

where $\Delta U(\mathbf{r})$ is a correction to the atomic potential that matches the periodic potential of the crystal [36]. $\psi_n(\mathbf{r})$ then also satisfies the crystal Schrödinger equation as long as $\Delta U(\mathbf{r})$ vanishes where $\psi_n(\mathbf{r})$ does not. If this condition holds, then for each of the N sites $\mathbf{R}$ in the lattice, each atomic level $\psi_n(\mathbf{r})$ yields N levels in the periodic potential with wavefunctions $\psi_n(\mathbf{r}-\mathbf{R})$ [36]. One may now write a wavefunction that is a linear combination of these N atomic orbitals

$$\psi_{n_{\mathbf{k}}}(\mathbf{r}) = \frac{1}{\sqrt{N}}\sum_{\mathbf{l}} \mathrm{e}^{i\mathbf{k}\cdot\mathbf{l}}\psi_n(\mathbf{r}-\mathbf{l}), \tag{3.6}$$

where $\mathbf{k}$ ranges through the N values of the first Brillouin zone and ψ_n are the atomic orbital functions [36]. This wavefunction satisfies Bloch's theorem[5] and contains the atomic character of the levels. The energy bands in this description correspond to the energy of the atomic level E_n regardless of the value of $\mathbf{k}$ [36]. Therefore, the wavefunction in Eq. (3.6) does not contain any specific information about the system in combination with the initial assumptions.

One way to fix this problem is by modifying the initial assumption. It is more realistic to assume that $\psi_n(\mathbf{r})$ becomes very small but non-zero when $\Delta U(\mathbf{r})$ comes into play [36]. One wants to find a solution to the full crystal Schrödinger equation in the form of Eq. (3.6). Now the Bloch function is

$$\psi_{n_{\mathbf{k}}}(\mathbf{r}) = \sum_{\mathbf{l}} \mathrm{e}^{i\mathbf{k}\cdot\mathbf{l}}\phi_n(\mathbf{r}-\mathbf{l}), \tag{3.7}$$

where $\phi_n(\mathbf{r}-\mathbf{l})$ is not an orbital function but a Wannier function [36]. Wannier functions describe the motion of the electrons as a function of position and they are independent of $\mathbf{k}$ [33]. For each electron band, there is a different Wannier function [33]. As $\psi_{n_{\mathbf{k}}}(\mathbf{r})$ describe a basis, $\phi_n(\mathbf{r}-\mathbf{l})$ also describe a basis. The orthogonality of the Bloch functions $\psi_{n_{\mathbf{k}}}$ and $\psi_{n'_{\mathbf{k}}}$ (where n and n' belong to different bands) means that the Wannier functions should also form an orthogonal basis. Moreover, Wannier functions on different sites should always be orthogonal to each other, even when they belong to the same energy band [33]. This means the following: if W_R is a Wannier function, the orthogonality condition states that $\langle W_R|W'_R\rangle = 0$ should hold, i.e.

$$\int_{-\infty}^{\infty} \mathrm{d}r W_R^*(r)W_{R'}(r) = \delta(R-R'). \tag{3.8}$$

[5]Remember that Bloch's theorem states that one can always write a wavefunction as $\psi_{\mathbf{k}}(\mathbf{r}) = \exp(i\mathbf{k}\cdot\mathbf{r})u_{\mathbf{k}}(\mathbf{r})$, where $u_{\mathbf{k}}(\mathbf{r})$ is periodic under lattice translation, i.e. $\psi_{\mathbf{k}}(\mathbf{r}+\mathbf{R}) = \exp(i\mathbf{k}\cdot\mathbf{R})\psi_{\mathbf{k}}(\mathbf{r})$ should hold.

This equation imposes a condition on when one can safely use the tight-binding approximation, namely for the integral to yield zero, the functions must have nodes. When the Wannier functions overlap with each other, electrons can hop. It is important to note at this point that Wannier functions are not eigenfunctions of the Hamiltonian and do not form an eigenbasis for the system. However, because the functions are so localized, they form a good basis to work with.

As discussed previously, three of the four valence electrons of carbon form σ bonds that bind the carbon atoms together in the honeycomb lattice. They do not play a role in the electronic properties exhibited by graphene. The π electrons are responsible for the low-energy excitations, whereas the σ electrons form bonds far away from the Fermi energy. This is why only the π electrons are included in the calculation to find the energy bands of graphene, following the example of Wallace. As explained before, p_z orbitals can be described perfectly using the tight-binding approximation. Therefore, tight-binding is a suitable model for finding the energy bands in graphene.

3.3.2 Tight-Binding Applied to Graphene in Second Quantized Language

In the tight-binding model described in this Section, it is assumed that electrons can hop to their nearest neighbor (between different sublattices) and next-nearest neighbor (within the same sublattice). The hopping is facilitated by overlapping orbital functions. Possible hopping to sites further away is not taken into account because the overlap between the orbitals is negligible. The Hamiltonian (with $\hbar = 1$) reads

$$H = -t \sum_{\langle i,j\rangle,\sigma} \left(a^\dagger_{\sigma,i} b_{\sigma,j} + h.c. \right) - t' \sum_{\langle\langle i,j\rangle\rangle,\sigma} \left(a^\dagger_{\sigma,i} a_{\sigma,j} + b^\dagger_{\sigma,i} b_{\sigma,j} + h.c. \right) \tag{3.9}$$

where $a_{i,\sigma}$ ($b_{i,\sigma}$) annihilates an electron with spin projection $\sigma = \uparrow, \downarrow$, and $a^\dagger_{i,\sigma}$ ($b^\dagger_{i,\sigma}$) creates the corresponding electron on site $\mathbf{R}_i$ on sublattice A (B) [32]. The sum in the first term runs over all nearest-neighbor sites $\langle i, j\rangle$, whereas the sum in the second term is over all next-nearest-neighbor sites $\langle\langle i, j\rangle\rangle$. The corresponding hopping parameters are $t \approx 2.8$ eV and t', respectively. The value of t' is not well-known. Calculations have shown it to be between $0.02t$ and $0.2t$ [32]. However, the sign of t' relative to t is debated. This issue is addressed in App. 6.2.1.

The energy bands describing the electron state in the system can be derived from this Hamiltonian. To find the bands, it is easier to treat the nearest-neighbor and next-nearest-neighbor terms in the Hamiltonian separately. First, the operators are Fourier transformed according to

$$a_n = \frac{1}{\sqrt{N}} \sum_{\mathbf{k}} \mathrm{e}^{-i\mathbf{k}\cdot\mathbf{R}_n} a(\mathbf{k}), \quad b_n = \frac{1}{\sqrt{N}} \sum_{\mathbf{k}} \mathrm{e}^{-i\mathbf{k}\cdot\mathbf{R}_n} b(\mathbf{k}), \tag{3.10}$$

where N is the number of atoms in each sublattice. Diagonalizing the Fourier transformed Hamiltonian and solving the Schrödinger equation then allows one to find the energy bands. They are

$$E_\pm(\mathbf{k}) = \pm t\sqrt{3 + f(\mathbf{k})} - t' f(\mathbf{k}), \tag{3.11}$$

with

$$f(\mathbf{k}) = 2\cos\left(k_{\mathbf{y}}\sqrt{3}a\right) + 4\cos\left(k_{\mathbf{x}}\frac{3a}{2}\right)\cos\left(k_{\mathbf{y}}\frac{\sqrt{3}a}{2}\right). \tag{3.12}$$

The derivation of these bands can be found in App. 6.2.2. The plus corresponds to the upper (π) band, the electron band, and the minus to the lower (π^*) band, the hole band [32]. Eq. (3.12) is symmetric such that, if $t' = 0$, the energy in Eq. (3.11) is symmetric around zero. However, if t' is finite, the electron-hole symmetry is broken and as a result the π and π^* bands will become asymmetric.

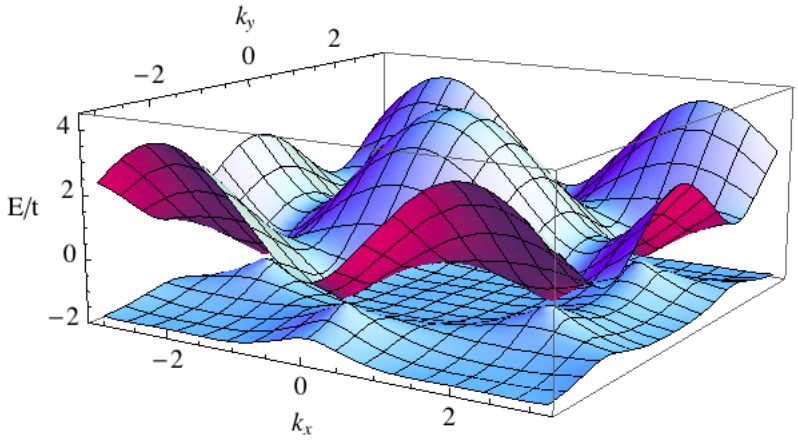

Figure 3.5: The energy-band structure of graphene with E in units of t, for $t' = -0.2t$ and the lattice spacing $a = 1$.

In Fig. 3.5, the full band structure of graphene with t and t' is shown.[6] The bands touch at the K and K' points forming Dirac cones, hence the name Dirac points. There are six Dirac cones, but only two of them are inequivalent, because vectors of the reciprocal lattice can connect the others. One Dirac cone is divided over three Brillouin zones, so there are exactly two inequivalent Dirac cones in one Brillouin zone.

The dispersion at the Dirac point can be found by expanding the band structure close to the $\mathbf{K}$ (or $\mathbf{K}'$) vector as $\mathbf{k} = \mathbf{K} + \mathbf{q}$ with $|\mathbf{q}| \ll |\mathbf{K}|$. Putting $t' = 0$ yields

$$E_{\pm}(\mathbf{K} + \mathbf{q}) = \pm v_F|\mathbf{q}| + \mathcal{O}\left[(\mathbf{q}/\mathbf{K})^2\right]. \tag{3.13}$$

The dispersion is derived in App. 6.2.3. The momentum $\mathbf{q}$ is measured relatively to the Dirac points and v_F is the Fermi velocity, $v_F = 3at/2 \approx 1 \times 10^6$ m/s. This is a remarkable outcome. Normally, one finds $\epsilon(\mathbf{q}) = \mathbf{q}^2/2m$ where m is the mass of the electron such that the velocity is $v = k/m = \sqrt{E/m}$ [32]. However, in the result obtained in Eq. (3.13) the Fermi velocity depends on neither the energy nor the momentum. Expanding the spectrum up to second order in $(\mathbf{q}/\mathbf{K})$ and including t' yields

$$E_{\pm}(\mathbf{K} + \mathbf{q}) = 3t' \pm v_F|\mathbf{q}| - \left[\frac{9t'a^2}{4} \pm \frac{3ta^2}{8}\sin(3\theta_{\mathbf{q}})\right]|\mathbf{q}|^2 + \mathcal{O}\left[(\mathbf{q}/\mathbf{K})^3\right] \tag{3.14}$$

[6]Note here the discrepancy with the statement made before where t' was attributed a positive sign with respect to t, whereas now t' has a negative sign in terms of t to find the energy bands.

with

$$\theta_{\mathbf{q}} = \arctan\left(\frac{q_x}{q_y}\right) \tag{3.15}$$

the angle in momentum space. The derivation of this dispersion relation can be found in App. 6.2.4. The dispersion in Eq. (3.14) depends on the direction of the momentum and is threefold symmetric [32].

The energy dispersion in Eq. (3.13) has the form of the energy of ultrarelativistic particles, $E = c\,p$. Quantum-mechanically such particles are described by the massless Dirac equation. Therefore, it can be concluded from Eq. (3.13) that the low-energy excitations in graphene are massless Dirac fermions.

3.4 Cyclotron Mass

In the previous Section, it was derived from theory that the dispersion relation of graphene is linear, which means that the excitations in the system are massless Dirac fermions. In this Section, support for this conclusion will be given by studying the cyclotron mass. This quantity can be measured experimentally and used to calculate other physical quantities, such as the Fermi velocity. The specific shape of the dispersion relation found in Eq. (3.13) should lead to a cyclotron mass which depends on the square root of the electronic density [32]. In the semiclassical approximation, the cyclotron mass is defined as

$$m^* = \frac{1}{2\pi}\left[\frac{\partial \mathcal{A}(E)}{\partial E}\right]_{E=E_F},$$

where $\mathcal{A}(E)$ is the area in k space given by $\mathcal{A}(E) = \pi q(E)^2$. $q(E)$ can be found by rewriting Eq. (3.13), so that the area is

$$\mathcal{A}(E) = \pi\frac{E^2}{v_F^2}.$$

The cyclotron mass is then

$$m^* = \frac{E_F}{v_F^2} = \frac{k_F}{v_F}.$$

This can be expressed in terms of the electronic density n using that $k_F^2/\pi = n$

$$m^* = \frac{\sqrt{n\pi}}{v_F}. \tag{3.16}$$

Hence, the cyclotron mass indeed depends on the square root of the electronic density. Eq. (3.16) can be fitted to experimental data to find an approximation of the Fermi velocity $v_F \approx 10^6$ m/s and the hopping energy $t \approx 3$ eV [32]. The experimental confirmation of the dependence of the cyclotron mass on $\sqrt{n}$ can be seen as evidence for the existence of massless Dirac quasiparticles in graphene, as opposed to the common parabolic Schrödinger dispersion which produces a constant cyclotron mass.

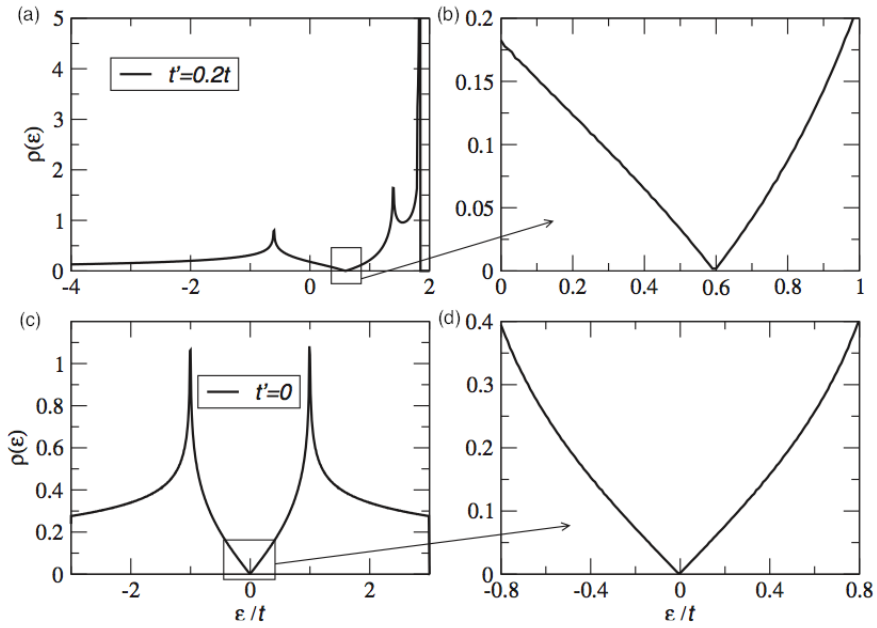

Figure 3.6: The density of states of graphene per unit cell given as function of energy in units of t. (a) and (b) $t' = 0.2\,t$. (c) and (d) $t' = 0$. (b) and (d) show a zoom-in on the density of states near the neutrality point of one electron per site. At $t' = 0$, the electron-hole symmetry is clearly visible. Figure from Ref. [32].

3.5 Density of States

The density of states is derived from the Hamiltonian in Eq. (3.9) and shown in Fig. 3.6. In both cases, for $t' = 0$ and for $t' \neq 0$, the density of states shows semimetallic behavior [32]. Considering only nearest-neighbor hopping, i.e. $t' = 0$, allows for the derivation of an analytical expression of the density of states per unit cell [32]. Using the energy dispersion in Eq. (3.11), one can compute the retarded Green's function, $G_{\mathrm{ret}} = E - \hat{H}(\mathbf{k}) + i\delta$ (with $\delta > 0$ to make sure the Green's function is retarded), and use this to find the density of states according to

$$\rho(E) = -\frac{1}{\pi}\mathrm{Im}\,\mathrm{Tr}\,(G_{\mathrm{ret}})^{-1}\,.$$

Computing the trace leads to the following result

$$\rho(E) = \frac{4}{\pi^2}\frac{|E|}{t^2}\frac{1}{\sqrt{Z_0}}\mathbf{F}\left(\frac{\pi}{2}, \sqrt{\frac{Z_1}{Z_0}}\right) \tag{3.17}$$

with

$$Z_0 = \begin{cases} \left(1 + \left|\frac{E}{t}\right|\right)^2 - \frac{[(E/t)^2-1]^2}{4}, & |E| \leq t, \\ 4\left|\frac{E}{t}\right|, & t \leq |E| \leq 3t, \end{cases}$$

and

$$Z_1 = \begin{cases} 4\left|\frac{E}{t}\right|, & |E| \leq t, \\ \left(1 + \left|\frac{E}{t}\right|\right)^2 - \frac{[(E/t)^2-1]^2}{4}, & t \leq |E| \leq 3t, \end{cases}$$

where

$$\mathbf{F}\left(\frac{\pi}{2}, k\right) = \int_0^{\pi/2} \frac{\mathrm{d}\theta}{\sqrt{1 - k^2 \sin^2\theta}} \tag{3.18}$$

is the complete elliptical integral of the first kind. The density of states per unit cell near the Dirac point can be found using the dispersion in Eq. (3.13) and leads to a much simpler expression

$$\rho(E) = \frac{2\mathcal{A}}{\pi}\frac{|E|}{v_F^2} \tag{3.19}$$

where $\mathcal{A}$ is the area of the unit cell $\mathcal{A} = 3\sqrt{3}a^2/2$. The derivation for both, the density of states in the system and the density of states near the Dirac points can be found in App. 6.2.5.

3.6 Effective Dirac Hamiltonian

Considering only nearest-neighbor hopping ($t' = 0$), the Hamiltonian for graphene can be written as an effective Hamiltonian resembling the massless Dirac-like Hamiltonian. Rewriting the Hamiltonian in Eq. (3.9) in terms of the Fourier transform of the operators as in Eq. (3.10), and expanding around the K and K' points as before, i.e. $\mathbf{k} = \mathbf{K} + \mathbf{q}$, leads to the following effective Hamiltonian

$$\begin{aligned}
&H \approx \\
&-\frac{t}{4}\int \mathrm{d}x\mathrm{d}y\, \Big\{\psi_1^\dagger \left[\begin{pmatrix} 0 & 3a\left(1-i\sqrt{3}\right) \\ -3a\left(1+i\sqrt{3}\right) & 0 \end{pmatrix}\partial_{\mathbf{x}} + \begin{pmatrix} 0 & 3a\left(-\sqrt{3}-i\right) \\ -3a\left(-\sqrt{3}+i\right) & 0 \end{pmatrix}\partial_{\mathbf{y}}\right]\psi_1 \\
&+\psi_2^\dagger \left[\begin{pmatrix} 0 & 3a\left(1+i\sqrt{3}\right) \\ -3a\left(1-i\sqrt{3}\right) & 0 \end{pmatrix}\partial_{\mathbf{x}} + \begin{pmatrix} 0 & 3a\left(-\sqrt{3}+i\right) \\ -3a\left(-\sqrt{3}-i\right) & 0 \end{pmatrix}\partial_{\mathbf{y}}\right]\psi_2\Big\} \\
&= -iv_F\int \mathrm{d}x\mathrm{d}y\left[\hat{\psi}_1^\dagger(\mathbf{r})\boldsymbol{\sigma}\cdot\nabla\hat{\psi}_1(\mathbf{r}) + \hat{\psi}_2^\dagger(\mathbf{r})\boldsymbol{\sigma}^*\cdot\nabla\hat{\psi}_2(\mathbf{r})\right],
\end{aligned} \tag{3.20}$$

with the Pauli matrices $\boldsymbol{\sigma} = (\sigma_x, \sigma_y)$, $\boldsymbol{\sigma}^* = (\sigma_x, -\sigma_y)$, and $\hat{\psi}_i^\dagger = (a_i^\dagger, b_i^\dagger)$ with $i = 1, 2$ where $i = 1$ ($i = 2$) refers to the K (K') point. The first (second) part of Eq. (3.20) represents the massless Dirac Hamiltonian around the K (K') point. Close to the K point, the two-component electron wavefunction $\psi(\mathbf{r})$ obeys the two-dimensional Dirac equation

$$-iv_F\boldsymbol{\sigma}\cdot\nabla\psi(\mathbf{r}) = E\,\psi(\mathbf{r}).$$

This wavefunction in momentum representation around $\mathbf{K}$ is

$$\psi_{\pm,\mathbf{K}}(\mathbf{k}) = \frac{1}{\sqrt{2}}\begin{pmatrix} \mathrm{e}^{-i\theta_{\mathbf{k}}/2} \\ \pm\mathrm{e}^{i\theta_{\mathbf{k}}/2} \end{pmatrix}$$

for $H_{\mathbf{K}} = v_F\boldsymbol{\sigma}\cdot\mathbf{k}$, where the $\pm$ correspond to the eigenenergies $E = \pm v_F k$, and $\theta_{\mathbf{k}}$ given by Eq. (3.15) [32]. Similarly, around the K' point the wavefunction is

$$\psi_{\pm,\mathbf{K}'}(\mathbf{k}) = \frac{1}{\sqrt{2}}\begin{pmatrix} \mathrm{e}^{i\theta_{\mathbf{k}}/2} \\ \pm\mathrm{e}^{-i\theta_{\mathbf{k}}/2} \end{pmatrix}$$

for $H_{\mathbf{K}'} = v_F\boldsymbol{\sigma}^*\cdot\mathbf{k}$. These two wavefunctions are connected through time-reversal symmetry. Taking point M in Fig. 3.1 as the origin of coordinates in momentum space, this symmetry is realized as a reflection over the x-axis, i.e. $(k_x, k_y) \to (k_x, -k_y)$. Rotating the phase θ by 2π changes the sign of the wavefunction. This means there is a phase of π which is called a Berry's

phase. This phase is topologically protected.[7] The sign change under rotation by π is typical for spinors.

The wavefunctions are the eigenfunctions of the helicity operator, which by definition is the projection of the momentum operator in the (pseudo)spin direction. The helicity operator is

$$\hat{h} = \frac{1}{2}\boldsymbol{\sigma} \cdot \frac{\mathbf{p}}{|\mathbf{p}|}. \tag{3.21}$$

$\psi_{\mathbf{K}}$ and $\psi_{\mathbf{K}'}$ are eigenstates of $\hat{h}$,

$$\hat{h}\psi_{\mathbf{K}}(\mathbf{r}) = \pm\frac{1}{2}\psi_{\mathbf{K}}(\mathbf{r}), \tag{3.22}$$

and the same for $\psi_{\mathbf{K}'}(\mathbf{r})$ with reversed sign. The plus sign corresponds to electrons and the minus sign to holes. The eigenvalue equation also shows that the eigenvalues of $\boldsymbol{\sigma}$ are either in the direction of the momentum ($\uparrow$) or in the opposite direction ($\downarrow$). This means that the states of the system have a well-defined chirality or helicity. The values of the helicity are good quantum numbers as long as Eq. (3.20) holds [32]. Consequently, the helicity is a good quantum number near the K and K' points. It loses this status when one moves away from these points or when t' becomes finite.

[7] The topological protection is a consequence of the specific shape of the Hamiltonian near the Dirac point. The Hamiltonian near K can be written as $H_K = \boldsymbol{\sigma} \cdot \mathbf{k}$ and describes a vortex. The wavefunction picks up a phase π when going around the vortex once.

Chapter 4

Superconductivity in Artificial Graphene

Superconductivity does not occur naturally in graphene. This is unfortunate because the relativistic quantum mechanics that govern the carbon system have interesting consequences for the physics of superconductivity that are worthwhile investigating, such as Andreev reflection [3]. Experiments using the proximity effect [15, 16] or doping [17] have shown that graphene is well-suited to support a supercurrent. Due to the ease with which the electronic properties of graphene can be altered, there is hope that the material may be tailored in such a way that it can be made intrinsically superconducting. However, such a discovery has not yet been made. Therefore, the realization of a Dirac superconductor has to come about using a different material with similar properties to graphene. This has led to the idea to study superconductivity in artificial graphene samples. The type of samples studied here are systems where nanocrystals with a truncated cubic shape are synthesized in honeycomb superlattices via self-assembly, as shown in Fig. 4.1 [18]. Boneschanscher et al. have experimentally realized these systems for rock-salt PbSe nanocrystals, which form honeycomb superlattices via the attachment of the {100} facet of the nanocrystal as shown in Fig. 4.2 with a lattice parameter of 6 nm [18]. This honeycomb superlattice has an octahedral symmetry that is buckled, which means that the nanocrystals occupy two parallel planes. Therefore, the superlattice resembles proposed atomic silicene honeycomb structures. Via cation exchange, the PbSe honeycomb superlattice was successfully transformed into a honeycomb superlattice composed of zinc-blende CdSe nanocrystals with a lattice parameter of 6 nm. This preservation of the lattice structure during this transformation is a sign of the robustness of the honeycomb geometry. The sheets produced have a size of over a hundred unit cells, which suggests that the nanocrystals attach from a preordered state. What drives the attachment into this specific geometry is not known, especially because more often than not the nanocrsytals self-assemble into square superlattices [37]. The energy spectrum of PbSe and CdSe honeycomb superlattices as well as of HgTe nanocrystals assembled in a honeycomb superlattice has been described theoretically and the presence of Dirac cones therein reflects the graphene-like nature of these materials [19, 20]. In this Chapter, the possibility of phonon-mediated superconductivity in a system of CdSe nanocrystals posited in a graphene-like structure is investigated.

To be able to find the energy bands of this specific system, Kalesaki et al. used an atomistic tight-binding method, where each atom in the lattice is described by a double set of $sp^3d^5s^*$ atomic orbitals including the spin degree of freedom [19]. The system was made of up to 6×10^4 atoms and 1.2×10^6 atomic orbitals. They used these results to compute the energy bands for

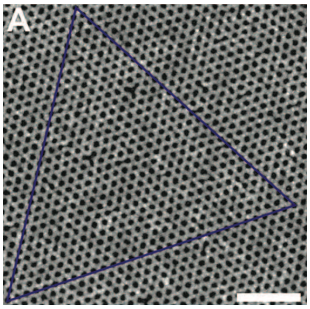

Figure 4.1: HAADF-STEM image of a honeycomb superlattice of nanocrystals. The scale bar is 50 nm. Figure from Ref [18].

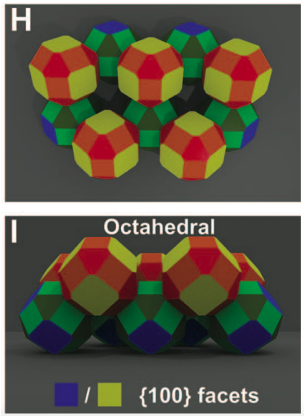

Figure 4.2: Nanocrystals with a truncated cubic shape attached via the {100} facet to form a honeycomb superlattice. Figure from Ref [18].

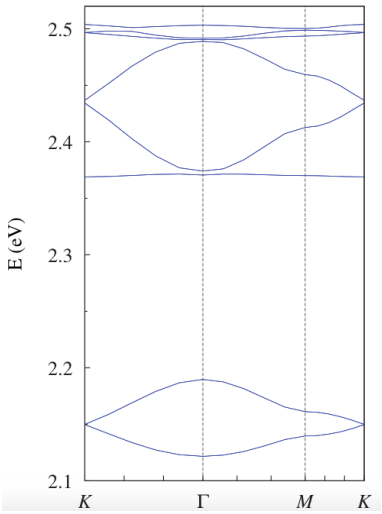

Figure 4.3: Conduction bands for CdSe nanocrystals arranged in a honeycomb superlattice. A Dirac cone appears at the s and p-like bands. Figure from Ref [20].

the graphene-like system. Just as in graphene, they find that there are Dirac cones at the K and K' points shown in Fig. 4.3. In the Figure, there are two well-separated sets of two and six bands. The lowest two bands correspond to the π and π^* bands in actual graphene and they are s-wave like [19]. The second set of bands are p-wave like and the Dirac cone is in fact made up of a superposition of p_x and p_y-bands. Each band is spin degenerate, hence actually there are 4 and 12 bands.

In Section 4.1, it will be explained that the system is described through an effective model where one nanocrystal is modeled as a superatom. The effective phonon of a single CdSe nanocrystal is the longitudinal optical one [21]. Optical phonons are gapped and for simplicity, it is assumed that there is one Einstein phonon per superatom site. Only the effective s-like electrons close to the lowest Dirac point shown in Fig. 4.3 are considered. It is assumed that a phonon can couple to electrons on-site and at nearest-neighbor sites. The system is described by a tight-binding Hamiltonian, which includes the chemical potential, electron-phonon coupling, nearest-neighbor hopping, and Hubbard terms for electron-pairing on-site and between nearest neighbors. In Section 4.2, a path-integral approach will be employed to integrate out the phonons to obtain the effective interaction. In case of a negative value for this interaction, the electrons will repell each other and the system is not superconducting. If this interaction is positive, the electrons will attract each other. A numerical analysis by the group of Prof. C. Delerue (Lille, France) allows for the determination of a value for this effective interaction. Order parameters for the on-site Cooper pairs and Cooper pairs between nearest-neighbor sites will be defined in Section 4.3 to be able to decouple the electron fields. For the nearest-neighbor interaction, the competition between the hidden order [4] and the Kekule order [5] will be studied extensively. Next, in Section 4.4, the Hamiltonians will be expanded around the Dirac points and written in Dirac-Nambu representation. To ensure that the Dirac description is valid, the Fermi level cannot move away too far from the Dirac points.

Then, by employing a mean-field approximation, the ground-state energy, gap equations at zero and finite temperature, and the critical temperatures will be obtained in Section 4.5.

4.1 Model

To describe superconductivity in this system, a model is used in which one nanocrystal is described as one superatom. Only the effective s-like electrons are considered such that there is no orbital degree of freedom. This results in a system that can be described using the same tight-binding approach as in graphene. It is known from the literature that in CdSe quantum dots the longitudinal optical phonon is dominant and it is assumed that this is also the case for its nanocrystals [21]. Therefore, only this phonon is considered and treated as local. Moreover, an optical phonon has a constant frequency, and it can thus be described by an Einstein mode ω_E. The phonon couples to the effective s-like electrons on the nanocrystals, which is justified by Schluter et al. [38]. Within BCS theory, phonons only couple to electrons at the Fermi level. Therefore, to build a Dirac superconductor, the Fermi level should remain sufficiently close to the Dirac points to ensure the validity of the linear description of the fermions. This means that the chemical potential, which raises and lowers the Fermi level in the system, cannot be larger than half of the nearest-neighbor hopping parameter t according to $\mu \leq 0.5t$, where $t \approx -11\,\mathrm{meV}$ in the CdSe honeycomb superlattice [19]. The complete system can now be referred to as a graphene superstructure build up of superatoms with one phonon living on each site coupling to effective s-like electrons.

The system is described using a tight-binding Hamiltonian, which consists of a Hubbard Hamiltonian including nearest-neighbor hopping and on-site and nearest-neighbor site electron-electron interactions, a Hamiltonian for the chemical potential and an electron-phonon Hamiltonian, which couples the phonons to on-site and nearest-neighbor site electrons. The following Hubbard Hamiltonian H_{Hub} is considered

$$\begin{aligned} H_{\mathrm{Hub}} &= -t \sum_{\langle i,j\rangle,\sigma} \left(a^\dagger_{i,\sigma} b_{j,\sigma} + b^\dagger_{j,\sigma} a_{i,\sigma} \right) + U \sum_i \left(a^\dagger_{i,\uparrow} a^\dagger_{i,\downarrow} a_{i,\downarrow} a_{i,\uparrow} + b^\dagger_{i,\uparrow} b^\dagger_{i,\downarrow} b_{i,\downarrow} b_{i,\uparrow} \right) \\ &\quad + V \sum_{\langle i,j\rangle;\sigma,\sigma'} a^\dagger_{i,\sigma} a_{i,\sigma} b^\dagger_{j,\sigma'} b_{j,\sigma'}, \end{aligned} \tag{4.1}$$

where $\sum_{\langle i,j\rangle}$ indicates that the sum in the first and last term runs over nearest-neighbor sites, $a^\dagger_{i,\sigma}$ ($a_{i,\sigma}$) is a creation (annihilation) operator of an electron on sublattice A at site i with spin σ, $t \approx -11\,\mathrm{meV}$ is the nearest-neighbor hopping parameter, and U and V are the on-site and the nearest-neighbor Coulomb interactions, respectively. The Hamiltonian for the chemical potential H_μ reads

$$H_\mu = -\mu \sum_{i,\sigma} \left(a^\dagger_{i,\sigma} a_{i,\sigma} + b^\dagger_{i,\sigma} b_{i,\sigma} \right). \tag{4.2}$$

The electron-phonon Hamiltonian $H_{\mathrm{el-ph}}$ is defined using that the phonon couples to electrons on-site and between nearest-neighbor sites. This means that a phonon on sublattice A couples to electrons on sublattices A and B, and likewise for a phonon on sublattice B. The phonon frequency for phonons on sublattices A and B is equal and given by the einstein mode ω_E. This

yields the following for the electron-phonon Hamiltonian $H_{\text{el}-\text{ph}}$

$$\begin{aligned} H_{\text{el}-\text{ph}} &= \hbar\omega_E \sum_i c^\dagger_{A,i} c_{A,i} + \sum_{i,j;\sigma} \left[V(\mathbf{r}_i - \mathbf{r}_j)\, a^\dagger_{\mathbf{r}_i,\sigma} a_{\mathbf{r}_i,\sigma} + \tilde{V}(\mathbf{r}_i - \mathbf{r}_j)\, b^\dagger_{\mathbf{r}_i,\sigma} b_{\mathbf{r}_i,\sigma} \right] \left(c^\dagger_{A,\mathbf{r}_j} + c_{A,\mathbf{r}_j} \right) \\ &\quad + A \leftrightarrow B, \end{aligned} \tag{4.3}$$

where $c^\dagger_{A,i}$ ($c_{A,i}$) creates (annihilates) a phonon on sublattice A at site i and where

$$V(\mathbf{r}_i - \mathbf{r}_j) = V_0\, \delta_{\mathbf{r}_i,\mathbf{r}_j}, \quad \text{and} \quad \tilde{V}(\mathbf{r}_i - \mathbf{r}_j) = \tilde{V}_0 \sum_\alpha \delta_{\mathbf{r}_i,\mathbf{r}_j - \boldsymbol{\delta}_\alpha},$$

with V_0 and $\tilde{V}_0$ some constants.

4.2 Effective Electron-Electron Interaction

To be able to determine whether the system can enter a superconducting phase, the effective interaction between electrons needs to be calculated. If this effective interaction is attractive, Cooper pairs can form and the system is superconducting. If the interaction is repulsive, superconductivity is not possible. To determine this effective interaction, the phonons need to be integrated out from Eq. (4.3) after which the Coulomb terms U and V in Eq. (4.1) can be renormalized. To integrate out the phonons, one uses a path-integral formalism

$$\mathcal{Z} = \int \mathcal{D}\left[\psi^\dagger, \psi\right] \int \mathcal{D}\left[\phi^\dagger, \phi\right] \mathrm{e}^{-\frac{1}{\hbar\beta} S\left[\psi^\dagger,\psi;\phi^\dagger,\phi\right]}, \tag{4.4}$$

where ψ is an electron field and ϕ a boson field and the action $S\left[\psi^\dagger, \psi; \phi^\dagger, \phi\right]$ is defined as

$$S\left[\psi^\dagger, \psi; \phi^\dagger, \phi\right] = \int_0^{\hbar\beta} \mathrm{d}\tau \left[\psi^\dagger(\tau)\partial_\tau \psi(\tau) + \phi^\dagger(\tau)\partial_\tau \phi(\tau) + H\left(\psi^\dagger, \psi; \phi^\dagger, \phi\right) \right]. \tag{4.5}$$

To be able to rewrite a Hamiltonian into an action, the operators need to be replaced by fields. The following transformations are used

$$\begin{aligned} a_{\mathbf{k},\sigma} &\rightarrow \psi_{A,\mathbf{k},\sigma}(\tau) = \frac{1}{\sqrt{\hbar\beta}} \sum_n \psi_{A,\mathbf{k},\sigma,n} \mathrm{e}^{-i\omega_n \tau}, \\ c_{A,\mathbf{q}} &\rightarrow \phi_{A,\mathbf{q}}(\tau) = \frac{1}{\sqrt{\hbar\beta}} \sum_n \phi_{A,\mathbf{q},n} \mathrm{e}^{-i\hat{\omega}_n \tau}, \end{aligned}$$

where $\omega_n = (2n+1)\pi/(\hbar\beta)$ and $\hat{\omega}_n = 2n\pi/(\hbar\beta)$ for $n \in \mathbb{Z}$ are the Matsubara frequencies for fermions and bosons, respectively, and ϕ (ψ) obey the boson (fermion) (anti)commutation relations.

To use this procedure, the electron-phonon Hamiltonian $H_{\text{el}-\text{ph}}$ first has to be written in reciprocal space. The following transformation is used

$$\begin{aligned} a_{i,\sigma} &= \frac{1}{\sqrt{N}} \sum_{\mathbf{k}} a_{\mathbf{k},\sigma} \mathrm{e}^{i\mathbf{k}\cdot\mathbf{r}_i}, \quad b_{i,\sigma} = \frac{1}{\sqrt{N}} \sum_{\mathbf{k}} b_{\mathbf{k},\sigma} \mathrm{e}^{i\mathbf{k}\cdot\mathbf{r}_i}, \\ c_{A,i} &= \frac{1}{\sqrt{N}} \sum_{\mathbf{q}} c_{A,\mathbf{q}} \mathrm{e}^{i\mathbf{q}\cdot\mathbf{r}_i}, \quad c_{B,i} = \frac{1}{\sqrt{N}} \sum_{\mathbf{q}} c_{B,\mathbf{q}} \mathrm{e}^{i\mathbf{q}\cdot\mathbf{r}_i}, \end{aligned}$$

where $a^\dagger_{\mathbf{k},\sigma}$ ($a_{\mathbf{k},\sigma}$) creates (annihilates) an electron on sublattice A with momentum $\mathbf{k}$ and spin σ, $c^\dagger_{A,\mathbf{q}}$ ($c_{A,\mathbf{q}}$) creates (annihilates) a phonon with momentum $\mathbf{q}$ on sublattice A, $\mathbf{r}_i$ is the real space vector connecting sites and it is assumed that there are $2N$ atoms in the system. This yields the following

$$\begin{aligned} H_{\text{el-ph}} &= \hbar\omega_E \sum_{\mathbf{q}} c^\dagger_{A,\mathbf{q}} c_{A,\mathbf{q}} + \sum_{\mathbf{k},\mathbf{q},\sigma} \left[u_0\, a^\dagger_{\mathbf{k}+\mathbf{q},\sigma} a_{\mathbf{k},\sigma} + v(q)\, b^\dagger_{\mathbf{k}+\mathbf{q},\sigma} b_{\mathbf{k},\sigma} \right] \left(c^\dagger_{A,-\mathbf{q}} + c_{A,\mathbf{q}} \right) \\ &\quad + A \leftrightarrow B, \end{aligned} \tag{4.6}$$

where

$$u_0 \equiv \frac{V_0}{\sqrt{N}}, \qquad v(q) \equiv \frac{\tilde{V}_0}{\sqrt{N}} \gamma_{\mathbf{q}}, \tag{4.7}$$

with

$$\gamma_{\mathbf{k}} \equiv \sum_{\alpha=1,2,3} \mathrm{e}^{i\mathbf{k}\cdot\boldsymbol{\delta}_\alpha}, \tag{4.8}$$

where $\boldsymbol{\delta}_\alpha$ is the real-space vector connecting nearest-neighbor sites. Eq. (4.7) shows that the on-site coupling u_0 is independent of the phonon momentum $\mathbf{q}$, whereas the coupling between nearest-neighbor sites $v(q)$ is dependent on the momentum. Replacing the operators in Eq. (4.6) with fields leads to the electron-phonon Hamiltonian

$$\begin{aligned} &H_{\text{el-ph}} \left(\psi^\dagger, \psi; \phi^\dagger, \phi \right) = \hbar\omega_E \sum_{\mathbf{q}} \phi^\dagger_{A,\mathbf{q}}(\tau) \phi_{A,\mathbf{q}}(\tau) \\ &+ \sum_{\mathbf{k},\mathbf{q},\sigma} \left[u_0\, \psi^\dagger_{A,\mathbf{k}+\mathbf{q},\sigma}(\tau) \psi_{A,\mathbf{k},\sigma}(\tau) + v(q)\, \psi^\dagger_{B,\mathbf{k}+\mathbf{q},\sigma}(\tau) \psi_{B,\mathbf{k},\sigma}(\tau) \right] \left[\phi^\dagger_{A,-\mathbf{q}}(\tau) + \phi_{A,\mathbf{q}}(\tau) \right] \\ &+ A \leftrightarrow B. \end{aligned} \tag{4.9}$$

Plugging this into Eq. (4.5), expanding in terms of the Matsubara frequencies and solving the integral over τ leads to the electron-phonon action

$$\begin{aligned} &S_{\text{el-ph}} \left[\psi^\dagger, \psi; \phi^\dagger, \phi \right] = \sum_{\mathbf{q},n} \phi^\dagger_{A,\mathbf{q},n} \left(-i\hat{\omega}_n + \hbar\omega_E \right) \phi_{A,\mathbf{q},n} \\ &+ \frac{1}{\sqrt{\hbar\beta}} \sum_{\mathbf{q},\sigma,n} \left[\left(u_0\, \rho_{A,\mathbf{q},\sigma,n} + v(q)\, \rho_{B,\mathbf{q},\sigma,n} \right) \phi^\dagger_{A,-\mathbf{q},-n} + \left(u_0\, \rho_{A,\mathbf{q},\sigma,n} + v(q)\, \rho_{B,\mathbf{q},\sigma,n} \right) \phi_{A,\mathbf{q},n} \right] \\ &+ A \leftrightarrow B, \end{aligned} \tag{4.10}$$

where the following definition for the density of electrons on sublattice A is used

$$\rho_{A,\mathbf{q},\sigma,n} \equiv \sum_{\mathbf{k},m} \psi^\dagger_{A,\mathbf{k}+\mathbf{q},\sigma,m+n} \psi_{A,\mathbf{k},\sigma,m}. \tag{4.11}$$

The explicit derivation of the electron-phonon action can be found in App. 6.3.1. To be able

to integrate out the phonons, the square needs to be completed. This yields

$$
\begin{aligned}
&S\left[\psi^\dagger,\psi;\phi^\dagger,\phi\right]\\
&=\sum_{\mathbf{q},n}\left(-i\hat{\omega}_n+\hbar\omega_E\right)\left[\phi^\dagger_{A,\mathbf{q},n}+\frac{1}{\sqrt{\hbar\beta}}\frac{1}{-i\hat{\omega}_n+\hbar\omega_E}\sum_\sigma\left(u_0\,\rho_{A,\mathbf{q},\sigma,n}+v(q)\,\rho_{B,\mathbf{q},\sigma,n}\right)\right]\\
&\times\left[\phi_{A,\mathbf{q},n}+\frac{1}{\sqrt{\hbar\beta}}\frac{1}{-i\hat{\omega}_n+\hbar\omega_E}\sum_{\sigma'}\left(u_0\,\rho_{A,-\mathbf{q},\sigma',-n}+v(-q)\,\rho_{B,-\mathbf{q},\sigma',-n}\right)\right]\\
&-\frac{1}{\hbar\beta}\sum_{\mathbf{q},\sigma,\sigma',n}\frac{1}{-i\hat{\omega}_n+\hbar\omega_E}\left(u_0\,\rho_{A,\mathbf{q},\sigma,n}+v(q)\,\rho_{B,\mathbf{q},\sigma,n}\right)\left(u_0\,\rho_{A,-\mathbf{q},\sigma',-n}+v(-q)\,\rho_{B,-\mathbf{q},\sigma',-n}\right)\\
&+A\leftrightarrow B.
\end{aligned}
\tag{4.12}
$$

Now, the phonons can be eliminated by integrating them out. The result reads

$$
\mathcal{Z}=\int\mathcal{D}\left[\psi^\dagger,\psi\right]\int\mathcal{D}\left[\phi^\dagger,\phi\right]\mathrm{e}^{-\frac{1}{\hbar\beta}\left(S_{\mathrm{el}}\left[\psi^\dagger,\psi\right]+S_{\mathrm{el-ph}}\left[\psi^\dagger,\psi;\phi^\dagger,\phi\right]\right)}=\int\mathcal{D}\left[\psi^\dagger,\psi\right]\mathrm{e}^{-\frac{1}{\hbar\beta}S_{\mathrm{eff}}\left[\psi^\dagger,\psi\right]},
$$

where

$$
S_{\mathrm{eff}}\left[\psi^\dagger,\psi\right]=S_{\mathrm{el}}\left[\psi^\dagger,\psi\right]-\frac{1}{\hbar\beta}\sum_{\mathbf{q},\sigma,\sigma',n}\frac{1}{-i\hat{\omega}_n+\hbar\omega_E}\left(S_{\mathrm{eff},A}\left[\psi^\dagger,\psi\right]+A\leftrightarrow B\right),
$$

with

$$
S_{\mathrm{eff},A}\left[\psi^\dagger,\psi\right]=\left(u_0\,\rho_{A,\mathbf{q},\sigma,n}+v(q)\,\rho_{B,\mathbf{q},\sigma,n}\right)\left(u_0\,\rho_{A,-\mathbf{q},\sigma',-n}+v(-q)\,\rho_{B,-\mathbf{q},\sigma',-n}\right).
$$

The elimination of the phonons is done explicitly in App. 6.3.1. Rewriting according to

$$
\sum_n\frac{1}{-i\hat{\omega}_n+\hbar\omega_E}\frac{i\hat{\omega}_n+\hbar\omega_E}{i\hat{\omega}_n+\hbar\omega_E}=\sum_n\frac{i\hat{\omega}_n+\hbar\omega_E}{\hat{\omega}_n^2+(\hbar\omega_E)^2}=\sum_n\frac{\hbar\omega_E}{\hat{\omega}_n^2+(\hbar\omega_E)^2},
$$

where $i\hat{\omega}_n$ disappears in the numerator because the function is symmetric in n, leads to the final result

$$
S_{\mathrm{eff}}\left[\psi^\dagger,\psi\right]=S_{\mathrm{el}}\left[\psi^\dagger,\psi\right]-\frac{1}{\hbar\beta}\sum_{\mathbf{q},\sigma,\sigma',n}\frac{\hbar\omega_E}{\hat{\omega}_n^2+(\hbar\omega_E)^2}\left(S_{\mathrm{eff},A}\left[\psi^\dagger,\psi\right]+A\leftrightarrow B\right),
\tag{4.13}
$$

with

$$
S_{\mathrm{eff},A}\left[\psi^\dagger,\psi\right]=\left(u_0\,\rho_{A,\mathbf{q},\sigma,n}+v(q)\,\rho_{B,\mathbf{q},\sigma,n}\right)\left(u_0\,\rho_{A,-\mathbf{q},\sigma',-n}+v(-q)\,\rho_{B,-\mathbf{q},\sigma',-n}\right).
\tag{4.14}
$$

To be able to renormalize the Coulomb interactions U and V, their respective Hamiltonians need to be written into an action. Transforming the U and V terms in Eq. (4.1) to reciprocal space leads to

$$
\begin{aligned}
H_{\mathrm{Hub},U,V} &= \frac{U}{N}\sum_{\mathbf{k},\mathbf{k}',\mathbf{q}}\left(a^\dagger_{\mathbf{k}-\mathbf{q},\uparrow}a^\dagger_{\mathbf{k}'+\mathbf{q},\downarrow}a_{\mathbf{k}',\downarrow}a_{\mathbf{k},\uparrow}+b^\dagger_{\mathbf{k}-\mathbf{q},\uparrow}b^\dagger_{\mathbf{k}'+\mathbf{q},\downarrow}b_{\mathbf{k}',\downarrow}b_{\mathbf{k},\uparrow}\right)\\
&\quad+\frac{V}{N}\sum_{\mathbf{k},\mathbf{k}',\mathbf{q}}\sum_{\sigma,\sigma'}\gamma_{\mathbf{q}}a^\dagger_{\mathbf{k}+\mathbf{q},\sigma}a_{\mathbf{k},\sigma}b^\dagger_{\mathbf{k}'-\mathbf{q},\sigma'}b_{\mathbf{k}',\sigma'},
\end{aligned}
\tag{4.15}
$$

where $\gamma_{\mathbf{k}}$ is given by Eq. (4.8). Replacing the operators by fields then yields the following action for the Hubbard U term

$$\begin{aligned} S_{\mathrm{Hub},U}\left[\psi_A^\dagger,\psi_A,\psi_B^\dagger,\psi_B\right] &= \frac{U}{N}\int_0^{\hbar\beta}\mathrm{d}\tau\sum_{\mathbf{k},\mathbf{k}',\mathbf{q}}\psi^\dagger_{A,\mathbf{k}-\mathbf{q},\uparrow}(\tau)\,\psi^\dagger_{A,\mathbf{k}'+\mathbf{q},\downarrow}(\tau)\,\psi_{A,\mathbf{k}',\downarrow}(\tau)\,\psi_{A,\mathbf{k},\uparrow}(\tau)+A\to B \\ &= \frac{1}{\hbar\beta}\frac{U}{N}\sum_{\mathbf{q},n}\left(\rho_{A,\mathbf{q},\downarrow,n}\rho_{A,-\mathbf{q},\uparrow,-n}+\rho_{B,\mathbf{q},\downarrow,n}\rho_{B,-\mathbf{q},\uparrow,-n}\right), \end{aligned} \tag{4.16}$$

and for the Hubbard V term one finds

$$\begin{aligned} S_{\mathrm{Hub},V}\left[\psi_A^\dagger,\psi_A,\psi_B^\dagger,\psi_B\right] &= \frac{V}{N}\int_0^{\hbar\beta}\mathrm{d}\tau\sum_{\mathbf{k},\mathbf{k}',\mathbf{q}}\sum_{\sigma,\sigma'}\gamma_{\mathbf{q}}\psi^\dagger_{A,\mathbf{k}+\mathbf{q},\sigma}(\tau)\,\psi_{A,\mathbf{k},\sigma}(\tau)\,\psi^\dagger_{B,\mathbf{k}'-\mathbf{q},\sigma'}(\tau)\,\psi^\dagger_{B,\mathbf{k}',\sigma'}(\tau) \\ &= \frac{1}{\hbar\beta}\frac{V}{N}\sum_{\mathbf{q},\sigma,\sigma',n}\gamma_{\mathbf{q}}\rho_{A,\mathbf{q},\sigma,n}\rho_{B,-\mathbf{q},\sigma',-n}. \end{aligned} \tag{4.17}$$

The details of this derivation can be found in App. 6.3.2.

Upon realizing that the electron dependence of Eqs. (4.13) and (4.14) corresponds to that of Eqs. (4.16) and (4.17), an effective electron-electron interaction term can be derived,

$$\begin{aligned} S_{\mathrm{eff},U,V}\left[\psi^\dagger,\psi\right] &= -\sum_{\mathbf{q},n}\tilde{U}(q)\left(\rho_{A,\mathbf{q},\downarrow,n}\rho_{A,-\mathbf{q},\uparrow,-n}+\rho_{B,\mathbf{q},\downarrow,n}\rho_{B,-\mathbf{q},\uparrow,-n}\right) \\ &\quad -\sum_{\mathbf{q};\sigma,\sigma';n}\tilde{V}(q)\rho_{A,\mathbf{q},\sigma,n}\rho_{B,-\mathbf{q},\sigma',-n}, \end{aligned} \tag{4.18}$$

where

$$\tilde{U}(q) = -\frac{1}{\hbar\beta}\left\{\frac{U}{N}-2\frac{\hbar\omega_E}{\hat{\omega}_n^2+(\hbar\omega_E)^2}\left[u_0^2+v(q)v(-q)\right]\right\}, \tag{4.19}$$

$$\tilde{V}(q) = -\frac{1}{\hbar\beta}\left\{\frac{V}{N}\gamma_{\mathbf{q}}-2\frac{\hbar\omega_E}{\hat{\omega}_n^2+(\hbar\omega_E)^2}\left[u_0v(-q)+u_0v(q)\right]\right\}. \tag{4.20}$$

The effective interactions $\tilde{U}(q)$ and $\tilde{V}(q)$ are defined with a minus sign, which means that for the electron interaction to be attractive these interactions must acquire a positive value.

The values for $\hbar\omega_E$, U, V, V_0 and $\tilde{V}_0$ have been calculated by Prof. C. Delerue (Lille, France), a collaborator of Prof. C. Morais Smith, using a static model. The following values were obtained

$$\begin{aligned} &\hbar\omega_E = 26\,\mathrm{meV}, \quad U = 469\,\mathrm{meV}, \quad V = 262\,\mathrm{meV}, \\ &V_0 = 31\,\mathrm{meV}, \quad \tilde{V}_0 = 8.5\,\mathrm{meV}. \end{aligned}$$

Writing Eq. (4.19) in terms of these parameters and plugging in their values yields

$$\tilde{U}(q) = -\frac{1}{\hbar\beta}\frac{1}{N}\left[U-\frac{2}{\hbar\omega_E}\left(V_0^2+9\tilde{V}_0^2\right)\right] \approx -\frac{1}{\hbar\beta}\frac{1}{N}345\,\mathrm{meV}, \tag{4.21}$$

where it was assumed that at finite temperature the zero mode of the Matsubara frequency is dominant and that

$$\mathrm{e}^{i\mathbf{q}\cdot\boldsymbol{\delta}_\alpha}\approx 1, \qquad \text{such that} \qquad \gamma_{\mathbf{q}}=\sum_\alpha \mathrm{e}^{i\mathbf{q}\cdot\boldsymbol{\delta}_\alpha}\approx 3.$$

For Eq. (4.20) the following is found

$$\tilde{V}(q) = -\frac{1}{\hbar\beta}\frac{1}{N}\left(3V - \frac{8}{\hbar\omega_E}V_0\tilde{V}_0\right) \approx -\frac{1}{\hbar\beta}\frac{1}{N}664\,\mathrm{meV}, \tag{4.22}$$

where the same approximation was used. Unfortunately, both values for $\tilde{U}(q)$ and $\tilde{V}(q)$ are negative, which means that the effective electron interaction for both on-site pairing and nearest-neighbor pairing is repulsive and no superconducting state in either can exist. However, the model introduced in this Chapter could also be used for other materials where the effective interaction could be positive. A good candidate is PbSe for which nanocrystals have also been synthesized in honeycomb superlattices and also there Dirac cones were discovered in the energy spectrum [19]. Moreover, the effective phonon here also is most like the longitudinal optical phonon. A numerical analysis by the group of Prof. C. Delerue will show whether a system PbSe nanocrystals in a honeycomb superstructure can indeed be superconducting.

4.3 Order Parameters and Mean Field Approximation

In this Section, order parameters are defined such that a mean-field approximation can be performed to decouple the electron-electron interaction in the effective action in Eq. (4.18). To be able to perform this procedure, the action will first be written back to a real-space Hamiltonian. Moreover, from now on it will be assumed that $\tilde{U}(q)$ and $\tilde{V}(q)$ have positive values such that they generate an attractive interaction between the electrons. Transforming back to real space, they are constants such that $\tilde{U}(q) \equiv \tilde{U}$ and $\tilde{V}(q) \equiv \tilde{V}$. This yields

$$H_{\text{eff,Hub}} = -\tilde{U}\sum_i \left(a^\dagger_{i,\downarrow}a_{i,\downarrow}a^\dagger_{i,\uparrow}a_{i,\uparrow} + b^\dagger_{i,\downarrow}b_{i,\downarrow}b^\dagger_{i,\uparrow}b_{i,\uparrow}\right) - \tilde{V}\sum_{\langle i,j\rangle}\sum_{\sigma,\sigma'} a^\dagger_{i,\sigma}b^\dagger_{j,\sigma'}b_{j,\sigma'}a_{i,\sigma}. \tag{4.23}$$

The following order parameters are defined for on-site pairing and nearest-neighbor pairing, respectively,

$$\Delta_0 = \langle a_{i,\downarrow}a_{i,\uparrow}\rangle = \langle b_{i,\downarrow}b_{i,\uparrow}\rangle\,, \tag{4.24}$$

$$\Delta_{\sigma',\sigma}\left(\mathbf{r}_i,\mathbf{r}_j\right) = \langle b_{j,\sigma'}a_{i,\sigma}\rangle\,, \tag{4.25}$$

where a very general form for the nearest-neighbor order parameter $\Delta_{\sigma',\sigma}\left(\mathbf{r}_i,\mathbf{r}_j\right)$ is assumed, which allows for different values of this order parameter depending on the spin of the electrons that are coupled.

To decouple the electron densities in the $\tilde{U}$ term in Eq. (4.23) the following mean-field approximation is used

$$a_{i,\downarrow}a_{i,\uparrow} \;=\; \langle a_{i,\downarrow}a_{i,\uparrow}\rangle + \delta\left(a_{i,\downarrow}a_{i,\uparrow}\right) = \Delta_0 + \delta\left(a_{i,\downarrow}a_{i,\uparrow}\right), \tag{4.26}$$

and the same for the b-operators. Plugging this into the first part of Eq. (4.23) and neglecting the term quadratic in fluctuations $\mathcal{O}\left(\delta^2\right)$ leads to

$$H_{\text{eff,Hub},U} = -\tilde{U}\sum_i\left[-2\left|\Delta_0\right|^2 + \Delta_0^\dagger\left(a_{i,\downarrow}a_{i,\uparrow} + b_{i,\downarrow}b_{i,\uparrow}\right) + \Delta_0\left(a^\dagger_{i,\uparrow}a^\dagger_{i,\downarrow} + b^\dagger_{i,\uparrow}b^\dagger_{i,\downarrow}\right)\right]. \tag{4.27}$$

For the $\tilde{V}$ term in Eq. (4.23), the mean-field approximation reads

$$b_{j,\sigma'}a_{i,\sigma} = \langle b_{j,\sigma'}a_{i,\sigma}\rangle + \delta\left(b_{j,\sigma'}a_{i,\sigma}\right) = \Delta_{\sigma',\sigma}\left(\mathbf{r}_j,\mathbf{r}_i\right) + \delta\left(b_{j,\sigma'}a_{i,\sigma}\right). \tag{4.28}$$

Plugging this into the second part of Eq. (4.23) and again neglecting the term quadratic in fluctuations $\mathcal{O}\left(\delta^2\right)$ yields

$$H_{\text{eff,Hub},V} = -\tilde{V}\sum_{\langle i,j\rangle}\left(-\left|\Delta_{\sigma',\sigma}\left(\mathbf{r}_j,\mathbf{r}_i\right)\right|^2 + \Delta^{\dagger}_{\sigma,\sigma'}\left(\mathbf{r}_i,\mathbf{r}_j\right)b_{j,\sigma'}a_{i,\sigma} + \Delta_{\sigma',\sigma}\left(\mathbf{r}_j,\mathbf{r}_i\right)a^{\dagger}_{i,\sigma}b^{\dagger}_{j,\sigma'}\right). \tag{4.29}$$

Therefore, after successfully decoupling the electron operators, the total real-space Hamiltonian describing the system reads

$$\begin{aligned} H_{\text{tot}} \;=\; & -t\sum_{\langle i,j\rangle,\sigma}\left(a^{\dagger}_{i,\sigma}b_{j,\sigma} + b^{\dagger}_{j,\sigma}a_{i,\sigma}\right) - \mu\sum_{i,\sigma}\left(a^{\dagger}_{i,\sigma}a_{i,\sigma} + b^{\dagger}_{i,\sigma}b_{i,\sigma}\right) \\ & -\tilde{U}\sum_{\mathbf{k}}\left[-2\left|\Delta_0\right|^2 + \Delta^{\dagger}_0\left(a_{\mathbf{k},\downarrow}a_{-\mathbf{k},\uparrow} + b_{\mathbf{k},\downarrow}b_{-\mathbf{k},\uparrow}\right) + \Delta_0\left(a^{\dagger}_{-\mathbf{k},\uparrow}a^{\dagger}_{\mathbf{k},\downarrow} + b^{\dagger}_{-\mathbf{k},\uparrow}b^{\dagger}_{\mathbf{k},\downarrow}\right)\right] \\ & -\tilde{V}\sum_{\langle i,j\rangle}\left(-\left|\Delta_{\sigma',\sigma}\left(\mathbf{r}_j,\mathbf{r}_i\right)\right|^2 + \Delta^{\dagger}_{\sigma,\sigma'}\left(\mathbf{r}_i,\mathbf{r}_j\right)b_{j,\sigma'}a_{i,\sigma} + \Delta_{\sigma',\sigma}\left(\mathbf{r}_j,\mathbf{r}_i\right)a^{\dagger}_{i,\sigma}b^{\dagger}_{j,\sigma'}\right). \end{aligned} \tag{4.30}$$

4.4 Dirac-Nambu Representation

Now, the Hamiltonian in Eq. (4.30) will be transformed to reciprocal space, expanded around the Dirac points $\mathbf{K}$ and $\mathbf{K}'$, where $\mathbf{K}' = -\mathbf{K}$, and then, following the example of Ref. [5], compactified using

$$H = \frac{1}{2}\sum_{\mathbf{q}}\psi^{\dagger}\left(\mathbf{q}\right)M\psi\left(\mathbf{q}\right) + E_0, \tag{4.31}$$

where E_0 is the energy of the condensate, the 16-component Dirac-Nambu spinors $\Psi^{\dagger} = \left(\Psi^{\dagger}_p, \Psi^{\dagger}_h\right)$, with $\Psi^{\dagger}_p = \left(\Psi^{\dagger}_{p\uparrow}, \Psi^{\dagger}_{p\downarrow}\right)$ and $\Psi^{\dagger}_h = \left(\Psi^{\dagger}_{h\downarrow}, -\Psi^{\dagger}_{h\uparrow}\right)$ are given by

$$\Psi^{\dagger}_{p,\sigma}\left(\mathbf{q}\right) = \begin{pmatrix} a^{\dagger}_{\mathbf{K}+\mathbf{q},\sigma} & b^{\dagger}_{\mathbf{K}+\mathbf{q},\sigma} & a^{\dagger}_{-\mathbf{K}+\mathbf{q},\sigma} & b^{\dagger}_{-\mathbf{K}+\mathbf{q},\sigma}\end{pmatrix}, \tag{4.32}$$

$$\Psi^{\dagger}_{h,\sigma}\left(\mathbf{q}\right) = \begin{pmatrix} b_{\mathbf{K}-\mathbf{q},\sigma} & a_{\mathbf{K}-\mathbf{q},\sigma} & b_{-\mathbf{K}-\mathbf{q},\sigma} & a_{-\mathbf{K}-\mathbf{q},\sigma}\end{pmatrix}, \tag{4.33}$$

and the matrix M is written in the following form

$$\Gamma_{ijk} = \tau_i \otimes \sigma_j \otimes \gamma_k, \tag{4.34}$$

where $i,j = 1,2,3$, $k = 0,1,2,3,5$, τ_i and σ_j are Pauli matrices

$$\tau_1 = \begin{pmatrix} 0 & 1 \\ 1 & 0\end{pmatrix}, \quad \tau_2 = \begin{pmatrix} 0 & -i \\ i & 0\end{pmatrix}, \quad \tau_3 = \begin{pmatrix} 1 & 0 \\ 0 & -1\end{pmatrix},$$

which act in the particle-hole space and spin space, respectively, and γ_k are the Dirac matrices given by

$$\begin{aligned} &\gamma_0 = \sigma_0 \otimes \sigma_3, \quad \gamma_1 = \sigma_3 \otimes \sigma_2, \quad \gamma_2 = \sigma_0 \otimes \sigma_1, \\ &\gamma_3 = \sigma_1 \otimes \sigma_2, \quad \gamma_5 = \sigma_2 \otimes \sigma_2, \end{aligned}$$

acting in the sublattice $\otimes$ valley space.

4.4.1 Dirac Hamiltonian

Transforming the Hamiltonian for the hopping parameter t to reciprocal space yields

$$H_t = -t \sum_{\mathbf{k},\sigma} \left(\gamma_{\mathbf{k}} a^\dagger_{\mathbf{k},\sigma} b_{\mathbf{k},\sigma} + \gamma^*_{\mathbf{k}} b^\dagger_{\mathbf{k},\sigma} a_{\mathbf{k},\sigma} \right),$$

where $\gamma_{\mathbf{k}}$ is given by Eq. (4.8). Expanding around the Dirac point using $\mathbf{k} = \pm\mathbf{K} + \mathbf{q}$, where $\mathbf{q}$ is small and making the particle and hole explicit leads to the following

$$\begin{aligned}
H_t &= -t \sum_{\mathbf{q},\sigma} \Big(\gamma_{\mathbf{K}+\mathbf{q}} a^\dagger_{\mathbf{K}+\mathbf{q},\sigma} b_{\mathbf{K}+\mathbf{q},\sigma} + \gamma^*_{\mathbf{K}+\mathbf{q}} b^\dagger_{\mathbf{K}+\mathbf{q},\sigma} a_{\mathbf{K}+\mathbf{q},\sigma} + \gamma_{-\mathbf{K}+\mathbf{q}} a^\dagger_{-\mathbf{K}+\mathbf{q},\sigma} b_{-\mathbf{K}+\mathbf{q},\sigma} \\
&+ \gamma^*_{-\mathbf{K}+\mathbf{q}} b^\dagger_{-\mathbf{K}+\mathbf{q},\sigma} a_{-\mathbf{K}+\mathbf{q},\sigma} \Big) \\
&= -\frac{v_F}{2} \sum_{\mathbf{q}} \Big(iq\, a^\dagger_{\mathbf{K}+\mathbf{q},\uparrow} b_{\mathbf{K}+\mathbf{q},\uparrow} - iq^*\, b^\dagger_{\mathbf{K}+\mathbf{q},\uparrow} a_{\mathbf{K}+\mathbf{q},\uparrow} + iq^*\, a^\dagger_{-\mathbf{K}+\mathbf{q},\uparrow} b_{-\mathbf{K}+\mathbf{q},\uparrow} - iq\, b^\dagger_{-\mathbf{K}+\mathbf{q},\uparrow} a_{-\mathbf{K}+\mathbf{q},\uparrow} \\
&+ iq\, a^\dagger_{\mathbf{K}+\mathbf{q},\downarrow} b_{\mathbf{K}+\mathbf{q},\downarrow} - iq^*\, b^\dagger_{\mathbf{K}+\mathbf{q},\downarrow} a_{\mathbf{K}+\mathbf{q},\downarrow} + iq^*\, a^\dagger_{-\mathbf{K}+\mathbf{q},\downarrow} b_{-\mathbf{K}+\mathbf{q},\downarrow} - iq\, b^\dagger_{-\mathbf{K}+\mathbf{q},\downarrow} a_{-\mathbf{K}+\mathbf{q},\downarrow} \Big) \\
&+ \frac{v_F}{2} \sum_{\mathbf{q}} \Big(iq\, a^\dagger_{\mathbf{K}-\mathbf{q},\uparrow} b_{\mathbf{K}-\mathbf{q},\uparrow} - iq^*\, b^\dagger_{\mathbf{K}-\mathbf{q},\uparrow} a_{\mathbf{K}-\mathbf{q},\uparrow} + iq^*\, a^\dagger_{-\mathbf{K}-\mathbf{q},\uparrow} b_{-\mathbf{K}-\mathbf{q},\uparrow} - iq\, b^\dagger_{-\mathbf{K}-\mathbf{q},\uparrow} a_{-\mathbf{K}-\mathbf{q},\uparrow} \\
&+ iq\, a^\dagger_{\mathbf{K}-\mathbf{q},\downarrow} b_{\mathbf{K}-\mathbf{q},\downarrow} - iq^*\, b^\dagger_{\mathbf{K}-\mathbf{q},\downarrow} a_{\mathbf{K}-\mathbf{q},\downarrow} + iq^*\, a^\dagger_{-\mathbf{K}-\mathbf{q},\downarrow} b_{-\mathbf{K}-\mathbf{q},\downarrow} - iq\, b^\dagger_{-\mathbf{K}-\mathbf{q},\downarrow} a_{-\mathbf{K}-\mathbf{q},\downarrow} \Big),
\end{aligned}$$

where $v_F = 3at/2$ and it is used that $\sum_\alpha \mathrm{e}^{i\mathbf{K}\cdot\boldsymbol{\delta}_\alpha} = 0$, $\sum_\alpha \mathrm{e}^{i\mathbf{q}\cdot\boldsymbol{\delta}_\alpha} \sim 1$, and

$$\sum_\alpha \mathrm{e}^{i(\mathbf{K}+\mathbf{q})\cdot\boldsymbol{\delta}_\alpha} = \frac{3ai}{4} q \left(1 + i\sqrt{3}\right) = \frac{3ai}{2} q \left(\frac{1+i\sqrt{3}}{2} \right) = \frac{3ai}{2} q\, \mathrm{e}^{i\pi/3} \to \frac{3ai}{2} q,$$

where q is rotated such that $q\,\mathrm{e}^{i\pi/3} \to q$ and $q = q_{\mathbf{x}} + iq_{\mathbf{y}}$. This also implies that

$$\sum_\alpha \mathrm{e}^{i(-\mathbf{K}+\mathbf{q})\cdot\boldsymbol{\delta}_\alpha} = \frac{3ai}{2} q^*, \quad \sum_\alpha \mathrm{e}^{-i(\mathbf{K}+\mathbf{q})\cdot\boldsymbol{\delta}_\alpha} = -\frac{3ai}{2} q^*, \quad \sum_\alpha \mathrm{e}^{-i(-\mathbf{K}+\mathbf{q})\cdot\boldsymbol{\delta}_\alpha} = -i\frac{3ai}{2} q.$$

Writing H_t in Dirac-Nambu representation neatly compactifies the expression

$$H_t = \frac{1}{2} \sum_{\mathbf{q}} \Psi^\dagger M_t \Psi, \quad \text{where} \quad M_t = v_F \tau_0 \otimes \sigma_0 \otimes \left(i\gamma_0\gamma_1 q_y - i\gamma_0\gamma_2 q_x \right). \tag{4.35}$$

This Hamiltonian is linear in momentum $\mathbf{q}$ and is referred to as the Dirac Hamiltonian.

4.4.2 Chemical Potential Hamiltonian

The Hamiltonian for chemical potential H_μ in reciprocal space reads

$$H_\mu = -\mu \sum_{\mathbf{k},\sigma} \left(a^\dagger_{\mathbf{k},\sigma} a_{\mathbf{k},\sigma} + b^\dagger_{\mathbf{k},\sigma} b_{\mathbf{k},\sigma} \right).$$

Expanding around the Dirac points yields

$$\begin{aligned} H_\mu &= -\frac{\mu}{2}\Big(a^\dagger_{\mathbf{K+q},\uparrow}a_{\mathbf{K+q},\uparrow} + b^\dagger_{\mathbf{K+q},\uparrow}b_{\mathbf{K+q},\uparrow} + a^\dagger_{-\mathbf{K+q},\uparrow}a_{-\mathbf{K+q},\uparrow} + b^\dagger_{-\mathbf{K+q},\uparrow}b_{-\mathbf{K+q},\uparrow} \\ &\quad + a^\dagger_{\mathbf{K+q},\downarrow}a_{\mathbf{K+q},\downarrow} + b^\dagger_{\mathbf{K+q},\downarrow}b_{\mathbf{K+q},\downarrow} + a^\dagger_{-\mathbf{K+q},\downarrow}a_{-\mathbf{K+q},\downarrow} + b^\dagger_{-\mathbf{K+q},\downarrow}b_{-\mathbf{K+q},\downarrow} \\ &\quad + a^\dagger_{\mathbf{K-q},\uparrow}a_{\mathbf{K-q},\uparrow} + b^\dagger_{\mathbf{K-q},\uparrow}b_{\mathbf{K-q},\uparrow} + a^\dagger_{-\mathbf{K-q},\uparrow}a_{-\mathbf{K-q},\uparrow} + b^\dagger_{-\mathbf{K-q},\uparrow}b_{-\mathbf{K-q},\uparrow} \\ &\quad + a^\dagger_{\mathbf{K-q},\downarrow}a_{\mathbf{K-q},\downarrow} + b^\dagger_{\mathbf{K-q},\downarrow}b_{\mathbf{K-q},\downarrow} + a^\dagger_{-\mathbf{K-q},\downarrow}a_{-\mathbf{K-q},\downarrow} + b^\dagger_{-\mathbf{K-q},\downarrow}b_{-\mathbf{K-q},\downarrow}\Big), \end{aligned}$$

such that in Dirac-Nambu representation this Hamiltonian reads

$$H_\mu = \frac{1}{2}\sum_{\mathbf{q}} \Psi^\dagger M_\mu \Psi, \quad \text{where} \quad M_\mu = -\mu\tau_3 \otimes \sigma_0 \otimes \mathbb{I}_{4\times 4}. \tag{4.36}$$

4.4.3 On-Site Pairing Hamiltonian

Transforming the term with the on-site order parameter Δ_0 to reciprocal space leads to

$$H_{\Delta_0} = -\tilde{U}\sum_{\mathbf{k}}\left[-2\left|\Delta_0\right|^2 + \Delta_0^\dagger\left(a_{\mathbf{k},\downarrow}a_{-\mathbf{k},\uparrow} + b_{\mathbf{k},\downarrow}b_{-\mathbf{k},\uparrow}\right) + \Delta_0\left(a^\dagger_{-\mathbf{k},\uparrow}a^\dagger_{\mathbf{k},\downarrow} + b^\dagger_{-\mathbf{k},\uparrow}b^\dagger_{\mathbf{k},\downarrow}\right)\right]. \tag{4.37}$$

Next, the momentum $\mathbf{k}$ is expanded around the Dirac point such that

$$\begin{aligned} H_{\Delta_0} &= -\frac{\tilde{U}}{2}\sum_{\mathbf{q}}\Big[-4\left|\Delta_0\right|^2 + \Delta_0^\dagger a_{\mathbf{K+q}\downarrow}a_{-\mathbf{K-q}\uparrow} + \Delta_0^\dagger a_{-\mathbf{K+q}\downarrow}a_{\mathbf{K-q}\uparrow} + \Delta_0 a^\dagger_{\mathbf{K+q}\uparrow}a^\dagger_{-\mathbf{K-q}\downarrow} \\ &\quad + \Delta_0 a^\dagger_{-\mathbf{K+q}\uparrow}a^\dagger_{\mathbf{K-q}\downarrow} + \Delta_0^\dagger a_{\mathbf{K-q}\downarrow}a_{-\mathbf{K+q}\uparrow} + \Delta_0^\dagger a_{-\mathbf{K-q}\downarrow}a_{\mathbf{K+q}\uparrow} + \Delta_0 a^\dagger_{\mathbf{K-q}\uparrow}a^\dagger_{-\mathbf{K+q}\downarrow} \\ &\quad + \Delta_0 a^\dagger_{-\mathbf{K-q}\uparrow}a^\dagger_{\mathbf{K+q}\downarrow} + a \to b\Big]. \end{aligned}$$

Writing this in Dirac-Nambu representation leads to

$$\begin{aligned} H_{\Delta_0} &= 4N\tilde{U}\left|\Delta_0\right|^2 + \frac{1}{2}\sum_{\mathbf{q}}\Psi^\dagger M_{\Delta_0}\Psi, \quad \text{where} \\ M_{\Delta_0} &= -\tilde{U}\left[\mathrm{Re}(\Delta_0)\tau_1 - \mathrm{Im}(\Delta_0)\tau_2\right]\otimes\sigma_0\otimes i\gamma_0\gamma_3, \end{aligned} \tag{4.38}$$

and it was used in the first term that $\sum_{\mathbf{q}} = 2N$ and $\Delta_0 = \mathrm{Re}(\Delta_0) + i\,\mathrm{Im}(\Delta_0)$. From this expression, it can be seen that Δ_0 indeed pairs on-site particles in opposite valleys and with opposite spin, as it should per definition.

4.4.4 Nearest-Neighbor Pairing Hamiltonian

For the nearest-neighbor pairing $\Delta_{\sigma',\sigma}(\mathbf{r}_j, \mathbf{r}_i)$, a slightly different route is taken. For the order parameter, the Kekule ansatz, as defined in Ref. [5], is applied. This ansatz transforms the real-space order parameter $\Delta_{\sigma',\sigma}(\mathbf{r}_j, \mathbf{r}_i)$ into a reciprocal-space order parameter close to the Dirac points. The ansatz is defined as

$$\Delta_{\sigma,\sigma;\alpha}(\mathbf{r}_i, \mathbf{r}_j) = \Delta_\sigma \cos\left(\mathbf{K}\cdot(\mathbf{r}_i + \mathbf{r}_j) + \gamma\right), \tag{4.39}$$

$$\frac{1}{2}\left(\Delta_{\downarrow,\uparrow;\alpha}(\mathbf{r}_i, \mathbf{r}_j) + \Delta_{\uparrow,\downarrow;\alpha}(\mathbf{r}_i, \mathbf{r}_j)\right) = \Delta\cos\left(\mathbf{K}\cdot(\mathbf{r}_i + \mathbf{r}_j) + \gamma\right), \tag{4.40}$$

$$\frac{1}{2}\left(\Delta_{\downarrow,\uparrow;\alpha}(\mathbf{r}_i, \mathbf{r}_j) - \Delta_{\uparrow,\downarrow;\alpha}(\mathbf{r}_i, \mathbf{r}_j)\right) = \Delta', \tag{4.41}$$

where γ is a parameterization angle, which contains information about the spatial patterns of the order parameter. Eqs. (4.39) and (4.40) form a spin triplet and are the Kekule order, whereas Eq. (4.41) represents a spin singlet and is called the hidden order. This nomenclature will become clearer later. The unit cell of the Kekule latice is shown in Fig. 4.4. It can be seen that the Kekule unit cell looks like benzene, the electronic structure of which was discovered by the German chemist Kekule, hence the name of the ansatz.

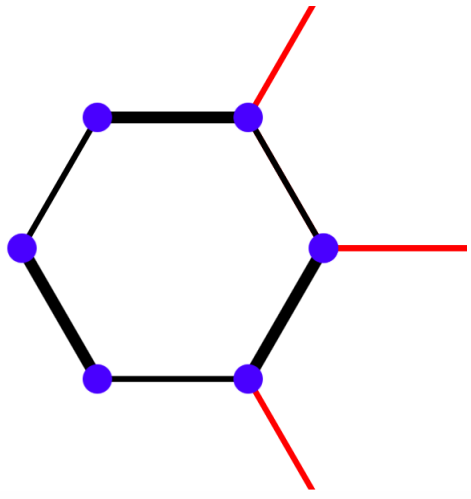

Figure 4.4: The unit cell of the Kekule lattice. Δ_σ and Δ are related to each other via an angle θ. By setting this angle such that $\Delta_\sigma = 0$ and subsequently mapping the superconducting problem onto the hopping problem, the unit cell looks like this. The hopping parameter is renormalized on the bold lines by $\Delta\cos(\gamma + 2\pi/3)$, on the thin lines by $\Delta\cos(\gamma - 2\pi/3)$ and on the red lines by $\Delta\cos(\gamma)$. Figure from Ref. [5].

Making the sum over spin explicit and then plugging in the Kekule ansatz leads to the following for $H_{\Delta_{\sigma',\sigma}}$

$$\begin{aligned}
H_{\Delta_{\sigma',\sigma}} &= -\tilde{V}\sum_{\langle i,j\rangle}\Big[-\left|\Delta_{\uparrow,\uparrow}\left(\mathbf{r}_j,\mathbf{r}_i\right)\right|^2-\left|\Delta_{\uparrow,\downarrow}\left(\mathbf{r}_j,\mathbf{r}_i\right)\right|^2-\left|\Delta_{\downarrow,\uparrow}\left(\mathbf{r}_j,\mathbf{r}_i\right)\right|^2-\left|\Delta_{\downarrow,\downarrow}\left(\mathbf{r}_j,\mathbf{r}_i\right)\right|^2 \\
&+\Delta_{\uparrow\uparrow}\left(\mathbf{r}_j,\mathbf{r}_i\right)a^\dagger_{i,\uparrow}b^\dagger_{j,\uparrow}+\Delta_{\downarrow\downarrow}\left(\mathbf{r}_j,\mathbf{r}_i\right)a^\dagger_{i,\downarrow}b^\dagger_{j,\downarrow}+\Delta_{\uparrow\downarrow}\left(\mathbf{r}_j,\mathbf{r}_i\right)a^\dagger_{i,\downarrow}b^\dagger_{j,\uparrow}+\Delta_{\downarrow\uparrow}\left(\mathbf{r}_j,\mathbf{r}_i\right)a^\dagger_{i,\uparrow}b^\dagger_{j,\downarrow}\Big] \\
&= -\tilde{V}\sum_{\langle i,j\rangle}\Big[-\left(\left|\Delta_\uparrow\right|^2+\left|\Delta_\downarrow\right|^2+2\left|\Delta\right|^2\right)\cos^2\left(\mathbf{K}\cdot\left(\mathbf{r}_i+\mathbf{r}_j\right)+\gamma\right)-2\left|\Delta'\right|^2 \\
&+\left(\Delta_\uparrow a^\dagger_{i,\uparrow}b^\dagger_{j,\uparrow}+\Delta_\downarrow a^\dagger_{i,\downarrow}b^\dagger_{j,\downarrow}+\Delta a^\dagger_{i,\downarrow}b^\dagger_{j,\uparrow}+\Delta a^\dagger_{i,\uparrow}b^\dagger_{j,\downarrow}\right)\cos\left(\mathbf{K}\cdot\left(\mathbf{r}_i+\mathbf{r}_j\right)+\gamma\right) \\
&+\Delta'\left(a^\dagger_{i,\uparrow}b^\dagger_{j,\downarrow}-a^\dagger_{i,\downarrow}b^\dagger_{j,\uparrow}\right)\Big]. \qquad (4.42)
\end{aligned}$$

Focusing first on the term proportional to Δ' and transforming to reciprocal space yields

$$H_{\Delta'} = 6\tilde{V}\sum_{\mathbf{q}}\left|\Delta'\right|^2-\tilde{V}\sum_{\mathbf{k},\alpha}\Delta'\left(a^\dagger_{\mathbf{k},\uparrow}b^\dagger_{-\mathbf{k},\downarrow}-a^\dagger_{\mathbf{k},\downarrow}b^\dagger_{-\mathbf{k},\uparrow}\right)\mathrm{e}^{i\mathbf{k}\cdot\boldsymbol{\delta}_\alpha},$$

where the factor of 6 in front of the first term comes from $\sum_{\langle i,j\rangle} = 3$. Expanding around the

Dirac points leads to

$$
\begin{aligned}
&H_{\Delta'} = 12N\tilde{V}\left|\Delta'\right|^2 \\
&-\frac{\tilde{V}}{2}\sum_{\mathbf{q}}\Bigg[\frac{3ai}{2}\Delta'\left(q\,a^\dagger_{\mathbf{K}+\mathbf{q},\uparrow}b^\dagger_{-\mathbf{K}-\mathbf{q},\downarrow} - q\,a^\dagger_{\mathbf{K}+\mathbf{q},\downarrow}b^\dagger_{-\mathbf{K}-\mathbf{q},\uparrow} + q^*\,a^\dagger_{-\mathbf{K}+\mathbf{q},\uparrow}b^\dagger_{\mathbf{K}-\mathbf{q},\downarrow} - q^*\,a^\dagger_{-\mathbf{K}+\mathbf{q},\downarrow}b^\dagger_{\mathbf{K}-\mathbf{q},\uparrow}\right) \\
&-\frac{3ai}{2}\Delta'^\dagger\left(q^*\,b_{-\mathbf{K}-\mathbf{q},\downarrow}a_{\mathbf{K}+\mathbf{q},\uparrow} - q^*b_{-\mathbf{K}-\mathbf{q},\uparrow}a_{\mathbf{K}+\mathbf{q},\downarrow} + q\,b_{\mathbf{K}-\mathbf{q},\downarrow}a_{-\mathbf{K}+\mathbf{q},\uparrow} - q\,b_{\mathbf{K}-\mathbf{q},\uparrow}a_{-\mathbf{K}+\mathbf{q},\downarrow}\right) \\
&-\frac{3ai}{2}\Delta'\left(q\,a^\dagger_{\mathbf{K}-\mathbf{q},\uparrow}b^\dagger_{-\mathbf{K}+\mathbf{q},\downarrow} - q\,a^\dagger_{\mathbf{K}-\mathbf{q},\downarrow}b^\dagger_{-\mathbf{K}+\mathbf{q},\uparrow} + q^*\,a^\dagger_{-\mathbf{K}-\mathbf{q},\uparrow}b^\dagger_{\mathbf{K}+\mathbf{q},\downarrow} - q^*\,a^\dagger_{-\mathbf{K}-\mathbf{q},\downarrow}b^\dagger_{\mathbf{K}+\mathbf{q},\uparrow}\right) \\
&+\frac{3ai}{2}\Delta'^\dagger\left(q^*\,b_{-\mathbf{K}+\mathbf{q},\downarrow}a_{\mathbf{K}-\mathbf{q},\uparrow} - q^*b_{-\mathbf{K}+\mathbf{q},\uparrow}a_{\mathbf{K}-\mathbf{q},\downarrow} + q\,b_{\mathbf{K}+\mathbf{q},\downarrow}a_{-\mathbf{K}-\mathbf{q},\uparrow} - q\,b_{\mathbf{K}+\mathbf{q},\uparrow}a_{-\mathbf{K}-\mathbf{q},\downarrow}\right)\Bigg].
\end{aligned}
$$

Compactifying then yields the following

$$
\begin{aligned}
H_{\Delta'} &= 12N\tilde{V}\left|\Delta'\right|^2 + \frac{1}{2}\sum_{\mathbf{q}}\psi^\dagger M_{\Delta'}\psi, \quad \text{where} \\
M_{\Delta'} &= \frac{3ai}{2}\tilde{V}\left[\mathrm{Re}\left(\Delta'\right)\tau_2 + \mathrm{Im}\left(\Delta'\right)\tau_1\right]\otimes\sigma_0\otimes i\gamma_0\gamma_3\left(i\gamma_0\gamma_1 q_y - i\gamma_0\gamma_2 q_x\right).
\end{aligned}
$$

Comparing this result to the Dirac Hamiltonian in Eq. (4.35), one can see that it is proportional to the latter and one can write

$$
M_{\Delta'} = \frac{2i}{t}\tilde{V}\left[\mathrm{Re}\left(\Delta'\right)\tau_2 + \mathrm{Im}\left(\Delta'\right)\tau_1\right]\otimes\sigma_0\otimes i\gamma_0\gamma_3 M_t. \tag{4.43}
$$

This dependence is an indication that instead of opening a superconducting gap the order parameter Δ' renormalizes the Fermi velocity v_F. Therefore, this order parameter is referred to as the hidden-order parameter, a term first coined by Ref. [4]. From this equation, it can be seen that Δ' is indeed a spin-singlet state.

Next, the remaining terms in Eq. (4.42) are considered. Transforming the operators to reciprocal space and writing the cosine in terms of exponentials yields

$$
\begin{aligned}
&H_{\Delta,\Delta_\uparrow,\Delta_\downarrow} = \frac{1}{4}\tilde{V}\sum_{\langle i,j\rangle}\sum_{\mathbf{q}}\left(\left|\Delta_\uparrow\right|^2 + \left|\Delta_\downarrow\right|^2 + 2\left|\Delta\right|^2\right)\left(\mathrm{e}^{2i\mathbf{K}\cdot(\mathbf{r}_i+\mathbf{r}_j)}\mathrm{e}^{2i\gamma} + \mathrm{e}^{-2i\mathbf{K}\cdot(\mathbf{r}_i+\mathbf{r}_j)}\mathrm{e}^{-2i\gamma} + 2\right) \\
&-\frac{\tilde{V}}{N}\sum_{i,\alpha}\sum_{\mathbf{k},\mathbf{k}'}\Bigg[\frac{1}{2}\left(\Delta_\uparrow a^\dagger_{\mathbf{k},\uparrow}b^\dagger_{\mathbf{k}',\uparrow} + \Delta_\downarrow a^\dagger_{\mathbf{k},\downarrow}b^\dagger_{\mathbf{k}',\downarrow} + \Delta a^\dagger_{\mathbf{k},\downarrow}b^\dagger_{\mathbf{k}',\uparrow} + \Delta a^\dagger_{\mathbf{k},\uparrow}b^\dagger_{\mathbf{k}',\downarrow}\right)\mathrm{e}^{-i(\mathbf{k}+\mathbf{k}'-2\mathbf{K})\cdot\mathbf{r}_i}\mathrm{e}^{-i(\mathbf{k}'-\mathbf{K})\cdot\boldsymbol{\delta}_\alpha}\mathrm{e}^{i\gamma} \\
&+\frac{1}{2}\left(\Delta_\uparrow a^\dagger_{\mathbf{k},\uparrow}b^\dagger_{\mathbf{k}',\uparrow} + \Delta_\downarrow a^\dagger_{\mathbf{k},\downarrow}b^\dagger_{\mathbf{k}',\downarrow} + \Delta a^\dagger_{\mathbf{k},\downarrow}b^\dagger_{\mathbf{k}',\uparrow} + \Delta a^\dagger_{\mathbf{k},\uparrow}b^\dagger_{\mathbf{k}',\downarrow}\right)\mathrm{e}^{-i(\mathbf{k}+\mathbf{k}'+2\mathbf{K})\cdot\mathbf{r}_i}\mathrm{e}^{-i(\mathbf{k}'+\mathbf{K})\cdot\boldsymbol{\delta}_\alpha}\mathrm{e}^{-i\gamma} + h.c.\Bigg] \\
&= 6N\tilde{V}\left[\frac{1}{2}\left(\left|\Delta_\uparrow\right|^2 + \left|\Delta_\downarrow\right|^2\right) + \left|\Delta\right|^2\right] \\
&-\frac{\tilde{V}}{2}\sum_{\mathbf{q}}\Big[\left(\Delta_\uparrow a^\dagger_{\mathbf{K}+\mathbf{q},\uparrow}b^\dagger_{\mathbf{K}-\mathbf{q},\uparrow} + \Delta_\downarrow a^\dagger_{\mathbf{K}+\mathbf{q},\downarrow}b^\dagger_{\mathbf{K}-\mathbf{q},\downarrow} + \Delta a^\dagger_{\mathbf{K}+\mathbf{q},\downarrow}b^\dagger_{\mathbf{K}-\mathbf{q},\uparrow} + \Delta a^\dagger_{\mathbf{K}+\mathbf{q},\uparrow}b^\dagger_{\mathbf{K}-\mathbf{q},\downarrow}\right)\mathrm{e}^{i\gamma} \\
&+\left(\Delta_\uparrow a^\dagger_{\mathbf{K}-\mathbf{q},\uparrow}b^\dagger_{\mathbf{K}+\mathbf{q},\uparrow} + \Delta_\downarrow a^\dagger_{\mathbf{K}-\mathbf{q},\downarrow}b^\dagger_{\mathbf{K}+\mathbf{q},\downarrow} + \Delta a^\dagger_{\mathbf{K}-\mathbf{q},\downarrow}b^\dagger_{\mathbf{K}+\mathbf{q},\uparrow} + \Delta a^\dagger_{\mathbf{K}-\mathbf{q},\uparrow}b^\dagger_{\mathbf{K}+\mathbf{q},\downarrow}\right)\mathrm{e}^{i\gamma} \\
&+\left(\Delta_\uparrow a^\dagger_{-\mathbf{K}+\mathbf{q},\uparrow}b^\dagger_{-\mathbf{K}-\mathbf{q},\uparrow} + \Delta_\downarrow a^\dagger_{-\mathbf{K}+\mathbf{q},\downarrow}b^\dagger_{-\mathbf{K}-\mathbf{q},\downarrow} + \Delta a^\dagger_{-\mathbf{K}+\mathbf{q},\downarrow}b^\dagger_{-\mathbf{K}-\mathbf{q},\uparrow} + \Delta a^\dagger_{-\mathbf{K}+\mathbf{q},\uparrow}b^\dagger_{-\mathbf{K}-\mathbf{q},\downarrow}\right)\mathrm{e}^{-i\gamma} \\
&+\left(\Delta_\uparrow a^\dagger_{-\mathbf{K}-\mathbf{q},\uparrow}b^\dagger_{-\mathbf{K}+\mathbf{q},\uparrow} + \Delta_\downarrow a^\dagger_{-\mathbf{K}-\mathbf{q},\downarrow}b^\dagger_{-\mathbf{K}+\mathbf{q},\downarrow} + \Delta a^\dagger_{-\mathbf{K}-\mathbf{q},\downarrow}b^\dagger_{-\mathbf{K}+\mathbf{q},\uparrow} + \Delta a^\dagger_{-\mathbf{K}-\mathbf{q},\uparrow}b^\dagger_{-\mathbf{K}+\mathbf{q},\downarrow}\right)\mathrm{e}^{-i\gamma} + h.c.\Big].
\end{aligned}
$$

Two values for the parameterization angle γ are considered: $\gamma = 0, \pi/2$. The first is referred to as the s-Kekule order and the second as the p-Kekule order, following Ref. [5]. This nomenclature will become clear later on. For $\gamma = 0$, the following result is found

$$\begin{aligned} H_{\Delta,\Delta_\uparrow,\Delta_\downarrow,\gamma=0} &= 6N\tilde{V}m^2 + \frac{1}{2}\sum_{\mathbf{q}} \psi^\dagger M_{\Delta,\Delta_\uparrow,\Delta_\downarrow,\gamma=0}\psi, \quad \text{where} \\ M_{\Delta,\Delta_\uparrow,\Delta_\downarrow,\gamma=0} &= -\tilde{V}\left[(X\tau_1 - Y\tau_2)\otimes\sigma_3 + (I_-\tau_2 - R_-\tau_1)\otimes\sigma_1 + (I_+\tau_1 + R_+\tau_2)\otimes\sigma_2\right]\otimes\gamma_0, \end{aligned} \tag{4.44}$$

with

$$\begin{aligned} m^2 &= X^2 + Y^2 + R_+^2 + I_+^2 + R_-^2 + I_-^2, \qquad X = \mathrm{Re}\left(\Delta\right), \qquad Y = \mathrm{Im}\left(\Delta\right), \\ R_\pm &= \frac{1}{2}\left[\mathrm{Re}\left(\Delta_\uparrow\right) \pm \mathrm{Re}\left(\Delta_\downarrow\right)\right], \qquad I_\pm = \frac{1}{2}\left[\mathrm{Im}\left(\Delta_\uparrow\right) \pm \mathrm{Im}\left(\Delta_\downarrow\right)\right]. \end{aligned}$$

From now on, m will be referred to as the Kekule order. Later on, it will be shown that it opens a superconducting gap. In accordance with the definition of Δ and Δ_σ, it can be seen from the Hamiltonian that the order parameter Δ facilitates nearest-neighbor pairing of particles coming from the same valley and with opposite spin and that the order parameters $\Delta_\uparrow$ and $\Delta_\downarrow$ also pair particles that are on nearest-neighbor sites with no valley mixing and equal spin. For $\gamma = \pi/2$ a similar expression is found, however, the dependence on the Dirac matrices is different

$$\begin{aligned} H_{\Delta,\Delta_\uparrow,\Delta_\downarrow,\gamma=\pi/2} &= 6N\tilde{V}m^2 + \frac{1}{2}\sum_{\mathbf{q}} \psi^\dagger M_{\Delta,\Delta_\uparrow,\Delta_\downarrow,\gamma=0}\psi, \quad \text{where} \\ M_{\Delta,\Delta_\uparrow,\Delta_\downarrow,\gamma=\pi/2} &= -\tilde{V}\left[-\left(Y\tau_1 + X\tau_2\right)\otimes\sigma_3 + (I_-\tau_1 + R_-\tau_2)\otimes\sigma_1 + (R_+\tau_1 - I_+\tau_2)\otimes\sigma_2\right]\otimes i\gamma_1\gamma_2. \end{aligned} \tag{4.45}$$

4.4.5 Total Hamiltonian

Changing the basis to absorb the particle-hole doubling according to

$$\frac{1}{2}\sum_{\mathbf{q}} \Psi^\dagger M \Psi \to \sum_{\mathbf{q}} \Psi^\dagger M \Psi.$$

leads to the following total Hamiltonian

$$H_{\mathrm{tot},\gamma} = E_{0,\mathrm{tot}} + \sum_{\mathbf{q}} \psi^\dagger M_{\mathrm{tot},\gamma}\psi, \tag{4.46}$$

where the energy of the condensate is

$$E_{0,\mathrm{tot}} = 4N\tilde{U}\left|\Delta_0\right|^2 + 6N\tilde{V}\left(m^2 + 2\left|\Delta'\right|^2\right). \tag{4.47}$$

For $\gamma = 0$, $M_{\text{tot},\gamma}$ reads

$$\begin{aligned} M_{\text{tot},\gamma=0} &= v_F\tau_0 \otimes \sigma_0 \otimes (i\gamma_0\gamma_1 q_y - i\gamma_0\gamma_2 q_x) - \mu\tau_3 \otimes \sigma_0 \otimes \mathbb{I}_{4\times 4} \\ &\quad -\tilde{U}\left[\text{Re}(\Delta_0)\tau_1 - \text{Im}(\Delta_0)\tau_2\right] \otimes \sigma_0 \otimes i\gamma_0\gamma_3 \\ &\quad +\frac{2i}{t}\tilde{V}\left[\text{Re}\left(\Delta'\right)\tau_2 + \text{Im}\left(\Delta'\right)\tau_1\right] \otimes \sigma_0 \otimes i\gamma_0\gamma_3 M_t \\ &\quad -\tilde{V}\left[(X\tau_1 - Y\tau_2) \otimes \sigma_3 + (I_-\tau_2 - R_-\tau_1) \otimes \sigma_1 + (I_+\tau_1 + R_+\tau_2) \otimes \sigma_2\right] \otimes \gamma_0, \end{aligned} \tag{4.48}$$

and for $\gamma = \pi/2$

$$\begin{aligned} M_{\text{tot},\gamma=\pi/2} &= v_F\tau_0 \otimes \sigma_0 \otimes (i\gamma_0\gamma_1 q_y - i\gamma_0\gamma_2 q_x) - \mu\tau_3 \otimes \sigma_0 \otimes \mathbb{I}_{4\times 4} \\ &\quad -\tilde{U}\left[\text{Re}(\Delta_0)\tau_1 - \text{Im}(\Delta_0)\tau_2\right] \otimes \sigma_0 \otimes i\gamma_0\gamma_3 \\ &\quad +\frac{2i}{t}\tilde{V}\left[\text{Re}\left(\Delta'\right)\tau_2 + \text{Im}\left(\Delta'\right)\tau_1\right] \otimes \sigma_0 \otimes i\gamma_0\gamma_3 M_t \\ &\quad -\tilde{V}\left[-\left(Y\tau_1 + X\tau_2\right) \otimes \sigma_3 + (I_-\tau_1 + R_-\tau_2) \otimes \sigma_1 + (R_+\tau_1 - I_+\tau_2) \otimes \sigma_2\right] \otimes i\gamma_1\gamma_2. \end{aligned} \tag{4.49}$$

4.4.6 Symmetries

In this representation, some generators can be defined such that the symmetries of the Hamiltonians can be determined. The number operator $\hat{N}$ is equal to plus the identity in the upper quadrant and minus the identity in the lower quadrant, such that there is a plus sign for the particles and a minus sign for the holes. Therefore,

$$\hat{N} = \tau_3 \otimes \sigma_0 \otimes \mathbb{I}.$$

The generator for translations $\hat{P}$ equals

$$\hat{P} = \tau_3 \otimes \sigma_0 \otimes i\gamma_3\gamma_5.$$

The generator that exchanges the two Dirac points $\hat{I}_K$ reads

$$\hat{I}_K = \tau_0 \otimes \sigma_0 \otimes i\gamma_1\gamma_5.$$

Upon writing it out in full, one can check that it exchanges the Dirac points when the axis is inversed according to $q_y \to -q_y$. The generator for sublattice exchange $\hat{I}_{ab}$ is

$$\hat{I}_{ab} = \tau_0 \otimes \sigma_0 \otimes \gamma_2.$$

Upon writing this generator out in full, one finds that it exchanges sublattices when the axis is inversed according to $q_x \to -q_x$. Lastly, the three generators of rotations of electron spin $\hat{\mathbf{S}}$ reads

$$\hat{\mathbf{S}} = \tau_0 \otimes \boldsymbol{\sigma} \otimes \mathbb{I}.$$

All these generators are defined in Ref. [5].

It is reviewed whether the Dirac Hamiltonian M_t commutes with the generators, as it should. It clearly commutes with the number operator, i.e. $\left[\hat{N}, M_t\right] = 0$. Next, for M_t to commute with $\hat{P}$, the following must hold

$$[i\gamma_3\gamma_5, i\gamma_0\gamma_1 q_y - i\gamma_0\gamma_2 q_x] = 0,$$

indeed $\gamma_3\gamma_5\gamma_0\gamma_1 = \gamma_0\gamma_1\gamma_3\gamma_5$ and $\gamma_3\gamma_5\gamma_0\gamma_2 = \gamma_0\gamma_2\gamma_3\gamma_5$, such that $\left[\hat{P}, M_t\right] = 0$. Then, for M_t to commute with $\hat{I}_K$, the following must hold

$$[i\gamma_1\gamma_5, i\gamma_0\gamma_1 q_y - i\gamma_0\gamma_2 q_x] = 0.$$

Using the requirement $q_y \to -q_y$ and that $\gamma_1\gamma_5\gamma_0\gamma_1 = -\gamma_0\gamma_1\gamma_1\gamma_5$ and $\gamma_1\gamma_5\gamma_0\gamma_2 = \gamma_0\gamma_2\gamma_1\gamma_5$, one finds that $\left[\hat{I}_K, M_t\right] = 0$. Next, M_t commutes with $\hat{I}_{ab}$ if

$$[\gamma_2, i\gamma_0\gamma_1 q_y - i\gamma_0\gamma_2 q_x] = 0$$

holds when accompanied by $q_x \to -q_x$. This holds because $\gamma_2\gamma_0\gamma_1 = \gamma_0\gamma_1\gamma_2$ and $\gamma_2\gamma_0\gamma_2 = -\gamma_0\gamma_2\gamma_2$, such that $\left[\hat{I}_{ab}, M_t\right] = 0$. Lastly, one can immediately see that $\left[\hat{\mathbf{S}}, M_t\right] = 0$. Therefore, M_t commutes with all generators, and it preserves particle-number, translation and spin-rotational symmetry. Moreover, M_t is even under exchange of the Dirac points as well as under sublattice exchange.

One can clearly see that M_μ commutes with all these generators, such that all symmetries are preserved, as is expected.

Next, using the same technique, it can easily be seen that M_U does not commute with $\hat{N}$ and $\hat{P}$, which means that M_U breaks particle-number and translation symmetry. The matrix, however, does commute with $\hat{I}_K$, $\hat{I}_{ab}$ and $\hat{\mathbf{I}}$, which means that M_U is even under Dirac point and sublattice exchange, and that it preserves spin-rotational symmetry. Therefore, M_U represents a spatially uniform s-wave singlet superconducting state.

Then, $M_{V,\Delta'}$ equals a factor times M_t, where this factor by itself would actually be a singlet s-wave order parameter. This factor anticommutes with M_t, which means that $M_{V,\Delta'}^\dagger = M_{V,\Delta'}$. $M_{V,\Delta'}$ represents the superconducting hidden order [4]. Roy and Herbut explain that the opening of the order parameter Δ' to lower the energy of the Dirac-Fermi sea is energetically not favorable because $M_{V,\Delta'}$ vanishes at the Dirac points [5]. It will be seen in the next Section that the Kekule order is indeed preferred over this order.

Lastly, $M_{V,\Delta,\Delta_\uparrow,\Delta_\downarrow,\gamma=0}$ does not commute with $\hat{N}$, $\hat{P}$, and $\hat{I}_{ab}$ and breaks two generators of $\hat{\mathbf{S}}$. It does, however, commute with $\hat{I}_K$. Therefore, $M_{V,\Delta,\Delta_\uparrow,\Delta_\downarrow,\gamma=0}$ is a spatially non-uniform superconductor, which is odd under sublattice exchange, but even under the exchange of Dirac points. It is called the s-Kekule superconducting state. As it violates the spin-rotational symmetry, $M_{V,\Delta,\Delta_\uparrow,\Delta_\downarrow,\gamma=0}$ represents a triplet superconducting state. On the other hand, $M_{V,\Delta,\Delta_\uparrow,\Delta_\downarrow,\gamma=\pi/2}$ does not commute with any of the generators, such that this state is called the p-Kekule superconducting state [5].

4.5 Competition Between Kekule and Hidden Order

In this Section, the competition between the Kekule order m and the hidden order Δ' will be investigated for both $\gamma = 0$ and $\gamma = \pi/2$. It is more interesting to study the competition between

the Kekule and hidden order because when all order parameters are non-zero, the s-wave order parameter wins. To show this, the s-wave superconductor is reviewed in Appendix 6.3.8. Therefore, the s-wave order parameter Δ_0 is set to zero in this Section, i.e. $\Delta_0 = 0$. When the on-site attraction is turned off and only nearest-neighbor attraction is taken into account, it is not *a priori* clear which superconducting order is preferred. In Ref. [5], Roy and Herbut use a similar model to the one used in this Chapter to show that the Kekule order dominates over the hidden order when considering graphene. They determine the ground-state energy, gap equation at zero temperature and critical couplings in the absence of chemical potential. In this Chapter, their research is expanded by including chemical potential and calculating gaps at zero temperature, gap equations at finite temperature and critical temperatures. The work in Ref. [5] was preceded by work done by Uchoa and Castro Neto [4], where they investigate the competition between on-site and nearest-neighbor coupling. For nearest-neighbor coupling they only consider the hidden order.

In the following Subsections, the ground-state energy, gap equations at zero and finite temperature, critical couplings, zero-temperature gaps and critical temperature will be calculated first for the s-Kekule order and then for the p-Kekule order. It will become clear that in the approximation used in this Chapter, the results will be the same for both cases. Only upon inclusion of higher-energy particles, it can be determined that the p-Kekule order is preferred over the s-Kekule order [5]. However, such calculations are outside the scope of this Thesis and the reader is referred to Ref. [5] for details. Lastly, in Subsection 4.5.3, the competition between the Kekule and hidden order is reviewed.

4.5.1 s-Kekule Order

In this Subsection, the ground-state energy is calculated for the s-Kekule order, for which $\gamma = 0$. This is followed by the computation of the gap equation at zero temperature and the critical couplings. The gap equation will be solved analytically in the strong- and weak-coupling limit to find the zero-temperature gap. Next, the gap equations at finite temperature are computed, which is then followed by the determination of the critical temperatures.

Ground-State Energy

The ground-state energy will first be calculated by diagonalizing Eqs. (4.46)-(4.48) for $\Delta' = 0$. Initially, the hidden order is turned off because by minimizing the resulting ground-state energy, a condition on the components of the Kekule order can be derived, which simplifies the ground-state energy. This will be followed by including the hidden order in the ground-state energy.

Ground-State Energy for $\Delta' = 0$
To find the energy, the following expression is used

$$\sum_{\mathbf{q}} \left(E_{0,m} + M_t + M_\mu + M_{m,\gamma=0}\right) \Psi = E_{m,\gamma=0} \Psi.$$

This yields

$$E_{0,m} = 6N\tilde{V}m^2.$$

$M_t + M_\mu + M_{m,\gamma=0}$ is first squared and then diagonalized,

$$
\begin{aligned}
&(M_t + M_\mu + M_{m,\gamma=0})^2 = \left(M_t + M_\mu + M_{\Delta,\gamma=0} + M^+_{\Delta_\uparrow,\Delta_\downarrow,\gamma=0} + M^-_{\Delta_\uparrow,\Delta_\downarrow,\gamma=0}\right)^2 \\
&= M_t^2 + M_\mu^2 + M^2_{\Delta,\gamma=0} + \left(M^+_{\Delta_\uparrow,\Delta_\downarrow,\gamma=0}\right)^2 + \left(M^-_{\Delta_\uparrow,\Delta_\downarrow,\gamma=0}\right)^2 \\
&+ \left\{M_t\,,\, M_\mu + M_{\Delta,\gamma=0} + M^+_{\Delta_\uparrow,\Delta_\downarrow,\gamma=0} + M^-_{\Delta_\uparrow,\Delta_\downarrow,\gamma=0}\right\} \\
&+ \left\{M_\mu\,,\, M_{\Delta,\gamma=0} + M^+_{\Delta_\uparrow,\Delta_\downarrow,\gamma=0} + M^-_{\Delta_\uparrow,\Delta_\downarrow,\gamma=0}\right\} \\
&+ \left\{M_{\Delta,\gamma=0}\,,\, M^+_{\Delta_\uparrow,\Delta_\downarrow,\gamma=0} + M^-_{\Delta_\uparrow,\Delta_\downarrow,\gamma=0}\right\} + \left\{M^+_{\Delta_\uparrow,\Delta_\downarrow,\gamma=0}\,,\, M^-_{\Delta_\uparrow,\Delta_\downarrow,\gamma=0}\right\},
\end{aligned}
$$

where M_t and M_μ are given by Eqs.(4.35) and (4.36), respectively, and

$$
\begin{aligned}
&M_{\Delta,\gamma=0} = -\tilde{V}\,(X\tau_1 - Y\tau_2)\otimes\sigma_3\otimes\gamma_0, \qquad M^+_{\Delta_\uparrow,\Delta_\downarrow,\gamma=0} = -\tilde{V}\,(I_+\tau_1 + R_+\tau_2)\otimes\sigma_2\otimes\gamma_0, \\
&M^-_{\Delta_\uparrow,\Delta_\downarrow,\gamma=0} = -\tilde{V}\,(I_-\tau_2 - R_-\tau_1)\otimes\sigma_1\otimes\gamma_0.
\end{aligned}
$$

Before computing $(M_t + M_\mu + M_{m,\gamma=0})^2$, the anticommutation relations will be reviewed. Using the anticommutation rules for the Pauli and Dirac matrices

$$
\{\tau_i,\tau_j\} = 2\delta_{i,j}, \qquad \tau_i\tau_j = i\,\epsilon_{ijk}\tau_k, \qquad \{\gamma_i,\gamma_j\} = 2\delta_{i,j},
$$

where the same anticommutation relations hold for the σ-matrices as for the τ-matrices and ϵ_{ijk} is the Levi-Civita symbol with $\epsilon_{123} = 1$, one can observe that

$$
\begin{aligned}
&\{M_t\,,\, M_\mu\} = 2M_tM_\mu, \quad \left\{M_t\,,\, M_{\Delta,\gamma=0} + M^+_{\Delta_\uparrow,\Delta_\downarrow,\gamma=0} + M^-_{\Delta_\uparrow,\Delta_\downarrow,\gamma=0}\right\} = 0, \\
&\left\{M_\mu\,,\, M_{\Delta,\gamma=0} + M^+_{\Delta_\uparrow,\Delta_\downarrow,\gamma=0} + M^-_{\Delta_\uparrow,\Delta_\downarrow,\gamma=0}\right\} = 0, \\
&\left\{M_{\Delta,\gamma=0}\,,\, M^+_{\Delta_\uparrow,\Delta_\downarrow,\gamma=0} + M^-_{\Delta_\uparrow,\Delta_\downarrow,\gamma=0}\right\} \neq 0, \quad \left\{M^+_{\Delta_\uparrow,\Delta_\downarrow,\gamma=0}\,,\, M^-_{\Delta_\uparrow,\Delta_\downarrow,\gamma=0}\right\} \neq 0.
\end{aligned}
$$

Therefore, one needs to compute

$$
\begin{aligned}
&(M_t + M_\mu + M_{m,\gamma=0})^2 = M_t^2 + M_\mu^2 + M^2_{\Delta,\gamma=0} + \left(M^+_{\Delta_\uparrow,\Delta_\downarrow,\gamma=0}\right)^2 + \left(M^-_{\Delta_\uparrow,\Delta_\downarrow,\gamma=0}\right)^2 \\
&+2M_tM_\mu + \left\{M_{\Delta,\gamma=0}\,,\, M^+_{\Delta_\uparrow,\Delta_\downarrow,\gamma=0}\right\} + \left\{M_{\Delta,\gamma=0}\,,\, M^-_{\Delta_\uparrow,\Delta_\downarrow,\gamma=0}\right\} + \left\{M^+_{\Delta_\uparrow,\Delta_\downarrow,\gamma=0}\,,\, M^-_{\Delta_\uparrow,\Delta_\downarrow,\gamma=0}\right\}.
\end{aligned}
$$

For the first six terms this yields

$$
\begin{aligned}
&M_t^2 = v_F^2|q|^2\,(\tau_0\otimes\sigma_0\otimes\mathbb{I})\,, \qquad M_\mu^2 = \mu^2\,(\tau_0\otimes\sigma_0\otimes\mathbb{I})\,, \qquad M^2_{\Delta,\gamma=0} = \tilde{V}^2\left(X^2+Y^2\right)(\tau_0\otimes\sigma_0\otimes\mathbb{I})\,, \\
&\left(M^+_{\Delta_\uparrow,\Delta_\downarrow,\gamma=0}\right)^2 = \tilde{V}^2(R_+^2 + I_+^2)\,(\tau_0\otimes\sigma_0\otimes\mathbb{I})\,, \qquad \left(M^-_{\Delta_\uparrow,\Delta_\downarrow,\gamma=0}\right)^2 = \tilde{V}^2(R_-^2 + I_-^2)\,(\tau_0\otimes\sigma_0\otimes\mathbb{I})\,, \\
&2M_tM_\mu = -2\mu\,v_F\,\tau_3\otimes\sigma_0\otimes(i\gamma_0\gamma_1 q_y - i\gamma_0\gamma_2 q_x)\,,
\end{aligned}
$$

where τ_0 and σ_0 are 2×2 identity matrices. The first anticomutation relation leads to

$$
\begin{aligned}
\left\{M_{\Delta,\gamma=0}\,,\, M^+_{\Delta_\uparrow,\Delta_\downarrow,\gamma=0}\right\} &= \tilde{V}^2\left[(XR_+ + YI_+)\,\tau_3 - i\,(XI_+ - YR_+)\,\tau_0\right]\otimes\sigma_1\otimes\mathbb{I} \\
&\quad +\tilde{V}^2\left[(XR_+ + YI_+)\,\tau_3 + i\,(XI_+ - YR_+)\,\tau_0\right]\otimes\sigma_1\otimes\mathbb{I} \\
&= 2\tilde{V}^2\,(XR_+ + YI_+)\,\tau_3\otimes\sigma_1\otimes\mathbb{I},
\end{aligned}
$$

where it is used that $\{\tau_1,\tau_1\}=\{\tau_2,\tau_2\}=\tau_0$, $\{\tau_1,\tau_2\}=i\,\tau_3=-\{\tau_2,\tau_1\}$ and $\{\sigma_3,\sigma_2\}=-i\,\sigma_1=-\{\sigma_3,\sigma_2\}$. In a similar fashion, the other two anticommutation relations can be computed

$$\left\{M_{\Delta,\gamma=0}\,,\,M^{-}_{\Delta_\uparrow,\Delta_\downarrow,\gamma=0}\right\}=2\tilde{V}^2\,(YR_- - XI_-)\,\tau_3\otimes\sigma_2\otimes\mathbb{I},$$
$$\left\{M^{+}_{\Delta_\uparrow,\Delta_\downarrow,\gamma=0}\,,\,M^{-}_{\Delta_\uparrow,\Delta_\downarrow,\gamma=0}\right\}=2\tilde{V}^2\,(R_+R_- + I_+I_-)\,\tau_3\otimes\sigma_3\otimes\mathbb{I}.$$

Therefore, the result is

$$\begin{aligned}(M_t+M_\mu+M_{m,\gamma=0})^2 &= \left(v_F^2|q|^2+\mu^2+\tilde{V}^2m^2\right)(\tau_0\otimes\sigma_0\otimes\mathbb{I})+2\tilde{V}^2\,\tau_3\otimes(\mathbf{n}\cdot\boldsymbol{\sigma})\otimes\mathbb{I}\\ &\quad -2\mu\,v_F\,\tau_3\otimes\sigma_0\otimes(i\gamma_0\gamma_1q_y-i\gamma_0\gamma_2q_x)\,,\end{aligned}\tag{4.50}$$

where

$$\mathbf{n}\equiv(XR_++YI_+\,,\,YR_--XI_-\,,\,R_+R_-+I_+I_-)\,.\tag{4.51}$$

Diagonalizing this term leads to the dispersion

$$(\omega_{m,\gamma=0;s,s'})^2=(v_F|q|+s\mu)^2+\tilde{V}^2m^2+2s'\,|\mathbf{n}|\,,$$

where $s,s'=\pm$. Now the energy is given by

$$E_{m,\gamma=0}=E_{0,m}+\sum_{\mathbf{q};s,s'=\pm}\sqrt{(\omega_{m,\gamma=0;s,s'})^2}=E_{0,m}\pm\sum_{\mathbf{q};s,s'=\pm}\omega_{m,\gamma=0;s,s'},$$

such that the ground-state energy reads

$$\begin{aligned}E_{\mathrm{g.s.},m,\gamma=0} &= E_{0,m}-\sum_{\mathbf{q};s,s'=\pm}\omega_{m,\gamma=0;s,s'}\\ &= 6N\tilde{V}m^2-2N\sum_{s,s'=\pm}\int\frac{\mathrm{d}\mathbf{q}}{(2\pi)^2}\sqrt{(v_F|q|+s\mu)^2+\tilde{V}^2m^2+2s'\,|\mathbf{n}|},\end{aligned}$$

where $\sum_{\mathbf{q}}\to 2N\int\mathrm{d}\mathbf{q}/(2\pi)^2$ and s and s' represent the particle-hole and spin degree of freedom, respectively. This leads to the final result for the ground state per honeycomb lattice site

$$\frac{E_{\mathrm{g.s.},m,\gamma=0}}{4N}=\frac{3\tilde{V}m^2}{2}-\frac{1}{2}\sum_{s,s'=\pm}\int\frac{\mathrm{d}\mathbf{q}}{(2\pi)^2}\sqrt{(v_F|q|+s\mu)^2+\tilde{V}^2m^2+2s'\,|\mathbf{n}|},\tag{4.52}$$

which, in the limit $\mu=0$, corresponds to the result found in Ref. [5].

Minimum of the Ground-State Energy

Differentiating Eq. (4.52) with respect to $|\mathbf{n}|$ to find the minimum of the ground-state energy leads to a condition for $|\mathbf{n}|$. Minimizing this yields

$$\begin{aligned}0 &= \frac{\mathrm{d}}{\mathrm{d}\,|\mathbf{n}|}\frac{E_{\mathrm{g.s.},m,\gamma=0}}{4N}=\frac{\mathrm{d}}{\mathrm{d}\,|\mathbf{n}|}\left\{\frac{3\tilde{V}m^2}{2}-\frac{1}{2}\sum_{s,s'=\pm}\int\frac{\mathrm{d}\mathbf{q}}{(2\pi)^2}\sqrt{(v_F|q|+s\mu)^2+\tilde{V}^2m^2+2s'\,|\mathbf{n}|}\right\}\\ &= -\frac{1}{2}\sum_{s,s'=\pm}\int\frac{\mathrm{d}\mathbf{q}}{(2\pi)^2}\frac{s'}{\sqrt{(v_F|q|+s\mu)^2+\tilde{V}^2m^2+2s'\,|\mathbf{n}|}}\\ &= -\frac{1}{2}\sum_{s=\pm}\int\frac{\mathrm{d}\mathbf{q}}{(2\pi)^2}\left(\frac{1}{\sqrt{(v_F|q|+s\mu)^2+\tilde{V}^2m^2+2\,|\mathbf{n}|}}-\frac{1}{\sqrt{(v_F|q|+s\mu)^2+\tilde{V}^2m^2-2\,|\mathbf{n}|}}\right),\end{aligned}$$

which is only zero if $|\mathbf{n}| = 0$ for any m. Using $\sum_{s'=\pm} = 2$, the ground-state energy now reads

$$\frac{E_{\text{g.s.},m,\gamma=0}}{4N} = \frac{3\tilde{V}m^2}{2} - \sum_{s=\pm}\int \frac{\mathrm{d}\mathbf{q}}{(2\pi)^2}\sqrt{\left(v_F|q| + s\mu\right)^2 + \tilde{V}^2m^2}, \tag{4.53}$$

The condition $|\mathbf{n}| = 0$ implies $n_1 = n_2 = n_3 = 0$. However, the conditions $n_1 = 0$ and $n_2 = 0$ in fact imply the condition $n_3 = 0$, i.e.

$$\begin{aligned}
&n_1 = 0 \Rightarrow XR_+ + Y_+ = 0 \Rightarrow X = -\frac{YI_+}{R_+}\\
&n_2 = 0 \Rightarrow YR_- - XI_- = 0\\
&YR_- \frac{YI_+}{R_+}I_- = 0 \Rightarrow R_+R_- + I_+I_- = 0 = n_3.
\end{aligned}$$

Therefore, the condition $|\mathbf{n}| = 0$ yields only two independent equations and not three. The condition $n_3 = 0$ implies

$$|\Delta_\uparrow|^2 - |\Delta_\downarrow|^2 = 0, \qquad \text{such that} \qquad |\Delta_\uparrow| = |\Delta_\downarrow|.$$

Using that $\Delta_\sigma = |\Delta_\sigma|\,\mathrm{e}^{i\phi_\sigma}$ and $\Delta = |\Delta|\,\mathrm{e}^{i\phi}$, the condition $n_1 = 0$ implies

$$\frac{1}{2}|\Delta|\,|\Delta_\uparrow|\left[\cos(\phi)\left(\cos(\phi_\uparrow) + \cos(\phi_\downarrow)\right) + \sin(\phi)\left(\sin(\phi_\uparrow) + \sin(\phi_\downarrow)\right)\right] = 0.$$

This leads to the following two conditions

$$0 = \cos(\phi)\left(\cos(\phi_\uparrow) + \cos(\phi_\downarrow)\right), \qquad 0 = \sin(\phi)\left(\sin(\phi_\uparrow) + \sin(\phi_\downarrow)\right).$$

Evaluating the first yields

$$0 = \frac{1}{2}\left[\cos\left(\phi_\uparrow - \phi\right) + \cos\left(\phi_\uparrow + \phi\right) + \cos\left(\phi_\downarrow - \phi\right) + \cos\left(\phi_\downarrow + \phi\right)\right],$$

such that

$$\begin{aligned}
&\cos\left(\phi_\uparrow - \phi\right) = 0 \Rightarrow \phi_\uparrow - \phi = n\pi,\\
&\cos\left(\phi_\downarrow - \phi\right) = 0 \Rightarrow \phi_\downarrow - \phi = n\pi,\\
&\phi_\uparrow + \phi_\downarrow - 2\phi = n\pi \Rightarrow \phi_\uparrow + \phi_\downarrow = 2\phi + n\pi,
\end{aligned}$$

where $n \in \mathbb{Z}$. Therefore, the condition $|\mathbf{n}| = 0$ yields two instead of three independent equations, and leads to two constraints

$$|\Delta_\uparrow| = |\Delta_\downarrow|, \qquad \text{and} \qquad \phi_\uparrow + \phi_\downarrow = 2\phi + n\pi, \tag{4.54}$$

which corresponds to what is found in Ref. [5].

Using the condition $|\mathbf{n}| = 0$ together with $\Delta_\sigma = |\Delta_\sigma|\,\mathrm{e}^{i\phi_\sigma}$ and $\Delta = |\Delta|\,\mathrm{e}^{i\phi}$ and the conditions in Eq. (4.54) leads to the following simplification for $M_{\Delta,\gamma=0}$, $M^+_{\Delta_\uparrow,\Delta_\downarrow,\gamma=0}$ and $M^-_{\Delta_\uparrow,\Delta_\downarrow,\gamma=0}$

$$\begin{aligned}
&\left(M_{\Delta,\gamma=0} + M^+_{\Delta_\uparrow,\Delta_\downarrow,\gamma=0} + M^-_{\Delta_\uparrow,\Delta_\downarrow,\gamma=0}\right)\Big|_{|\mathbf{n}|=0}\\
&= -\tilde{V}\left[\cos(\phi)\tau_1 - \sin(\phi)\tau_2\right] \otimes \left[\sigma_3\,|\Delta| + \sigma_1\,|\Delta_\uparrow|\cos\left(\phi_\downarrow - \phi\right) + \sigma_2\,|\Delta_\uparrow|\sin\left(\phi_\downarrow - \phi\right)\right] \otimes \gamma_0.
\end{aligned}$$

Writing $|\Delta| = m_0 \cos(\theta)$ and $|\Delta_\uparrow| = m_0 \sin(\theta)$, where $m = m_0$ at the minimum of the energy, leads to

$$\begin{aligned}&\left(M_{\Delta,\gamma=0} + M^+_{\Delta_\uparrow,\Delta_\downarrow,\gamma=0} + M^-_{\Delta_\uparrow,\Delta_\downarrow,\gamma=0}\right)\Big|_{|\mathbf{n}|=0} \\ &= -\tilde{V} m_0 \left[\cos(\phi)\tau_1 - \sin(\phi)\tau_2\right] \otimes \left[\cos(\theta)\,\sigma_3 + \sin(\theta)\left(\sigma_1 \cos\left(\phi_\downarrow - \phi\right) + \sigma_2 \sin\left(\phi_\downarrow - \phi\right)\right)\right] \otimes \gamma_0.\end{aligned} \tag{4.55}$$

Ground-State Energy for $\Delta' \neq 0$
Now, the ground-state energy can be calculated including both the Kekule and hidden order using the condition $|\mathbf{n}| = 0$. The same relation as before is used to determine the energy

$$\sum_{\mathbf{q}} \left(E_{0,m,\Delta'} + M_t + M_\mu + M_{m,\gamma=0} + M_{\Delta'}\right) \Psi = E_{m,\Delta'\gamma=0} \Psi.$$

This yields

$$E_{0,m,\Delta'} = 6N\tilde{V}\left(m^2 + 2\left|\Delta'\right|^2\right).$$

Squaring $M_t + M_\mu + M_{m,\gamma=0} + M_{\Delta'}$ leads to

$$\begin{aligned}&\left(M_t + M_\mu + M_{m,\gamma=0} + M_{\Delta'}\right)^2 = \left(M_t + M_\mu + M_{m,\gamma=0}\right)^2 + M^2_{\Delta'} \\ &+ \left\{M_t + M_\mu + M_{\Delta,\gamma=0} + M^+_{\Delta_\uparrow,\Delta_\downarrow,\gamma=0} + M^-_{\Delta_\uparrow,\Delta_\downarrow,\gamma=0}\,,\, M_{\Delta'}\right\}.\end{aligned}$$

One can compute that

$$\left\{M_t\,,\, M_{\Delta'}\right\} = 0, \qquad \left\{M_\mu\,,\, M_{\Delta'}\right\} = 0.$$

The following is imposed

$$\left\{M_{\Delta,\gamma=0} + M^+_{\Delta_\uparrow,\Delta_\downarrow,\gamma=0} + M^-_{\Delta_\uparrow,\Delta_\downarrow,\gamma=0}\,,\, M_{\Delta',}\right\} = 0.$$

For this to hold, a condition needs to be derived for the relative phase between the Kekule and hidden order. To do this, one looks at Eq. (4.55), which describes the Kekule order at minimal energy. One can see immediately that the terms for the spin and sublattice-valley space anticommute. Therefore, this condition is computed in the particle-hole space. For all the components of the Kekule order, the dependence in the particle-hole space is the same. This yields the following

$$\begin{aligned}&\left\{\cos(\phi)\,\tau_1 - \sin(\phi)\,\tau_2\,,\, \mathrm{Re}(\Delta')\tau_2 + \mathrm{Im}(\Delta')\tau_1\right\} = 2\cos(\phi)\,\mathrm{Im}(\Delta') - 2\sin(\phi)\,\mathrm{Re}(\Delta') \\ &= 2\left|\Delta'\right|\left[\cos(\phi)\sin(\varphi) - \sin(\phi)\cos(\varphi)\right] = 2\left|\Delta'\right|\sin\left(\phi - \varphi\right),\end{aligned}$$

where $\Delta' = |\Delta'|\,\mathrm{e}^{i\varphi}$. Therefore, for the anticommutation relation to be zero the relative phase between the Kekule and hidden-order parameters should be zero. This leads to the following

$$\left(M_t + M_\mu + M_{m,\gamma=0} + M_{\Delta'}\right)^2 = \left(M_t + M_\mu + M_{m,\gamma=0}\right)^2 + M^2_{\Delta'}.$$

The first part was already calculated before and the last term leads to

$$M^2_{\Delta'} = \frac{v_F^2}{t^2}|q|^2 \tilde{V}^2 \left|\Delta'\right|^2 \left(\tau_0 \otimes \sigma_0 \otimes \mathbb{I}\right).$$

Therefore, the result is

$$\begin{aligned}(M_t + M_\mu + M_{m,\gamma=0} + M_{\Delta'})^2 &= \left(v_F^2|q|^2 + \mu^2 + \tilde{V}^2 m^2 + \frac{v_F^2}{t^2}|q|^2\tilde{V}^2\,|\Delta'|^2\right)(\tau_0 \otimes \sigma_0 \otimes \mathbb{I}) \\ &\quad -2\mu\, v_F\left[\tau_3 \otimes \sigma_0 \otimes (i\gamma_0\gamma_1 q_y - i\gamma_0\gamma_2 q_x)\right],\end{aligned}$$

where the condition $|\mathbf{n}| = 0$ was applied. Diagonalizing this term leads to the dispersion

$$(\omega_{m,\Delta',\gamma=0;s})^2 = (v_F|q| + s\mu)^2 + \tilde{V}^2 m^2 + \frac{v_F^2}{t^2}|q|^2\tilde{V}^2\,|\Delta'|^2,$$

where $s = \pm$. Now the energy is given by

$$E_{m,\Delta',\gamma=0} = E_{0,m,\Delta'} \pm \sum_{\mathbf{q};s=\pm} \omega_{m,\Delta',\gamma=0;s},$$

such that the ground-state energy reads

$$\begin{aligned}E_{\text{g.s.},m,\Delta',\gamma=0} &= E_{0,m,\Delta'} - \sum_{\mathbf{q};s=\pm} \omega_{m,\Delta',\gamma=0;s} \\ &= 6N\tilde{V}\left(m^2 + 2\,|\Delta'|^2\right) - 4N\sum_{s=\pm}\int \frac{\mathrm{d}\mathbf{q}}{(2\pi)^2}\sqrt{(v_F|q| + s\mu)^2 + \tilde{V}^2 m^2 + \frac{v_F^2}{t^2}|q|^2\tilde{V}^2\,|\Delta'|^2},\end{aligned}$$

where $\sum_{\mathbf{q}} \to 4N\int \mathrm{d}\mathbf{q}/(2\pi)^2$ with the extra factor of 2 coming from the spin degree of freedom and s representing the particle-hole degree of freedom, respectively. This leads to the final result for the ground state per honeycomb lattice site

$$\frac{E_{\text{g.s.},m,\Delta',\gamma=0}}{4N} = \frac{3\tilde{V}\left(m^2 + 2\,|\Delta'|^2\right)}{2} - \sum_{s=\pm}\int \frac{\mathrm{d}\mathbf{q}}{(2\pi)^2}\sqrt{(v_F|q| + s\mu)^2 + \tilde{V}^2 m^2 + \frac{v_F^2}{t^2}|q|^2\tilde{V}^2\,|\Delta'|^2}, \tag{4.56}$$

which in the limit $\mu = 0$ corresponds to the result found in Ref. [5]. One can clearly see how the Kekule order m acts as a mass term opening up a gap in the energy spectrum, as shown in Fig. 4.5. The hidden order, on the other hand, is linear in q and upon sending μ to zero it can be seen that it renormalizes the Fermi velocity v_F as shown in Fig. 4.6.

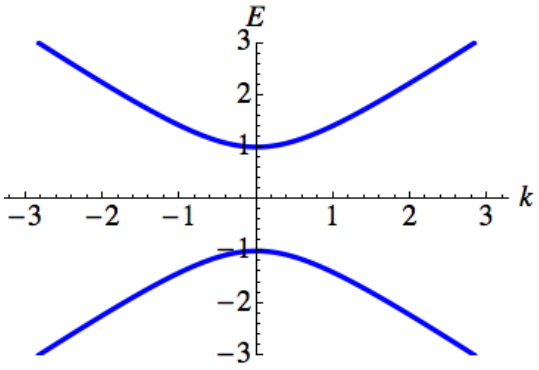

Figure 4.5: Schematic plot of how the Kekule order m opens a gap in the energy spectrum according to $E = \sqrt{k^2 + m^2}$.

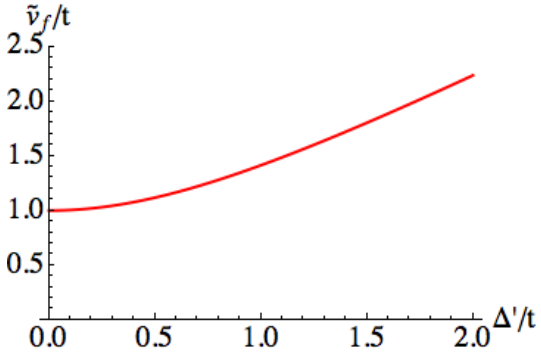

Figure 4.6: Schematic plot of how, at zero chemical potential, the hidden order Δ' renormalizes v_F according to $\tilde{v}_F/t = \sqrt{1 + |\Delta'|^2/t^2}$, where $\tilde{v}_F$ is the renormalized Ferm velocity.

Zero Temperature

Now, the zero-temperature gap equation, critical couplings and zero-temperature gaps will be computed.

Zero-Temperature Gap Equation
To find the zero-temperature gap equations for the Kekule and hidden order, one needs to minimize the ground-state energy in Eq. (4.56) with respect to the corresponding order parameter. For the Kekule order, this yields

$$0 = \frac{3\tilde{V}}{2} - \frac{\tilde{V}^2}{2} \sum_{s=\pm} \int \frac{\mathrm{d}\mathbf{q}}{(2\pi)^2} \frac{1}{\sqrt{(v_F|q| + s\mu)^2 + \tilde{V}^2 m^2(0) + \frac{v_F^2}{t^2}|q|^2 \tilde{V}^2 |\Delta'(0)|^2}},$$

such that the zero-temperature gap equation for the Kekule order reads

$$1 = \frac{\tilde{V}}{3} \sum_{s=\pm} \int \frac{\mathrm{d}\mathbf{q}}{(2\pi)^2} \frac{1}{\sqrt{(v_F|q| + s\mu)^2 + \tilde{V}^2 m^2(0) + \frac{v_F^2}{t^2}|q|^2 \tilde{V}^2 |\Delta'(0)|^2}}. \tag{4.57}$$

In Fig. 4.7 one can find the solution for this equation. Performing the same procedure for the hidden order leads to the zero-temperature gap equation for the hidden order

$$1 = \frac{\tilde{V}}{6} \frac{v_F^2}{t^2} \sum_{s=\pm} \int \frac{\mathrm{d}\mathbf{q}}{(2\pi)^2} \frac{|q|^2}{\sqrt{(v_F|q| + s\mu)^2 + \tilde{V}^2 m^2(0) + \frac{v_F^2}{t^2}|q|^2 \tilde{V}^2 |\Delta'(0)|^2}}. \tag{4.58}$$

In Fig. 4.8, the solution to this equation is shown.

Critical Couplings
At half-filling, i.e. $\mu = 0$, the Fermi energy is exactly at the Dirac points, at which the density of states ρ is zero, as was shown in Fig. 3.6. This means that the system is in a quantum critical regime. In this regime, there is a critical interaction at which the superconducting

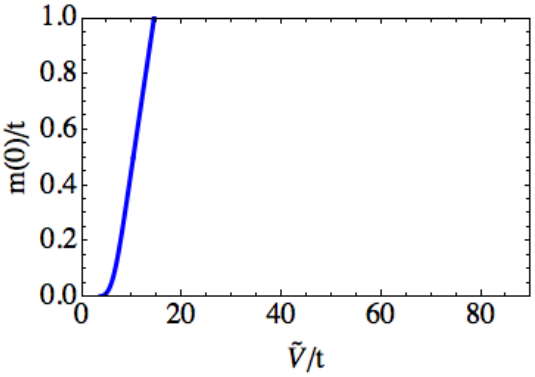

Figure 4.7: Solutions of the zero-temperature gap equation for the Kekule order with $v_F/t = \Lambda = 1$, $\Delta' = 0$ and $\mu/t = 0.25$.

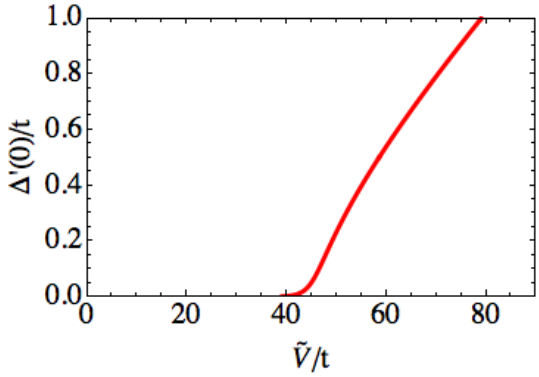

Figure 4.8: Solutions of the zero-temperature gap equation for the hidden order with $v_F/t = \Lambda = 1$, $m = 0$ and $\mu/t = 0.25$.

order appears. The value of the critical couplings can be calculated for both orders using Eqs. (4.57) and (4.58) and using that the gap is closed at the critical coupling. For the Kekule order this leads to

$$1 = \frac{2\tilde{V}_c}{3}\int \frac{\mathrm{d}\mathbf{q}}{(2\pi)^2}\frac{1}{v_F|q|} = \frac{2\tilde{V}_c}{3}\int_0^{2\pi}\mathrm{d}\theta\int_0^{\Lambda}\frac{\mathrm{d}q}{(2\pi)^2}\frac{q}{v_F|q|} = \frac{\tilde{V}_c}{3\pi v_F}\Lambda,$$

where Λ is the high-energy cut-off that goes with $1/a$. Therefore, the critical coupling $\tilde{V}_c$ for the Kekule order reads

$$\tilde{V}_c = \frac{3\pi v_F}{\Lambda}. \tag{4.59}$$

Similarly, for the hidden order one finds

$$1 = \frac{\tilde{V}_c'}{3}\frac{v_F^2}{t^2}\int \frac{\mathrm{d}\mathbf{q}}{(2\pi)^2}\frac{|q|^2}{v_F|q|} = \frac{\tilde{V}_c'}{3}\frac{v_F}{t^2}\int_0^{2\pi}\mathrm{d}\theta\int_0^{\Lambda}\frac{\mathrm{d}q}{(2\pi)^2}\,q^2 = \frac{\tilde{V}_c'}{6\pi}\frac{v_F}{t^2}\cdot\frac{1}{3}\Lambda^3 = \frac{\tilde{V}_c' v_F\Lambda^3}{18\pi t^2},$$

such that critical coupling $\tilde{V}_c'$ for the hidden order reads

$$\tilde{V}_c' = \frac{18\pi t^2}{v_F\Lambda^3}. \tag{4.60}$$

Setting $v_F/t = \Lambda = 1$ yields $\tilde{V}_c/t = 3\pi$ and $\tilde{V}_c'/t = 18\pi$ for the critical couplings for the Kekule and hidden order, respectively. Clearly, in this limit $\tilde{V}_c/t < \tilde{V}_c'/t$, which means that a much smaller interaction strength is needed to enter the Kekule order than the hidden order. This is the first evidence that the Kekule order is preferred over the hidden order.[1]

Zero-Temperature Gap for Kekule Order

As mentioned before, Eqs. (4.57) and (4.58) can be solved analytically in the strong- and weak-coupling limit with $|\tilde{V}| > |\tilde{V}_c|$ and $|\tilde{V}| < |\tilde{V}_c|$, respectively. The zero-temperature gap will be calculated at zero and finite chemical potential. First the Kekule gap and then the hidden order gap is determined.

[1]Roy and Herbut rightfully point out that this conclusion might become invalid upon including particles further away from the Fermi energy.

To find the zero-temperature gap $m(0)$, Eq. (4.57) is solved for finite μ and $\Delta' = 0$. This yields

$$\begin{aligned} 1 &= \frac{\tilde{V}}{3}\sum_{s=\pm}\int \frac{\mathrm{d}\mathbf{q}}{(2\pi)^2}\frac{1}{\sqrt{(v_F|q|+s\mu)^2+\tilde{V}^2m^2(0)}} \\ &= \frac{\tilde{V}}{3}\sum_{s=\pm}\int_0^{2\pi}\mathrm{d}\theta\int_0^{\Lambda}\frac{\mathrm{d}q}{(2\pi)^2}\frac{q}{\sqrt{(v_F|q|+s\mu)^2+\tilde{V}^2m^2(0)}} \\ &= \frac{\tilde{V}}{6\pi v_F^2}\left[2\left(v_F\Lambda-\sqrt{\mu^2+\tilde{V}^2m^2(0)}\right)+\mu\ln\left(\frac{\mu+\sqrt{\mu^2+\tilde{V}^2m^2(0)}}{-\mu+\sqrt{\mu^2+\tilde{V}^2m^2(0)}}\right)\right]. \end{aligned} \tag{4.61}$$

The integral is solved explicitly in Appendix 6.3.3.

First, this equation is solved for the zero-temperature gap at $\mu = 0$, $m(0, \mu = 0)$. This leads to

$$1 = \frac{\tilde{V}}{3\pi v_F^2}\left[v_F\Lambda - \tilde{V}m(0,\mu=0)\right],$$

such that

$$m(0,\mu=0) = \frac{3\pi v_F}{\tilde{V}_c\tilde{V}}\left(1-\frac{\tilde{V}_c}{\tilde{V}}\right). \tag{4.62}$$

Next, Eq. (4.61) is solved for the zero-temperature gap $m(0)$ in the strong-coupling limit, $|\tilde{V}| > |\tilde{V}_c|$ and $m(0)/\mu \gg 1$. Note that the last condition implies that $\mu \ll 1$, which means that the Fermi energy is very close to the Dirac points and the density of states ρ is nearly negligible. Therefore, in this limit the system is far away from the BCS limit, which requires a finite ρ, and the resulting zero-temperature gap is expected to have power-law behavior. Rewriting Eq. (4.61) yields

$$1 = \frac{\tilde{V}}{6\pi v_F^2}\left[2v_F\Lambda - 2\mu\sqrt{1+\tilde{V}^2\frac{m^2(0)}{\mu^2}}+\mu\ln\left(\frac{\sqrt{1+\tilde{V}^2\frac{m^2(0)}{\mu^2}}+1}{\sqrt{1+\tilde{V}^2\frac{m^2(0)}{\mu^2}}-1}\right)\right]. \tag{4.63}$$

Now, the limit $m(0)/\mu \to \infty$ is taken. This leads to

$$\begin{aligned} 1 &= \frac{\tilde{V}}{6\pi v_F^2}\left[2v_F\Lambda - 2\mu\tilde{V}\frac{m(0)}{\mu}+\mu\ln\left(\frac{\sqrt{1+\tilde{V}^2\frac{m^2(0)}{\mu^2}}+1}{\sqrt{1+\tilde{V}^2\frac{m^2(0)}{\mu^2}}-1}\right)\Bigg|_{m(0)/\mu\to\infty}\right] \\ &= \frac{\tilde{V}}{3\pi v_F^2}\left[v_F\Lambda - \tilde{V}m(0)+\frac{\mu^2}{\tilde{V}m(0)}\right], \end{aligned}$$

where the derivation of the limit of the natural logarithm can be found in Appendix 6.3.4. This leads to the following quadratic equation

$$\tilde{V}^2m^2(0) - \tilde{V}^2m(0,\mu=0)m(0) - \mu^2 = 0.$$

Using the limit $|\tilde{V}| > |\tilde{V}_c|$ leads to the final answer

$$m(0) \to \frac{m\left(0, \mu = 0\right)}{2} \left[1 + \sqrt{1 + \frac{4\mu^2}{\tilde{V}^2 m^2\left(0, \mu = 0\right)}}\right]. \tag{4.64}$$

Indeed, as predicted, there is power-law behavior.

Lastly, Eq. (4.61) is evaluated the weak-coupling limit, $|\tilde{V}| < |\tilde{V}_c|$ and $m(0)/\mu \ll 1$. Note that in this case the last condition implies that $\mu \gg 1$, which means that the Fermi energy is far away from the Dirac points and the density of states ρ is large. Therefore, in this limit the system is in the BCS limit and BCS-like behavior is expected for the resulting zero-temperature gap. In the weak-coupling limit, Eq. (4.63) can be written as

$$1 = \frac{\tilde{V}}{6\pi v_F^2} \left[2v_F\Lambda - 2\mu + \mu \ln\left(\frac{\sqrt{1 + \tilde{V}^2 \frac{m^2(0)}{\mu^2}} + 1}{\sqrt{1 + \tilde{V}^2 \frac{m^2(0)}{\mu^2}} - 1}\right)\Bigg|_{m(0)/\mu \to 0}\right].$$

The limit in the natural logarithm is straightforwardly solved using

$$\ln\left(\frac{\sqrt{1+x^2}+1}{\sqrt{1+x^2}-1}\right) \approx \ln\left(\frac{\sqrt{1+x^2}+1}{1+\frac{x^2}{2}+\mathcal{O}\left(x^4\right)-1}\right) \xrightarrow{x\to 0} \ln\left(\frac{2}{\frac{x^2}{2}}\right) = \ln\left(\frac{4}{x^2}\right) = 2\ln\left(\frac{2}{x}\right).$$

This yields

$$1 = \frac{\tilde{V}}{6\pi v_F^2} \left[2v_F\Lambda - 2\mu + 2\mu \ln\left(\frac{2\mu}{\tilde{V} m(0)}\right)\right].$$

Solving for $m(0)$ leads to

$$m(0) \to \frac{2\mu}{\tilde{V}} \mathrm{e}^{\frac{\tilde{V}}{\mu} m(0,\mu=0) - 1}. \tag{4.65}$$

Therefore, the final result is

$$m(0, \mu = 0) = \frac{3\pi v_F}{\tilde{V}_c \tilde{V}} \left(1 - \frac{\tilde{V}_c}{\tilde{V}}\right),$$

and

$$m\left(0, \mu\right) \to \begin{cases} \frac{m(0,\mu=0)}{2}\left[1 + \sqrt{1 + \frac{4\mu^2}{\tilde{V}_0^2\, m(0,\mu=0)^2}}\right], & |\tilde{V}| > |\tilde{V}_c|,\ m(0)/\mu \gg 1, \\ \frac{2\mu}{\tilde{V}} \mathrm{e}^{\frac{\tilde{V}}{\mu} m(0,\mu=0) - 1}, & |\tilde{V}| < |\tilde{V}_c|,\ m(0)/\mu \ll 1, \end{cases}$$

where now it is written explicitly that $m(0) \equiv m\left(0, \mu\right)$ depends on a finite chemical potential.

Zero-Temperature Gap for Hidden Order

Next, the zero-temperature gap equation for the hidden order in Eq. (4.58) is evaluated in the strong- and weak-coupling limit for finite μ and $m = 0$. This yields

$$\begin{aligned}
1 &= \frac{\tilde{V}}{6}\frac{v_F^2}{t^2}\sum_{s=\pm}\int\frac{\mathrm{d}\mathbf{q}}{(2\pi)^2}\frac{|q|^2}{\sqrt{\left(v_F|q|+s\mu\right)^2+\tilde{V}^2m^2(0)+\frac{v_F^2}{t^2}|q|^2\tilde{V}^2\left|\Delta'(0)\right|^2}} \\
&= \frac{\tilde{V}}{6}\frac{v_F^2}{t^2}\sum_{s=\pm}\int_0^{2\pi}\mathrm{d}\theta\int_0^{\Lambda}\frac{\mathrm{d}q}{(2\pi)^2}\frac{|q|^3}{\sqrt{\left(v_F|q|+s\mu\right)^2+\tilde{V}^2m^2(0)+\frac{v_F^2}{t^2}|q|^2\tilde{V}^2\left|\Delta'(0)\right|^2}} \\
&= \frac{\tilde{V}}{6}\frac{v_F}{t^2}\frac{1}{2\pi}\left\{2\Lambda\left[\frac{\Lambda^2}{3\sqrt{1+\alpha^2}}+\frac{\mu^2}{v_F^2}\left(\frac{3-\alpha^2}{(1+\alpha^2)^{5/2}}\right)\right]\right. \\
&\quad \left.+\frac{\mu^3}{v_F^3}\left[\frac{4\alpha^2-11}{9\left(1+\alpha^2\right)^3}+\ln\left(\frac{\sqrt{1+\alpha^2}+1}{\alpha}\right)\left(\frac{2-3\alpha^2}{(1+\alpha^2)^{7/2}}\right)\right]\right\},
\end{aligned} \tag{4.66}$$

where $\alpha \equiv \frac{\tilde{V}|\Delta'(0)|}{t}$. This integral is explicitly derived in Appendix 6.3.5.

In the limit $\mu \to 0$, the following is found

$$\begin{aligned}
1 &= \frac{\tilde{V}}{18}\frac{v_F}{\pi t^2}\frac{\Lambda^3}{\sqrt{1+\alpha(\mu=0)^2}} \\
\sqrt{1+\alpha(\mu=0)^2} &= \frac{\tilde{V}}{18}\frac{v_F}{\pi t^2}\Lambda^3 \\
1+\alpha(\mu=0)^2 &= \frac{\tilde{V}^2}{324}\frac{v_F^2}{\pi^2t^4}\Lambda^6 \\
\alpha(\mu=0) &= \sqrt{\frac{\tilde{V}^2}{324}\frac{v_F^2}{\pi^2t^4}\Lambda^6-1} \\
|\Delta'(0,\mu=0)| &= \frac{t}{\tilde{V}}\sqrt{\frac{\tilde{V}^2}{324}\frac{v_F^2}{\pi^2t^4}\Lambda^6-1},
\end{aligned}$$

such that the gap $|\Delta'(0,\mu=0)|$ is

$$|\Delta'(0,\mu=0)| = \frac{t}{\tilde{V}_c'}\sqrt{1-\left(\frac{\tilde{V}_c'}{\tilde{V}}\right)^2}. \tag{4.67}$$

Next, Eq. (4.66) is solved for the zero-temperature gap $\Delta'(0)$ in the strong-coupling limit, $|\tilde{V}| > |\tilde{V}_c'|$ and $|\Delta'(0)|/t \gg 1$. This yields

$$\begin{aligned}
1 &\approx \frac{\tilde{V}}{6}\frac{v_F}{t^2}\frac{1}{2\pi}\left\{2\Lambda\left[\frac{\Lambda^2}{3\alpha}+\frac{\mu^2}{v_F^2}\left(\frac{-\alpha^2}{\alpha^5}\right)\right]+\frac{\mu^3}{v_F^3}\left[\frac{4\alpha^2}{9\alpha^6}+\ln\left(\frac{\alpha}{\alpha}\right)\left(\frac{-3\alpha^2}{\alpha^7}\right)\right]\right\} \approx \frac{\tilde{V}}{18}\frac{v_F}{\pi t^2}\frac{\Lambda^3}{\alpha} \\
\alpha &\approx \frac{\tilde{V}}{18}\frac{v_F}{\pi t^2}\Lambda^3,
\end{aligned}$$

such that $|\Delta'(0)|$ reads

$$|\Delta'(0)| \to \frac{t}{\tilde{V}_c'}. \tag{4.68}$$

Lastly, Eq. (4.66) is evaluated in the weak-coupling limit, $|\tilde{V}| < |\tilde{V}_c'|$ and $|\Delta'(0)|/t \ll 1$. This leads to

$$1 \approx \frac{\tilde{V}}{6}\frac{v_F}{t^2}\frac{1}{2\pi}\left\{2\Lambda\left(\frac{\Lambda^2}{3}+3\frac{\mu^2}{v_F^2}\right)+\frac{\mu^3}{v_F^3}\left[2\ln\left(\frac{2}{\alpha}\right)-\frac{11}{3}\right]\right\},$$

where the second term can be neglected because $\Lambda \gg \mu/v_F$, such that

$$\begin{aligned} 1 &\approx \frac{\tilde{V}}{6}\frac{v_F}{t^2}\frac{1}{2\pi}\left\{\frac{2\Lambda^3}{3}+\frac{\mu^3}{v_F^3}\left[2\ln\left(\frac{2}{\alpha}\right)-\frac{11}{9}\right]\right\} \\ 2\ln\left(\frac{2}{\alpha}\right) &\approx \frac{11}{9}+\frac{12\pi t^2 v_F^2}{\tilde{V}\mu^3}-\frac{2\Lambda^3 v_F^3}{3\mu^3} \\ \alpha &\approx 2\exp\left(\frac{\Lambda^3 v_F^3}{3\mu^3}-\frac{6\pi t^2 v_F^2}{\tilde{V}\mu^3}-\frac{11}{18}\right), \end{aligned}$$

which leads to the following solution for $|\Delta'(0)|$:

$$|\Delta'(0)| \to \frac{2t}{\tilde{V}}\exp\left[\frac{6\pi t^2 v_F^2}{\tilde{V}_c'\mu^3}\left(1-\frac{\tilde{V}_c'}{\tilde{V}}\right)-\frac{11}{18}\right]. \tag{4.69}$$

Therefore, the final result is

$$|\Delta'(0,\mu=0)| = \frac{t}{\tilde{V}_c'}\sqrt{1-\left(\frac{\tilde{V}_c'}{\tilde{V}}\right)^2},$$

and

$$|\Delta'|(0,\mu) \to \begin{cases} \frac{t}{\tilde{V}_c'}, & |\tilde{V}| > |\tilde{V}_c|,\ |\Delta'(0)|/t \gg 1, \\ \frac{2t}{\tilde{V}}\,\mathrm{e}^{\frac{6\pi t^2 v_F^2}{\tilde{V}_c'\mu^3}\left(1-\frac{\tilde{V}_c'}{\tilde{V}}\right)-\frac{11}{18}}, & |\tilde{V}| < |\tilde{V}_c|,\ |\Delta'(0)|/t \ll 1, \end{cases}$$

where now it is written explicitly that $|\Delta'(0)| \equiv |\Delta'(0,\mu)|$ depends on a finite chemical potential.

Finite-Temperature Gap Equations

Next, the gap equations for m and Δ' are computed at finite temperature. These equations can be found by minimizing the thermodynamical potential $\Omega_{m,\Delta'}$. Therefore, first the thermodynamical potential will be derived followed by the computation of the finite-temperature gap equations for the Kekule and hidden order. Lastly, it is evaluated how the critical couplings in Eqs. (4.59) and (4.60) behave when the temperature is non-zero.

Thermodynamical Potential
To find a general expression for the thermodynamical potential Ω, one needs to start from the partition function

$$Z = \mathrm{e}^{-\beta\Omega} = \mathrm{Tr}\left(\mathrm{e}^{-\beta H}\right),$$

where $\beta = 1/(k_B T)$. Plugging in a general form of the Hamiltonian $H = E_0 + \sum_{\mathbf{q}} \Psi^\dagger_{\mathbf{q}} \omega \Psi_{\mathbf{q}}$ leads to

$$Z = \mathrm{Tr}\left(\mathrm{e}^{-\beta H}\right) = \mathrm{Tr}\left[\mathrm{e}^{-\beta\left(E_0 + \sum_{\mathbf{q}} \Psi^\dagger_{\mathbf{q}} \omega \Psi_{\mathbf{q}}\right)}\right] = \mathrm{e}^{-\beta E_0} \mathrm{Tr}\left[\mathrm{e}^{-\beta \sum_{\mathbf{q}} \Psi^\dagger_{\mathbf{q}} \omega \Psi_{\mathbf{q}}}\right].$$

The dispersion relation can be written as

$$\sum_{\mathbf{q}} \Psi^\dagger_{\mathbf{q}} \omega \Psi_{\mathbf{q}} = \sum_{\mathbf{q}} \hat{\omega} \Psi^\dagger_{\mathbf{q}} \Psi_{\mathbf{q}} = \sum_{\mathbf{q}} \tilde{\omega} \hat{n}_{\mathbf{q}},$$

where $\tilde{\omega}$ are the eigenvalues of the equation, and $\hat{n}_{\mathbf{q}} = \Psi^\dagger_{\mathbf{q}} \Psi_{\mathbf{q}}$ is the number operator. This yields the following for the partition function

$$Z = \mathrm{e}^{-\beta E_0} \mathrm{Tr}\left[\mathrm{e}^{-\beta \sum_{\mathbf{q}} \tilde{\omega} \hat{n}_{\mathbf{q}}}\right] = \mathrm{e}^{-\beta E_0} \prod_{\mathbf{q}} \sum_{\mathbf{q}} \langle n_{\mathbf{q}} | \, \mathrm{e}^{-\beta \tilde{\omega} \hat{n}_{\mathbf{q}}} \, | n_{\mathbf{q}} \rangle .$$

$\hat{n}_{\mathbf{q}}$ is the number operator for fermions, and can therefore only have the values zero or one. This leads to

$$\begin{aligned} Z &= \mathrm{e}^{-\beta E_0} \prod_{\mathbf{q}} \left(\langle 0 | \, \mathrm{e}^0 \, | 0 \rangle + \langle 1 | \, \mathrm{e}^{-\beta \tilde{\omega}} \, | 1 \rangle \right) = \mathrm{e}^{-\beta E_0} \prod_{\mathbf{q}} \left(1 + \mathrm{e}^{-\beta \tilde{\omega}}\right) \\ &= \mathrm{e}^{-\beta E_0} \prod_{\mathbf{q}} \mathrm{e}^{\ln\left(1 + \mathrm{e}^{-\beta \tilde{\omega}}\right)} = \mathrm{e}^{-\beta E_0} \mathrm{e}^{\sum_{\mathbf{q}} \ln\left(1 + \mathrm{e}^{-\beta \tilde{\omega}}\right)} = \mathrm{e}^{-\beta \Omega}, \end{aligned}$$

such that the thermodynamic potential reads

$$\Omega = E_0 - \frac{1}{\beta} \sum_{\mathbf{q}} \ln\left(1 + \mathrm{e}^{-\beta \tilde{\omega}}\right). \tag{4.70}$$

Plugging in the energy for the condensate $E_{0,m,\Delta'}$ and the dispersion relation $\omega_{m,\Delta';s,s'}$ for the Kekule and hidden order yields the following for the thermodynamical potential $\Omega_{m,\Delta'}$

$$\begin{aligned} \Omega_{m,\Delta'} &= 6N\tilde{V}^2 \left(m^2 + 2\left|\Delta'\right|^2\right) \\ &\quad - \frac{1}{\beta} \sum_{\mathbf{q};s,s'=\pm} \ln\left[1 + \exp\left(-\beta s \sqrt{\left(v_F|q| + s'\mu\right)^2 + \tilde{V}^2 m^2 + \frac{v_F^2}{t^2}|q|^2 \tilde{V}^2 \left|\Delta'\right|^2}\right)\right]. \end{aligned} \tag{4.71}$$

In Figs. 4.9 and 4.10, it is shown how the thermodynamical potential behaves with increasing order parameter. When the system enters the superconducting phase, a second-order phase transition takes place, which is clearly visible in the Figures.

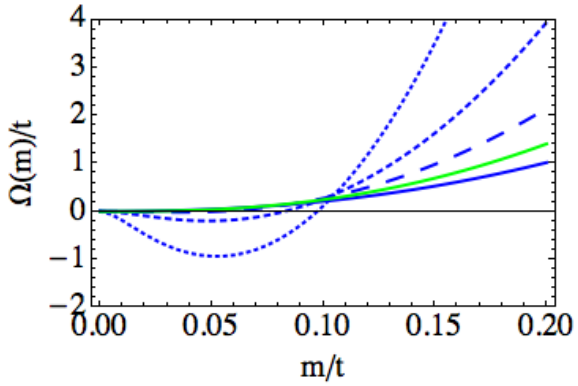

Figure 4.9: The evolution of the thermodynamical potential for the Kekule order with $v_F/t = \Lambda = 1$, $\mu/t = 0$ and $\Delta'/t = 0$ for different couplings: $\tilde{V}/t = 2\pi$ (solid), $\tilde{V}/t = 3\pi$ (green), $\tilde{V}/t = 5\pi$ (large dashed), $\tilde{V}/t = 10\pi$ (small dashed) and $\tilde{V}/t = 25\pi$ (dotted).

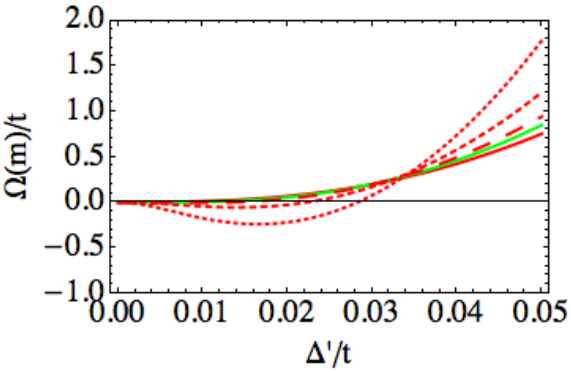

Figure 4.10: The evolution of the thermodynamical potential for the hidden order with $v_F/t = \Lambda = 1$, $\mu/t = 0$ and $m/t = 0$ for different couplings: $\tilde{V}/t = 15\pi$ (solid), $\tilde{V}/t = 18\pi$ (green), $\tilde{V}/t = 21\pi$ (large dashed), $\tilde{V}/t = 30\pi$ (small dashed) and $\tilde{V}/t = 50\pi$ (dotted).

Kekule Order

Minimizing Eq. (4.71) with respect to the Kekule gap m leads to

$$0 = 12N\tilde{V}m - \frac{1}{\beta}\sum_{\mathbf{q};s,s'=\pm}\frac{1}{1+\mathrm{e}^{-\beta\omega_{m,\Delta';s,s'}}}\left(\frac{\mathrm{d}}{\mathrm{d}m}\mathrm{e}^{-\beta\omega_{m,\Delta';s,s'}}\right), \tag{4.72}$$

where

$$\omega_{m,\Delta';s,s'} = s\sqrt{\left(v_F|q|+s'\mu\right)^2 + \tilde{V}^2m^2 + \frac{v_F^2}{t^2}|q|^2\tilde{V}^2\left|\Delta'\right|^2}.$$

The derivative in the second term yields

$$\begin{aligned}\frac{\mathrm{d}}{\mathrm{d}m}\mathrm{e}^{-\beta\omega_{m,\Delta';s,s'}} &= -\beta\left(\frac{\mathrm{d}}{\mathrm{d}m}s\sqrt{\left(v_F|q|+s'\mu\right)^2 + \tilde{V}^2m^2 + \frac{v_F^2}{t^2}|q|^2\tilde{V}^2\left|\Delta'\right|^2}\right)\mathrm{e}^{-\beta\omega_{m,\Delta';s,s'}}\\ &= \frac{-\beta s\tilde{V}^2m}{\sqrt{\left(v_F|q|+s'\mu\right)^2 + \tilde{V}^2m^2 + \frac{v_F^2}{t^2}|q|^2\tilde{V}^2\left|\Delta'\right|^2}}\mathrm{e}^{-\beta\omega_{m,\Delta';s,s'}} = -\frac{\beta\tilde{V}^2m}{\omega_{m,\Delta';s,s'}}\mathrm{e}^{-\beta\omega_{m,\Delta';s,s'}}.\end{aligned}$$

Plugging this result back into Eq. (4.72) leads to

$$12N\tilde{V}m = -\tilde{V}^2m\sum_{\mathbf{q};s,s'=\pm}\frac{N_{FD}\left(\omega_{m,\Delta';s,s'}\right)}{\omega_{m,\Delta';s,s'}},$$

where $N_{FD}\left(\omega_{m,\Delta';s,s'}\right)$ is the Fermi-Dirac distribution $N_{FD}\left(\omega_{m,\Delta';s,s'}\right) = \left(\mathrm{e}^{\beta\omega_{m,\Delta';s,s'}}+1\right)^{-1}$. Making the sum over s explicit in the last term leads to

$$\begin{aligned}&\sum_{s=\pm}\frac{1}{\mathrm{e}^{\beta s\omega_{m,\Delta';s'}}+1}\frac{1}{s\omega_{m,\Delta';s'}} = \frac{1}{\omega_{m,\Delta';s'}}\left(\frac{1}{\mathrm{e}^{\beta\omega_{m,\Delta';s'}}+1} - \frac{1}{\mathrm{e}^{-\beta\omega_{m,\Delta';s'}}+1}\right)\\ &= \frac{1}{\omega_{m,\Delta';s'}}\left(\frac{\mathrm{e}^{-\frac{\beta}{2}\omega_{m,\Delta';s'}}}{\mathrm{e}^{\frac{\beta}{2}\omega_{m,\Delta';s'}}+\mathrm{e}^{-\frac{\beta}{2}\omega_{m,\Delta';s'}}} - \frac{\mathrm{e}^{\frac{\beta}{2}\omega_{m,\Delta';s'}}}{\mathrm{e}^{-\frac{\beta}{2}\omega_{m,\Delta';s'}}+\mathrm{e}^{\frac{\beta}{2}\omega_{m,\Delta';s'}}}\right) = -\frac{1}{\omega_{m,\Delta';s'}}\tanh\left(\frac{\beta\omega_{m,\Delta';s'}}{2}\right),\end{aligned}$$

such that

$$\begin{aligned} 12N\tilde{V}m &= \tilde{V}^2 m \sum_{\mathbf{q};s=\pm} \frac{1}{\omega_{m,\Delta';s}} \tanh\left(\frac{\beta\omega_{m,\Delta';s}}{2}\right) \\ 1 &= \frac{\tilde{V}}{12N} \sum_{\mathbf{q};s=\pm} \frac{1}{\omega_{m,\Delta';s}} \tanh\left(\frac{\beta\omega_{m,\Delta';s}}{2}\right). \end{aligned}$$

Writing the sum over $\mathbf{q}$ as an integral according to $\sum_{\mathbf{q}} \to 4N \int \mathrm{d}\mathbf{q}/(2\pi)^2$ leads to the gap equation for the Kekule order

$$1 = \frac{\tilde{V}}{3} \sum_{s=\pm} \int \frac{\mathrm{d}\mathbf{q}}{(2\pi)^2} \frac{1}{\omega_{m,\Delta';s}} \tanh\left(\frac{\beta\omega_{m,\Delta';s}}{2}\right), \tag{4.73}$$

where

$$\omega_{m,\Delta';s} = \sqrt{\left(v_F|q| + s\mu\right)^2 + \tilde{V}^2 m^2 + \frac{v_F^2}{t^2}|q|^2\tilde{V}^2\left|\Delta'\right|^2}. \tag{4.74}$$

In the limit $T \to 0$, the tangent hyperbolic goes to one and this gap equation corresponds to the zero-temperature gap equation in Eq. (4.57), as it should.

Hidden Order
Minimizing Eq. (4.71) with respect to the hidden gap $|\Delta'|$ leads to

$$0 = 24N\tilde{V}\left|\Delta'\right| - \frac{1}{\beta} \sum_{\mathbf{q};s,s'=\pm} \frac{1}{1+\mathrm{e}^{-\beta\omega_{m,\Delta';s,s'}}} \left(\frac{\mathrm{d}}{\mathrm{d}\left|\Delta'\right|} \mathrm{e}^{-\beta\omega_{m,\Delta';s,s'}}\right), \tag{4.75}$$

where $\omega_{m,\Delta';s,s'} = s\,\omega_{m,\Delta';s'}$, with $\omega_{m,\Delta';s'}$ given by Eq. (4.74). Solving the derivative in the second term in the same manner as before leads to

$$\begin{aligned} &\frac{\mathrm{d}}{\mathrm{d}\Delta'^{\dagger}} \mathrm{e}^{-\beta\omega_{m,\Delta';s,s'}} = -\beta \left(\frac{\mathrm{d}}{\mathrm{d}\Delta'^{\dagger}} s\sqrt{\left(v_F|q| + s'\mu\right)^2 + \tilde{V}^2 m^2 + \frac{v_F^2}{t^2}|q|^2\tilde{V}^2\left|\Delta'\right|^2}\right) \mathrm{e}^{-\beta\omega_{m,\Delta';s,s'}} \\ &= \frac{-\beta s \frac{v_F^2}{t^2}|q|^2\tilde{V}^2\Delta'}{\sqrt{\left(v_F|q| + s'\mu\right)^2 + \tilde{V}^2 m^2 + \frac{v_F^2}{t^2}|q|^2\tilde{V}^2\left|\Delta'\right|^2}} \mathrm{e}^{-\beta\omega_{m,\Delta';s,s'}} = -\beta\frac{v_F^2|q|^2}{t^2}\frac{\tilde{V}^2\Delta'}{\omega_{m,\Delta';s,s'}} \mathrm{e}^{-\beta\omega_{m,\Delta';s,s'}}. \end{aligned}$$

Plugging this result back into Eq. (4.75) leads to

$$24N\tilde{V}\left|\Delta'\right| = -\frac{v_F^2|q|^2}{t^2}\tilde{V}^2\Delta' \sum_{\mathbf{q};s,s'=\pm} \frac{N_{FD}\left(\omega_{m,\Delta';s,s'}\right)}{\omega_{m,\Delta';s,s'}} = \frac{v_F^2|q|^2}{t^2}\tilde{V}^2\Delta' \sum_{\mathbf{q};s=\pm} \frac{1}{\omega_{m,\Delta';s}} \tanh\left(\frac{\beta\omega_{m,\Delta';s}}{2}\right),$$

where the sum over s was made explicit to obtain the last term in a similar fashion as before. Writing the sum over $\mathbf{q}$ as an integral leads to the following gap equation for the hidden order

$$1 = \frac{\tilde{V}}{6}\frac{v_F^2}{t^2} \sum_{s=\pm} \int \frac{\mathrm{d}\mathbf{q}}{(2\pi)^2} \frac{|q|^2}{\omega_{m,\Delta';s}} \tanh\left(\frac{\beta\omega_{m,\Delta';s}}{2}\right), \tag{4.76}$$

where $\omega_{m,\Delta';s}$ is given by Eq. (4.74). In the limit $T \to 0$, this gap equation corresponds to the zero-temperature gap equation in Eq. (4.58), as desired.

Critical Couplings for Finite Temperature
In Subsection 4.5.1, the critical couplings $\tilde{V}_c$ for the Kekule in Eq. (4.59) and $\tilde{V}'_C$ for the hidden order in Eq. (4.60) were calculated for zero temperature. With the gap equations in Eqs. (4.73) and (4.76), it is now possible to evaluate these critical couplings for non-zero temperature by requiring that the chemical potential is zero and the gaps are closed. In Fig. 4.11 it is shown that the critical couplings in fact increase with increasing temperature. From this figure it can be concluded that indeed the Kekule order is preferred over the hidden order.

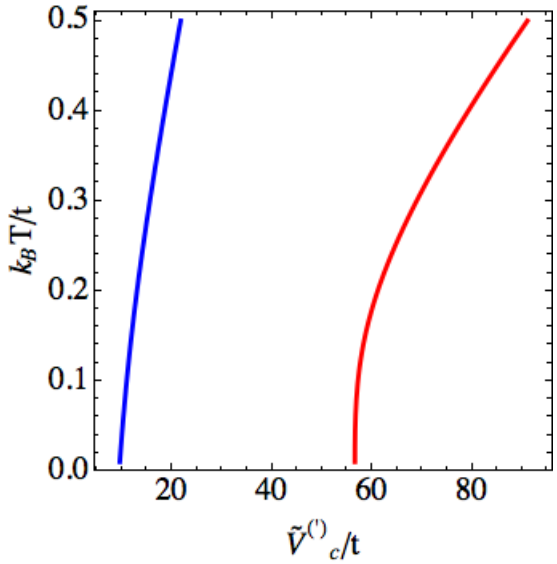

Figure 4.11: Solutions of the finite-temperature gap equation for the Kekule order (blue) and hidden order (red) with $v_F/t = \Lambda = 1$, $\mu/t = 0$ and $m/t = \Delta'/t = 0$. The critical coupling increases with increasing temperature.

Critical Temperature

The next step is the determination of the critical temperatures for the Kekule and hidden order. When a superconductor is cooled and the critical temperature is reached, it enters the superconducting phase and a superconducting gap opens. Therefore, this critical temperature can be found by requiring that the gap is zero at this temperature. First, the critical temperature for the Kekule order will be calculated followed by that of the hidden order. The critical temperature can be found analytically in the strong- and weak-coupling limit. Lastly, the critical temperatures for both superconducting states is reviewed to see how it behaves with increasing chemical potential and coupling.

Kekule Order

To find the critical temperature for the Kekule order, Eq. (4.73) is solved imposing that $m(T_c) = 0$ and $\Delta' = 0$. This yields

$$\begin{aligned} 1 &= \frac{\tilde{V}}{3}\sum_{s=\pm}\int \frac{\mathrm{d}\mathbf{q}}{(2\pi)^2}\frac{1}{v_F|q|+s\mu}\tanh\left(\frac{\beta\left(v_F|q|+s\mu\right)}{2}\right) \\ &= \frac{\tilde{V}}{6\pi v_F}\left\{\frac{4}{\beta_c v_F}\ln\left[\frac{\cosh(\frac{\beta_c}{2}v_F\Lambda)}{\cosh(\frac{\beta_c}{2}\mu)}\right]+\frac{2\mu}{v_F}\int_0^{\frac{\beta_c}{2}\mu}\mathrm{d}u\,\frac{\tanh(u)}{u}\right\}. \end{aligned} \tag{4.77}$$

The integral is solved explicitly in Appendix. 6.3.6. In Fig. 4.12 the behavior of the gap with increasing temperature that follows from this equation is shown. It can clearly be seen there that with increasing temperature the gap decreases. The gap closes at the critical temperature. It can also be seen that with increasing chemical potential the gap is larger and the critical temperature is also larger. An explicit expression for the critical temperature can be derived in the strong- and weak-coupling limit.

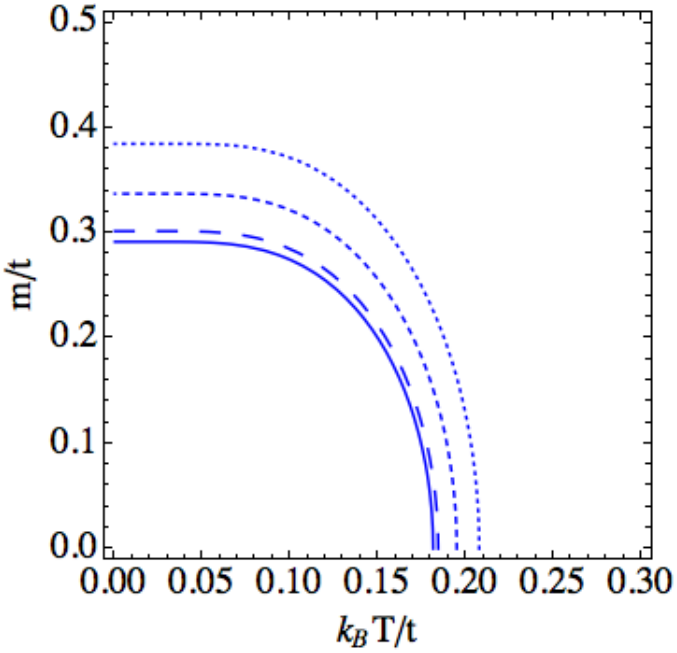

Figure 4.12: Solutions of the finite-temperature gap equation for the Kekule order with $v_F/t = \Lambda = 1$, $\Delta' = 0$ and $\tilde{V}/t = 4\pi$ for different values of the chemical potential: $\mu/t = 0$ (solid), $\mu/t = 0.1$ (large dashed), $\mu/t = 0.25$ (small dashed) and $\mu/t = 0.5$ (dotted).

In the strong-coupling limit, the critical temperature is much larger than the chemical potential, i.e. $\beta_c\mu \ll 1$. This leads to the following for Eq. (4.77)

$$\cosh\left(\frac{\beta_c}{2}\mu\right) = \frac{\mathrm{e}^{\frac{\beta_c}{2}\mu}+\mathrm{e}^{-\frac{\beta_c}{4}\mu}}{2} \xrightarrow{\beta_c\mu\ll 1} \frac{1+1}{2}+\mathcal{O}\left(\beta_c\mu\right) = 1+\mathcal{O}\left(\beta_c\mu\right),$$

such that

$$\ln\left[\cosh(\frac{\beta_c}{2}v_F\Lambda)\right] = \ln\left(\frac{\mathrm{e}^{\frac{\beta_c}{2}v_F\Lambda}+\mathrm{e}^{-\frac{\beta_c}{2}v_F\Lambda}}{2}\right) \xrightarrow{\Lambda\gg 1} \ln\left(\frac{\mathrm{e}^{\frac{\beta_c}{2}v_F\Lambda}}{2}\right) = \frac{\beta_c}{2}v_F\Lambda - \ln(2).$$

The integral leads to

$$\int_0^{\frac{\beta_c}{2}\mu} \mathrm{d}u \, \frac{\tanh(u)}{u} \xrightarrow{\beta_c\mu \ll 1} \tanh\left(\frac{\beta_c}{2}\mu\right) \frac{2}{\beta_c\mu} \approx 1,$$

where it is used that $\tanh(x)/x \approx 1 - x^2/3 + \mathcal{O}(x^4)$. Therefore, in the limit $\beta_c\mu \ll 1$, Eq. (4.77) yields

$$1 = \frac{\tilde{V}}{6\pi v_F}\left\{\frac{4}{\beta_c v_F}\left[\frac{\beta_c}{2}v_F\Lambda - \ln(2)\right] + \frac{2\mu}{v_F}\right\} = \frac{\tilde{V}}{6\pi v_F}\left[2\Lambda - \frac{4\ln(2)}{\beta_c v_F} + \frac{2\mu}{v_F}\right].$$

Using that $\beta_c = (k_B T_c)^{-1}$ and rewriting leads to the following expression for T_c in the limit $\beta_c\mu \ll 1$

$$T_c \to \frac{v_F}{2\ln(2)k_B}\left[\frac{3\pi v_F}{\tilde{V}_c}\left(1 - \frac{\tilde{V}_c}{\tilde{V}}\right) + \frac{\mu}{v_F}\right].$$

Plugging in Eq. (4.62), then yields the final result

$$T_c \to \frac{1}{2\ln(2)k_B}\left[m\left(0, \mu = 0\right) + \mu\right] = \frac{1}{2\ln(2)k_B}\left[\frac{\tilde{V}^2 m(0,\mu)^2}{\mu + \tilde{V}^2 m(0,\mu)} + \mu\right], \tag{4.78}$$

where Eq. (4.64) was used in the last expression. As mentioned before, in the strong-coupling limit the system is not in the BCS-like regime and indeed the resulting critical temperature shows power law behavior in μ.

In the weak-coupling limit, the critical temperature is much smaller than the chemical potential, i.e. $\beta_c\mu \gg 1$. This leads to the following for Eq. (4.77)

$$\cosh\left(\frac{\beta_c}{2}\mu\right) = \frac{\mathrm{e}^{\frac{\beta_c}{2}\mu} + \mathrm{e}^{-\frac{\beta_c}{2}\mu}}{2} \xrightarrow{\beta_c\mu \gg 1} \frac{1}{2}\mathrm{e}^{\frac{\beta_c}{2}\mu},$$

and secondly,

$$\int_0^{\frac{\beta_c}{2}\mu} \mathrm{d}u \, \frac{\tanh(u)}{u} \xrightarrow{\beta_c\mu \gg 1} \ln\left(\frac{4\mathrm{e}^{\gamma}}{\pi}\frac{\beta_c\mu}{2}\right) = \ln\left(\frac{2\beta_c}{\pi}\mu\mathrm{e}^{\gamma}\right).$$

where $\gamma = 0.577$ is Euler's constant. Noticing that Λ is taken to be extremely large, such that

$$\cosh\left(\frac{\beta_c}{2}v_F\Lambda\right) \to \frac{1}{2}\mathrm{e}^{\frac{\beta_c}{2}v_F\Lambda},$$

leads to

$$\begin{aligned} 1 &= \frac{\tilde{V}}{6\pi v_F}\left\{\frac{4}{\beta_c v_F}\left[\ln\left(\frac{1}{2}\mathrm{e}^{\frac{\beta_c}{2}v_F\Lambda}\right) - \ln\left(\frac{1}{2}\mathrm{e}^{\frac{\beta_c}{2}\mu}\right)\right] + \frac{2\mu}{v_F}\ln\left(\frac{2\beta_c}{\pi}\mu\mathrm{e}^{\gamma}\right)\right\} \\ &= \frac{\tilde{V}\mu}{3\pi v_F^2}\left[\frac{v_F\Lambda}{\mu} - 1 + \ln\left(\frac{2\beta_c}{\pi}\mu\mathrm{e}^{\gamma}\right)\right]. \end{aligned}$$

Such that the critical temperature in the limit $\beta_c\mu \gg 1$ reads

$$T_c \to \frac{2\mu\mathrm{e}^{\gamma}}{k_B\pi}\mathrm{e}^{\frac{\tilde{V}m(0,\mu=0)}{\mu}-1} = \frac{e^{\gamma}}{k_B\pi}\tilde{V}m(0,\mu), \tag{4.79}$$

where Eq. (4.65) was used. As mentioned before, in the weak-coupling limit the system is in the BCS regime and indeed the critical temperature behaves like in the BCS model.

Therefore, the final result is

$$T_c \to \begin{cases} \frac{1}{2\ln(2)k_B}\left[\frac{\tilde{V}^2 m(0,\mu)^2}{\mu+\tilde{V}^2 m(0,\mu)}+\mu\right], & |\tilde{V}|>|\tilde{V}_c|,\ \beta_c\mu \ll 1, \\ \frac{e^\gamma}{k_B\pi}\tilde{V}m(0,\mu), & |\tilde{V}|<|\tilde{V}_c|,\ \beta_c\mu \gg 1. \end{cases}$$

Hidden Order

To find the critical temperature for the hidden order, Eq. (4.76) is solved imposing that $\Delta'(T_c) = 0$ and $m = 0$. This yields the following

$$\begin{aligned} 1 &= \frac{\tilde{V}}{6}\frac{v_F^2}{t^2}\sum_{s=\pm}\int\frac{\mathrm{d}\mathbf{q}}{(2\pi)^2}\frac{|q|^2}{v_F|q|+s\mu}\tanh\left(\frac{\beta\left(v_F|q|+s\mu\right)}{2}\right) \\ &= \frac{\tilde{V}}{6}\frac{1}{t^2v_F^2}\frac{1}{\pi}\frac{1}{\beta_c^3}\left[2\int_{\frac{\beta_c}{2}\mu}^{\frac{\beta_c}{2}v_F\Lambda}\mathrm{d}v\left(4v^2+3\beta_c^2\mu^2\right)\tanh\left(v\right)+\beta_c\mu\int_0^{\frac{\beta_c}{2}\mu}\frac{\mathrm{d}v}{v}\left(12v^2+\beta_c^2\mu^2\right)\tanh\left(v\right)\right]. \end{aligned} \tag{4.80}$$

The integral is solved explicitly in Appendix 6.3.7. In Fig. 4.13 the behavior of the gap with increasing temperature that follows from this equation is shown. It can clearly be seen there that with increasing temperature the gap decreases. As is the case for the Kekule order, the gap closes at critical temperature. It can also be seen that with increasing chemical potential the gap is larger and the critical temperature is also larger. One cannot see from this figure that the hidden order is not actually a superconducting gap but instead renormalizes the Fermi velocity v_F. An explicit expression for the critical temperature can be derived in the strong and weak coupling limit.

In the strong-coupling limit, $\beta_c\mu \ll 1$, the following is found for the first integral in Eq. (4.80)

$$\begin{aligned} &2\int_{\frac{\beta_c}{2}\mu}^{\frac{\beta_c}{2}v_F\Lambda}\mathrm{d}v\left(4v^2+3\beta_c^2\mu^2\right)\tanh\left(v\right) = 8\int_{\frac{\beta_c}{2}\mu}^{\frac{\beta_c}{2}v_F\Lambda}\mathrm{d}v\,v^2\tanh\left(v\right)+6\left(\beta_c\mu\right)^2\int_{\frac{\beta_c}{2}\mu}^{\frac{\beta_c}{2}v_F\Lambda}\mathrm{d}v\tanh\left(v\right) \\ &= 8\left[\frac{v^3}{3}+v^2\ln\left|1+\mathrm{e}^{-2v}\right|-v\mathrm{Li}_2\left(-\mathrm{e}^{-2v}\right)-\frac{1}{2}\mathrm{Li}_3\left(-\mathrm{e}^{-2v}\right)\right]_{\frac{\beta_c}{2}\mu}^{\frac{\beta_c}{2}v_F\Lambda}+6\left(\beta_c\mu\right)^2\left[\ln\left(\cosh(v)\right)\right]_{\frac{\beta_c}{2}\mu}^{\frac{\beta_c}{2}v_F\Lambda} \\ &\xrightarrow{\beta_c\mu\ll1;\Lambda\gg1} 8\left[\frac{1}{3}\left(\frac{\beta_c v_F\Lambda}{2}\right)^3+\left(\frac{\beta_c v_F\Lambda}{2}\right)^2\ln|1|-\frac{\beta_c v_F\Lambda}{2}\mathrm{Li}_2\left(0\right)-\frac{1}{2}\mathrm{Li}_3\left(0\right)-\frac{1}{3}\left(\frac{\beta_c\mu}{2}\right)^3\right. \\ &\left.-\left(\frac{\beta_c\mu}{2}\right)^2\ln|2|+\frac{\beta_c\mu}{2}\mathrm{Li}_2(-1)+\frac{1}{2}\mathrm{Li}_3(-1)\right]+6\left(\beta_c\mu\right)^2\ln\left[\frac{\cosh(\frac{\beta_c}{2}v_F\Lambda)}{\cosh(\frac{\beta_c}{2}\mu)}\right] \\ &= \frac{\left(\beta_c v_F\Lambda\right)^3}{3}-\frac{\left(\beta_c\mu\right)^3}{3}-2\left(\beta_c\mu\right)^2\ln|2|-3\pi^2\beta_c\mu-3\zeta(3)+3\left(\beta_c\mu\right)^2\beta_c v_F\Lambda-6\ln(2)\left(\beta_c\mu\right)^2. \end{aligned}$$

The second integral in Eq. (4.80) yields

$$\begin{aligned} &\beta_c\mu\int_0^{\frac{\beta_c}{2}\mu}\frac{\mathrm{d}v}{v}\left[12v^2+\left(\beta_c\mu\right)^2\right]\tanh\left(v\right) = \beta_c\mu\int_0^{\frac{\beta_c}{2}\mu}\mathrm{d}v\left[12v+\frac{\left(\beta_c\mu\right)^2}{v}\right]\tanh\left(v\right) \\ &\xrightarrow{\beta_c\mu\ll1}\beta_c\mu\left[12\frac{\beta_c\mu}{2}+\left(\beta_c\mu\right)^2\frac{2}{\beta_c\mu}\right]\tanh\left(\frac{\beta_c\mu}{2}\right) = \left[6\left(\beta_c\mu\right)^2+2\left(\beta_c\mu\right)^2\right]\tanh\left(\frac{\beta_c\mu}{2}\right). \end{aligned}$$

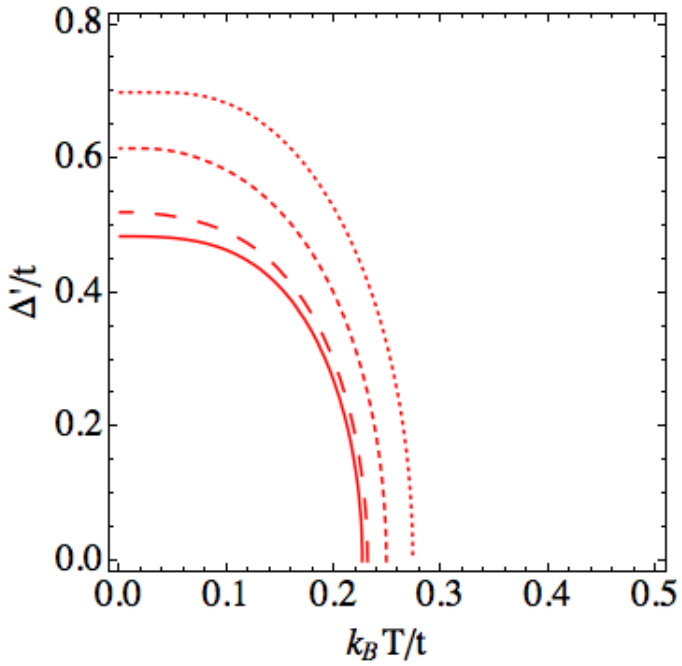

Figure 4.13: Solutions of the finite-temperature gap equation for the hidden order with $v_F/t = \Lambda = 1$, $\Delta' = 0$ and $\tilde{V}/t = 4\pi$ for different values of the chemical potential: $\mu/t = 0$ (solid), $\mu/t = 0.1$ (large dashed), $\mu/t = 0.25$ (small dashed) and $\mu/t = 0.5$ (dotted).

Using $\tanh(x) \approx x - x^3/3 + \mathcal{O}(x^5)$ leads to the following

$$\left[6\left(\beta_c\mu\right)^2 + 2\left(\beta_c\mu\right)^2\right]\tanh\left(\frac{\beta_c\mu}{2}\right) = 8\left(\beta_c\mu\right)^2\frac{\beta_c\mu}{2} = 4\left(\beta_c\mu\right)^3.$$

This yields the following for Eq. (4.80)

$$\begin{aligned} 1 \;=\; & \frac{\tilde{V}}{6}\frac{1}{t^2v_F^2}\frac{1}{\pi}\frac{1}{\beta_c^3}\left[\frac{\left(\beta_c v_F\Lambda\right)^3}{3} - \frac{\left(\beta_c\mu\right)^3}{3} - 2\left(\beta_c\mu\right)^2\ln|2| - 3\pi^2\beta_c\mu - 3\zeta(3)\right. \\ & \left. +3\left(\beta_c\mu\right)^2\beta_c v_F\Lambda - 6\ln(2)\left(\beta_c\mu\right)^2 + 4\left(\beta_c\mu\right)^3\right] \\ & \xrightarrow{\beta_c\mu\ll 1} \frac{\tilde{V}}{6}\frac{1}{t^2v_F^2}\frac{1}{\pi}\frac{1}{\beta_c^3}\left[\frac{\left(\beta_c v_F\Lambda\right)^3}{3} - 3\zeta(3)\right], \end{aligned}$$

such that the critical temperature in the limit $\beta_c\mu \ll 1$ reads

$$T_c' \to \frac{1}{k_B}\left[\frac{2\pi t^2v_F^2}{\zeta(3)\tilde{V}}\left(\frac{\tilde{V}}{\tilde{V}_c'} - 1\right)\right]^{1/3} = \frac{1}{k_B}\left[\frac{2\pi t^2v_F^2}{\zeta(3)\tilde{V}}\left(\frac{\tilde{V}\left|\Delta'(0,\mu)\right|}{t} - 1\right)\right]^{1/3}, \tag{4.81}$$

where Eq. (4.68) was used.

In the weak-coupling limit, $\beta_c\mu \gg 1$, the first integral in Eq. (4.80) leads to

$$
\begin{aligned}
&8\int_{\frac{\beta_c}{2}\mu}^{\frac{\beta_c}{2}v_F\Lambda} \mathrm{d}v\, v^2 \tanh(v) + 6(\beta_c\mu)^2 \int_{\frac{\beta_c}{2}\mu}^{\frac{\beta_c}{2}v_F\Lambda} \mathrm{d}v \tanh(v) \\
&= 8\left[\frac{v^3}{3} + v^2 \ln\left|1+\mathrm{e}^{-2v}\right| - v\mathrm{Li}_2\left(-\mathrm{e}^{-2v}\right) - \frac{1}{2}\mathrm{Li}_3\left(-\mathrm{e}^{-2v}\right)\right]_{\frac{\beta_c}{2}\mu}^{\frac{\beta_c}{2}v_F\Lambda} + 6(\beta_c\mu)^2\left[\ln(\cosh(v))\right]_{\frac{\beta_c}{2}\mu}^{\frac{\beta_c}{2}v_F\Lambda} \\
&\xrightarrow{\beta_c\mu\gg 1;\Lambda\gg 1} 8\left[\frac{1}{3}\left(\frac{\beta_c v_F\Lambda}{2}\right)^3 + \left(\frac{\beta_c v_F\Lambda}{2}\right)^2 \ln|1| - \frac{\beta_c v_F\Lambda}{2}\mathrm{Li}_2(0) - \frac{1}{2}\mathrm{Li}_3(0) - \frac{1}{3}\left(\frac{\beta_c\mu}{2}\right)^3\right. \\
&\left. - \left(\frac{\beta_c\mu}{2}\right)^2 \ln|1| + \frac{\beta_c\mu}{2}\mathrm{Li}_2(0) + \frac{1}{2}\mathrm{Li}_3(0)\right] + 6(\beta_c\mu)^2 \ln\left[\frac{\cosh\left(\frac{\beta_c v_F\Lambda}{2}\right)}{\cosh\left(\frac{\beta_c\mu}{2}\right)}\right] \\
&= \frac{(\beta_c v_F\Lambda)^3}{3} - \frac{(\beta_c\mu)^3}{3} + 3(\beta_c\mu)^2(\beta_c v_F\Lambda - \beta_c\mu).
\end{aligned}
$$

The second integral in Eq. (4.80) yields

$$
\begin{aligned}
&\beta_c\mu\int_0^{\frac{\beta_c}{2}\mu} \frac{\mathrm{d}v}{v}\left(12v^2 + \beta_c^2\mu^2\right)\tanh(v) = 12\beta_c\mu\int_0^{\frac{\beta_c}{2}\mu} \mathrm{d}v\, v\tanh(v) + (\beta_c\mu)^3\int_0^{\frac{\beta_c}{2}\mu} \mathrm{d}v \frac{\tanh(v)}{v} \\
&= 12\beta_c\mu\left[\frac{v^2}{2} + v\ln\left(1+\mathrm{e}^{-2v}\right) - \frac{1}{2}\mathrm{Li}_2\left(-\mathrm{e}^{-2v}\right)\right]_0^{\frac{\beta_c\mu}{2}} + (\beta_c\mu)^3\ln\left(\frac{4\mathrm{e}^\gamma}{\pi}\frac{\beta_c\mu}{2}\right) \\
&\xrightarrow{\beta_c\mu\gg 1;\Lambda\gg 1} 12\beta_c\mu\left[\frac{1}{2}\left(\frac{\beta_c\mu}{2}\right)^2 + \frac{\beta_c\mu}{2}\ln(1) - \frac{1}{2}\mathrm{Li}_2(0) - 0 - 0 + \frac{1}{2}\mathrm{Li}_2(-1)\right] \\
&+ (\beta_c\mu)^3\left[\gamma + \ln\left(\frac{2\beta_c\mu}{\pi}\right)\right] \\
&= \frac{3(\beta_c\mu)^3}{2} - \frac{\pi^2}{3}(\beta_c\mu) + (\beta_c\mu)^3\left[\gamma + \ln\left(\frac{2\beta_c\mu}{\pi}\right)\right].
\end{aligned}
$$

Eq. (4.80) can then be rewritten as

$$
\begin{aligned}
1 \;=\; & \frac{\tilde{V}}{6}\frac{1}{t^2 v_F^2}\frac{1}{\pi}\frac{1}{\beta_c^3}\left[\frac{(\beta_c v_F\Lambda)^3}{3} - \frac{(\beta_c\mu)^3}{3} + 3(\beta_c\mu)^2(\beta_c v_F\Lambda - \beta_c\mu)\right. \\
& \left. + \frac{3(\beta_c\mu)^3}{2} - \frac{\pi^2}{3}(\beta_c\mu) + (\beta_c\mu)^3\left[\gamma + \ln\left(\frac{2\beta_c\mu}{\pi}\right)\right]\right] \\
& \xrightarrow{\beta_c\mu\gg 1} \frac{\tilde{V}}{6}\frac{1}{t^2 v_F^2}\frac{1}{\pi}\frac{1}{\beta_c^3}\left\{\frac{(\beta_c v_F\Lambda)^3}{3} - \frac{11}{6}(\beta_c\mu)^3 + (\beta_c\mu)^3\left[\gamma + \ln\left(\frac{2\beta_c\mu}{\pi}\right)\right]\right\},
\end{aligned}
$$

such that the critical temperature in the limit $\beta_c\mu \gg 1$ reads

$$
T_c' \to \frac{2\mu}{k_B\pi}\exp\left[\frac{6\pi t^2 v_F^2}{\tilde{V}_c'\mu^3}\left(1 - \frac{\tilde{V}_c'}{\tilde{V}}\right) - \frac{11}{6} + \gamma\right] = \frac{\mu\mathrm{e}^{\gamma-\frac{11}{9}}}{k_B\pi}\frac{\tilde{V}\left|\Delta'(0,\mu)\right|}{t}, \tag{4.82}
$$

where Eq. (4.69) was used.

Therefore, the final result is

$$T_c' \to \begin{cases} \frac{1}{k_B}\left[\frac{2\pi t^2 v_F^2}{\zeta(3)\tilde{V}}\left(\frac{\tilde{V}|\Delta'(0,\mu)|}{t}-1\right)\right]^{1/3}, & |\tilde{V}| > |\tilde{V}_c|,\ \beta_c\mu \ll 1, \\ \frac{\mu e^{\gamma-\frac{11}{9}}}{k_B\pi}\frac{\tilde{V}|\Delta'(0,\mu)|}{t}, & |\tilde{V}| < |\tilde{V}_c|,\ \beta_c\mu \gg 1. \end{cases}$$

4.5.2 p-Kekule Order

In this Subsection, the p-Kekule order will be reviewed for which $\gamma = \pi/2$. It will be shown that the ground-state energy and the thermodynamical potential are equal to that of the s-Kekule order, such that the gap equations and critical temperatures are also equal.

Ground-State Energy

The ground-state energy will be calculated by diagonalizing Eqs. (4.46)-(4.49) for $\Delta' = 0$. As in the previous Subsection, the hidden order is turned off initially because by minimizing the resulting ground-state energy, a condition on the components of the Kekule order can be derived, which simplifies the ground-state energy. This will be followed by including the hidden order in the ground-state energy. It will be shown that the ground-state energy found here is equal to Eq. (4.52).

Ground-State Energy for $\Delta' = 0$
To find the energy, the following is used

$$\sum_{\mathbf{q}} \left(E_{0,m} + M_t + M_\mu + M_{m,\gamma=\pi/2}\right)\psi = E_{m,\gamma=\pi/2}\psi,$$

where

$$E_{0,m} = 6N\tilde{V}m^2.$$

Squaring $M_t + M_\mu + M_{m,\gamma=\pi/2}$ leads to

$$\begin{aligned}
&\left(M_t + M_\mu + M_{m,\gamma=\pi/2}\right)^2 = \left(M_t + M_\mu + M_{\Delta,\gamma=\pi/2} + M^+_{\Delta_\uparrow,\Delta_\downarrow,\gamma=\pi/2} + M^-_{\Delta_\uparrow,\Delta_\downarrow,\gamma=\pi/2}\right)^2 \\
&= M_t^2 + M_\mu^2 + M^2_{\Delta,\gamma=\pi/2} + \left(M^+_{\Delta_\uparrow,\Delta_\downarrow,\gamma=\pi/2}\right)^2 + \left(M^-_{\Delta_\uparrow,\Delta_\downarrow,\gamma=\pi/2}\right)^2 + 2M_tM_\mu \\
&+ \left\{M_t\,,\, M_{\Delta,\gamma=\pi/2} + M^+_{\Delta_\uparrow,\Delta_\downarrow,\gamma=\pi/2} + M^-_{\Delta_\uparrow,\Delta_\downarrow,\gamma=\pi/2}\right\} \\
&+ \left\{M_\mu\,,\, M_{\Delta,\gamma=\pi/2} + M^+_{\Delta_\uparrow,\Delta_\downarrow,\gamma=\pi/2} + M^-_{\Delta_\uparrow,\Delta_\downarrow,\gamma=\pi/2}\right\} \\
&+ \left\{M_{\Delta,\gamma=\pi/2}\,,\, M^+_{\Delta_\uparrow,\Delta_\downarrow,\gamma=\pi/2} + M^-_{\Delta_\uparrow,\Delta_\downarrow,\gamma=\pi/2}\right\} + \left\{M^+_{\Delta_\uparrow,\Delta_\downarrow,\gamma=\pi/2}\,,\, M^-_{\Delta_\uparrow,\Delta_\downarrow,\gamma=\pi/2}\right\},
\end{aligned}$$

where M_t and M_μ are given by Eqs.(4.35) and (4.36), respectively, and it was used that $\{M_t, M_\mu\} = 2M_tM_\mu$. Moreover,

$$\begin{aligned}
M_{\Delta,\gamma=\pi/2} &= \tilde{V}\left(Y\tau_1 + X\tau_2\right)\otimes\sigma_3\otimes i\gamma_1\gamma_2, \\
M^+_{\Delta_\uparrow,\Delta_\downarrow,\gamma=\pi/2} &= -\tilde{V}\left(R_+\tau_1 - I_+\tau_2\right)\otimes\sigma_2\otimes i\gamma_1\gamma_2 \\
M^-_{\Delta_\uparrow,\Delta_\downarrow,\gamma=\pi/2} &= -\tilde{V}\left(I_-\tau_1 + R_-\tau_2\right)\otimes\sigma_1\otimes i\gamma_1\gamma_2.
\end{aligned}$$

One can compute that

$$\left\{M_\mu\,,\,M_{\Delta,\gamma=\pi/2}+M^+_{\Delta_\uparrow,\Delta_\downarrow,\gamma=\pi/2}+M^-_{\Delta_\uparrow,\Delta_\downarrow,\gamma=\pi/2}\right\}=0.$$

Therefore, the following needs to be computed

$$\begin{aligned}&\left(M_t+M_\mu+M_{m,\gamma=\pi/2}\right)^2=M_t^2+M_\mu^2+M^2_{\Delta,\gamma=\pi/2}+\left(M^+_{\Delta_\uparrow,\Delta_\downarrow,\gamma=\pi/2}\right)^2+\left(M^-_{\Delta_\uparrow,\Delta_\downarrow,\gamma=\pi/2}\right)^2\\&+2M_tM_\mu+\left\{M_{\Delta,\gamma=\pi/2}\,,\,M^+_{\Delta_\uparrow,\Delta_\downarrow,\gamma=\pi/2}\right\}+\left\{M_{\Delta,\gamma=\pi/2}\,,\,M^-_{\Delta_\uparrow,\Delta_\downarrow,\gamma=\pi/2}\right\}\\&+\left\{M^+_{\Delta_\uparrow,\Delta_\downarrow,\gamma=\pi/2}\,,\,M^-_{\Delta_\uparrow,\Delta_\downarrow,\gamma=\pi/2}\right\}.\end{aligned}$$

M_t^2, M_μ and $2M_tM_\mu$ where computed before. Moreover, it can be seen that $M^2_{\Delta,\gamma=\pi/2}=M^2_{\Delta,\gamma=0}$ because the τ and σ-dependence is the same and $(i\gamma_1\gamma_2)=\mathbb{I}=\gamma_0^2$. The same holds for squaring $M^+_{\Delta_\uparrow,\Delta_\downarrow,\gamma=\pi/2}$ and $M^-_{\Delta_\uparrow,\Delta_\downarrow,\gamma=\pi/2}$. Therefore, only the anticommutation relations need to be computed here. This leads to

$$\begin{aligned}\left\{M_{\Delta,\gamma=\pi/2}\,,\,M^+_{\Delta_\uparrow,\Delta_\downarrow,\gamma=\pi/2}\right\}&=\tilde{V}^2\left[i\left(YR_+-XI_+\right)\tau_0+\left(XR_++YI_+\right)\tau_3\right]\otimes\sigma_1\otimes\mathbb{I}\\&\quad+\tilde{V}^2\left[-i\left(YR_+-XI_+\right)\tau_0+\left(XR_++YI_+\right)\tau_3\right]\otimes\sigma_1\otimes\mathbb{I}\\&=2\tilde{V}^2\left(XR_++YI_+\right)\left(\tau_3\otimes\sigma_1\otimes\mathbb{I}\right)\\&=\left\{M_{\Delta,\gamma=0}\,,\,M^+_{\Delta_\uparrow,\Delta_\downarrow,\gamma=0}\right\}.\end{aligned}$$

Likewise,

$$\begin{aligned}&\left\{M_{\Delta,\gamma=\pi/2}\,,\,M^-_{\Delta_\uparrow,\Delta_\downarrow,\gamma=\pi/2}\right\}=2\tilde{V}^2\left(YR_--XI_-\right)\tau_3\otimes\sigma_2\otimes\mathbb{I}=\left\{M_{\Delta,\gamma=0}\,,\,M^-_{\Delta_\uparrow,\Delta_\downarrow,\gamma=0}\right\}\\&\left\{M^+_{\Delta_\uparrow,\Delta_\downarrow,\gamma=\pi/2}\,,\,M^-_{\Delta_\uparrow,\Delta_\downarrow,\gamma=\pi/2}\right\}=2\tilde{V}^2\left(R_+R_-+I_+I_-\right)\tau_3\otimes\sigma_3\otimes\mathbb{I}=\left\{M^+_{\Delta_\uparrow,\Delta_\downarrow,\gamma=0}\,,\,M^-_{\Delta_\uparrow,\Delta_\downarrow,\gamma=0}\right\}.\end{aligned}$$

Therefore,

$$\left(M_t+M_\mu+M_{m,\gamma=\pi/2}\right)^2=\left(M_t+M_\mu+M_{m,\gamma=0}\right)^2,$$

which means that the ground-state energy $E_{\text{g.s.},m,\gamma=\pi/2}$ is equal to $E_{\text{g.s.},m,\gamma=0}$ in Eq. (4.52).

Minimum of the Ground-State Energy
Minimizing the ground-state energy yields the same conditions as were obtained in the previous Subsection, i.e.

$$|\mathbf{n}|=0,\qquad\text{such that}\qquad|\Delta_\uparrow|=|\Delta_\downarrow|\,,\qquad\text{and}\qquad\phi_\uparrow+\phi_\downarrow=2\phi+n\pi.$$

Using these conditions together with $\Delta_\sigma=|\Delta_\sigma|\,\mathrm{e}^{i\phi_\sigma}$ and $\Delta=|\Delta|\,\mathrm{e}^{i\phi}$ leads to the following simplification for $M_{\Delta,\gamma=\pi/2}$, $M^+_{\Delta_\uparrow,\Delta_\downarrow,\gamma=\pi/2}$ and $M^-_{\Delta_\uparrow,\Delta_\downarrow,\gamma=\pi/2}$:

$$\begin{aligned}&\left(M_{\Delta,\gamma=\pi/2}+M^+_{\Delta_\uparrow,\Delta_\downarrow,\gamma=\pi/2}+M^-_{\Delta_\uparrow,\Delta_\downarrow,\gamma=\pi/2}\right)\Big|_{|\mathbf{n}|=0}\\&=\tilde{V}\left[\sin(\phi)\tau_1+\cos(\phi)\tau_2\right]\otimes\left[\sigma_3\left|\Delta\right|+\sigma_1\left|\Delta_\uparrow\right|\cos(\phi_\downarrow-\phi)+\sigma_2\left|\Delta_\uparrow\right|\sin(\phi_\downarrow-\phi)\right]\otimes i\gamma_1\gamma_2.\end{aligned}$$

Writing $|\Delta| = m_0 \cos(\theta)$ and $|\Delta_\uparrow| = m_0 \sin(\theta)$, where $m = m_0$ at the minimum of the energy, leads to

$$\begin{aligned}&\left(M_{\Delta,\gamma=\pi/2} + M^+_{\Delta_\uparrow,\Delta_\downarrow,\gamma=\pi/2} + M^-_{\Delta_\uparrow,\Delta_\downarrow,\gamma=\pi/2}\right)\Big|_{|\mathbf{n}|=0} \\ &= \tilde{V} m_0 \left[\sin(\phi)\tau_1 + \cos(\phi)\tau_2\right] \otimes \left[\cos(\theta)\,\sigma_3 + \sin(\theta)\left(\sigma_1 \cos\left(\phi_\downarrow - \phi\right) + \sigma_2 \sin\left(\phi_\downarrow - \phi\right)\right)\right] \otimes i\gamma_1\gamma_2.\end{aligned} \tag{4.83}$$

Ground-State Energy for $\Delta' \neq 0$
Now, the ground-state energy can be calculated including both the Kekule and hidden order using the condition $|\mathbf{n}| = 0$. The same relation as before is used to determine the energy

$$\sum_{\mathbf{q}} \left(E_{0,m,\Delta'} + M_t + M_\mu + M_{m,\gamma=\pi/2} + M_{\Delta'}\right) \Psi = E_{m,\Delta'\gamma=\pi/2}\Psi,$$

where

$$E_{0,m,\Delta'} = 6N\tilde{V}\left(m^2 + 2\left|\Delta'\right|^2\right).$$

Squaring $M_t + M_\mu + M_{m,\gamma=\pi/2} + M_{\Delta'}$ yields

$$\begin{aligned}&\left(M_t + M_\mu + M_{m,\gamma=\pi/2} + M_{\Delta'}\right)^2 = \left(M_t + M_\mu + M_{m,\gamma=\pi/2}\right)^2 + M^2_{\Delta'} \\ &+ \left\{M_{\Delta,\gamma=\pi/2} + M^+_{\Delta_\uparrow,\Delta_\downarrow,\gamma=\pi/2} + M^-_{\Delta_\uparrow,\Delta_\downarrow,\gamma=\pi/2}\,,\, M_{\Delta'}\right\},\end{aligned}$$

where it was used that $\{M_t + M_\mu\,,\, M_{\Delta'}\} = 0$. Again, the following condition will be imposed

$$\left\{M_{\Delta,\gamma=\pi/2} + M^+_{\Delta_\uparrow,\Delta_\downarrow,\gamma=\pi/2} + M^-_{\Delta_\uparrow,\Delta_\downarrow,\gamma=\pi/2}\,,\, M_{\Delta'}\right\} = 0.$$

For this to hold, a condition needs to be derived for the relative phase between the Kekule and hidden order. To do this, one considers Eq. (4.83), which describes the Kekule order at minimal energy. One can see immediately that the terms for the spin and sublattice-valley space anticommute. Therefore, this condition is computed in the particle-hole space. For all the components of the Kekule order, the dependence in the particle-hole space is the same. This yields

$$\begin{aligned}&\left\{\sin(\phi)\,\tau_1 + \cos(\phi)\tau_2\,,\, \mathrm{Re}(\Delta')\tau_2 + \mathrm{Im}(\Delta')\tau_1\right\} = 2\sin(\phi)\,\mathrm{Im}(\Delta') + 2\cos(\phi)\,\mathrm{Re}(\Delta') \\ &= 2\left|\Delta'\right|\left[\sin(\phi)\sin(\varphi) + \cos(\phi)\cos(\varphi)\right] = 2\left|\Delta'\right|\cos\left(\phi - \varphi\right),\end{aligned}$$

where $\Delta' = |\Delta'|\,\mathrm{e}^{i\varphi}$. Therefore, for the anticommutation relation to be zero the relative phase between the Kekule and hidden order parameters should be $\pi/2$. This leads to

$$\begin{aligned}\left(M_t + M_\mu + M_{m,\gamma=\pi/2} + M_{\Delta'}\right)^2 &= \left(M_t + M_\mu + M_{m,\gamma=\pi/2}\right)^2 + M^2_{\Delta'} \\ &= \left(M_t + M_\mu + M_{m,\gamma=0} + M_{\Delta'}\right)^2,\end{aligned}$$

which means that the ground-state energy is equal to $E_{\mathrm{g.s.},m,\Delta',\gamma=0}$ in Eq. (4.56).

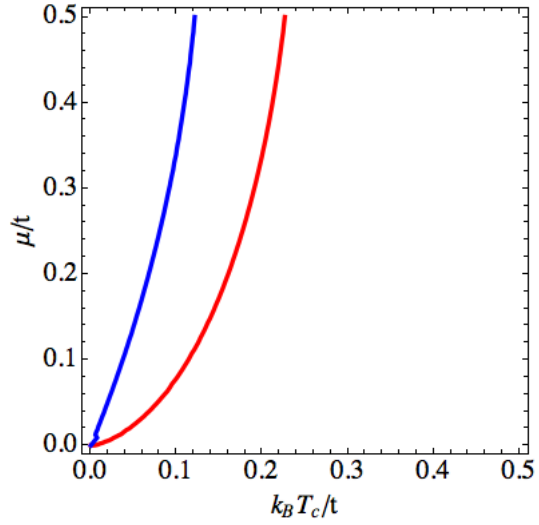

Figure 4.14: Solutions of the finite-temperature gap equation for the Kekule and hidden order at critical temperature with $v_F/t = \Lambda = 1$, $m(T_c) = \Delta'(T_c') = 0$. For the Kekule order the coupling is $\tilde{V}/t = 3\pi$ and for the hidden order $\tilde{V}/t = 18\pi$. The critical temperature increases with increasing μ.

Comparison between s-Kekule Order and p-Kekule Order

The fact that the ground-state energies for the s and p-Kekule order are identical means that also their thermodynamical potential must be the same. Therefore, as mentioned before, the zero- and finite-temperature gap equations, critical couplings, zero-temperature gaps and critical temperatures for the p-Kekule order correspond to those for the s-Kekule order in this approximation. However, Roy and Herbut show that when electrons away from the Fermi level are taken into account, the p-Kekule is preferred over the s-Kekule order, which implies that the results for the critical couplings and critical temperatures will be different for the s and p-Kekule order in that approximation [5].

4.5.3 Competition Between Kekule and Hidden Order Reviewed

In the previous Subsections, it was already mentioned that the Kekule order is preferred over the hidden order. In this Subsection, the behavior of both orders, as well as the competition between them is reviewed. In Fig. 4.11, it was already shown that the critical coupling for the Kekule order is smaller than that for the hidden order, which is a first indication that the first is preferred over the second. Then, in Fig. 4.14 the behavior of the critical temperature with respect to chemical potential is reviewed. One can see that the critical temperature increases with increasing chemical potential, which was already shown in Figs. 4.12 and 4.13. As different couplings are taken to solve the finite-temperature gap equations for the Kekule and hidden order, the critical temperature values cannot be compared in this Figure. Next, in Figs. 4.15 and 4.16 the behavior of the coupling with respect to increasing critical temperature is shown. One can see that for increasing chemical potential the coupling decreases. Moreover, with increasing interaction strength, the critical temperature also increases. Lastly, the finite-temperature gap equations in Eqs. (4.73) and (4.76) have been solved self-consistently, the result of which can be found in Fig. 4.17. There, it can be seen that the Kekule gap opens at a higher temperature than the hidden order gap. Therefore, the critical temperature of the Kekule order is higher

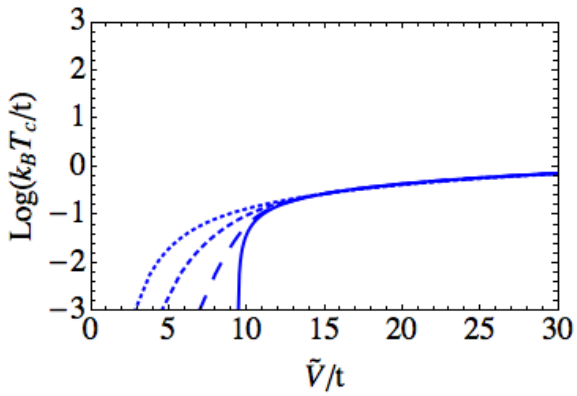

Figure 4.15: Solutions of the finite-temperature gap equation for the Kekule order at critical temperature with $v_F/t = \Lambda = 1$, $m(T_c) = 0$ and $\Delta' = 0$ for different values of the chemical potential: $\mu/t = 0$ (solid), $\mu/t = 0.1$ (large dashed), $\mu/t = 0.25$ (small dashed) and $\mu/t = 0.5$ (dotted). With increasing interaction the critical temperature also increases. For increasing chemical potential the critical coupling is smaller.

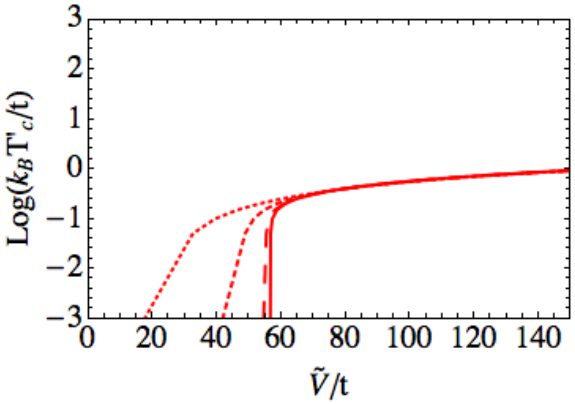

Figure 4.16: Solutions of the finite-temperature gap equation for the hidden order at critical temperature with $v_F/t = \Lambda = 1$, $\Delta'(T_c') = 0$ and $m = 0$ for different values of the chemical potential: $\mu/t = 0$ (solid), $\mu/t = 0.1$ (large dashed), $\mu/t = 0.25$ (small dashed) and $\mu/t = 0.5$ (dotted). With increasing interaction the critical temperature also increases. For increasing chemical potential the critical coupling is smaller.

than that of the hidden order. Seeing that the critical coupling for the Kekule order is lower than that for the hidden order and the critical temperature is higher, it can be concluded that the Kekule order is preferred over the hidden order when only electrons at Fermi level are considered.

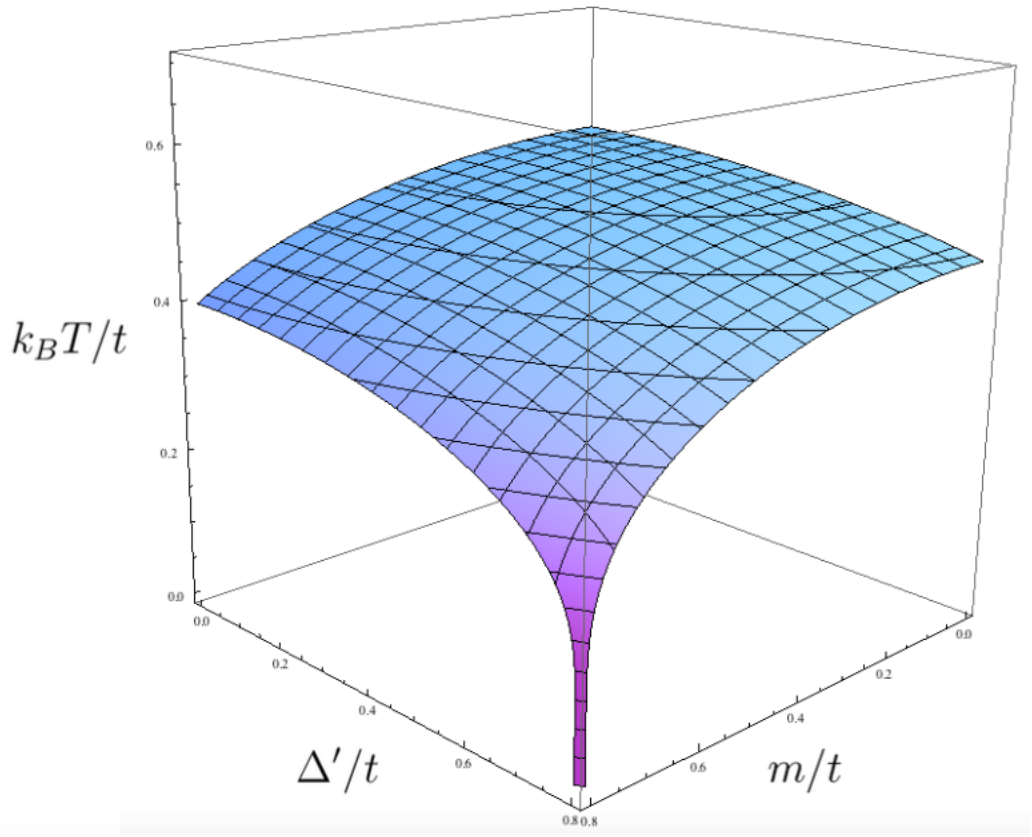

Figure 4.17: Finite-temperature gap equations solved self-consistently for $v_F/t = \Lambda = 1$, $\mu/t = 0.25$ and $\tilde{V}/t = 58$. The Kekule gap opens at higher temperature than the hidden order gap and remains larger for any temperature.

Chapter 5

Conclusion

In this Master's Thesis, superconductivity in artificial graphene samples has been investigated. To that end, first BCS theory was studied in Chapter 2 to provide a theoretical basis for treating superconductivity. Considering a system with a square lattice, it was shown how an attractive potential between electrons can be generated and how a superconducting gap can be opened in the energy spectrum. In the following Chapter, graphene was reviewed. Due to the geometrical similarity between graphene and artificial graphene, studying graphene provides the basis of the understanding of artificial-graphene systems. The tight-binding model for graphene was explained extensively and it was shown that the low-energy excitations in the system are massless Dirac fermions. Combining the knowledge from Chapters 2 and 3 then allowed for the investigation of how superconductivity is manifested in graphene-like systems. A honeycomb superlattice made of CdSe nanocrystals was considered with a longitudinal optical phonon coupling to effective s-like electrons on the same site and on nearest-neighbor sites. Superconducting order parameters were defined for on-site and nearest-neighbor electron coupling. The latter resulted in a competition between the Kekule and hidden order.

Two main results were obtained in this Thesis. Firstly, an expression for the effective on-site electron-electron interaction and nearest-neighbor electron-electron interaction was derived. A numerical analysis by the group of Prof. C. Delerue (Lille, France) shows that the effective interactions for both cases remains repulsive. This means that the honeycomb superstructure of CdSe nanocrystals may not be superconductive. The model studied in this Thesis can also be used for other materials, such as for instance PbSe nanocrystals assembled in a honeycomb geometry. An analysis of the numerical values there will show whether superconductivity is possible. Secondly, the competition between the Kekule and hidden order was investigated and the results show that the first is preferred over the second. The critical coupling for the Kekule order is lower, whereas the critical temperature for the Kekule order is higher than those for the hidden order, which proves that indeed the Kekule order is preferred over the hidden order. For both the s and p-Kekule order, the same results were obtained. Upon including electrons further away from the Fermi level, this will be overturned, as shown by Ref. [5], and one will find that the p-Kekule is preferred over the s-Kekule order. It was also found that the system behaves BCS-like in the weak-coupling limit.

In the future, the research in this Thesis could be expanded in several directions. First of all, the research in this Thesis could be expanded by including electrons that are further away from the Fermi level as is done in Ref. [5] to show that the p-Kekule is preferred over

the s-Kekule order. Secondly, orbital degree of freedom could be included in the model. The conduction bands of CdSe nanocrystals arranged in a honeycomb superlattice reveal a Dirac-like manifold for the s-like electrons as well as the p-like electrons, of which only the first were considered in this research. Experimentally, the nanocrystals can be doped with electrons such that p-like states can be filled. Theoretically, however, it is not clear yet how the p-like electrons can be included in the tight-binding description. Including these electrons would increase the theoretical understanding of tight-binding models, as well as lead to the formation of exotic superconducting states. Thirdly, following the example of Ref. [11], the effect of straining on the system could be studied, as it leads to exotic electron pairings. Lastly, in the conduction bands of HgTe nanocrystals arranged in a honeycomb configuration topologically non-trivial gaps were found [20]. One could study what happens when superconductivity is induced in this system. The topological nature of the gaps will lead to non-trivial results for the superconducting states.

Chapter 6

Appendix

6.1 Appendix to Chapter 2

6.1.1 Derivation of $H_{\mathrm{el-ph}}$

The electron-phonon Hamiltonian is derived in second quantized language.[1] A simple model for a metal is considered, where conduction electrons interact with ions of a crystal. It is assumed that there is one ion per unit cell at a position $\mathbf{R}_i$. The ions are arranged in a square lattice with N lattice sites.

In first quantization, the electron-ion Hamiltonian of the system is

$$H_{ei} = \sum_{i,j} V_{ei}\left(\mathbf{r}_i - \mathbf{R}_j\right),$$

where $i, j = 1, ..., N$, and $V_{ei}\left(\mathbf{r}_i - \mathbf{R}_j\right)$ is the interaction energy between electrons at position $\mathbf{r}_i$ and ions at positions $\mathbf{R}_j$.

The ion coordinates $\mathbf{R}_i$ have small fluctuations around their equilibrium position

$$\mathbf{R}_i = \mathbf{R}_i^0 + \delta\mathbf{R}_i.$$

Therefore, the electron-ion interaction can be expanded as

$$\sum_{i,j} V_{ei}\left(\mathbf{r}_i - \mathbf{R}_j\right) = \sum_{i,j} V_{ei}\left(\mathbf{r}_i - \mathbf{R}_j^0\right) + \sum_{i,j} \delta\mathbf{R}_j \nabla V_{ei}\left(\mathbf{r}_i - \mathbf{R}_j^0\right). \tag{6.1}$$

All higher order terms are neglected. The first term is an external potential for the electron coming from the periodicity of the crystalline lattice and contributes to the electron Hamiltonian. Therefore, this term is neglected here. The second term describes the interaction of the electrons with lattice deformations to the lowest order.

The potential term can be diagonalized by introducing normal modes

$$\delta\mathbf{R}_i = \frac{1}{\sqrt{NM}} \sum_{\mathbf{q},\lambda} Q_{\mathbf{q},\lambda} \mathcal{E}_\lambda\left(\mathbf{q}\right) \mathrm{e}^{i\mathbf{q}\cdot\mathbf{R}_i^0}, \tag{6.2}$$

$$\mathbf{P}_i = \sqrt{\frac{M}{N}} \sum_{\mathbf{q},\lambda} \Pi_{\mathbf{q},\lambda} \mathcal{E}_\lambda\left(\mathbf{q}\right) \mathrm{e}^{-i\mathbf{q}\cdot\mathbf{R}_i^0}, \tag{6.3}$$

[1] This derivation is based on Section 2.6 in Ref. [29].

where $\mathcal{E}_\lambda(\mathbf{q})$, $\lambda = 1,2,3$ are the polarization vectors. The commutation relation between $\mathbf{R}_i$ and $\mathbf{P}_i$ is well-known

$$\left[\mathbf{R}_i^\mu, \mathbf{P}_j^\nu\right] = i\hbar\delta_{i,j}\delta_{\mu,\nu}.$$

This relation can be used to derive the commutation relation between $Q_{\mathbf{q},\lambda}$ and $\Pi_{\mathbf{q},\lambda}$

$$\left[\delta\mathbf{R}_i^\mu, \mathbf{P}_j^\nu\right] = \frac{1}{\sqrt{NM}}\sqrt{\frac{M}{N}}\sum_{\mathbf{q},\lambda}\sum_{\mathbf{q}',\lambda'}\left[Q_{\mathbf{q},\lambda}, \Pi_{\mathbf{q}',\lambda'}\right]\mathcal{E}_\lambda^\mu(\mathbf{q})\,\mathcal{E}_{\lambda'}^\nu(\mathbf{q}')\,\mathrm{e}^{i\mathbf{q}\cdot\mathbf{R}_i^0}\mathrm{e}^{-i\mathbf{q}'\cdot\mathbf{R}_j^0} = i\hbar\delta_{i,j}\delta_{\mu,\nu}$$

only if

$$\left[Q_{\mathbf{q},\lambda}, \Pi_{\mathbf{q}',\lambda'}\right] = i\hbar\delta_{\mathbf{q},\mathbf{q}'}\delta_{\lambda,\lambda'}. \tag{6.4}$$

Moreover, $[\mathbf{R}_i, \mathbf{R}_j] = 0 = [\mathbf{P}_i, \mathbf{P}_j]$ imply

$$\left[Q_{\mathbf{q},\lambda}, Q_{\mathbf{q}',\lambda'}\right] = \left[\Pi_{\mathbf{q},\lambda}, \Pi_{\mathbf{q}',\lambda'}\right] = 0. \tag{6.5}$$

The explicit form of the functions $Q_{\mathbf{q},\lambda}$ and $\Pi_{\mathbf{q},\lambda}$ can be derived using the ladder operators for bosons

$$\begin{aligned} b_{\mathbf{q},\lambda}^\dagger &= \sqrt{\frac{\omega_{\mathbf{q},\lambda}}{2\hbar}}\left(Q_{\mathbf{q},\lambda}^\dagger - \frac{i}{\omega_{\mathbf{q},\lambda}}\Pi_{-\mathbf{q},\lambda}^\dagger\right), \\ b_{\mathbf{q},\lambda} &= \sqrt{\frac{\omega_{\mathbf{q},\lambda}}{2\hbar}}\left(Q_{\mathbf{q},\lambda} + \frac{i}{\omega_{\mathbf{q},\lambda}}\Pi_{-\mathbf{q},\lambda}\right), \end{aligned}$$

and the conditions $Q_{-\mathbf{q}} = Q_{\mathbf{q}}^\dagger$ and $\Pi_{-\mathbf{q}} = \Pi_{\mathbf{q}}^\dagger$. For $Q_{\mathbf{q},\lambda}$ this leads to

$$b_{\mathbf{q},\lambda} + b_{-\mathbf{q},\lambda}^\dagger = \sqrt{\frac{\omega_{\mathbf{q},\lambda}}{2\hbar}}\left(Q_{\mathbf{q},\lambda} + \frac{i}{\omega_{\mathbf{q},\lambda}}\Pi_{-\mathbf{q},\lambda} + Q_{-\mathbf{q},\lambda}^\dagger - \frac{i}{\omega_{\mathbf{q},\lambda}}\Pi_{\mathbf{q},\lambda}^\dagger\right) = \sqrt{\frac{2\omega_{\mathbf{q},\lambda}}{\hbar}}Q_{\mathbf{q},\lambda},$$

such that

$$Q_{\mathbf{q},\lambda} = \sqrt{\frac{\hbar}{2\omega_{\mathbf{q},\lambda}}}\left(b_{\mathbf{q},\lambda} + b_{-\mathbf{q},\lambda}^\dagger\right). \tag{6.6}$$

Next, $\Pi_{\mathbf{q},\lambda}$ is retrieved

$$b_{\mathbf{q},\lambda}^\dagger - b_{-\mathbf{q},\lambda} = \sqrt{\frac{\omega_{\mathbf{q},\lambda}}{2\hbar}}\left(Q_{\mathbf{q},\lambda}^\dagger - \frac{i}{\omega_{\mathbf{q},\lambda}}\Pi_{-\mathbf{q},\lambda}^\dagger - Q_{-\mathbf{q},\lambda} - \frac{i}{\omega_{\mathbf{q},\lambda}}\Pi_{\mathbf{q},\lambda}\right) = \frac{1}{i}\sqrt{\frac{2}{\hbar\omega_{\mathbf{q},\lambda}}}\Pi_{\mathbf{q},\lambda},$$

such that

$$\Pi_{\mathbf{q},\lambda} = i\sqrt{\frac{\hbar\omega_{\mathbf{q},\lambda}}{2}}\left(b_{\mathbf{q},\lambda}^\dagger - b_{-\mathbf{q},\lambda}\right). \tag{6.7}$$

The ladder operators $b^\dagger$ and b obey Bose-Einstein statistics and their commutation relations are

$$\left[b_{\mathbf{q},\lambda}, b_{\mathbf{q}',\lambda'}^\dagger\right] = \delta_{\mathbf{q},\mathbf{q}'}\delta_{\lambda,\lambda'}, \quad \left[b_{\mathbf{q},\lambda}, b_{\mathbf{q}',\lambda'}\right] = \left[b_{\mathbf{q},\lambda}^\dagger, b_{\mathbf{q}',\lambda'}^\dagger\right] = 0.$$

Inserting Eq. (6.2) into the second term in Eq. (6.1) yields

$$\sum_j \delta\mathbf{R}_j\nabla V_{ei}\left(\mathbf{r} - \mathbf{R}_j^0\right) = \frac{1}{\sqrt{NM}}\sum_{j,\mathbf{q},\lambda} Q_{\mathbf{q},\lambda}\mathcal{E}_\lambda(\mathbf{q})\,\mathrm{e}^{i\mathbf{q}\cdot\mathbf{R}_j^0}\nabla V_{ei}\left(\mathbf{r} - \mathbf{R}_j^0\right).$$

Denoting with $a^{\dagger}_{\mathbf{k},\sigma}$ and $a_{\mathbf{k},\sigma}$ the creation and annihilation operators of electrons in the basis of Bloch functions $\chi_{\mathbf{k}}(\mathbf{r})$, this expression can be written as

$$\begin{aligned}
&\frac{1}{\sqrt{NM}}\sum_{j,\mathbf{q},\lambda} Q_{\mathbf{q},\lambda}\mathcal{E}_{\lambda}(\mathbf{q})\,\mathrm{e}^{i\mathbf{q}\cdot\mathbf{R}^0_j}\nabla V_{ei}\left(\mathbf{r}-\mathbf{R}^0_j\right)\\
=\;&\frac{1}{\sqrt{NM}}\sum_{j,\mathbf{q},\lambda}\sum_{\mathbf{k},\mathbf{k}',\sigma} Q_{\mathbf{q},\lambda}\mathcal{E}_{\lambda}(\mathbf{q})\,\mathrm{e}^{i\mathbf{q}\cdot\mathbf{R}^0_j}\int \mathrm{d}\mathbf{r}\overline{\chi_{\mathbf{k}}(\mathbf{r})}\nabla V_{ei}\left(\mathbf{r}-\mathbf{R}^0_j\right)\chi_{\mathbf{k}'}(\mathbf{r})\,a^{\dagger}_{\mathbf{k},\sigma}a_{\mathbf{k}',\sigma}\\
=\;&\frac{1}{\sqrt{NM}}\sum_{j,\mathbf{q},\lambda}\sum_{\mathbf{k},\mathbf{k}',\sigma} Q_{\mathbf{q},\lambda}\mathcal{E}_{\lambda}(\mathbf{q})\,\mathrm{e}^{i\mathbf{q}\cdot\mathbf{R}^0_j}\int \mathrm{d}\mathbf{r}\overline{\chi_{\mathbf{k}}\left(\mathbf{r}+\mathbf{R}^0_j\right)}\nabla V_{ei}(\mathbf{r})\,\chi_{\mathbf{k}'}\left(\mathbf{r}+\mathbf{R}^0_j\right)a^{\dagger}_{\mathbf{k},\sigma}a_{\mathbf{k}',\sigma}.
\end{aligned}$$

Using Bloch's theorem

$$\chi_{\mathbf{k}}(\mathbf{r}+\mathbf{R}) = \mathrm{e}^{i\mathbf{k}\cdot\mathbf{R}}\chi_{\mathbf{k}}(\mathbf{r}), \tag{6.8}$$

where $\mathbf{R}$ is a lattice vector, leads to the following

$$\begin{aligned}
&\frac{1}{\sqrt{NM}}\sum_{j,\mathbf{q},\lambda}\sum_{\mathbf{k},\mathbf{k}',\sigma} Q_{\mathbf{q},\lambda}\mathcal{E}_{\lambda}(\mathbf{q})\,\mathrm{e}^{i\mathbf{q}\cdot\mathbf{R}^0_j}\int \mathrm{d}\mathbf{r}\overline{\chi_{\mathbf{k}}\left(\mathbf{r}+\mathbf{R}^0_j\right)}\nabla V_{ei}(\mathbf{r})\,\chi_{\mathbf{k}'}\left(\mathbf{r}+\mathbf{R}^0_j\right)a^{\dagger}_{\mathbf{k},\sigma}a_{\mathbf{k}',\sigma}\\
=\;&\frac{1}{\sqrt{NM}}\sum_{j,\mathbf{q},\lambda}\sum_{\mathbf{k},\mathbf{k}',\sigma} Q_{\mathbf{q},\lambda}\mathcal{E}_{\lambda}(\mathbf{q})\,\mathrm{e}^{i\mathbf{q}\cdot\mathbf{R}^0_j}\int \mathrm{d}\mathbf{r}\overline{\chi_{\mathbf{k}}(\mathbf{r})}\mathrm{e}^{-i\mathbf{k}\cdot\mathbf{R}^0_j}\nabla V_{ei}(\mathbf{r})\,\chi_{\mathbf{k}'}(\mathbf{r})\,\mathrm{e}^{i\mathbf{k}'\cdot\mathbf{R}^0_j}a^{\dagger}_{\mathbf{k},\sigma}a_{\mathbf{k}',\sigma}\\
=\;&\frac{1}{\sqrt{NM}}\sum_{j,\mathbf{q},\lambda}\sum_{\mathbf{k},\mathbf{k}',\sigma} Q_{\mathbf{q},\lambda}\mathcal{E}_{\lambda}(\mathbf{q})\,\mathrm{e}^{i(\mathbf{k}'-\mathbf{k}+\mathbf{q})\cdot\mathbf{R}^0_j}\int \mathrm{d}\mathbf{r}\overline{\chi_{\mathbf{k}}(\mathbf{r})}\nabla V_{ei}(\mathbf{r})\,\chi_{\mathbf{k}'}(\mathbf{r})\,a^{\dagger}_{\mathbf{k},\sigma}a_{\mathbf{k}',\sigma}\\
=\;&\sqrt{\frac{N}{M}}\sum_{\mathbf{q},\lambda}\sum_{\mathbf{k},\mathbf{k}',\mathbf{G},\sigma} Q_{\mathbf{q},\lambda}\mathcal{E}_{\lambda}(\mathbf{q})\,\delta_{\mathbf{k}'-\mathbf{k}+\mathbf{q},\mathbf{G}}\left\langle\mathbf{k}\right|\nabla V_{ei}\left|\mathbf{k}'\right\rangle a^{\dagger}_{\mathbf{k},\sigma}a_{\mathbf{k}',\sigma},
\end{aligned}$$

where $\mathbf{G}$ is a vector of the dual lattice, i.e. $\mathrm{e}^{i\mathbf{G}\cdot\mathbf{R}}=1$ and

$$\int \mathrm{d}\mathbf{r}\overline{\chi_{\mathbf{k}}(\mathbf{r})}\nabla V_{ei}(\mathbf{r})\,\chi_{\mathbf{k}'}(\mathbf{r}) \equiv \left\langle\mathbf{k}\right|\nabla V_{ei}\left|\mathbf{k}'\right\rangle.$$

Therefore, the electron-phonon Hamiltonian in terms of normal modes is

$$H^{\mathrm{nm}}_{\mathrm{el-ph}} = \sqrt{\frac{N}{M}}\sum_{\mathbf{q},\lambda}\sum_{\mathbf{k},\mathbf{k}',\mathbf{G},\sigma}\left\langle\mathbf{k}\right|\nabla V_{ei}\left|\mathbf{k}'\right\rangle\mathcal{E}_{\lambda}(\mathbf{q})\,\delta_{\mathbf{k}'-\mathbf{k}+\mathbf{q},\mathbf{G}}Q_{\mathbf{q},\lambda}a^{\dagger}_{\mathbf{k},\sigma}a_{\mathbf{k}',\sigma}. \tag{6.9}$$

Eq. (6.9) can be expressed in terms of boson operators using Eq. (6.6)

$$\begin{aligned}
H_{\mathrm{el-ph}} &= \sqrt{\frac{N}{M}}\sum_{\mathbf{q},\lambda}\sum_{\mathbf{k},\mathbf{k}',\mathbf{G},\sigma}\left\langle\mathbf{k}\right|\nabla V_{ei}\left|\mathbf{k}'\right\rangle\mathcal{E}_{\lambda}(\mathbf{q})\,\delta_{\mathbf{k}'-\mathbf{k}+\mathbf{q},\mathbf{G}}Q_{\mathbf{q},\lambda}a^{\dagger}_{\mathbf{k},\sigma}a_{\mathbf{k}',\sigma}\\
&= \sum_{\mathbf{q},\lambda}\sum_{\mathbf{k},\mathbf{k}',\mathbf{G},\sigma}\sqrt{\frac{\hbar N}{2\omega_{\mathbf{q},\lambda}M}}\left\langle\mathbf{k}\right|\nabla V_{ei}\left|\mathbf{k}'\right\rangle\mathcal{E}_{\lambda}(\mathbf{q})\,\delta_{\mathbf{k}'-\mathbf{k}+\mathbf{q},\mathbf{G}}\left(b_{\mathbf{q},\lambda}+b^{\dagger}_{-\mathbf{q},\lambda}\right)a^{\dagger}_{\mathbf{k},\sigma}a_{\mathbf{k}',\sigma}\\
&= \sum_{\mathbf{q},\lambda}\sum_{\mathbf{k},\mathbf{k}',\mathbf{G},\sigma} g_{\mathbf{k},\mathbf{k}'}(\mathbf{q})\,\delta_{\mathbf{k}'-\mathbf{k}+\mathbf{q},\mathbf{G}}\left(b_{\mathbf{q},\lambda}+b^{\dagger}_{-\mathbf{q},\lambda}\right)a^{\dagger}_{\mathbf{k},\sigma}a_{\mathbf{k}',\sigma},
\end{aligned} \tag{6.10}$$

where $g_{\mathbf{k},\mathbf{k}'}(\mathbf{q})$ describes the electron-phonon coupling

$$g_{\mathbf{k},\mathbf{k}'}(\mathbf{q}) = \sqrt{\frac{\hbar N}{2\omega_{\mathbf{q},\lambda} M}} \langle \mathbf{k}| \nabla V_{ei} |\mathbf{k}'\rangle \mathcal{E}_\lambda(\mathbf{q}). \tag{6.11}$$

This expression can be simplified by setting $\mathbf{G} = 0$

$$\begin{aligned} H_{\text{el-ph}} &= \sum_{\mathbf{q},\lambda} \sum_{\mathbf{k},\mathbf{k}',\sigma} \sqrt{\frac{\hbar N}{2\omega_{\mathbf{q},\lambda} M}} \langle \mathbf{k}| \nabla V_{ei} |\mathbf{k}'\rangle \mathcal{E}_\lambda(\mathbf{q}) \delta_{\mathbf{k}'-\mathbf{k}+\mathbf{q},0} \left(b_{\mathbf{q},\lambda} + b^\dagger_{-\mathbf{q},\lambda}\right) a^\dagger_{\mathbf{k},\sigma} a_{\mathbf{k}',\sigma} \\ &= \sum_{\mathbf{k},\mathbf{q},\lambda,\sigma} \sqrt{\frac{\hbar N}{2\omega_{\mathbf{q},\lambda} M}} \langle \mathbf{k}+\mathbf{q}| \nabla V_{ei} |\mathbf{k}\rangle \mathcal{E}_\lambda(\mathbf{q}) \left(b_{\mathbf{q},\lambda} + b^\dagger_{-\mathbf{q},\lambda}\right) a^\dagger_{\mathbf{k}+\mathbf{q},\sigma} a_{\mathbf{k},\sigma} \\ &= \sum_{\mathbf{q},\lambda,\sigma} \sqrt{\hbar N} \frac{iq_j}{\sqrt{2\omega_{\mathbf{q},\lambda} M}} \mathcal{E}_\lambda(\mathbf{q}) \left(b_{\mathbf{q},\lambda} + b^\dagger_{-\mathbf{q},\lambda}\right) \hat{n}_{\mathbf{q},\sigma} \\ &= \gamma \sum_{\mathbf{q},\lambda,\sigma} \frac{iq_j}{\sqrt{2\omega_{\mathbf{q},\lambda} M}} \left(b_{\mathbf{q},\lambda} + b^\dagger_{-\mathbf{q},\lambda}\right) \hat{n}_{\mathbf{q},\sigma}, \end{aligned} \tag{6.12}$$

where $\hat{n}_{\mathbf{q},\sigma} = \sum_{\mathbf{k}} a^\dagger_{\mathbf{k}+\mathbf{q},\sigma} a_{\mathbf{k},\sigma}$ and $\gamma = \sqrt{\hbar N}\mathcal{E}_\lambda(\mathbf{q})$.

6.1.2 Derivation of S_{ph} and $S_{\text{el-ph}}$

To find the action, the following definition is used

$$S\left[\psi^\dagger, \psi\right] = \int_0^{\hbar\beta} \mathrm{d}\tau \left[\psi^\dagger(\tau)\partial_\tau \psi(\tau) + H\left(\psi^\dagger, \psi\right)\right], \tag{6.13}$$

where the first term contributes to the kinetic term in H. To write the Hamiltonians in terms of the fields, the operators are transformed to fields using the following

$$\begin{aligned} a_{\mathbf{q}} &\rightarrow \psi_{\mathbf{q}}(\tau) = \frac{1}{\sqrt{\hbar\beta}} \sum_n \psi_{\mathbf{q},n} \mathrm{e}^{-i\omega_n \tau}, \\ c_{\mathbf{q},j} &\rightarrow \phi_{\mathbf{q},j}(\tau) = \frac{1}{\sqrt{\hbar\beta}} \sum_n \phi_{\mathbf{q},j,n} \mathrm{e}^{-i\hat{\omega}_n \tau}, \end{aligned}$$

where $\omega_n = (2n+1)\pi/(\hbar\beta)$ and $\hat{\omega}_n = 2n\pi/(\hbar\beta)$ for $n \in \mathbb{Z}$ are the Matsubara frequencies for fermions and bosons, respectively, and $\phi^\dagger$ ($\psi^\dagger$) and ϕ (ψ) obey the boson (fermion) (anti)commutation relations.

For the phonon action $S_{\text{ph}}\left[\phi^\dagger, \phi\right]$ this yields

$$\begin{aligned} S_{\text{ph}}\left[\phi^\dagger, \phi\right] &= \int_0^{\hbar\beta} \mathrm{d}\tau \sum_{\mathbf{q},j} \left[\phi^\dagger_{\mathbf{q},j}(\tau)\partial_\tau \phi_{\mathbf{q},j}(\tau) + \omega_q \phi^\dagger_{\mathbf{q},j}(\tau)\phi_{\mathbf{q},j}(\tau)\right] \\ &= \frac{1}{\hbar\beta} \int_0^{\hbar\beta} \mathrm{d}\tau \sum_{\mathbf{q},j} \sum_{n,n'} \mathrm{e}^{i(\hat{\omega}_n - \hat{\omega}_{n'})\tau} \left[\phi^\dagger_{\mathbf{q},j,n}\left(-i\hat{\omega}_{n'}\right)\phi_{\mathbf{q},j,n'} + \omega_q \phi^\dagger_{\mathbf{q},j,n}\phi_{\mathbf{q},j,n'}\right] \\ &= \frac{1}{\hbar\beta} \sum_{\mathbf{q},j} \sum_{n,n'} \hbar\beta\, \delta(n-n') \left[\phi^\dagger_{\mathbf{q},j,n}\left(-i\hat{\omega}_{n'}\right)\phi_{\mathbf{q},j,n'} + \omega_q \phi^\dagger_{\mathbf{q},j,n}\phi_{\mathbf{q},j,n'}\right] \\ &= \sum_{\mathbf{q},j,n} \phi^\dagger_{\mathbf{q},j,n}\left(-i\hat{\omega}_n + \omega_q\right)\phi_{\mathbf{q},j,n} = \sum_{q,j} \phi^\dagger_{q,j}\left(-i\hat{\omega}_n + \omega_q\right)\phi_{q,j}, \end{aligned}$$

where $q = (n, \mathbf{q})$, and the following identity was used

$$\int_0^{\hbar\beta} \mathrm{d}\tau\, \mathrm{e}^{i(\hat{\omega}_n - \hat{\omega}_{n'})\tau} = 2\pi\delta\left(\omega_n - \omega_{n'}\right) = 2\pi\delta\left(\frac{2n\pi}{\hbar\beta} - \frac{2n'\pi}{\hbar\beta}\right)$$
$$= 2\pi\delta\left(\frac{2\pi}{\hbar\beta}(n-n')\right) = 2\pi\frac{1}{\frac{2\pi}{\hbar\beta}}\delta(n-n') = \hbar\beta\,\delta(n-n').$$

Next, the electron-phonon action $S_{\mathrm{el-ph}}\left[\psi^\dagger, \psi, \phi^\dagger, \phi\right]$ is determined. This term does not contain any terms contributing to the kinetic term, so the first term in Eq. (6.13) is not included in this calculation. The following is found

$$S_{\mathrm{el-ph}}\left[\psi^\dagger, \psi, \phi^\dagger, \phi\right] = \gamma\int_0^{\hbar\beta}\mathrm{d}\tau\sum_{\mathbf{k},\mathbf{q},j}\frac{iq_j}{\left(2m\omega_q\right)^{1/2}}\psi^\dagger_{\mathbf{k}+\mathbf{q}}(\tau)\psi_{\mathbf{k}}(\tau)\left(\phi^\dagger_{-\mathbf{q},j}(\tau) + \phi_{\mathbf{q},j}(\tau)\right)$$
$$= \frac{\gamma}{\hbar\beta\sqrt{\hbar\beta}}\int_0^{\hbar\beta}\mathrm{d}\tau\sum_{\mathbf{k},\mathbf{q},j}\sum_{n,n',n''}\frac{iq_j}{\left(2m\omega_q\right)^{1/2}}$$
$$\times\left(\mathrm{e}^{i(\omega_n-\omega_{n'}+\hat{\omega}_{n''})\tau}\psi^\dagger_{\mathbf{k}+\mathbf{q},n}\psi_{\mathbf{k},n'}\phi^\dagger_{-\mathbf{q},j,n''} + \mathrm{e}^{i(\omega_n-\omega_{n'}-\hat{\omega}_{n''})\tau}\psi^\dagger_{\mathbf{k}+\mathbf{q},n}\psi_{\mathbf{k},n'}\phi_{\mathbf{q},j,n''}\right)$$
$$= \frac{\gamma}{\hbar\beta\sqrt{\hbar\beta}}\sum_{\mathbf{k},\mathbf{q},j}\sum_{n,n',n''}\hbar\beta\frac{iq_j}{\left(2m\omega_q\right)^{1/2}}\psi^\dagger_{\mathbf{k}+\mathbf{q},n}\psi_{\mathbf{k},n'}\left(\delta(n-n'+n'')\phi^\dagger_{-\mathbf{q},j,n''} + \delta(n-n'-n'')\phi_{\mathbf{q},j,n''}\right)$$
$$= \frac{\gamma}{\sqrt{\hbar\beta}}\sum_{\mathbf{k},\mathbf{q},j}\sum_{n,n'}\frac{iq_j}{\left(2m\omega_q\right)^{1/2}}\psi^\dagger_{\mathbf{k}+\mathbf{q},n}\psi_{\mathbf{k},n'}\left(\phi^\dagger_{-\mathbf{q},j,n'-n} + \phi_{\mathbf{q},j,n-n'}\right).$$

Therefore, $S_{\mathrm{ph}}\left[\phi^\dagger, \phi\right]$ and $S_{\mathrm{el-ph}}\left[\psi^\dagger, \psi, \phi^\dagger, \phi\right]$ read

$$S_{\mathrm{ph}}\left[\phi^\dagger, \phi\right] = \sum_{q,j}\phi^\dagger_{q,j}\left(-i\hat{\omega}_n + \omega_q\right)\phi_{q,j}, \tag{6.14}$$

$$S_{\mathrm{el-ph}}\left[\psi^\dagger, \psi, \phi^\dagger, \phi\right] = \frac{\gamma}{\sqrt{\hbar\beta}}\sum_{\mathbf{k},\mathbf{q},j}\sum_{n,n'}\frac{iq_j}{\left(2m\omega_q\right)^{1/2}}\psi^\dagger_{\mathbf{k}+\mathbf{q},n}\psi_{\mathbf{k},n'}\left(\phi^\dagger_{-\mathbf{q},j,n'-n} + \phi_{\mathbf{q},j,n-n'}\right). \tag{6.15}$$

6.1.3 Derivation of Effective Action

Using the definition for ρ_q, the solution for $S_{\mathrm{el-ph}}\left[\psi^\dagger, \psi, \phi^\dagger, \phi\right]$ can be rewritten as

$$S_{\mathrm{el-ph}}\left[\psi^\dagger, \psi, \phi^\dagger, \phi\right] = \frac{\gamma}{\sqrt{\hbar\beta}}\sum_{\mathbf{k},\mathbf{q},j}\sum_{n,n'}\frac{iq_j}{\left(2m\omega_q\right)^{1/2}}\psi^\dagger_{\mathbf{k}+\mathbf{q},n}\psi_{\mathbf{k},n'}\left(\phi^\dagger_{-\mathbf{q},j,n'-n} + \phi_{\mathbf{q},j,n-n'}\right)$$
$$= \frac{\gamma}{\sqrt{\hbar\beta}}\sum_{\mathbf{k},\mathbf{q},j}\sum_{n,m}\frac{iq_j}{\left(2m\omega_q\right)^{1/2}}\psi^\dagger_{\mathbf{k}+\mathbf{q},m}\psi_{\mathbf{k},m-n}\left(\phi^\dagger_{-\mathbf{q},j,n} + \phi_{\mathbf{q},j,-n}\right)$$
$$= \gamma\sum_{\mathbf{q},j,n}\frac{iq_j}{\left(2m\omega_q\right)^{1/2}}\rho_{\mathbf{q},-n}\left(\phi^\dagger_{-\mathbf{q},j,-n} + \phi_{\mathbf{q},j,n}\right) = \gamma\sum_{\mathbf{q},j,n}\frac{iq_j}{\left(2m\omega_q\right)^{1/2}}\rho_{\mathbf{q},-n}\left(\phi^\dagger_{-q,j} + \phi_{q,j}\right).$$

Using the solution for the phonon action $S_{\rm ph}\left[\phi^\dagger,\phi\right]$ yields the following coherent state integral

$$\begin{aligned}\mathcal{Z} &= \int D\left[\psi^\dagger,\psi\right]\int D\left[\phi^\dagger,\phi\right]\exp\left\{-\left[S_{\rm el}\left[\psi^\dagger,\psi\right]+\sum_{q,j,\omega_n}\phi^\dagger_{q,j}\left(-i\omega_n+\omega_q\right)\phi_{q,j}\right.\right.\\ &\left.\left.+\gamma\sum_{\mathbf{q},j,n}\frac{iq_j}{\left(2m\omega_q\right)^{1/2}}\rho_{\mathbf{q},-n}\left(\phi^\dagger_{-q,j}+\phi_{q,j}\right)\right]/\hbar\right\}.\end{aligned}$$

To be able to integrate out the phonon fields, the square needs to be completed. This yields

$$\begin{aligned}&-\sum_{q,j}\phi^\dagger_{q,j}\left(-i\hat{\omega}_n+\omega_q\right)\phi_{q,j}-\gamma\sum_{\mathbf{q},j,n}\frac{iq_j}{\left(2m\omega_q\right)^{1/2}}\rho_{\mathbf{q},-n}\left(\phi^\dagger_{-q,j}+\phi_{q,j}\right)\\ &=-\sum_{q,j}\left(-i\hat{\omega}_n+\omega_q\right)\phi^\dagger_{q,j}\phi_{q,j}+\gamma\sum_{q,j}\frac{iq_j}{\left(2m\omega_q\right)^{1/2}}\rho_{-\mathbf{q},n}\phi^\dagger_{q,j}-\gamma\sum_{q,j}\frac{iq_j}{\left(2m\omega_q\right)^{1/2}}\rho_{\mathbf{q},-n}\phi_{q,j}\\ &=-\sum_{q,j}\left(-i\hat{\omega}_n+\omega_q\right)\left(\phi^\dagger_{q,j}-\frac{i\gamma q_j}{\left(2m\omega_q\right)^{1/2}}\rho_{\mathbf{q},-n}\frac{1}{-i\hat{\omega}_n+\omega_q}\right)\\ &\times\left(\phi_{q,j}+\frac{i\gamma q_j}{\left(2m\omega_q\right)^{1/2}}\rho_{-\mathbf{q},n}\frac{1}{-i\hat{\omega}_n+\omega_q}\right)+\sum_{\mathbf{q},n}\frac{\gamma^2q^2}{2m\omega_q}\frac{1}{-i\hat{\omega}_n+\omega_q}\rho_{\mathbf{q},-n}\rho_{-\mathbf{q},n}.\end{aligned}$$

Plugging this into partition function yields a Gaussian integral. Integrating out the phonon field leads to the desired result

$$\begin{aligned}&\mathcal{Z}=\int D\left[\psi^\dagger,\psi\right]\int D\left[\phi^\dagger,\phi\right]\exp\left[-S_{\rm el}\left[\psi^\dagger,\psi\right]/\hbar\right.\\ &-\frac{1}{\hbar}\sum_{q,j}\left(-i\hat{\omega}_n+\omega_q\right)\left(\phi^\dagger_{q,j}-\frac{i\gamma q_j}{\left(2m\omega_q\right)^{1/2}}\rho_{\mathbf{q},-n}\frac{1}{-i\hat{\omega}_n+\omega_q}\right)\\ &\left.\times\left(\phi_{q,j}+\frac{i\gamma q_j}{\left(2m\omega_q\right)^{1/2}}\rho_{-\mathbf{q},n}\frac{1}{-i\hat{\omega}_n+\omega_q}\right)+\frac{1}{\hbar}\sum_{\mathbf{q},n}\frac{\gamma^2q^2}{2m\omega_q}\frac{1}{-i\hat{\omega}_n+\omega_q}\rho_{\mathbf{q},-n}\rho_{-\mathbf{q},n}\right]\\ &=\int D\left[\psi^\dagger,\psi\right]\exp\left[-S_{\rm el}\left[\psi^\dagger,\psi\right]/\hbar+\frac{\gamma^2}{2\hbar m}\sum_{\mathbf{q},n}\frac{q^2}{\omega_q}\frac{1}{-i\hat{\omega}_n+\omega_q}\rho_{\mathbf{q},n}\rho_{-\mathbf{q},n}\right].\end{aligned}$$

Using that $\hat{\omega}_n=-\hat{\omega}_{-n}$, sending $n\to-n$ yields

$$\begin{aligned}\mathcal{Z} &= \int D\left[\psi^\dagger,\psi\right]\exp\left[-S_{\rm el}\left[\psi^\dagger,\psi\right]/\hbar+\frac{\gamma^2}{2\hbar m}\sum_{q,n}\frac{q^2}{\omega_q}\frac{1}{-i\hat{\omega}_{-n}+\omega_q}\rho_{\mathbf{q},n}\rho_{-\mathbf{q},-n}\right]\\ &= \int D\left[\psi^\dagger,\psi\right]\exp\left[-S_{\rm el}\left[\psi^\dagger,\psi\right]/\hbar+\frac{\gamma^2}{2\hbar m}\sum_{q,n}\frac{q^2}{\omega_q}\frac{1}{i\hat{\omega}_n+\omega_q}\rho_q\rho_{-q}\right],\end{aligned}$$

such that

$$S_{\rm eff}\left[\psi^\dagger,\psi\right]=S_{\rm el}\left[\psi^\dagger,\psi\right]-\frac{\gamma^2}{2m}\sum_q\frac{q^2}{\omega_q}\frac{1}{i\hat{\omega}_n+\omega_q}\rho_q\rho_{-q}.$$

This result can be rewritten

$$\begin{aligned} S_{\text{eff}}\left[\psi^{\dagger},\psi\right] &= S_{\text{el}}\left[\psi^{\dagger},\psi\right]-\frac{\gamma^{2}}{2m}\sum_{q}\frac{q^{2}}{\omega_{q}}\frac{1}{i\hat{\omega}_{n}+\omega_{q}}\frac{-i\hat{\omega}_{n}+\omega_{q}}{-i\hat{\omega}_{n}+\omega_{q}}\rho_{q}\rho_{-q} \\ &= S_{\text{el}}\left[\psi^{\dagger},\psi\right]-\frac{\gamma^{2}}{2m}\sum_{q}\frac{q^{2}}{\omega_{q}}\frac{-i\hat{\omega}_{n}+\omega_{q}}{\hat{\omega}_{n}^{2}+\omega_{q}^{2}}\rho_{q}\rho_{-q}. \end{aligned} \tag{6.16}$$

$i\hat{\omega}_n$ in the numerator will drop out because the function is symmetric. This leads to the desired result

$$S_{\text{eff}}\left[\psi^{\dagger},\psi\right]=S_{\text{el}}\left[\psi^{\dagger},\psi\right]-\frac{\gamma^{2}}{2m}\sum_{q}\frac{q^{2}}{\hat{\omega}_{n}^{2}+\omega_{q}^{2}}\rho_{q}\rho_{-q}. \tag{6.17}$$

6.2 Appendix to Chapter 3

6.2.1 Derivation of Energy Bands in First Quantized Language

In the tight-binding model discussed in this Chapter, the energy bands produced by the σ bonds are neglected, and only the energy bands of the π electrons are taken into consideration. The body of this Chapter employs second quantization techniques to find these bands. However, as mentioned in the text, the relative sign between t (the nearest-neighbor hopping parameter) and t' (the next-nearest neighbor hopping parameter) does not follow from the second quantized approach. That is why, in this Appendix, the energy bands for the π electrons will be derived in the first quantized language to show that the relative sign between the two parameters should be negative when both parameters are defined with equal sign in the Hamiltonian.

Graphene has two atoms per unit cell, this means that one can write a trial wavefunction

$$\psi_{\mathbf{k}}\left(\mathbf{r}\right)=\alpha_{\mathbf{k}}\psi_{\mathbf{k}}^{(A)}\left(\mathbf{r}\right)+\beta_{\mathbf{k}}\psi_{\mathbf{k}}^{(B)}\left(\mathbf{r}\right),$$

where $\alpha_{\mathbf{k}}$ and $\beta_{\mathbf{k}}$ are complex functions of the quasimomentum $\mathbf{k}$. $\psi_{\mathbf{k}}^{(A)}\left(\mathbf{r}\right)$ and $\psi_{\mathbf{k}}^{(B)}\left(\mathbf{r}\right)$ are Bloch functions

$$\psi_{\mathbf{k}}^{(j)}\left(\mathbf{r}\right)=\sum_{\mathbf{R}_{l}}\mathrm{e}^{i\mathbf{k}\cdot\mathbf{R}_{l}}\phi^{(j)}\left(\mathbf{r}+\mathbf{r}_{j}-\mathbf{R}_{l}\right),\quad\text{with}\quad j=A,B \tag{6.18}$$

where $\mathbf{r}_j$ connects the sites of the underlying Bravais lattice of the j atom with the unit cell [35]. The functions $\phi^{(j)}\left(\mathbf{r}+\mathbf{r}_{j}-\mathbf{R}_{l}\right)$ are the atomic orbitals for electrons in the vicinity of atom j located at a position $\mathbf{R}_l-\mathbf{r}_j$ at the Bravais lattice site $\mathbf{R}_l$ [35].

Assuming that this trial wavefunction is correct, it can be used to find solutions to the Schrödinger equation $H\psi_{\mathbf{k}}=\epsilon_{\mathbf{k}}\psi_{\mathbf{k}}$. Multiplying with $\psi_{\mathbf{k}}^{*}$ from the left gives $\psi_{\mathbf{k}}^{*}H\psi_{\mathbf{k}}=\epsilon_{\mathbf{k}}\psi_{\mathbf{k}}^{*}\psi_{\mathbf{k}}$. The left hand side is

$$\begin{aligned} &\psi_{\mathbf{k}}^{*}H\psi_{\mathbf{k}}=\left(\alpha_{\mathbf{k}}^{*}\psi_{\mathbf{k}}^{*(A)}+\beta_{\mathbf{k}}^{*}\psi_{\mathbf{k}}^{*(B)}\right)H\left(\alpha_{\mathbf{k}}\psi_{\mathbf{k}}^{(A)}+\beta_{\mathbf{k}}\psi_{\mathbf{k}}^{(B)}\right) \\ &=\alpha^{*}\psi_{\mathbf{k}}^{*(A)}H\alpha\psi_{\mathbf{k}}^{(A)}+\alpha^{*}\psi_{\mathbf{k}}^{*(A)}H\beta\psi_{\mathbf{k}}^{(B)}+\beta^{*}\psi_{\mathbf{k}}^{*(B)}H\alpha\psi_{\mathbf{k}}^{(A)}+\beta^{*}\psi_{\mathbf{k}}^{*(B)}H\beta\psi_{\mathbf{k}}^{(B)} \\ &=\begin{pmatrix}\alpha_{\mathbf{k}}^{*} & \beta_{\mathbf{k}}^{*}\end{pmatrix}\begin{pmatrix}\psi_{\mathbf{k}}^{*(A)}H\psi_{\mathbf{k}}^{(A)} & \psi_{\mathbf{k}}^{*(A)}H\psi_{\mathbf{k}}^{(B)}\\ \psi_{\mathbf{k}}^{*(B)}H\psi_{\mathbf{k}}^{(A)} & \psi_{\mathbf{k}}^{*(B)}H\psi_{\mathbf{k}}^{(B)}\end{pmatrix}\begin{pmatrix}\alpha_{\mathbf{k}}\\ \beta_{\mathbf{k}}\end{pmatrix}=\begin{pmatrix}\alpha_{\mathbf{k}}^{*} & \beta_{\mathbf{k}}^{*}\end{pmatrix}\mathcal{H}_{\mathbf{k}}\begin{pmatrix}\alpha_{\mathbf{k}}\\ \beta_{\mathbf{k}}\end{pmatrix}, \end{aligned} \tag{6.19}$$

where

$$\mathcal{H}_{\mathbf{k}} \equiv \begin{pmatrix} \psi_{\mathbf{k}}^{*(A)} H \psi_{\mathbf{k}}^{(A)} & \psi_{\mathbf{k}}^{*(A)} H \psi_{\mathbf{k}}^{(B)} \\ \psi_{\mathbf{k}}^{*(B)} H \psi_{\mathbf{k}}^{(A)} & \psi_{\mathbf{k}}^{*(B)} H \psi_{\mathbf{k}}^{(B)} \end{pmatrix}. \tag{6.20}$$

This matrix is Hermitian

$$\begin{aligned} \mathcal{H}_{\mathbf{k}}^{\dagger} &= \begin{pmatrix} \psi_{\mathbf{k}}^{*(A)} H \psi_{\mathbf{k}}^{(A)} & \psi_{\mathbf{k}}^{*(A)} H \psi_{\mathbf{k}}^{(B)} \\ \psi_{\mathbf{k}}^{*(B)} H \psi_{\mathbf{k}}^{(A)} & \psi_{\mathbf{k}}^{*(B)} H \psi_{\mathbf{k}}^{(B)} \end{pmatrix}^{\dagger} = \begin{pmatrix} \psi_{\mathbf{k}}^{(A)} H \psi_{\mathbf{k}}^{*(A)} & \psi_{\mathbf{k}}^{(A)} H \psi_{\mathbf{k}}^{*(B)} \\ \psi_{\mathbf{k}}^{(B)} H \psi_{\mathbf{k}}^{*(A)} & \psi_{\mathbf{k}}^{(B)} H \psi_{\mathbf{k}}^{*(B)} \end{pmatrix}^{*} \\ &= \begin{pmatrix} \psi_{\mathbf{k}}^{*(A)} H \psi_{\mathbf{k}}^{(A)} & \psi_{\mathbf{k}}^{*(A)} H \psi_{\mathbf{k}}^{(B)} \\ \psi_{\mathbf{k}}^{*(B)} H \psi_{\mathbf{k}}^{(A)} & \psi_{\mathbf{k}}^{*(B)} H \psi_{\mathbf{k}}^{(B)} \end{pmatrix} = \mathcal{H}_{\mathbf{k}}, \end{aligned}$$

where in the first step the transpose was taken of the matrix, and in the second the complex conjugate. The right hand side of the Schrödinger equation gives

$$\begin{aligned} &\epsilon_{\mathbf{k}} \psi_{\mathbf{k}}^{*} \psi_{\mathbf{k}} = \epsilon_{\mathbf{k}} \left(\alpha_{\mathbf{k}}^{*} \psi_{\mathbf{k}}^{*(A)} + \beta_{\mathbf{k}}^{*} \psi_{\mathbf{k}}^{*(B)} \right) \left(\alpha_{\mathbf{k}} \psi_{\mathbf{k}}^{(A)} + \beta_{\mathbf{k}} \psi_{\mathbf{k}}^{(B)} \right) \\ &= \epsilon_{\mathbf{k}} \begin{pmatrix} \alpha_{\mathbf{k}}^{*} & \beta_{\mathbf{k}}^{*} \end{pmatrix} \begin{pmatrix} \psi_{\mathbf{k}}^{*(A)} \psi_{\mathbf{k}}^{(A)} & \psi_{\mathbf{k}}^{*(A)} \psi_{\mathbf{k}}^{(B)} \\ \psi_{\mathbf{k}}^{*(B)} \psi_{\mathbf{k}}^{(A)} & \psi_{\mathbf{k}}^{*(B)} \psi_{\mathbf{k}}^{(B)} \end{pmatrix} \begin{pmatrix} \alpha_{\mathbf{k}} \\ \beta_{\mathbf{k}} \end{pmatrix} = \epsilon_{\mathbf{k}} \begin{pmatrix} \alpha_{\mathbf{k}}^{*} & \beta_{\mathbf{k}}^{*} \end{pmatrix} \mathcal{S}_{\mathbf{k}} \begin{pmatrix} \alpha_{\mathbf{k}} \\ \beta_{\mathbf{k}} \end{pmatrix}, \end{aligned} \tag{6.21}$$

where

$$\mathcal{S}_{\mathbf{k}} \equiv \begin{pmatrix} \psi_{\mathbf{k}}^{*(A)} \psi_{\mathbf{k}}^{(A)} & \psi_{\mathbf{k}}^{*(A)} \psi_{\mathbf{k}}^{(B)} \\ \psi_{\mathbf{k}}^{*(B)} \psi_{\mathbf{k}}^{(A)} & \psi_{\mathbf{k}}^{*(B)} \psi_{\mathbf{k}}^{(B)} \end{pmatrix}, \tag{6.22}$$

called the overlap matrix. From the hermicity of $\mathcal{H}_{\mathbf{k}}$ it is clear that $\mathcal{S}_{\mathbf{k}}$ is also hermitian $\mathcal{S}_{\mathbf{k}} = \mathcal{S}_{\mathbf{k}}^{\dagger}$. This leads to the following relation

$$\begin{pmatrix} \alpha_{\mathbf{k}}^{*} & \beta_{\mathbf{k}}^{*} \end{pmatrix} \mathcal{H}_{\mathbf{k}} \begin{pmatrix} \alpha_{\mathbf{k}} \\ \beta_{\mathbf{k}} \end{pmatrix} = \epsilon_{\mathbf{k}} \begin{pmatrix} \alpha_{\mathbf{k}}^{*} & \beta_{\mathbf{k}}^{*} \end{pmatrix} \mathcal{S}_{\mathbf{k}} \begin{pmatrix} \alpha_{\mathbf{k}} \\ \beta_{\mathbf{k}} \end{pmatrix}. \tag{6.23}$$

The energy bands of the π electrons correspond to the eigenvalues of $\epsilon_{\mathbf{k}}$

$$\begin{aligned} \mathcal{H}_{\mathbf{k}} \begin{pmatrix} \alpha_{\mathbf{k}} \\ \beta_{\mathbf{k}} \end{pmatrix} &= \epsilon_{\mathbf{k}} \mathcal{S}_{\mathbf{k}} \begin{pmatrix} \alpha_{\mathbf{k}} \\ \beta_{\mathbf{k}} \end{pmatrix} \\ \begin{pmatrix} \mathcal{H}_{\mathbf{k}} \alpha_{\mathbf{k}} \\ \mathcal{H}_{\mathbf{k}} \beta_{\mathbf{k}} \end{pmatrix} &= \begin{pmatrix} \epsilon_{\mathbf{k}} \mathcal{S}_{\mathbf{k}} \alpha_{\mathbf{k}} \\ \epsilon_{\mathbf{k}} \mathcal{S}_{\mathbf{k}} \beta_{\mathbf{k}} \end{pmatrix} \\ \begin{pmatrix} \mathcal{H}_{\mathbf{k}} \alpha_{\mathbf{k}} - \epsilon_{\mathbf{k}} \mathcal{S}_{\mathbf{k}} \alpha_{\mathbf{k}} \\ \mathcal{H}_{\mathbf{k}} \beta_{\mathbf{k}} - \epsilon_{\mathbf{k}} \mathcal{S}_{\mathbf{k}} \beta_{\mathbf{k}} \end{pmatrix} &= 0 \\ \det \left(\mathcal{H}_{\mathbf{k}} - \epsilon_{\mathbf{k}}^{\lambda} \mathcal{S}_{\mathbf{k}} \right) &= 0. \end{aligned}$$

The solution to the last equation yields the energy bands. The index λ on the energy indicates that there is more than one solution, in this case two, because there are two atoms in one unit cell [35].

To solve this equation, it can be written in terms of the orbital functions using Eq. (6.18). The Hamiltonian H is split into a part for the atomic orbital $H^a = -(\hbar^2/2p)\Delta + V(\mathbf{r} + \boldsymbol{\delta}_j - \mathbf{R}_l)$ and a part ΔV, which is a perturbation that corrects the atomic potential so that the potential of the Hamiltonian corresponds to the potential of the crystal (just like was done in Section 3.2).

H^a satisfies the eigenvalue equation $H^a\phi^{(j)}(\mathbf{r}+\boldsymbol{\delta}_j-\mathbf{R}_l)=\epsilon^{(j)}\phi^{(j)}(\mathbf{r}+\boldsymbol{\delta}_j-\mathbf{R}_l)$ [35]. As all atoms in the system are the same, they yield the same on-site energy. This means that this energy only shifts the energy bands, and can therefore be omitted from the calculation by setting it to zero, i.e. $H^a\phi^{(j)}=0$. The Bravais lattice vectors correspond to those of the A sublattice, such that $\mathbf{r}_A=0$, and the equivalent site on sublattice B is found by the displacement $\mathbf{r}_B=\boldsymbol{\delta}_3$ [35].[2] The orbital wavefunctions are normalized such that $\int \mathrm{d}^2r\phi^{*(j)}(\mathbf{r})\,\phi^{(j)}(\mathbf{r})=1$. Lastly, overlap by orbitals that are not nearest-neighbor are neglected.

The four matrix elements of $\mathcal{H}_\mathbf{k}-\epsilon^\lambda_\mathbf{k}\mathcal{S}_\mathbf{k}$ will be treated seperately. First, the off-diagonal elements will be evaluated. $\mathcal{H}^{AB}_\mathbf{k}=(\mathcal{H}^{BA}_\mathbf{k})^*$ yields a hopping term. The nearest-neighbor hopping amplitude is defined as

$$t_{NN}\equiv-\int \mathrm{d}^2r\,\phi^{*(A)}(\mathbf{r})\,\Delta V\phi^{(B)}(\mathbf{r}+\boldsymbol{\delta}_3) \tag{6.24}$$

An atom at site A has three nearest-neighbors. In Eq. (6.24), the hopping is defined as going from site A to site B with a vector $\boldsymbol{\delta}_3$. Therefore, to cover the other two possibilities, Eq. (6.24) needs to be shifted with a phase factor as appears in Eq. (6.18). To go to the nearest-neighbor at $\mathbf{r}+\boldsymbol{\delta}_1$, Eq. (6.24) needs to be multiplied by $\exp(i\mathbf{k}\cdot\mathbf{a}_1)$. To go to $\mathbf{r}+\boldsymbol{\delta}_2$, Eq. (6.24) needs to be multiplied by $\exp(i\mathbf{k}\cdot\mathbf{a}_2)$. This leads to the following off-diagonal term

$$\mathcal{H}^{AB}_\mathbf{k}=-t_{NN}\left(1+\mathrm{e}^{i\mathbf{k}\cdot\mathbf{a}_2}+\mathrm{e}^{i\mathbf{k}\cdot\mathbf{a}_3}\right)=-t_{NN}\,\gamma_\mathbf{k}, \tag{6.25}$$

where

$$\gamma_\mathbf{k}\equiv 1+\mathrm{e}^{i\mathbf{k}\cdot\mathbf{a}_2}+\mathrm{e}^{i\mathbf{k}\cdot\mathbf{a}_3}. \tag{6.26}$$

Next, $-\epsilon^\lambda_\mathbf{k}\mathcal{S}^{AB}_\mathbf{k}=(-\epsilon^\lambda_\mathbf{k}\mathcal{S}^{BA}_\mathbf{k})^*$ yields a correction to the overlap of atomic orbitals. It is assumed that only orbitals on nearest-neighbor sites overlap. The overlap correction is defined as

$$s\equiv\int \mathrm{d}^2r\,\phi^{*(A)}(\mathbf{r})\,\phi^{(B)}(\mathbf{r}+\boldsymbol{\delta}_3)\,. \tag{6.27}$$

Using the same reasoning as before, the result is

$$-\epsilon^\lambda_\mathbf{k}\mathcal{S}^{AB}_\mathbf{k}=-\epsilon^\lambda_\mathbf{k}s\left(1+\mathrm{e}^{i\mathbf{k}\cdot\mathbf{a}_1}+\mathrm{e}^{i\mathbf{k}\cdot\mathbf{a}_2}\right)=-\epsilon^\lambda_\mathbf{k}s\gamma_\mathbf{k}.$$

So the off-diagonal terms are

$$\mathcal{H}^{AB}_\mathbf{k}-\epsilon^\lambda_\mathbf{k}\mathcal{S}^{AB}_\mathbf{k}=-\left(t_{NN}+\epsilon^\lambda_\mathbf{k}s\right)\gamma_\mathbf{k},\qquad \mathcal{H}^{BA}_\mathbf{k}-\epsilon^\lambda_\mathbf{k}\mathcal{S}^{AB}_\mathbf{k}=-\left(t_{NN}+\epsilon^\lambda_\mathbf{k}s\right)\gamma^*_\mathbf{k}. \tag{6.28}$$

Next, the diagonal terms will be evaluated. $\mathcal{H}^{AA}_\mathbf{k}=\mathcal{H}^{BB}_\mathbf{k}$ yields a hopping term between next-nearest neighbor sites separated from each other by the lattice vectors in Eq. (3.1). The following is found

$$\mathcal{H}^{AA}_\mathbf{k}=\psi^{*(A)}_\mathbf{k}H\psi^{(A)}_\mathbf{k}=\int \mathrm{d}^2r\,\phi^{*(A)}(\mathbf{r})\,\Delta V\left[\mathrm{e}^{i\mathbf{k}\cdot\mathbf{a}_1}\phi^{(A)}(\mathbf{r}-\mathbf{a}_1)+\mathrm{e}^{-i\mathbf{k}\cdot\mathbf{a}_1}\phi^{(A)}(\mathbf{r}+\mathbf{a}_1)\right.$$
$$\left.+\mathrm{e}^{i\mathbf{k}\cdot\mathbf{a}_2}\phi^{(A)}(\mathbf{r}-\mathbf{a}_2)+\mathrm{e}^{-i\mathbf{k}\cdot\mathbf{a}_2}\phi^{(A)}(\mathbf{r}+\mathbf{a}_2)+\mathrm{e}^{i\mathbf{k}\cdot\mathbf{a}_3}\phi^{(A)}(\mathbf{r}-\mathbf{a}_3)+\mathrm{e}^{-i\mathbf{k}\cdot\mathbf{a}_3}\phi^{(A)}(\mathbf{r}+\mathbf{a}_3)\right].$$

[2] One can choose any of the other vectors $\boldsymbol{\delta}_j$ without changing the physics.

All sites A are equivalent to each other, i.e.

$$\phi^{(A)}(\mathbf{r}-\mathbf{a}_1)=\phi^{(A)}(\mathbf{r}+\mathbf{a}_1)=\phi^{(A)}(\mathbf{r}-\mathbf{a}_2)=\phi^{(A)}(\mathbf{r}+\mathbf{a}_2)=\phi^{(A)}(\mathbf{r}-\mathbf{a}_3)=\phi^{(A)}(\mathbf{r}+\mathbf{a}_3).$$

Defining the next-nearest hopping amplitude as

$$t_{NNN}\equiv-\int \mathrm{d}^2r\,\phi^{*(A)}(\mathbf{r})\,\Delta V\phi^{(A)}(\mathbf{r}+\mathbf{a}_3) \tag{6.29}$$

the following is retrieved

$$\begin{aligned}\mathcal{H}_{\mathbf{k}}^{AA}&=-t_{NNN}\left(\mathrm{e}^{i\mathbf{k}\cdot\mathbf{a}_1}+\mathrm{e}^{-i\mathbf{k}\cdot\mathbf{a}_1}+\mathrm{e}^{i\mathbf{k}\cdot\mathbf{a}_2}+\mathrm{e}^{-i\mathbf{k}\cdot\mathbf{a}_2}+\mathrm{e}^{i\mathbf{k}\cdot\mathbf{a}_3}+\mathrm{e}^{-i\mathbf{k}\cdot\mathbf{a}_3}\right)\\&=-2\,t_{NNN}\sum_i\cos(\mathbf{k}\cdot\mathbf{a}_i)=-t_{NNN}\left(|\gamma_{\mathbf{k}}|^2-3\right).\end{aligned} \tag{6.30}$$

That this last equality holds can be easily checked

$$\begin{aligned}|\gamma_{\mathbf{k}}|^2-3&=\left(1+\mathrm{e}^{-i\mathbf{k}\cdot\mathbf{a}_2}+\mathrm{e}^{-i\mathbf{k}\cdot\mathbf{a}_3}\right)\left(1+\mathrm{e}^{i\mathbf{k}\cdot\mathbf{a}_2}+\mathrm{e}^{i\mathbf{k}\cdot\mathbf{a}_3}\right)-3\\&=1+1+1+\mathrm{e}^{i\mathbf{k}\cdot\mathbf{a}_2}+\mathrm{e}^{-i\mathbf{k}\cdot\mathbf{a}_2}+\mathrm{e}^{i\mathbf{k}\cdot\mathbf{a}_3}+\mathrm{e}^{-i\mathbf{k}\cdot\mathbf{a}_3}+\mathrm{e}^{i\mathbf{k}\cdot(\mathbf{a}_2-\mathbf{a}_3)}+\mathrm{e}^{-i\mathbf{k}\cdot(\mathbf{a}_2-\mathbf{a}_3)}-3\\&=2\cos(\mathbf{k}\cdot\mathbf{a}_1)+2\cos(\mathbf{k}\cdot\mathbf{a}_2)+2\cos(\mathbf{k}\cdot\mathbf{a}_3)=2\sum_i\cos(\mathbf{k}\cdot\mathbf{a}_i).\end{aligned} \tag{6.31}$$

The second part of this equation yields

$$-\epsilon_{\mathbf{k}}^{\lambda}\psi_{\mathbf{k}}^{*(A)}\psi_{\mathbf{k}}^{(A)}=-\epsilon_{\mathbf{k}}^{\lambda}\int\mathrm{d}^2r\sum_{\mathbf{R}_l,\mathbf{R}'_l}\mathrm{e}^{-i\mathbf{k}\cdot(\mathbf{R}_l-\mathbf{R}'_l)}\phi^{*(A)}(\mathbf{r}-\mathbf{R}_l)\,\phi^{(A)}(\mathbf{r}-\mathbf{R}'_l).$$

Any overlap of orbitals that are not nearest neighbor is neglected, hence this equation yields zero unless $\mathbf{r}-\mathbf{R}_l=\mathbf{r}-\mathbf{R}'_l$, because then the renormalization condition can be used. Therefore, the solution to this equation is

$$-\epsilon_{\mathbf{k}}^{\lambda}\psi_{\mathbf{k}}^{*(A)}\psi_{\mathbf{k}}^{(A)}=-\epsilon_{\mathbf{k}}^{\lambda}.$$

So the diagonal terms are

$$\mathcal{H}_{\mathbf{k}}^{AA}-\epsilon_{\mathbf{k}}^{\lambda}\mathcal{S}_{\mathbf{k}}^{AA}=\mathcal{H}_{\mathbf{k}}^{BB}-\epsilon_{\mathbf{k}}^{\lambda}\mathcal{S}_{\mathbf{k}}^{BB}=-t_{NNN}\left(|\gamma_{\mathbf{k}}|^2-3\right)-\epsilon_{\mathbf{k}}^{\lambda}. \tag{6.32}$$

These considerations lead to the following equation

$$\det\begin{bmatrix}-t_{NNN}\left(|\gamma_{\mathbf{k}}|^2-3\right)-\epsilon_{\mathbf{k}}^{\lambda} & -\left(t_{NN}+\epsilon_{\mathbf{k}}^{\lambda}s\right)\gamma_{\mathbf{k}}\\ -\left(t_{NN}+\epsilon_{\mathbf{k}}^{\lambda}s\right)\gamma_{\mathbf{k}}^{*} & -t_{NNN}\left(|\gamma_{\mathbf{k}}|^2-3\right)-\epsilon_{\mathbf{k}}^{\lambda}\end{bmatrix}=0.$$

Solving yields

$$\begin{aligned}\left[t_{NNN}\left(|\gamma_{\mathbf{k}}|^2-3\right)+\epsilon_{\mathbf{k}}^{\lambda}\right]^2&=\left(t_{NN}+\epsilon_{\mathbf{k}}^{\lambda}s\right)^2|\gamma_{\mathbf{k}}|^2\\ t_{NNN}\left(|\gamma_{\mathbf{k}}|^2-3\right)+\epsilon_{\mathbf{k}}^{\lambda}&=\pm\left(t_{NN}+\epsilon_{\mathbf{k}}^{\lambda}s\right)|\gamma_{\mathbf{k}}|\\ \epsilon_{\mathbf{k}}^{\lambda}\left(1\mp s\,|\gamma_{\mathbf{k}}|\right)&=\pm t_{NN}\,|\gamma_{\mathbf{k}}|-t_{NNN}\left(|\gamma_{\mathbf{k}}|^2-3\right)\\ \epsilon_{\mathbf{k}}^{\lambda}&=\frac{t_{NNN}\left(|\gamma_{\mathbf{k}}|^2-3\right)\pm t_{NN}\,|\gamma_{\mathbf{k}}|}{1\mp s\,|\gamma_{\mathbf{k}}|}\\ \epsilon_{\mathbf{k}}^{\lambda}&=\frac{t_{NNN}\left(|\gamma_{\mathbf{k}}|^2-3\right)+\lambda t_{NN}\,|\gamma_{\mathbf{k}}|}{1-\lambda s\,|\gamma_{\mathbf{k}}|},\end{aligned} \tag{6.33}$$

where $\lambda = \pm$. This equation can be expanded using that $s \ll 1$ and $t_{NNN} \ll t_{NN}$. The orbital wavefunctions are defined to be localized, so their overlap is assumed to be extremely small, hence the first assumption. The second assumption rests on the same argument and implies that the overlap between orbital functions of next-nearest neighbors is much smaller than the overlap of nearest-neighbor orbitals. The following is found

$$\begin{aligned}
\epsilon_{\mathbf{k}}^{\lambda} &\approx \left[t_{NNN}\left(|\gamma_{\mathbf{k}}|^2 - 3\right) + \lambda t_{NN}|\gamma_{\mathbf{k}}|\right]\left[1 + \lambda s|\gamma_{\mathbf{k}}|\right] \\
&= t_{NNN}\left(|\gamma_{\mathbf{k}}|^2 - 3\right) + \lambda t_{NN}|\gamma_{\mathbf{k}}| + \lambda t_{NNN} s|\gamma_{\mathbf{k}}|\left(|\gamma_{\mathbf{k}}|^2 - 3\right) + t_{NN} s|\gamma_{\mathbf{k}}|^2 \\
&= (t_{NNN} + t_{NN}s)|\gamma_{\mathbf{k}}|^2 - 3t_{NNN} + \lambda t_{NN}|\gamma_{\mathbf{k}}| + \lambda t_{NNN} s|\gamma_{\mathbf{k}}|\left(|\gamma_{\mathbf{k}}|^2 - 3\right) \\
&= t'_{NNN}|\gamma_{\mathbf{k}}|^2 - 3t_{NNN} + \lambda t_{NN}|\gamma_{\mathbf{k}}| + \lambda t_{NNN} s|\gamma_{\mathbf{k}}|\left(|\gamma_{\mathbf{k}}|^2 - 3\right),
\end{aligned}$$

where $t'_{NNN} \equiv t_{NNN} + t_{NN}s$ is the effective next-nearest neighbor parameter. The last term in this equation can be neglected because it is extremely small compared to the other terms. Moreover, the term $-3t_{NNN}$ is just a constant that shifts the energy bands and can be left out. Using Eq. (6.31) leads to the following

$$\epsilon_{\mathbf{k}}^{\lambda} = t'_{NNN}\left[3 + 2\sum_i \cos\left(\mathbf{k}\cdot\mathbf{a}_i\right)\right] + \lambda t_{NN}\sqrt{3 + 2\sum_i \cos\left(\mathbf{k}\cdot\mathbf{a}_i\right)}. \tag{6.34}$$

Using Eq. (3.1), the energy bands can be computed explicitly. The cosine leads to the following

$$\begin{aligned}
&2\sum_i \cos\left(\mathbf{k}\cdot\mathbf{a}_i\right) = 2\cos\left(\mathbf{k}\cdot\mathbf{a}_1\right) + 2\cos\left(\mathbf{k}\cdot\mathbf{a}_2\right) + 2\cos\left(\mathbf{k}\cdot\mathbf{a}_3\right) \\
&= 2\cos\left[k_{\mathbf{x}}(a_1)_{\mathbf{x}} + k_{\mathbf{y}}(a_1)_{\mathbf{y}}\right] + 2\cos\left[k_{\mathbf{x}}(a_2)_{\mathbf{x}} + k_{\mathbf{y}}(a_2)_{\mathbf{y}}\right] + 2\cos\left[k_{\mathbf{x}}(a_1 - a_2)_{\mathbf{x}} + k_{\mathbf{y}}(a_1 - a_2)_{\mathbf{y}}\right] \\
&= 2\cos\left(k_{\mathbf{x}}\frac{3a}{2} + k_{\mathbf{y}}\frac{\sqrt{3}a}{2}\right) + 2\cos\left(k_{\mathbf{x}}\frac{3a}{2} - k_{\mathbf{y}}\frac{\sqrt{3}a}{2}\right) + 2\cos\left(k_{\mathbf{y}}\sqrt{3}a\right) \\
&= 2\cos\left(k_{\mathbf{x}}\frac{3a}{2}\right)\cos\left(k_{\mathbf{y}}\frac{\sqrt{3}a}{2}\right) - 2\sin\left(k_{\mathbf{x}}\frac{3a}{2}\right)\sin\left(k_{\mathbf{y}}\frac{\sqrt{3}a}{2}\right) + 2\cos\left(k_{\mathbf{x}}\frac{3a}{2}\right)\cos\left(k_{\mathbf{y}}\frac{\sqrt{3}a}{2}\right) \\
&+2\sin\left(k_{\mathbf{x}}\frac{3a}{2}\right)\sin\left(k_{\mathbf{y}}\frac{\sqrt{3}a}{2}\right) + 2\cos\left(k_{\mathbf{y}}\sqrt{3}a\right) \\
&= 2\cos\left(k_{\mathbf{y}}\sqrt{3}a\right) + 4\cos\left(k_{\mathbf{x}}\frac{3a}{2}\right)\cos\left(k_{\mathbf{y}}\frac{\sqrt{3}a}{2}\right) \equiv f\left(\mathbf{k}\right).
\end{aligned}$$

The energy bands are

$$\begin{aligned}
\epsilon_{\mathbf{k}}^{\lambda} &= t'_{NNN}\left[3 + 2\cos\left(k_{\mathbf{y}}\sqrt{3}a\right) + 4\cos\left(k_{\mathbf{x}}\frac{3a}{2}\right)\cos\left(k_{\mathbf{y}}\frac{\sqrt{3}a}{2}\right)\right] \\
&\quad + \lambda t_{NN}\sqrt{3 + 2\cos\left(k_{\mathbf{y}}\sqrt{3}a\right) + 4\cos\left(k_{\mathbf{x}}\frac{3a}{2}\right)\cos\left(k_{\mathbf{y}}\frac{\sqrt{3}a}{2}\right)} \\
&= \lambda t_{NN}\sqrt{3 + f\left(\mathbf{k}\right)} + t'_{NNN}\left[3 + f\left(\mathbf{k}\right)\right].
\end{aligned} \tag{6.35}$$

The values of the hopping parameters can be found by fitting the energy dispersion to the energy dispersion calculated numerically in more rigourous band-structure calculations. The value of the nearest-neighbor hopping parameter is $t_{NN} \approx -3$ eV [35]. For the next-nearest neighbor hopping $t'_{NNN} \approx 0.1 t_{NN}$, so indeed $t_{NNN} \ll t_{NN}$. This shows that in this case, where t_{NN} and t_{NNN} are defined with equal sign, also have an equal sign in their value. Comparing to the second quantized case shows that there t and t' show up in the dispersion relation with opposite sign. Therefore, their values fitted to first principle calculations, should be opposite.

6.2.2 Derivation of Energy Bands in Second Quantized Language

To find the energy bands from the Hamiltonian in Eq. (3.9), it is easiest to treat the nearest-neighbor (nn) and next-nearest neighbor (nnn) parts separately. The nn part of the Hamiltonian is

$$H_{nn} = -t \sum_{\langle i,j \rangle, \sigma} \left(a^\dagger_{\sigma,i} b_{\sigma,j} + b^\dagger_{\sigma,j} a_{\sigma,i} \right).$$

The nn of position $\mathbf{r}_i$ is $\mathbf{r}_j = \mathbf{r}_i + \boldsymbol{\delta}_\alpha$ with $\alpha = 1, 2, 3$ where $\boldsymbol{\delta}_\alpha$ is defined in Eq. (3.2). The Fourier transform of the operators a and b is

$$a_{\sigma,i} = \frac{1}{\sqrt{N}} \sum_{\mathbf{k}} a_{\sigma,\mathbf{k}} \mathrm{e}^{i\mathbf{k}\cdot\mathbf{r}_i}, \qquad b_{\sigma,i} = \frac{1}{\sqrt{N}} \sum_{\mathbf{k}} b_{\sigma,\mathbf{k}} \mathrm{e}^{i\mathbf{k}\cdot\mathbf{r}_i},$$

where N is the number of atoms in each sublattice. Plugging the Fourier transform into H_{nn} leads to the following

$$\begin{aligned}
H_{nn} &= -\frac{t}{N} \sum_{\sigma} \sum_{\mathbf{r}_i, \mathbf{r}_j} \sum_{\mathbf{k},\mathbf{q}} \left(a^\dagger_{\sigma,\mathbf{k}} b_{\sigma,\mathbf{q}} \mathrm{e}^{-i\mathbf{k}\cdot\mathbf{r}_i + i\mathbf{q}\cdot\mathbf{r}_j} + b^\dagger_{\sigma,\mathbf{q}} a_{\sigma,\mathbf{k}} \mathrm{e}^{-i\mathbf{q}\cdot\mathbf{r}_j + i\mathbf{k}\cdot\mathbf{r}_i} \right) \\
&= -\frac{t}{N} \sum_{\sigma} \sum_{\mathbf{r}_i, \boldsymbol{\delta}_\alpha} \sum_{\mathbf{k},\mathbf{q}} \left(a^\dagger_{\sigma,\mathbf{k}} b_{\sigma,\mathbf{q}} \mathrm{e}^{-i\mathbf{k}\cdot\mathbf{r}_i + i\mathbf{q}\cdot(\mathbf{r}_i + \boldsymbol{\delta}_\alpha)} + b^\dagger_{\sigma,\mathbf{q}} a_{\sigma,\mathbf{k}} \mathrm{e}^{-i\mathbf{q}\cdot(\mathbf{r}_i + \boldsymbol{\delta}_\alpha) + i\mathbf{k}\cdot\mathbf{r}_i} \right) \\
&= -\frac{t}{N} \sum_{\sigma} \sum_{\mathbf{r}_i, \boldsymbol{\delta}_\alpha} \sum_{\mathbf{k},\mathbf{q}} \left(a^\dagger_{\sigma,\mathbf{k}} b_{\sigma,\mathbf{q}} \mathrm{e}^{-i(\mathbf{k}-\mathbf{q})\cdot\mathbf{r}_i + i\mathbf{q}\cdot\boldsymbol{\delta}_\alpha} + b^\dagger_{\sigma,\mathbf{q}} a_{\sigma,\mathbf{k}} \mathrm{e}^{-i(\mathbf{q}-\mathbf{k})\cdot\mathbf{r}_i - i\mathbf{q}\cdot\boldsymbol{\delta}_\alpha} \right).
\end{aligned}$$

The following relation is used

$$\sum_i \mathrm{e}^{i(\mathbf{k}-\mathbf{q})\cdot\mathbf{r}_i} = N \delta_{\mathbf{k},\mathbf{q}}$$

to find

$$\begin{aligned}
H_{nn} &= -\frac{t}{N} \sum_{\sigma,\boldsymbol{\delta}_\alpha} \sum_{\mathbf{k},\mathbf{q}} \left(a^\dagger_{\sigma,\mathbf{k}} b_{\sigma,\mathbf{q}} N \delta_{\mathbf{k},\mathbf{q}} \mathrm{e}^{i\mathbf{q}\cdot\boldsymbol{\delta}_\alpha} + b^\dagger_{\sigma,\mathbf{q}} a_{\sigma,\mathbf{k}} N \delta_{\mathbf{k},\mathbf{q}} \mathrm{e}^{-i\mathbf{q}\cdot\boldsymbol{\delta}_\alpha} \right) \\
&= -t \sum_{\sigma,\boldsymbol{\delta}_\alpha,\mathbf{k}} \left(a^\dagger_{\sigma,\mathbf{k}} b_{\sigma,\mathbf{k}} \mathrm{e}^{i\mathbf{k}\cdot\boldsymbol{\delta}_\alpha} + b^\dagger_{\sigma,\mathbf{k}} a_{\sigma,\mathbf{k}} \mathrm{e}^{-i\mathbf{k}\cdot\boldsymbol{\delta}_\alpha} \right).
\end{aligned}$$

Defining the function

$$g(\mathbf{k}) \equiv -t \sum_{\boldsymbol{\delta}_\alpha} \mathrm{e}^{i\mathbf{k}\cdot\boldsymbol{\delta}_\alpha}, \tag{6.36}$$

allows H_{nn} to be written as

$$H_{nn} = \sum_{\sigma,\mathbf{k}} \begin{pmatrix} a^\dagger_{\sigma,\mathbf{k}} & b^\dagger_{\sigma,\mathbf{k}} \end{pmatrix} \begin{pmatrix} 0 & g(\mathbf{k}) \\ g^*(\mathbf{k}) & 0 \end{pmatrix} \begin{pmatrix} a_{\sigma,\mathbf{k}} \\ b_{\sigma,\mathbf{k}} \end{pmatrix}. \tag{6.37}$$

This leads to the following relation

$$\begin{aligned} \begin{pmatrix} 0 & g(\mathbf{k}) \\ g^*(\mathbf{k}) & 0 \end{pmatrix} \begin{pmatrix} a_{\sigma,\mathbf{k}} \\ b_{\sigma,\mathbf{k}} \end{pmatrix} &= E_{\mathbf{k},nn} \begin{pmatrix} a_{\sigma,\mathbf{k}} \\ b_{\sigma,\mathbf{k}} \end{pmatrix} \\ \begin{pmatrix} g(\mathbf{k}) b_{\sigma,\mathbf{k}} \\ g^*(\mathbf{k}) a_{\sigma,\mathbf{k}} \end{pmatrix} &= \begin{pmatrix} E_{\mathbf{k},nn} a_{\sigma,\mathbf{k}} \\ E_{\mathbf{k},nn} b_{\sigma,\mathbf{k}} \end{pmatrix}. \end{aligned}$$

There are two equations that need to be satisfied

$$\begin{aligned} g(\mathbf{k}) b_{\sigma,\mathbf{k}} &= E_{\mathbf{k},nn} a_{\sigma,\mathbf{k}}, \\ g^*(\mathbf{k}) a_{\sigma,\mathbf{k}} &= E_{\mathbf{k},nn} b_{\sigma,\mathbf{k}}. \end{aligned}$$

Rewriting

$$\begin{aligned} E_{\mathbf{k},nn} a_{\sigma,\mathbf{k}} - g(\mathbf{k}) b_{\sigma\mathbf{k}} &= 0 \\ -g^*(\mathbf{k}) a_{\sigma\mathbf{k}} + E_{\mathbf{k},nn} b_{\sigma,\mathbf{k}} &= 0 \end{aligned}$$

leads to

$$\begin{vmatrix} E_{\mathbf{k},nn} & -g(\mathbf{k}) \\ -g^*(\mathbf{k}) & E_{\mathbf{k},nn} \end{vmatrix} = 0.$$

Such that the energy band for nn is

$$\begin{aligned} E^2_{\mathbf{k},nn} - |g(\mathbf{k})|^2 &= 0 \\ E^2_{\mathbf{k},nn} &= |g(\mathbf{k})|^2 \\ E_{\mathbf{k},nn} &= \pm |g(\mathbf{k})|. \end{aligned} \tag{6.38}$$

Next, $E_{\mathbf{k},nn}$ will be computed explicitly. Starting with

$$\begin{aligned} g^*(\mathbf{k}) g(\mathbf{k}) &= \left(-t \sum_{\boldsymbol{\delta}_\alpha} \mathrm{e}^{-i\mathbf{k}\cdot\boldsymbol{\delta}_\alpha} \right) \left(-t \sum_{\boldsymbol{\delta}_\beta} \mathrm{e}^{i\mathbf{k}\cdot\boldsymbol{\delta}_\beta} \right) \\ &= t^2 \left(\mathrm{e}^{-i\mathbf{k}\cdot\boldsymbol{\delta}_1} + \mathrm{e}^{-i\mathbf{k}\cdot\boldsymbol{\delta}_2} + \mathrm{e}^{-i\mathbf{k}\cdot\boldsymbol{\delta}_3} \right) \left(\mathrm{e}^{i\mathbf{k}\cdot\boldsymbol{\delta}_1} + \mathrm{e}^{i\mathbf{k}\cdot\boldsymbol{\delta}_2} + \mathrm{e}^{i\mathbf{k}\cdot\boldsymbol{\delta}_3} \right) \\ &= t^2 \left(1 + \mathrm{e}^{-i\mathbf{k}\cdot(\boldsymbol{\delta}_2 - \boldsymbol{\delta}_1)} + \mathrm{e}^{-i\mathbf{k}\cdot(\boldsymbol{\delta}_3 - \boldsymbol{\delta}_1)} + \mathrm{e}^{-i\mathbf{k}\cdot(\boldsymbol{\delta}_1 - \boldsymbol{\delta}_2)} + 1 + \mathrm{e}^{-i\mathbf{k}\cdot(\boldsymbol{\delta}_3 - \boldsymbol{\delta}_2)} + \mathrm{e}^{-i\mathbf{k}\cdot(\boldsymbol{\delta}_1 - \boldsymbol{\delta}_3)} + \mathrm{e}^{-i\mathbf{k}\cdot(\boldsymbol{\delta}_2 - \boldsymbol{\delta}_3)} + 1 \right) \\ &= t^2 \left(3 + \mathrm{e}^{i\mathbf{k}\cdot(\boldsymbol{\delta}_1 - \boldsymbol{\delta}_2)} + \mathrm{e}^{-i\mathbf{k}\cdot(\boldsymbol{\delta}_1 - \boldsymbol{\delta}_2)} + \mathrm{e}^{i\mathbf{k}\cdot(\boldsymbol{\delta}_1 - \boldsymbol{\delta}_3)} + \mathrm{e}^{-i\mathbf{k}\cdot(\boldsymbol{\delta}_1 - \boldsymbol{\delta}_3)} + \mathrm{e}^{i\mathbf{k}\cdot(\boldsymbol{\delta}_2 - \boldsymbol{\delta}_3)} + \mathrm{e}^{-i\mathbf{k}\cdot(\boldsymbol{\delta}_2 - \boldsymbol{\delta}_3)} \right) \\ &= t^2 \left[3 + 2\cos(\mathbf{k}(\boldsymbol{\delta}_1 - \boldsymbol{\delta}_2)) + 2\cos(\mathbf{k}(\boldsymbol{\delta}_1 - \boldsymbol{\delta}_3)) + 2\cos(\mathbf{k}(\boldsymbol{\delta}_2 - \boldsymbol{\delta}_3)) \right], \end{aligned} \tag{6.39}$$

which can be evaluated explicitly using Eq. (3.2). The cosines are

$$\begin{aligned} &2\cos\left[\mathbf{k}(\boldsymbol{\delta}_1 - \boldsymbol{\delta}_2)\right] = 2\cos\left[k_\mathbf{x}(\delta_1 - \delta_2)_\mathbf{x} + k_\mathbf{y}(\delta_1 - \delta_2)_\mathbf{y}\right] \\ &= 2\cos\left[k_\mathbf{x}\left(\frac{a}{2} - \frac{a}{2}\right) + k_\mathbf{y}\left(\frac{\sqrt{3}a}{2} + \frac{\sqrt{3}a}{2}\right) \right] = 2\cos\left(k_\mathbf{y}\sqrt{3}a\right), \end{aligned}$$

$$
\begin{aligned}
&2\cos\left[\mathbf{k}(\boldsymbol{\delta}_1-\boldsymbol{\delta}_3)\right]=2\cos\left[k_{\mathbf{x}}(\delta_1-\delta_3)_{\mathbf{x}}+k_{\mathbf{y}}(\delta_1-\delta_3)_{\mathbf{y}}\right]\\
&=2\cos\left[k_{\mathbf{x}}\left(\frac{a}{2}+a\right)+k_{\mathbf{y}}\left(\frac{\sqrt{3}a}{2}-0\right)\right]=2\cos\left(k_{\mathbf{x}}\frac{3a}{2}+k_{\mathbf{y}}\frac{\sqrt{3}a}{2}\right)\\
&=2\cos\left(k_{\mathbf{x}}\frac{3a}{2}\right)\cos\left(k_{\mathbf{y}}\frac{\sqrt{3}a}{2}\right)-2\sin\left(k_{\mathbf{x}}\frac{3a}{2}\right)\sin\left(k_{\mathbf{y}}\frac{\sqrt{3}a}{2}\right),
\end{aligned}
$$

and

$$
\begin{aligned}
&2\cos\left[\mathbf{k}(\boldsymbol{\delta}_2-\boldsymbol{\delta}_3)\right]=2\cos\left[k_{\mathbf{x}}(\delta_2-\delta_3)_{\mathbf{x}}+k_{\mathbf{y}}(\delta_2-\delta_3)_{\mathbf{y}}\right]\\
&=2\cos\left[k_{\mathbf{x}}\left(\frac{a}{2}+a\right)+k_{\mathbf{y}}\left(-\frac{\sqrt{3}a}{2}+0\right)\right]=2\cos\left(k_{\mathbf{x}}\frac{3a}{2}-k_{\mathbf{y}}\frac{\sqrt{3}a}{2}\right)\\
&=2\cos\left(k_{\mathbf{x}}\frac{3a}{2}\right)\cos\left(k_{\mathbf{y}}\frac{\sqrt{3}a}{2}\right)+2\sin\left(k_{\mathbf{x}}\frac{3a}{2}\right)\sin\left(k_{\mathbf{y}}\frac{\sqrt{3}a}{2}\right).
\end{aligned}
$$

Plugging these results back into Eq. (6.39) leads to

$$
\begin{aligned}
&g^*(\mathbf{k})g(\mathbf{k})=t^2\left[3+2\cos\left(k_{\mathbf{y}}\sqrt{3}a\right)+2\cos\left(k_{\mathbf{x}}\frac{3a}{2}\right)\cos\left(k_{\mathbf{y}}\frac{\sqrt{3}a}{2}\right)\right.\\
&\left.-2\sin\left(k_{\mathbf{x}}\frac{3a}{2}\right)\sin\left(k_{\mathbf{y}}\frac{\sqrt{3}a}{2}\right)+2\cos\left(k_{\mathbf{x}}\frac{3a}{2}\right)\cos\left(k_{\mathbf{y}}\frac{\sqrt{3}a}{2}\right)+2\sin\left(k_{\mathbf{x}}\frac{3a}{2}\right)\sin\left(k_{\mathbf{y}}\frac{\sqrt{3}a}{2}\right)\right]\\
&=t^2\left[3+2\cos\left(k_{\mathbf{y}}\sqrt{3}a\right)+4\cos\left(k_{\mathbf{x}}\frac{3a}{2}\right)\cos\left(k_{\mathbf{y}}\frac{\sqrt{3}a}{2}\right)\right],
\end{aligned}
$$

such that

$$
E_{\mathbf{k},nn}=\pm t\sqrt{3+f(\mathbf{k})}, \tag{6.40}
$$

with

$$
f(\mathbf{k})=2\cos\left(k_{\mathbf{y}}\sqrt{3}a\right)+4\cos\left(k_{\mathbf{x}}\frac{3a}{2}\right)\cos\left(k_{\mathbf{y}}\frac{\sqrt{3}a}{2}\right), \tag{6.41}
$$

as desired.

Next, the nnn hopping will be included. The nnn-part of the Hamiltonian is

$$
H_{nnn}=-t'\sum_{\langle\langle i,j\rangle\rangle,\sigma}\left(a^\dagger_{\sigma,i}a_{\sigma,j}+b^\dagger_{\sigma,i}b_{\sigma,j}+a^\dagger_{\sigma,j}a_{\sigma,i}+b^\dagger_{\sigma,j}b_{\sigma,i}\right).
$$

The nnn of position $\mathbf{r}_i$ is $\mathbf{r}_j=\mathbf{r}_i+\boldsymbol{\delta}_\alpha-\boldsymbol{\delta}_\beta$ with $\alpha,\beta=1,2,3$ and $\alpha\neq\beta$ where $\boldsymbol{\delta}_{\alpha,\beta}$ is defined

in Eq. (3.2). Transforming to reciprocal space following the same procedure as before leads to

$$
\begin{aligned}
H_{nnn} &= -\frac{t'}{2N}\sum_{\sigma}\sum_{\mathbf{r}_i,\mathbf{r}_j}\sum_{\mathbf{k},\mathbf{q}}\left[\left(a^{\dagger}_{\sigma,\mathbf{k}}a_{\sigma,\mathbf{q}}+b^{\dagger}_{\sigma,\mathbf{k}}b_{\sigma,\mathbf{q}}\right)\mathrm{e}^{-i\mathbf{k}\cdot\mathbf{r}_i+i\mathbf{q}\cdot\mathbf{r}_j}+\left(a^{\dagger}_{\sigma,\mathbf{q}}a_{\sigma,\mathbf{k}}+b^{\dagger}_{\sigma,\mathbf{q}}b_{\sigma,\mathbf{k}}\right)\mathrm{e}^{-i\mathbf{q}\cdot\mathbf{r}_i+i\mathbf{k}\cdot\mathbf{r}_j}\right]\\
&= -\frac{t'}{2N}\sum_{\sigma}\sum_{\substack{\mathbf{r}_i,\boldsymbol{\delta}_\alpha,\boldsymbol{\delta}_\beta\\ \alpha\neq\beta}}\sum_{\mathbf{k},\mathbf{q}}\left[\left(a^{\dagger}_{\sigma,\mathbf{k}}a_{\sigma,\mathbf{q}}+b^{\dagger}_{\sigma,\mathbf{k}}b_{\sigma,\mathbf{q}}\right)\mathrm{e}^{-i\mathbf{k}\cdot\mathbf{r}_i+i\mathbf{q}\cdot\left(\mathbf{r}_i+\boldsymbol{\delta}_\alpha-\boldsymbol{\delta}_\beta\right)}\right.\\
&\left.+\left(a^{\dagger}_{\sigma,\mathbf{q}}a_{\sigma,\mathbf{k}}+b^{\dagger}_{\sigma,\mathbf{q}}b_{\sigma,\mathbf{k}}\right)\mathrm{e}^{-i\mathbf{q}\cdot\mathbf{r}_i+i\mathbf{k}\cdot\left(\mathbf{r}_i+\boldsymbol{\delta}_\alpha-\boldsymbol{\delta}_\beta\right)}\right]\\
&= -\frac{t'}{2N}\sum_{\sigma}\sum_{\substack{\mathbf{r}_i,\boldsymbol{\delta}_\alpha,\boldsymbol{\delta}_\beta\\ \alpha\neq\beta}}\sum_{\mathbf{k},\mathbf{q}}\left[\left(a^{\dagger}_{\sigma,\mathbf{k}}a_{\sigma,\mathbf{q}}+b^{\dagger}_{\sigma,\mathbf{k}}b_{\sigma,\mathbf{q}}\right)\mathrm{e}^{-i(\mathbf{k}-\mathbf{q})\cdot\mathbf{r}_i+i\mathbf{q}\cdot\left(\boldsymbol{\delta}_\alpha-\boldsymbol{\delta}_\beta\right)}\right.\\
&\left.+\left(a^{\dagger}_{\sigma,\mathbf{q}}a_{\sigma,\mathbf{k}}+b^{\dagger}_{\sigma,\mathbf{q}}b_{\sigma,\mathbf{k}}\right)\mathrm{e}^{-i(\mathbf{q}-\mathbf{k})\cdot\mathbf{r}_i+i\mathbf{k}\cdot\left(\boldsymbol{\delta}_\alpha-\boldsymbol{\delta}_\beta\right)}\right]\\
&= -\frac{t'}{2N}\sum_{\sigma}\sum_{\substack{\boldsymbol{\delta}_\alpha,\boldsymbol{\delta}_\beta\\ \alpha\neq\beta}}\sum_{\mathbf{k},\mathbf{q}}\left[\left(a^{\dagger}_{\sigma,\mathbf{k}}a_{\sigma,\mathbf{q}}+b^{\dagger}_{\sigma,\mathbf{k}}b_{\sigma,\mathbf{q}}\right)N\delta_{\mathbf{k},\mathbf{q}}\mathrm{e}^{i\mathbf{q}\cdot\left(\boldsymbol{\delta}_\alpha-\boldsymbol{\delta}_\beta\right)}+\left(a^{\dagger}_{\sigma,\mathbf{q}}a_{\sigma,\mathbf{k}}+b^{\dagger}_{\sigma,\mathbf{q}}b_{\sigma,\mathbf{k}}\right)N\delta_{\mathbf{k},\mathbf{q}}\mathrm{e}^{i\mathbf{k}\cdot\left(\boldsymbol{\delta}_\alpha-\boldsymbol{\delta}_\beta\right)}\right]\\
&= -\frac{t'}{2}\sum_{\sigma,\mathbf{k}}\sum_{\substack{\boldsymbol{\delta}_\alpha,\boldsymbol{\delta}_\beta\\ \alpha\neq\beta}}\left[\left(a^{\dagger}_{\sigma,\mathbf{k}}a_{\sigma,\mathbf{k}}+b^{\dagger}_{\sigma,\mathbf{k}}b_{\sigma,\mathbf{k}}\right)\mathrm{e}^{i\mathbf{k}\cdot\left(\boldsymbol{\delta}_\alpha-\boldsymbol{\delta}_\beta\right)}+\left(a^{\dagger}_{\sigma,\mathbf{k}}a_{\sigma,\mathbf{k}}+b^{\dagger}_{\sigma,\mathbf{k}}b_{\sigma,\mathbf{k}}\right)\mathrm{e}^{i\mathbf{k}\cdot\left(\boldsymbol{\delta}_\alpha-\boldsymbol{\delta}_\beta\right)}\right],
\end{aligned}
$$

where the following relation was used

$$\sum_{\langle\langle i,j\rangle\rangle}=\frac{1}{2}\sum_{\mathbf{r}_i,\mathbf{r}_j}$$

to prevent double counting. Defining the following

$$h(\mathbf{k})\equiv -t'\sum_{\substack{\boldsymbol{\delta}_\alpha,\boldsymbol{\delta}_\beta\\ \alpha\neq\beta}}\mathrm{e}^{i\mathbf{k}\cdot\left(\boldsymbol{\delta}_\alpha-\boldsymbol{\delta}_\beta\right)}, \tag{6.42}$$

allows for H_{nnn} to be rewritten according to

$$H_{nnn}=\frac{1}{2}\sum_{\sigma,\mathbf{k}}\begin{pmatrix}a^{\dagger}_{\sigma,\mathbf{k}} & b^{\dagger}_{\sigma,\mathbf{k}}\end{pmatrix}\begin{pmatrix}h(\mathbf{k})+h^{*}(\mathbf{k}) & 0\\ 0 & h(\mathbf{k})+h^{*}(\mathbf{k})\end{pmatrix}\begin{pmatrix}a_{\sigma,\mathbf{k}}\\ b_{\sigma,\mathbf{k}}\end{pmatrix}. \tag{6.43}$$

This leads to the following relation

$$
\begin{aligned}
\frac{1}{2}\begin{pmatrix}h(\mathbf{k})+h^{*}(\mathbf{k}) & 0\\ 0 & h(\mathbf{k})+h^{*}(\mathbf{k})\end{pmatrix}\begin{pmatrix}a_{\sigma,\mathbf{k}}\\ b_{\sigma,\mathbf{k}}\end{pmatrix} &= E_{\mathbf{k},nnn}\begin{pmatrix}a_{\sigma,\mathbf{k}}\\ b_{\sigma,\mathbf{k}}\end{pmatrix}\\
\frac{1}{2}\begin{pmatrix}(h(\mathbf{k})+h^{*}(\mathbf{k}))a_{\sigma,\mathbf{k}}\\ (h(\mathbf{k})+h^{*}(\mathbf{k}))b_{\sigma,\mathbf{k}}\end{pmatrix} &= \begin{pmatrix}E_{\mathbf{k},nnn}a_{\sigma,\mathbf{k}}\\ E_{\mathbf{k},nnn}b_{\sigma,\mathbf{k}}\end{pmatrix}.
\end{aligned}
$$

Hence,

$$E_{\mathbf{k},nnn}=\frac{1}{2}\left[h(\mathbf{k})+h^{*}(\mathbf{k})\right]. \tag{6.44}$$

The next step is to explicitly compute $h(\mathbf{k})$

$$\begin{aligned} h(\mathbf{k}) &= -t' \sum_{\boldsymbol{\delta}_\alpha, \boldsymbol{\delta}_\beta, \alpha \neq \beta} \mathrm{e}^{i\mathbf{k}\cdot\left(\boldsymbol{\delta}_\alpha - \boldsymbol{\delta}_\beta\right)} = -t' \sum_{\boldsymbol{\delta}_\beta, \alpha \neq \beta} \left(\mathrm{e}^{i\mathbf{k}\cdot\left(\boldsymbol{\delta}_1 - \boldsymbol{\delta}_\beta\right)} + \mathrm{e}^{i\mathbf{k}\cdot\left(\boldsymbol{\delta}_2 - \boldsymbol{\delta}_\beta\right)} + \mathrm{e}^{i\mathbf{k}\cdot\left(\boldsymbol{\delta}_3 - \boldsymbol{\delta}_\beta\right)} \right) \\ &= -t' \left(\mathrm{e}^{i\mathbf{k}\cdot(\boldsymbol{\delta}_1 - \boldsymbol{\delta}_2)} + \mathrm{e}^{i\mathbf{k}\cdot(\boldsymbol{\delta}_1 - \boldsymbol{\delta}_3)} + \mathrm{e}^{i\mathbf{k}\cdot(\boldsymbol{\delta}_2 - \boldsymbol{\delta}_1)} + \mathrm{e}^{i\mathbf{k}\cdot(\boldsymbol{\delta}_2 - \boldsymbol{\delta}_3)} + \mathrm{e}^{i\mathbf{k}\cdot(\boldsymbol{\delta}_3 - \boldsymbol{\delta}_1)} + \mathrm{e}^{i\mathbf{k}\cdot(\boldsymbol{\delta}_3 - \boldsymbol{\delta}_2)} \right) \\ &= -t' \left(\mathrm{e}^{i\mathbf{k}\cdot(\boldsymbol{\delta}_1 - \boldsymbol{\delta}_2)} + \mathrm{e}^{-i\mathbf{k}\cdot(\boldsymbol{\delta}_1 - \boldsymbol{\delta}_2)} + \mathrm{e}^{i\mathbf{k}\cdot(\boldsymbol{\delta}_1 - \boldsymbol{\delta}_3)} + \mathrm{e}^{-i\mathbf{k}\cdot(\boldsymbol{\delta}_1 - \boldsymbol{\delta}_3)} + \mathrm{e}^{i\mathbf{k}\cdot(\boldsymbol{\delta}_2 - \boldsymbol{\delta}_3)} + \mathrm{e}^{-i\mathbf{k}\cdot(\boldsymbol{\delta}_2 - \boldsymbol{\delta}_3)} \right). \end{aligned}$$

Comparing this result to Eq. (6.39) immediately yields the solution

$$h(\mathbf{k}) = -t' \left(2\cos\left(k_{\mathbf{y}}\sqrt{3}a\right) + 4\cos\left(k_{\mathbf{x}}\frac{3a}{2}\right)\cos\left(k_{\mathbf{y}}\frac{\sqrt{3}a}{2}\right) \right).$$

Moreover, from Eq. (**??**) it is clear that $h(\mathbf{k}) = h^*(\mathbf{k})$, such that the energy bands for nnn are

$$E_{\mathbf{k},nnn} = -t' \left(2\cos\left(k_{\mathbf{y}}\sqrt{3}a\right) + 4\cos\left(k_{\mathbf{x}}\frac{3a}{2}\right)\cos\left(k_{\mathbf{y}}\frac{\sqrt{3}a}{2}\right) \right). \tag{6.45}$$

Therefore, the energy bands derived from the Hamiltonian in Eq. (3.9) have the form

$$E_{\mathbf{k}} = \pm t\sqrt{3 + f(\mathbf{k})} - t' f(\mathbf{k}), \tag{6.46}$$

with

$$f(\mathbf{k}) = 2\cos\left(k_{\mathbf{y}}\sqrt{3}a\right) + 4\cos\left(k_{\mathbf{x}}\frac{3a}{2}\right)\cos\left(k_{\mathbf{y}}\frac{\sqrt{3}a}{2}\right). \tag{6.47}$$

6.2.3 Expansion of Energy Bands around Dirac Points for Nearest-Neighbor Hopping up to $\mathcal{O}(\mathbf{q}/\mathbf{K})$

The full band structure close to the $\mathbf{K}$ point is determined by expanding as $\mathbf{k} = \mathbf{K} + \mathbf{q}$ with $|\mathbf{q}| \ll |\mathbf{K}|$, where $\mathbf{K}$ is defined in Eq. (3.5). Only nn-hopping is considered. At $\mathbf{k} = \mathbf{K}$, $E_{\mathbf{K},nn} = 0$. This can be shown explicitly,

$$E_{\mathbf{K},nn} = \pm t\sqrt{3 + f(\mathbf{K})} = 0, \qquad \text{such that} \qquad 3 + f(\mathbf{K}) = 0.$$

So $f(\mathbf{K}) = -3$. To see whether this holds, Eqs. (3.5) and (3.12) are used to obtain the following

$$\begin{aligned} f(\mathbf{K}) = 2\cos\left(K_{\mathbf{y}}\sqrt{3}a\right) + 4\cos\left(K_{\mathbf{x}}\frac{3a}{2}\right)\cos\left(K_{\mathbf{y}}\frac{\sqrt{3}a}{2}\right) &= -3 \\ 2\cos\left(\frac{2\pi}{3}\right) + 4\cos\left(\frac{\pi}{3}\right)\cos(\pi) &= -3 \\ 2 \times -\frac{1}{2} + 4 \times \frac{1}{2} \times -1 &= -3 \\ -3 &= -3, \end{aligned}$$

such that indeed $E_{\mathbf{K},nn} = 0$. Now $\mathbf{k}$ will be expanded around $\mathbf{K}$ using Eqs. (6.36) and (6.38). This leads to the following

$$g(\mathbf{K} + \mathbf{q}) = g(\mathbf{K}) + q_i \partial_{k_i} g\big|_{\mathbf{K}} = g(\mathbf{K}) + q_{\mathbf{x}} \partial_{k_{\mathbf{x}}} g\big|_{\mathbf{K}} + q_{\mathbf{y}} \partial_{k_{\mathbf{y}}} g\big|_{\mathbf{K}}.$$

From the fact that $E_{\mathbf{K},nn} = 0$, $g(\mathbf{K})$ should be zero,

$$
\begin{aligned}
g(\mathbf{K}) &= -t \sum_{\boldsymbol{\delta}_\alpha} \mathrm{e}^{i\mathbf{K}\cdot\boldsymbol{\delta}_\alpha} = -t\left(\mathrm{e}^{i\mathbf{K}\cdot\boldsymbol{\delta}_1} + \mathrm{e}^{i\mathbf{K}\cdot\boldsymbol{\delta}_2} + \mathrm{e}^{i\mathbf{K}\cdot\boldsymbol{\delta}_3}\right) \\
&= -t\left\{\exp\left[i\left(\frac{2\pi}{3a}\cdot\frac{a}{2} + \frac{2\pi}{3\sqrt{3}a}\cdot\frac{\sqrt{3}a}{2}\right)\right] + \exp\left[i\left(\frac{2\pi}{3a}\cdot\frac{a}{2} - \frac{2\pi}{3\sqrt{3}a}\cdot\frac{\sqrt{3}a}{2}\right)\right] + \exp\left(-i\frac{2\pi}{3a}\cdot a\right)\right\} \\
&= -t\left(\mathrm{e}^{i2\pi/3} + 1 + \mathrm{e}^{-i2\pi/3}\right) = -t\left[2\cos\left(\frac{2\pi}{3}\right) + 1\right] = -t(-1+1) = 0.
\end{aligned}
$$

The other two functions in the expansion are

$$
\partial_{k_\mathbf{x}} g|_\mathbf{K} = -t\sum_{\boldsymbol{\delta}_\alpha}\left(i\delta_{\alpha,\mathbf{x}}\mathrm{e}^{i\mathbf{k}\cdot\boldsymbol{\delta}_\alpha}\right)\Big|_\mathbf{K} = -it\sum_{\boldsymbol{\delta}_\alpha}\left(\delta_{\alpha,\mathbf{x}}\mathrm{e}^{i\mathbf{K}\cdot\boldsymbol{\delta}_\alpha}\right),
$$

and likewise

$$
\partial_{k_\mathbf{y}} g|_\mathbf{K} = -it\sum_{\boldsymbol{\delta}_\alpha}\left(\delta_{\alpha,\mathbf{y}}\mathrm{e}^{i\mathbf{K}\cdot\boldsymbol{\delta}_\alpha}\right).
$$

This leads to

$$
g(\mathbf{K}+\mathbf{q}) = q_i\partial_{k_i} g|_\mathbf{K} = -it\sum_{\boldsymbol{\delta}_\alpha}\left(q_\mathbf{x}\delta_{\alpha,\mathbf{x}} + q_\mathbf{y}\delta_{\alpha,\mathbf{y}}\right)\mathrm{e}^{i\mathbf{K}\cdot\boldsymbol{\delta}_\alpha}.
$$

This equation can be computed explicitly using Eqs. (3.2) and (3.5)

$$
\begin{aligned}
&g(\mathbf{K}+\mathbf{q}) = -it\sum_{\boldsymbol{\delta}_\alpha}\left(q_\mathbf{x}\delta_{\alpha,\mathbf{x}} + q_\mathbf{y}\delta_{\alpha,\mathbf{y}}\right)\mathrm{e}^{i\mathbf{K}\cdot\boldsymbol{\delta}_\alpha} \\
&= -it\left[\left(q_\mathbf{x}\delta_{1,\mathbf{x}} + q_\mathbf{y}\delta_{1,\mathbf{y}}\right)\mathrm{e}^{i\mathbf{K}\cdot\boldsymbol{\delta}_1} + \left(q_\mathbf{x}\delta_{2,\mathbf{x}} + q_\mathbf{y}\delta_{2,\mathbf{y}}\right)\mathrm{e}^{i\mathbf{K}\cdot\boldsymbol{\delta}_2} + \left(q_\mathbf{x}\delta_{3,\mathbf{x}} + q_\mathbf{y}\delta_{3,\mathbf{y}}\right)\mathrm{e}^{i\mathbf{K}\cdot\boldsymbol{\delta}_3}\right] \\
&= -it\left[\left(q_\mathbf{x}\frac{a}{2} + q_\mathbf{y}\frac{a\sqrt{3}}{2}\right)\mathrm{e}^{i(K_\mathbf{x}\delta_{1,\mathbf{x}} + K_\mathbf{y}\delta_{1,\mathbf{y}})} + \left(q_\mathbf{x}\frac{a}{2} - q_\mathbf{y}\frac{a\sqrt{3}}{2}\right)\mathrm{e}^{i(K_\mathbf{x}\delta_{2,\mathbf{x}} + K_\mathbf{y}\delta_{2,\mathbf{y}})} - q_\mathbf{x}a\,\mathrm{e}^{i(K_\mathbf{x}\delta_{3,\mathbf{x}} + K_\mathbf{y}\delta_{3,\mathbf{y}})}\right] \\
&= -it\left[\left(q_\mathbf{x}\frac{a}{2} + q_\mathbf{y}\frac{a\sqrt{3}}{2}\right)\mathrm{e}^{i\frac{2\pi}{3}} + \left(q_\mathbf{x}\frac{a}{2} - q_\mathbf{y}\frac{a\sqrt{3}}{2}\right)\mathrm{e}^{i\left(\frac{\pi}{3}-\frac{\pi}{3}\right)} - q_\mathbf{x}a\,\mathrm{e}^{-i\frac{2\pi}{3a}a}\right] \\
&= -it\left\{\left(q_\mathbf{x}\frac{a}{2} + q_\mathbf{y}\frac{a\sqrt{3}}{2}\right)\left[\cos\left(\frac{2\pi}{3}\right) + i\sin\left(\frac{2\pi}{3}\right)\right] + q_\mathbf{x}\frac{a}{2} - q_\mathbf{y}\frac{a\sqrt{3}}{2}\right. \\
&\left. -q_\mathbf{x}a\left[\cos\left(\frac{2\pi}{3}\right) - i\sin\left(\frac{2\pi}{3}\right)\right]\right\} \\
&= -it\left[\left(q_\mathbf{x}\frac{a}{2} + q_\mathbf{y}\frac{a\sqrt{3}}{2}\right)\left(-\frac{1}{2} + \frac{i}{2}\sqrt{3}\right) + q_\mathbf{x}\frac{a}{2} - q_\mathbf{y}\frac{a\sqrt{3}}{2} - q_\mathbf{x}a\left(-\frac{1}{2} - \frac{i}{2}\sqrt{3}\right)\right] \\
&= -it\left[q_\mathbf{x}\frac{3a}{4}\left(1 + i\sqrt{3}\right) + q_\mathbf{y}\frac{3a}{4}\left(-\sqrt{3} + i\right)\right].
\end{aligned}
$$

Such that

$$
g^*(\mathbf{K}+\mathbf{q}) = it\left[q_\mathbf{x}\frac{3a}{4}\left(1 - i\sqrt{3}\right) + q_\mathbf{y}\frac{3a}{4}\left(-\sqrt{3} - i\right)\right].
$$

This leads to

$$g^*(\mathbf{K}+\mathbf{q})g(\mathbf{K}+\mathbf{q}) = \frac{9a^2t^2}{16}\left[\left(q_\mathbf{x}-\sqrt{3}q_\mathbf{y}\right)+i\left(\sqrt{3}q_\mathbf{x}+q_\mathbf{y}\right)\right]\left[\left(q_\mathbf{x}-\sqrt{3}q_\mathbf{y}\right)-i\left(\sqrt{3}q_\mathbf{x}+q_\mathbf{y}\right)\right]$$
$$= \frac{9a^2t^2}{16}\left[\left(q_\mathbf{x}-\sqrt{3}q_\mathbf{y}\right)^2+\left(\sqrt{3}q_\mathbf{x}+q_\mathbf{y}\right)^2\right] = \frac{9a^2t^2}{16}\left[q_\mathbf{x}^2+3q_\mathbf{y}^2-2\sqrt{3}q_\mathbf{x}q_\mathbf{y}+3q_\mathbf{x}^2+q_\mathbf{y}^2+2\sqrt{3}q_\mathbf{x}q_\mathbf{y}\right]$$
$$= \frac{9a^2t^2}{16}\left[4q_\mathbf{x}^2+4q_\mathbf{y}^2\right] = \frac{9a^2t^2}{4}\left[q_\mathbf{x}^2+q_\mathbf{y}^2\right]. \tag{6.48}$$

Such that the final result reads

$$E_{nn}(\mathbf{K}+\mathbf{q}) = \sqrt{\frac{9a^2t^2}{4}\left[q_\mathbf{x}^2+q_\mathbf{y}^2\right]} = \pm\frac{3at}{2}|\mathbf{q}| = \pm v_F|\mathbf{q}|, \tag{6.49}$$

with the Fermi velocity $v_F = 3at/2$.

6.2.4 Expansion of Energy Bands around Dirac Points Including Next-Nearest Neighbor Hopping up to $\mathcal{O}\left(\mathbf{q}^2/\mathbf{K}^2\right)$

A similar procedure as in App. 6.2.3 can be followed to find the expansion of the energy bands around the Dirac points including nnn-hopping up $\mathcal{O}\left(\mathbf{q}^2/\mathbf{K}^2\right)$. First nn is considered followed by nnn.

Expansion of Energy Bands around Dirac Points for Nearest-Neighbor Hopping up to $\mathcal{O}\left(\mathbf{q}^2/\mathbf{K}^2\right)$

To find the energy bands up to $\mathcal{O}\left(\mathbf{q}^2/\mathbf{K}^2\right)$, the same procedure as in the previous Appendices is used, except that now $g(\mathbf{q}+\mathbf{K})$ needs to be expanded up to the third order in $\mathbf{q}$. To see why, one should consider the following expansion

$$g(\mathbf{K}+\mathbf{q}) = g(\mathbf{K}) + q_i\partial_{k_i}g|_\mathbf{K} + \frac{1}{2!}q_iq_j\partial_{k_i}\partial_{k_j}f\Big|_\mathbf{K} + \frac{1}{3!}q_iq_jq_k\partial_{k_i}\partial_{k_j}\partial_{k_k}g\Big|_\mathbf{K}$$
$$= A(\mathbf{q}^0)+B(\mathbf{q}^1)+C(\mathbf{q}^2)+D(\mathbf{q}^3),$$

where

$$A(\mathbf{q}^0) \equiv g(\mathbf{K}), \qquad B(\mathbf{q}^1) \equiv q_i\partial_{k_i}g|_\mathbf{K},$$
$$C(\mathbf{q}^2) \equiv \frac{1}{2!}q_iq_j\partial_{k_i}\partial_{k_j}g\Big|_\mathbf{K}, \qquad D(\mathbf{q}^3) \equiv \frac{1}{3!}q_iq_jq_k\partial_{k_i}\partial_{k_j}\partial_{k_k}g\Big|_\mathbf{K}.$$

In App. 6.2.3, it was found that $g(\mathbf{K}) = 0$, such that $g(\mathbf{q}+\mathbf{K})$ only needs to be expanded up to third order in $\mathbf{q}$. Therefore, computing $E_{nn}(\mathbf{q})$ up to $\mathcal{O}\left(\mathbf{q}^2/\mathbf{K}^2\right)$ yields

$$E_{nn}(\mathbf{K}+\mathbf{q}) = \pm|g(\mathbf{K}+\mathbf{q})| = \sqrt{g^*(\mathbf{K}+\mathbf{q})g(\mathbf{K}+\mathbf{q})}$$
$$= \sqrt{\left[B^*(\mathbf{q}^1)+C^*(\mathbf{q}^2)+D^*(\mathbf{q}^3)\right]\left[B(\mathbf{q}^1)+C(\mathbf{q}^2)+D(\mathbf{q}^3)\right]}$$
$$= \big\{B^*(\mathbf{q}^1)B(\mathbf{q}^1)+B^*(\mathbf{q}^1)C(\mathbf{q}^2)+B^*(\mathbf{q}^1)D(\mathbf{q}^3)+C^*(\mathbf{q}^2)B(\mathbf{q}^1)$$
$$+C^*(\mathbf{q}^2)C(\mathbf{q}^2)+D^*(\mathbf{q}^3)B(\mathbf{q}^1)\big\}^{1/2}+\mathcal{O}(\mathbf{q}^3/\mathbf{K}^3) \tag{6.50}$$

The result for the first term, $B^*(\mathbf{q}^1)B(\mathbf{q}^1)$, was calculated in App. 6.2.3 and reads

$$B^*(\mathbf{q}^1)B(\mathbf{q}^1) = \frac{9a^2t^2}{4}\left[q_{\mathbf{x}}^2 + q_{\mathbf{y}}^2\right].$$

Next, the terms $B(\mathbf{q}^1)$, $C(\mathbf{q}^2)$, $D(\mathbf{q}^3)$ and their complex conjugates need to be found. The terms $B(\mathbf{q}^1)$ and $B^*(\mathbf{q}^1)$ were calculated in App. 6.2.3. They are

$$B(\mathbf{q}^1) = q_i\partial_{k_i}g|_{\mathbf{K}} = t\left[q_{\mathbf{x}}\frac{3a}{4}\left(\sqrt{3}-i\right) + q_{\mathbf{y}}\frac{3a}{4}\left(1+i\sqrt{3}\right)\right],$$

and $B^*(\mathbf{q}^1)$ the complex conjugate of this equation. Next, $C(\mathbf{q}^2)$ needs to be computed

$$C(\mathbf{q}^2) = \frac{1}{2!}q_iq_j\partial_{k_i}\partial_{k_j}g\Big|_{\mathbf{K}} = \frac{1}{2}q_{\mathbf{x}}^2\partial_{k_{\mathbf{x}}}^2 g\Big|_{\mathbf{K}} + \frac{1}{2}q_{\mathbf{y}}^2\partial_{k_{\mathbf{y}}}^2 g\Big|_{\mathbf{K}} + q_{\mathbf{x}}q_{\mathbf{y}}\partial_{k_{\mathbf{x}}}\partial_{k_{\mathbf{y}}}g|_{\mathbf{K}} = \mathrm{I_C} + \mathrm{II_C} + \mathrm{III_C},$$

where

$$\mathrm{I_C} \equiv \frac{1}{2}q_{\mathbf{x}}^2\partial_{k_{\mathbf{x}}}^2 g\Big|_{\mathbf{K}}, \qquad \mathrm{II_C} \equiv \frac{1}{2}q_{\mathbf{y}}^2\partial_{k_{\mathbf{y}}}^2 g\Big|_{\mathbf{K}}, \qquad \mathrm{III_C} \equiv q_{\mathbf{x}}q_{\mathbf{y}}\partial_{k_{\mathbf{x}}}\partial_{k_{\mathbf{y}}}g|_{\mathbf{K}}.$$

The first term leads to the following

$$\begin{aligned}
\mathrm{I_C} &= \frac{1}{2}q_{\mathbf{x}}^2\partial_{k_{\mathbf{x}}}^2 g\Big|_{\mathbf{K}} = \frac{1}{2}q_{\mathbf{x}}^2\partial_{k_{\mathbf{x}}}^2\left(-t\sum_{\boldsymbol{\delta}_\alpha}\mathrm{e}^{i\mathbf{k}\cdot\boldsymbol{\delta}_\alpha}\right)\Bigg|_{\mathbf{K}} = \frac{t}{2}q_{\mathbf{x}}^2\sum_{\boldsymbol{\delta}_\alpha}\delta_{\alpha,\mathbf{x}}^2\mathrm{e}^{i\mathbf{K}\cdot\boldsymbol{\delta}_\alpha} \\
&= \frac{t}{2}q_{\mathbf{x}}^2\left[\delta_{1,\mathbf{x}}^2\mathrm{e}^{i\mathbf{K}\cdot\boldsymbol{\delta}_1} + \delta_{2,\mathbf{x}}^2\mathrm{e}^{i\mathbf{K}\cdot\boldsymbol{\delta}_2} + \delta_{3,\mathbf{x}}^2\mathrm{e}^{i\mathbf{K}\cdot\boldsymbol{\delta}_3}\right] \\
&= \frac{t}{2}q_{\mathbf{x}}^2\left\{\left(\frac{a}{2}\right)^2\exp\left[i\left(\frac{2\pi}{3a}\cdot\frac{a}{2} + \frac{2\pi}{3\sqrt{3}a}\cdot\frac{\sqrt{3}a}{2}\right)\right] + \left(\frac{a}{2}\right)^2\exp\left[i\left(\frac{2\pi}{3a}\cdot\frac{a}{2} + \frac{2\pi}{3\sqrt{3}a}\cdot-\frac{\sqrt{3}a}{2}\right)\right]\right. \\
&\left. + (-a)^2\exp\left[i\left(\frac{2\pi}{3a}\cdot-a\right)\right]\right\} = \frac{t}{2}q_{\mathbf{x}}^2a^2\left[\frac{1}{4}\mathrm{e}^{2i\pi/3} + \frac{1}{4} + \mathrm{e}^{-2i\pi/3}\right] \\
&= \frac{t}{2}q_{\mathbf{x}}^2a^2\left\{\frac{1}{4}\left[\cos\left(\frac{2\pi}{3}\right) + i\sin\left(\frac{2\pi}{3}\right)\right] + \frac{1}{4} + \cos\left(\frac{2\pi}{3}\right) - i\sin\left(\frac{2\pi}{3}\right)\right\} \\
&= \frac{t}{2}q_{\mathbf{x}}^2a^2\left[\frac{5}{4}\cos\left(\frac{2\pi}{3}\right) - \frac{3i}{4}\sin\left(\frac{2\pi}{3}\right) + \frac{1}{4}\right] = \frac{t}{2}q_{\mathbf{x}}^2a^2\left(-\frac{5}{8} - \frac{3\sqrt{3}i}{8} + \frac{1}{4}\right) = -\frac{3t}{16}q_{\mathbf{x}}^2a^2\left(1+\sqrt{3}i\right).
\end{aligned}$$

The second term leads to

$$\begin{aligned}
\mathrm{II_C} &= \frac{1}{2}q_{\mathbf{y}}^2\partial_{k_{\mathbf{y}}}^2 g\Big|_{\mathbf{K}} = \frac{1}{2}q_{\mathbf{y}}^2\partial_{\mathbf{k_y}}^2\left(-t\sum_{\boldsymbol{\delta}_\alpha}\mathrm{e}^{i\mathbf{k}\cdot\boldsymbol{\delta}_\alpha}\right)\Big|_{\mathbf{K}} = \frac{t}{2}q_{\mathbf{y}}^2\sum_{\boldsymbol{\delta}_\alpha}\delta_{\alpha,\mathbf{y}}^2\mathrm{e}^{i\mathbf{K}\cdot\boldsymbol{\delta}_\alpha} \\
&= \frac{t}{2}q_{\mathbf{y}}^2\left[\delta_{1,\mathbf{y}}^2\mathrm{e}^{i\mathbf{K}\cdot\boldsymbol{\delta}_1}+\delta_{2,\mathbf{y}}^2\mathrm{e}^{i\mathbf{K}\cdot\boldsymbol{\delta}_2}+\delta_{3,\mathbf{y}}^2\mathrm{e}^{i\mathbf{K}\cdot\boldsymbol{\delta}_3}\right] \\
&= \frac{t}{2}q_{\mathbf{y}}^2\left\{\left(\frac{\sqrt{3}a}{2}\right)^2\exp\left[i\left(\frac{2\pi}{3a}\cdot\frac{a}{2}+\frac{2\pi}{3\sqrt{3}a}\cdot\frac{\sqrt{3}a}{2}\right)\right]\right. \\
&\left.+\left(-\frac{\sqrt{3}a}{2}\right)^2\exp\left[i\left(\frac{2\pi}{3a}\cdot\frac{a}{2}+\frac{2\pi}{3\sqrt{3}a}\cdot-\frac{\sqrt{3}a}{2}\right)\right]\right\} = \frac{3t}{8}q_{\mathbf{y}}^2a^2\left[\mathrm{e}^{2i\pi/3}+1\right] \\
&= \frac{3t}{8}q_{\mathbf{y}}^2a^2\left[\cos\left(\frac{2\pi}{3}\right)+i\sin\left(\frac{2\pi}{3}\right)+1\right] = \frac{3t}{8}q_{\mathbf{y}}^2a^2\left(\frac{1}{2}+\frac{i}{2}\sqrt{3}\right) = \frac{3t}{16}q_{\mathbf{y}}^2a^2\left(1+\sqrt{3}i\right).
\end{aligned}$$

The third term yields

$$\begin{aligned}
\mathrm{III_C} &= q_{\mathbf{x}}q_{\mathbf{y}}\partial_{k_{\mathbf{x}}}\partial_{k_{\mathbf{y}}}g\big|_{\mathbf{K}} = q_{\mathbf{x}}q_{\mathbf{y}}\partial_{k_{\mathbf{x}}}\partial_{k_{\mathbf{y}}}\left(-t\sum_{\boldsymbol{\delta}_\alpha}\mathrm{e}^{i\mathbf{k}\cdot\boldsymbol{\delta}_\alpha}\right)\Big|_{\mathbf{K}} = tq_{\mathbf{x}}q_{\mathbf{y}}\sum_{\boldsymbol{\delta}_\alpha}\delta_{\alpha,\mathbf{x}}\delta_{\alpha,\mathbf{y}}\mathrm{e}^{i\mathbf{K}\cdot\boldsymbol{\delta}_\alpha} \\
&= tq_{\mathbf{x}}q_{\mathbf{y}}\left[\delta_{1,\mathbf{x}}\delta_{1,\mathbf{y}}\mathrm{e}^{i\mathbf{K}\cdot\boldsymbol{\delta}_1}+\delta_{2,\mathbf{x}}\delta_{2,\mathbf{y}}\mathrm{e}^{i\mathbf{K}\cdot\boldsymbol{\delta}_2}+\delta_{3,\mathbf{x}}\delta_{3,\mathbf{y}}\mathrm{e}^{i\mathbf{K}\cdot\boldsymbol{\delta}_3}\right] \\
&= tq_{\mathbf{x}}q_{\mathbf{y}}\left[\frac{a}{2}\cdot\frac{\sqrt{3}a}{2}\mathrm{e}^{2i\pi/3}-\frac{a}{2}\cdot\frac{\sqrt{3}a}{2}\right] = \frac{\sqrt{3}t}{4}q_{\mathbf{x}}q_{\mathbf{y}}a^2\left[-\frac{1}{2}+\frac{i}{2}\sqrt{3}-1\right] = -\frac{3t}{8}q_{\mathbf{x}}q_{\mathbf{y}}a^2\left(\sqrt{3}-i\right).
\end{aligned}$$

$C(\mathbf{q}^2)$ then reads

$$C(\mathbf{q}^2) = -\frac{3t}{16}\left(q_{\mathbf{x}}^2-q_{\mathbf{y}}^2\right)a^2\left(1+\sqrt{3}i\right)-\frac{3t}{8}q_{\mathbf{x}}q_{\mathbf{y}}a^2\left(\sqrt{3}-i\right),$$

and $C^*(\mathbf{q}^2)$ the complex conjugate of this equation. Lastly, $D(\mathbf{q}^3)$ is evaluated

$$\begin{aligned}
D(\mathbf{q}^3) &= \frac{1}{3!}q_iq_jq_k\partial_{k_i}\partial_{k_j}\partial_{k_k}g\Big|_{\mathbf{K}} = \left(\frac{1}{6}q_{\mathbf{x}}^3\partial_{k_{\mathbf{x}}}^3+\frac{1}{6}q_{\mathbf{y}}^3\partial_{k_{\mathbf{y}}}^3+\frac{1}{2}q_{\mathbf{x}}^2q_{\mathbf{y}}\partial_{k_{\mathbf{x}}}^2\partial_{k_{\mathbf{y}}}+\frac{1}{2}q_{\mathbf{x}}q_{\mathbf{y}}^2\partial_{k_{\mathbf{x}}}\partial_{k_{\mathbf{y}}}^2\right)g\Big|_{\mathbf{K}} \\
&= \mathrm{I_D}+\mathrm{II_D}+\mathrm{III_D}+\mathrm{IV_D},
\end{aligned}$$

where

$$\begin{aligned}
\mathrm{I_D} &\equiv \frac{1}{6}q_{\mathbf{x}}^3\partial_{k_{\mathbf{x}}}^3 g\Big|_{\mathbf{K}}, & \mathrm{II_D} &\equiv \frac{1}{6}q_{\mathbf{y}}^3\partial_{k_{\mathbf{y}}}^3 g\Big|_{\mathbf{K}}, \\
\mathrm{III_D} &\equiv \frac{1}{2}q_{\mathbf{x}}^2q_{\mathbf{y}}\partial_{k_{\mathbf{x}}}^2\partial_{k_{\mathbf{y}}}g\Big|_{\mathbf{K}}, & \mathrm{IV_D} &\equiv \frac{1}{2}q_{\mathbf{x}}q_{\mathbf{y}}^2\partial_{k_{\mathbf{x}}}\partial_{k_{\mathbf{y}}}^2 g\Big|_{\mathbf{K}}.
\end{aligned}$$

The first term leads to

$$\mathrm{I_D} = \frac{1}{6}q_{\mathbf{x}}^3\partial_{k_{\mathbf{x}}}^3 g\Big|_{\mathbf{K}} = \frac{1}{6}q_{\mathbf{x}}^3\partial_{k_{\mathbf{x}}}^3\left(-t\sum_{\boldsymbol{\delta}_\alpha}\mathrm{e}^{i\mathbf{k}\cdot\boldsymbol{\delta}_\alpha}\right)\Big|_{\mathbf{K}} = \frac{it}{6}q_{\mathbf{x}}^3\sum_{\boldsymbol{\delta}_\alpha}\delta_{\alpha,\mathbf{x}}^3\mathrm{e}^{i\mathbf{K}\cdot\boldsymbol{\delta}_\alpha}$$
$$= \frac{it}{6}q_{\mathbf{x}}^3\left[\delta_{1,\mathbf{x}}^3\mathrm{e}^{i\mathbf{K}\cdot\boldsymbol{\delta}_1}+\delta_{2,\mathbf{x}}^3\mathrm{e}^{i\mathbf{K}\cdot\boldsymbol{\delta}_2}+\delta_{3,\mathbf{x}}^3\mathrm{e}^{i\mathbf{K}\cdot\boldsymbol{\delta}_3}\right] = \frac{it}{6}q_{\mathbf{x}}^3\left[\left(\frac{a}{2}\right)^3\mathrm{e}^{2i\pi/3}+\left(\frac{a}{2}\right)^3+(-a)^3\,\mathrm{e}^{-2i\pi/3}\right]$$
$$= \frac{it}{6}q_{\mathbf{x}}^3a^3\left\{\frac{1}{8}\left[\cos\left(\frac{2\pi}{3}\right)+i\sin\left(\frac{2\pi}{3}\right)\right]+\frac{1}{8}-\cos\left(\frac{2\pi}{3}\right)+i\sin\left(\frac{2\pi}{3}\right)\right\}$$
$$= \frac{it}{6}q_{\mathbf{x}}^3a^3\left[-\frac{7}{8}\cos\left(\frac{2\pi}{3}\right)+\frac{1}{8}+\frac{9i}{8}\sin\left(\frac{2\pi}{3}\right)\right] = \frac{it}{6}q_{\mathbf{x}}^3a^3\left(\frac{9}{16}+i\frac{9\sqrt{3}}{16}\right) = -\frac{3t}{32}q_{\mathbf{x}}^3a^3\left(\sqrt{3}-i\right).$$

The second term reads

$$\mathrm{II_D} = \frac{1}{6}q_{\mathbf{y}}^3\partial_{k_{\mathbf{y}}}^3 g\Big|_{\mathbf{K}} = \frac{1}{6}q_{\mathbf{y}}^3\partial_{k_{\mathbf{y}}}^3\left(-t\sum_{\boldsymbol{\delta}_\alpha}\mathrm{e}^{i\mathbf{k}\cdot\boldsymbol{\delta}_\alpha}\right)\Big|_{\mathbf{K}} = \frac{it}{6}q_{\mathbf{y}}^3\sum_{\boldsymbol{\delta}_\alpha}\delta_{\alpha,\mathbf{y}}^3\mathrm{e}^{i\mathbf{K}\cdot\boldsymbol{\delta}_\alpha}$$
$$= \frac{it}{6}q_y^3\left[\delta_{1,\mathbf{y}}^3\mathrm{e}^{i\mathbf{K}\cdot\boldsymbol{\delta}_1}+\delta_{2,\mathbf{y}}^3\mathrm{e}^{i\mathbf{K}\cdot\boldsymbol{\delta}_2}+\delta_{3,\mathbf{y}}^3\mathrm{e}^{i\mathbf{K}\cdot\boldsymbol{\delta}_3}\right] = \frac{it}{6}q_{\mathbf{y}}^3\left[\left(\frac{\sqrt{3}a}{2}\right)^3\mathrm{e}^{2i\pi/3}+\left(-\frac{\sqrt{3}a}{2}\right)^3\right]$$
$$= \frac{\sqrt{3}it}{16}q_{\mathbf{y}}^3a^3\left\{\left[\cos\left(\frac{2\pi}{3}\right)+i\sin\left(\frac{2\pi}{3}\right)\right]-1\right\} = \frac{\sqrt{3}it}{16}q_{\mathbf{y}}^3a^3\left(-\frac{3}{2}+\frac{i}{2}\sqrt{3}\right) = -\frac{3t}{32}q_{\mathbf{y}}^3a^3\left(1+i\sqrt{3}\right).$$

The third term yields

$$\mathrm{III_D} = \frac{1}{2}q_{\mathbf{x}}^2q_{\mathbf{y}}\partial_{k_{\mathbf{x}}}^2\partial_{k_{\mathbf{y}}}g\Big|_{\mathbf{K}} = \frac{1}{2}q_{\mathbf{x}}^2q_{\mathbf{y}}\partial_{k_{\mathbf{x}}}^2\partial_{k_{\mathbf{y}}}\left(-t\sum_{\boldsymbol{\delta}_\alpha}\mathrm{e}^{i\mathbf{k}\cdot\boldsymbol{\delta}_\alpha}\right)\Big|_{\mathbf{K}} = \frac{it}{2}q_{\mathbf{x}}^2q_{\mathbf{y}}\sum_{\boldsymbol{\delta}_\alpha}\delta_{\alpha,\mathbf{x}}^2\delta_{\alpha,\mathbf{y}}\mathrm{e}^{i\mathbf{K}\cdot\boldsymbol{\delta}_\alpha}$$
$$= \frac{it}{2}q_{\mathbf{x}}^2q_{\mathbf{y}}\left[\delta_{1,\mathbf{x}}^2\delta_{1,\mathbf{y}}\mathrm{e}^{i\mathbf{K}\cdot\boldsymbol{\delta}_1}+\delta_{2,\mathbf{x}}^2\delta_{2,\mathbf{y}}\mathrm{e}^{i\mathbf{K}\cdot\boldsymbol{\delta}_2}+\delta_{3,\mathbf{x}}^2\delta_{3,\mathbf{y}}\mathrm{e}^{i\mathbf{K}\cdot\boldsymbol{\delta}_3}\right]$$
$$= \frac{it}{2}q_{\mathbf{x}}^2q_{\mathbf{y}}\left[\left(\frac{a}{2}\right)^2\left(\frac{\sqrt{3}a}{2}\right)\mathrm{e}^{2i\pi/3}+\left(\frac{a}{2}\right)^2\left(-\frac{\sqrt{3}a}{2}\right)\right] = \frac{\sqrt{3}it}{16}q_{\mathbf{x}}^2q_{\mathbf{y}}a^3\left[\cos\left(\frac{2\pi}{3}\right)+i\sin\left(\frac{2\pi}{3}\right)-1\right]$$
$$= \frac{\sqrt{3}it}{16}q_{\mathbf{x}}^2q_{\mathbf{y}}a^3\left(-\frac{3}{2}+\frac{i}{2}\sqrt{3}\right) = -\frac{3t}{32}q_{\mathbf{x}}^2q_{\mathbf{y}}a^3\left(1+i\sqrt{3}\right).$$

The last term leads to

$$\mathrm{IV_D} = \frac{1}{2}q_{\mathbf{x}}q_{\mathbf{y}}^2\partial_{k_{\mathbf{x}}}\partial_{k_{\mathbf{y}}}^2 g\Big|_{\mathbf{K}} = \frac{1}{2}q_{\mathbf{x}}q_{\mathbf{y}}^2\partial_{k_{\mathbf{x}}}\partial_{k_{\mathbf{y}}}^2\left(-t\sum_{\boldsymbol{\delta}_\alpha}\mathrm{e}^{i\mathbf{k}\cdot\boldsymbol{\delta}_\alpha}\right)\Big|_{\mathbf{K}} = \frac{it}{2}q_{\mathbf{x}}q_{\mathbf{y}}^2\sum_{\boldsymbol{\delta}_\alpha}\delta_{\alpha,\mathbf{x}}\delta_{\alpha,\mathbf{y}}^2\mathrm{e}^{i\mathbf{K}\cdot\boldsymbol{\delta}_\alpha}$$
$$= \frac{it}{2}q_{\mathbf{x}}q_{\mathbf{y}}^2\left[\delta_{1,\mathbf{x}}\delta_{1,\mathbf{y}}^2\mathrm{e}^{i\mathbf{K}\cdot\boldsymbol{\delta}_1}+\delta_{2,\mathbf{x}}\delta_{2,\mathbf{y}}^2\mathrm{e}^{i\mathbf{K}\cdot\boldsymbol{\delta}_2}+\delta_{3,\mathbf{x}}\delta_{3,\mathbf{y}}^2\mathrm{e}^{i\mathbf{K}\cdot\boldsymbol{\delta}_3}\right]$$
$$= \frac{it}{2}q_{\mathbf{x}}q_{\mathbf{y}}^2\left[\left(\frac{a}{2}\right)\left(\frac{\sqrt{3}a}{2}\right)^2\mathrm{e}^{2i\pi/3}+\left(\frac{a}{2}\right)\left(-\frac{\sqrt{3}a}{2}\right)^2\right] = \frac{3it}{16}q_{\mathbf{x}}q_{\mathbf{y}}^2a^3\left[\cos\left(\frac{2\pi}{3}\right)+i\sin\left(\frac{2\pi}{3}\right)+1\right]$$
$$= \frac{3it}{16}q_{\mathbf{x}}q_{\mathbf{y}}^2a^3\left(\frac{1}{2}+\frac{i}{2}\sqrt{3}\right) = -\frac{3t}{32}q_{\mathbf{x}}q_{\mathbf{y}}^2a^3\left(\sqrt{3}-i\right).$$

$D(\mathbf{q}^3)$ then reads

$$D(\mathbf{q}^3) = -\frac{3t}{32}a^3\left[\left(q_{\mathbf{x}}^3 + q_{\mathbf{x}}q_{\mathbf{y}}^2\right)\left(\sqrt{3}-i\right) + \left(q_{\mathbf{y}}^3 + q_{\mathbf{x}}^2 q_{\mathbf{y}}\right)\left(1+i\sqrt{3}\right)\right],$$

and $D^*(\mathbf{q}^3)$ the complex conjugate of this equation. Now, the remaining terms in Eq. (6.50) can be computed explicitly. First, $B^*(\mathbf{q}^1)C(\mathbf{q}^2)$ is computed

$$\begin{aligned}
B^*(\mathbf{q}^1)C(\mathbf{q}^2) &= \left\{t\left[q_{\mathbf{x}}\frac{3a}{4}\left(\sqrt{3}+i\right) + q_{\mathbf{y}}\frac{3a}{4}\left(1-i\sqrt{3}\right)\right]\right\} \\
&\times\left\{-\frac{3t}{16}\left(q_{\mathbf{x}}^2 - q_{\mathbf{y}}^2\right)a^2\left(1+i\sqrt{3}\right) - \frac{3t}{8}q_{\mathbf{x}}q_{\mathbf{y}}a^2\left(\sqrt{3}-i\right)\right\} \\
&= -\frac{t^2a^3}{6}\left[q_{\mathbf{x}}\left(\sqrt{3}+i\right) + q_{\mathbf{y}}\left(1-i\sqrt{3}\right)\right]\left[\left(q_{\mathbf{x}}^2 - q_{\mathbf{y}}^2\right)\left(1+i\sqrt{3}\right) + 2q_{\mathbf{x}}q_{\mathbf{y}}\left(\sqrt{3}-i\right)\right] \\
&= -\frac{2t^2a^3}{3}\left[iq_{\mathbf{x}}^3 - 3iq_{\mathbf{x}}q_{\mathbf{y}}^2 + 3q_{\mathbf{x}}^2q_{\mathbf{y}} - q_{\mathbf{y}}^3\right],
\end{aligned}$$

and $B(\mathbf{q}^1)C^*(\mathbf{q}^2)$ the complex conjugate of this equation, such that $B^*(\mathbf{q}^1)C(\mathbf{q}^2)+C^*(\mathbf{q}^2)B(\mathbf{q}^1)$ reads

$$\begin{aligned}
B^*(\mathbf{q}^1)C(\mathbf{q}^2) + C^*(\mathbf{q}^2)B(\mathbf{q}^1) &= -\frac{2t^2a^3}{3}\left[iq_{\mathbf{x}}^3 - 3iq_{\mathbf{x}}q_{\mathbf{y}}^2 + 3q_{\mathbf{x}}^2q_{\mathbf{y}} - q_{\mathbf{y}}^3\right] \\
-\frac{2t^2a^3}{3}\left[-iq_{\mathbf{x}}^3 + 3iq_{\mathbf{x}}q_{\mathbf{y}}^2 + 3q_{\mathbf{x}}^2q_{\mathbf{y}} - q_{\mathbf{y}}^3\right] &= \frac{4t^2a^3}{3}\left(q_{\mathbf{y}}^3 - 3q_{\mathbf{x}}^2q_{\mathbf{y}}\right).
\end{aligned}$$

Next, $B^*(\mathbf{q}^1)D(\mathbf{q}^3)$ is computed

$$\begin{aligned}
B^*(\mathbf{q}^1)D(\mathbf{q}^3) &= \left\{t\left[q_{\mathbf{x}}\frac{3a}{4}\left(\sqrt{3}+i\right) + q_{\mathbf{y}}\frac{3a}{4}\left(1-i\sqrt{3}\right)\right]\right\} \\
&\times\left\{-\frac{3t}{32}a^3\left[\left(q_{\mathbf{x}}^3 + q_{\mathbf{x}}q_{\mathbf{y}}^2\right)\left(\sqrt{3}-i\right) + \left(q_{\mathbf{y}}^3 + q_{\mathbf{x}}^2q_{\mathbf{y}}\right)\left(1+i\sqrt{3}\right)\right]\right\} \\
&= -\frac{9t^2a^4}{128}\left[q_{\mathbf{x}}\left(\sqrt{3}+i\right) + q_{\mathbf{y}}\left(1-i\sqrt{3}\right)\right]\left[\left(q_{\mathbf{x}}^3 + q_{\mathbf{x}}q_{\mathbf{y}}^2\right)\left(\sqrt{3}-i\right) + \left(q_{\mathbf{y}}^3 + q_{\mathbf{x}}^2q_{\mathbf{y}}\right)\left(1+i\sqrt{3}\right)\right] \\
&= -\frac{9t^2a^4}{32}\left(q_{\mathbf{x}}^4 + 2q_{\mathbf{x}}^2q_{\mathbf{y}}^2 + q_{\mathbf{y}}^4\right) = -\frac{9t^2a^4}{32}\left(q_{\mathbf{x}}^2 + q_{\mathbf{y}}^2\right)^2,
\end{aligned}$$

where its complex conjugate $B(\mathbf{q}^1)D^*(\mathbf{q}^3)$ is the same, such that

$$B^*(\mathbf{q}^1)D(\mathbf{q}^3) + D^*(\mathbf{q}^3)B(\mathbf{q}^1) = -\frac{9t^2a^4}{16}\left(q_{\mathbf{x}}^2 + q_{\mathbf{y}}^2\right)^2.$$

Lastly, $C^*(\mathbf{q}^2)C(\mathbf{q}^2)$ is computed

$$\begin{aligned}
C^*(\mathbf{q}^2)C(\mathbf{q}^2) &= \left\{-\frac{3t}{16}\left(q_{\mathbf{x}}^2 - q_{\mathbf{y}}^2\right)a^2\left(1-i\sqrt{3}\right) - \frac{3t}{8}q_{\mathbf{x}}q_{\mathbf{y}}a^2\left(\sqrt{3}+i\right)\right\} \\
&\times\left\{-\frac{3t}{16}\left(q_{\mathbf{x}}^2 - q_{\mathbf{y}}^2\right)a^2\left(1+i\sqrt{3}\right) - \frac{3t}{8}q_{\mathbf{x}}q_{\mathbf{y}}a^2\left(\sqrt{3}-i\right)\right\} \\
&= \frac{9t^2a^4}{256}\left[\left(q_{\mathbf{x}}^2 - q_{\mathbf{y}}^2\right)\left(1-i\sqrt{3}\right) + 2q_{\mathbf{x}}q_{\mathbf{y}}\left(\sqrt{3}+i\right)\right] \\
&\times\left[\left(q_{\mathbf{x}}^2 - q_{\mathbf{y}}^2\right)\left(1+i\sqrt{3}\right) + 2q_{\mathbf{x}}q_{\mathbf{y}}\left(\sqrt{3}-i\right)\right] = \frac{9t^2a^4}{64}\left(q_{\mathbf{x}}^2 + q_{\mathbf{y}}^2\right)^2.
\end{aligned}$$

Combining these results leads to a solution for the energy bands near the Dirac point for nearest-neighbor hopping expanded up to $\mathcal{O}\left(\mathbf{q}^2/\mathbf{K}^2\right)$

$$\begin{aligned}
E_{nn}(\mathbf{K}+\mathbf{q}) &= \left[\frac{9a^2t^2}{4}\left(q_{\mathbf{x}}^2+q_{\mathbf{y}}^2\right)+\frac{9t^2a^4}{64}\left(q_{\mathbf{x}}^2+q_{\mathbf{y}}^2\right)^2-\frac{9t^2a^4}{16}\left(q_{\mathbf{x}}^2+q_{\mathbf{y}}^2\right)^2+\frac{4t^2a^3}{3}\left(q_{\mathbf{y}}^3-3q_{\mathbf{x}}^2q_{\mathbf{y}}\right)\right]^{1/2} \\
&= \left[\frac{9a^2t^2}{4}\left|\mathbf{q}\right|^2-\frac{27t^2a^4}{64}\left|\mathbf{q}\right|^4+\frac{4t^2a^3}{3}\left(q_{\mathbf{y}}^3-3q_{\mathbf{x}}^2q_{\mathbf{y}}\right)\right]^{1/2} \\
&= \pm\frac{3ta}{2}\left|\mathbf{q}\right|^2\sqrt{1-\frac{a^2}{6}\left|\mathbf{q}\right|^2+\frac{8a}{9\left|\mathbf{q}\right|^2}\left(q_{\mathbf{y}}^3-3q_{\mathbf{x}}^2q_{\mathbf{y}}\right)} \\
&= \pm v_F|\mathbf{q}|\mp\frac{3ta^2}{8}\sin(3\theta_{\mathbf{q}})|\mathbf{q}|^2+\mathcal{O}\left[(\mathbf{q}/\mathbf{K})^3\right], \qquad (6.51)
\end{aligned}$$

with

$$\theta_{\mathbf{q}}=\arctan\left(\frac{q_x}{q_y}\right) \qquad (6.52)$$

the angle in momentum space.

Expansion of Energy Bands around Dirac Points for Next-Nearest Neighbor Hopping up to $\mathcal{O}\left(\mathbf{q}^2/\mathbf{K}^2\right)$

Now, the same procedure will be followed for nnn. This procedure is much more straightforward because for nnn the Hamiltonian is diagonal. Using Eq. (6.44) it is evident that to find $E_{nnn}(\mathbf{q})$ up to second order in $(\mathbf{q}/\mathbf{K})$, $h(\mathbf{q}+\mathbf{K})$ needs to be expanded up to $\mathcal{O}\left(\mathbf{q}^2/\mathbf{K}^2\right)$

$$h(\mathbf{K}+\mathbf{q})=h(\mathbf{K})+q_i\partial_{k_i}h|_{\mathbf{K}}+\frac{1}{2!}q_iq_j\partial_{k_i}\partial_{k_j}h\Big|_{\mathbf{K}}.$$

Upon explicit computation, one finds

$$\begin{aligned}
h(\mathbf{K}) &= -t'\sum_{\substack{\boldsymbol{\delta}_\alpha,\boldsymbol{\delta}_\beta\\ \alpha\neq\beta}}\mathrm{e}^{i\mathbf{K}\cdot\left(\boldsymbol{\delta}_\alpha-\boldsymbol{\delta}_\beta\right)}=-t'\sum_{\boldsymbol{\delta}_\beta,\alpha\neq\beta}\left(\mathrm{e}^{i\mathbf{K}\cdot\left(\boldsymbol{\delta}_1-\boldsymbol{\delta}_\beta\right)}+\mathrm{e}^{i\mathbf{K}\cdot\left(\boldsymbol{\delta}_2-\boldsymbol{\delta}_\beta\right)}+\mathrm{e}^{i\mathbf{K}\cdot\left(\boldsymbol{\delta}_3-\boldsymbol{\delta}_\beta\right)}\right) \\
&= -t'\left(\mathrm{e}^{i\mathbf{K}\cdot(\boldsymbol{\delta}_1-\boldsymbol{\delta}_2)}+\mathrm{e}^{i\mathbf{K}\cdot(\boldsymbol{\delta}_1-\boldsymbol{\delta}_3)}+\mathrm{e}^{i\mathbf{K}\cdot(\boldsymbol{\delta}_2-\boldsymbol{\delta}_1)}+\mathrm{e}^{i\mathbf{K}\cdot(\boldsymbol{\delta}_2-\boldsymbol{\delta}_3)}+\mathrm{e}^{i\mathbf{K}\cdot(\boldsymbol{\delta}_3-\boldsymbol{\delta}_1)}+\mathrm{e}^{i\mathbf{K}\cdot(\boldsymbol{\delta}_3-\boldsymbol{\delta}_2)}\right) \\
&= -t'\left(\mathrm{e}^{i\mathbf{K}\cdot(\boldsymbol{\delta}_1-\boldsymbol{\delta}_2)}+\mathrm{e}^{-i\mathbf{K}\cdot(\boldsymbol{\delta}_1-\boldsymbol{\delta}_2)}+\mathrm{e}^{i\mathbf{K}\cdot(\boldsymbol{\delta}_1-\boldsymbol{\delta}_3)}+\mathrm{e}^{-i\mathbf{K}\cdot(\boldsymbol{\delta}_1-\boldsymbol{\delta}_3)}+\mathrm{e}^{i\mathbf{K}\cdot(\boldsymbol{\delta}_2-\boldsymbol{\delta}_3)}+\mathrm{e}^{-i\mathbf{K}\cdot(\boldsymbol{\delta}_2-\boldsymbol{\delta}_3)}\right) \\
&= -2t'\left\{\cos\left[\mathbf{K}\left(\boldsymbol{\delta}_1-\boldsymbol{\delta}_2\right)\right]+\cos\left[\mathbf{K}\left(\boldsymbol{\delta}_1-\boldsymbol{\delta}_3\right)\right]+\cos\left[\mathbf{K}\left(\boldsymbol{\delta}_2-\boldsymbol{\delta}_3\right)\right]\right\} \\
&= -2t'\left\{\cos\left[K_{\mathbf{x}}\left(\delta_1-\delta_2\right)_{\mathbf{x}}+K_{\mathbf{y}}\left(\delta_1-\delta_2\right)_{\mathbf{y}}\right]+\cos\left[K_{\mathbf{x}}\left(\delta_1-\delta_3\right)_{\mathbf{x}}\right.\right. \\
&\left.\left.+K_{\mathbf{y}}\left(\delta_1-\delta_3\right)_{\mathbf{y}}\right]+\cos\left[K_{\mathbf{x}}\left(\delta_2-\delta_3\right)_{\mathbf{x}}+K_{\mathbf{y}}\left(\delta_2-\delta_3\right)_{\mathbf{y}}\right]\right\} \\
&= -2t'\left\{\cos\left[\frac{2\pi}{3a}\left(\frac{a}{2}-\frac{a}{2}\right)+\frac{2\pi}{3\sqrt{3}a}\left(\frac{a\sqrt{3}}{2}+\frac{a\sqrt{3}}{2}\right)\right]+\cos\left[\frac{2\pi}{3a}\left(\frac{a}{2}+a\right)\right.\right. \\
&\left.\left.+\frac{2\pi}{3\sqrt{3}a}\left(\frac{a\sqrt{3}}{2}\right)\right]+\cos\left[\frac{2\pi}{3a}\left(\frac{a}{2}+a\right)+\frac{2\pi}{3\sqrt{3}a}\left(-\frac{a\sqrt{3}}{2}\right)\right]\right\} \\
&= -2t'\left[\cos\left(\frac{2\pi}{3}\right)+\cos\left(\frac{4\pi}{3}\right)+\cos\left(\frac{2\pi}{3}\right)\right]=-2t'\left(-\frac{1}{2}-\frac{1}{2}-\frac{1}{2}\right)=3t'.
\end{aligned}$$

The second term in the expansion leads to

$$\begin{aligned} q_i\partial_{k_i}h|_{\mathbf{K}} &= -t'\,q_{\mathbf{x}}\partial_{k_{\mathbf{x}}}\sum_{\substack{\boldsymbol{\delta}_\alpha,\boldsymbol{\delta}_\beta\\ \alpha\neq\beta}}\mathrm{e}^{i\mathbf{k}\cdot\left(\boldsymbol{\delta}_\alpha-\boldsymbol{\delta}_\beta\right)}\Bigg|_{\mathbf{K}} - t'\,q_{\mathbf{y}}\partial_{k_{\mathbf{y}}}\sum_{\substack{\boldsymbol{\delta}_\alpha,\boldsymbol{\delta}_\beta\\ \alpha\neq\beta}}\mathrm{e}^{i\mathbf{k}\cdot\left(\boldsymbol{\delta}_\alpha-\boldsymbol{\delta}_\beta\right)}\Bigg|_{\mathbf{K}} \\ &= -it'\,q_{\mathbf{x}}\sum_{\substack{\boldsymbol{\delta}_\alpha,\boldsymbol{\delta}_\beta\\ \alpha\neq\beta}}\left(\delta_\alpha-\delta_\beta\right)_{\mathbf{x}}\mathrm{e}^{i\mathbf{K}\cdot\left(\boldsymbol{\delta}_\alpha-\boldsymbol{\delta}_\beta\right)} - it'\,q_{\mathbf{y}}\sum_{\substack{\boldsymbol{\delta}_\alpha,\boldsymbol{\delta}_\beta\\ \alpha\neq\beta}}\left(\delta_\alpha-\delta_\beta\right)_{\mathbf{y}}\mathrm{e}^{i\mathbf{K}\cdot\left(\boldsymbol{\delta}_\alpha-\boldsymbol{\delta}_\beta\right)} \\ &= -it'\,q_{\mathbf{x}}\,\mathrm{I_h} - it'\,q_{\mathbf{y}}\,\mathrm{II_h}, \end{aligned}$$

where

$$\mathrm{I_h}\equiv\sum_{\substack{\boldsymbol{\delta}_\alpha,\boldsymbol{\delta}_\beta\\ \alpha\neq\beta}}\left(\delta_\alpha-\delta_\beta\right)_{\mathbf{x}}\mathrm{e}^{i\mathbf{K}\cdot\left(\boldsymbol{\delta}_\alpha-\boldsymbol{\delta}_\beta\right)},\qquad \mathrm{II_h}\equiv\sum_{\substack{\boldsymbol{\delta}_\alpha,\boldsymbol{\delta}_\beta\\ \alpha\neq\beta}}\left(\delta_\alpha-\delta_\beta\right)_{\mathbf{y}}\mathrm{e}^{i\mathbf{K}\cdot\left(\boldsymbol{\delta}_\alpha-\boldsymbol{\delta}_\beta\right)}.$$

The first part yields

$$\begin{aligned} \mathrm{I} &= \sum_{\substack{\boldsymbol{\delta}_\alpha,\boldsymbol{\delta}_\beta\\ \alpha\neq\beta}}\left(\delta_\alpha-\delta_\beta\right)_{\mathbf{x}}\mathrm{e}^{i\mathbf{K}\cdot\left(\boldsymbol{\delta}_\alpha-\boldsymbol{\delta}_\beta\right)} \\ &= \sum_{\boldsymbol{\delta}_\beta,\alpha\neq\beta}\left[\left(\delta_1-\delta_\beta\right)_{\mathbf{x}}\mathrm{e}^{i\mathbf{K}\cdot\left(\boldsymbol{\delta}_1-\boldsymbol{\delta}_\beta\right)} + \left(\delta_2-\delta_\beta\right)_{\mathbf{x}}\mathrm{e}^{i\mathbf{K}\cdot\left(\boldsymbol{\delta}_2-\boldsymbol{\delta}_\beta\right)} + \left(\delta_3-\delta_\beta\right)_{\mathbf{x}}\mathrm{e}^{i\mathbf{K}\cdot\left(\boldsymbol{\delta}_3-\boldsymbol{\delta}_\beta\right)}\right] \\ &= \left(\delta_1-\delta_2\right)_{\mathbf{x}}\left[\mathrm{e}^{i\mathbf{K}\cdot\left(\boldsymbol{\delta}_1-\boldsymbol{\delta}_2\right)}-\mathrm{e}^{-i\mathbf{K}\cdot\left(\boldsymbol{\delta}_1-\boldsymbol{\delta}_2\right)}\right] + \left(\delta_1-\delta_3\right)_{\mathbf{x}}\left[\mathrm{e}^{i\mathbf{K}\cdot\left(\boldsymbol{\delta}_1-\boldsymbol{\delta}_3\right)}-\mathrm{e}^{-i\mathbf{K}\cdot\left(\boldsymbol{\delta}_1-\boldsymbol{\delta}_3\right)}\right] \\ &+ \left(\delta_2-\delta_3\right)_{\mathbf{x}}\left[\mathrm{e}^{i\mathbf{K}\cdot\left(\boldsymbol{\delta}_2-\boldsymbol{\delta}_3\right)}-\mathrm{e}^{-i\mathbf{K}\cdot\left(\boldsymbol{\delta}_2-\boldsymbol{\delta}_3\right)}\right] \\ &= 2i\left\{\left(\frac{a}{2}-\frac{a}{2}\right)\sin\left[\mathbf{K}\cdot\left(\boldsymbol{\delta}_1-\boldsymbol{\delta}_2\right)\right] + \left(\frac{a}{2}+a\right)\sin\left[\mathbf{K}\cdot\left(\boldsymbol{\delta}_1-\boldsymbol{\delta}_3\right)\right] + \left(\frac{a}{2}+a\right)\sin\left[\mathbf{K}\cdot\left(\boldsymbol{\delta}_2-\boldsymbol{\delta}_3\right)\right]\right\} \\ &= 3ia\left[\sin\left(\frac{4\pi}{3}\right)+\sin\left(\frac{2\pi}{3}\right)\right] = 3ia\left(-\frac{1}{2}\sqrt{3}+\frac{1}{2}\sqrt{3}\right) = 0. \end{aligned}$$

The second part leads to

$$\begin{aligned} \mathrm{II_h} &= \sum_{\substack{\boldsymbol{\delta}_\alpha,\boldsymbol{\delta}_\beta\\ \alpha\neq\beta}}\left(\delta_\alpha-\delta_\beta\right)_{\mathbf{y}}\mathrm{e}^{i\mathbf{K}\cdot\left(\boldsymbol{\delta}_\alpha-\boldsymbol{\delta}_\beta\right)} \\ &= \left(\delta_1-\delta_2\right)_{\mathbf{y}}\left[\mathrm{e}^{i\mathbf{K}\cdot\left(\boldsymbol{\delta}_1-\boldsymbol{\delta}_2\right)}-\mathrm{e}^{-i\mathbf{K}\cdot\left(\boldsymbol{\delta}_1-\boldsymbol{\delta}_2\right)}\right] + \left(\delta_1-\delta_3\right)_{\mathbf{y}}\left[\mathrm{e}^{i\mathbf{K}\cdot\left(\boldsymbol{\delta}_1-\boldsymbol{\delta}_3\right)}-\mathrm{e}^{-i\mathbf{K}\cdot\left(\boldsymbol{\delta}_1-\boldsymbol{\delta}_3\right)}\right] \\ &+ \left(\delta_2-\delta_3\right)_{\mathbf{y}}\left[\mathrm{e}^{i\mathbf{K}\cdot\left(\boldsymbol{\delta}_2-\boldsymbol{\delta}_3\right)}-\mathrm{e}^{-i\mathbf{K}\cdot\left(\boldsymbol{\delta}_2-\boldsymbol{\delta}_3\right)}\right] \\ &= 2i\left\{\left(\delta_1-\delta_2\right)_{\mathbf{y}}\sin\left[\mathbf{K}\cdot\left(\boldsymbol{\delta}_1-\boldsymbol{\delta}_2\right)\right] + \left(\delta_1-\delta_3\right)_{\mathbf{y}}\sin\left[\mathbf{K}\cdot\left(\boldsymbol{\delta}_1-\boldsymbol{\delta}_3\right)\right] + \left(\delta_2-\delta_3\right)_{\mathbf{y}}\sin\left[\mathbf{K}\cdot\left(\boldsymbol{\delta}_2-\boldsymbol{\delta}_3\right)\right]\right\} \\ &= 2i\left[\left(\frac{\sqrt{3}a}{2}+\frac{\sqrt{3}a}{2}\right)\sin\left(\frac{2\pi}{3}\right) + \frac{\sqrt{3}a}{2}\sin\left(\frac{4\pi}{3}\right) - \frac{\sqrt{3}a}{2}\sin\left(\frac{2\pi}{3}\right)\right] \\ &= \sqrt{3}ia\left[2\sin\left(\frac{2\pi}{3}\right)+\sin\left(\frac{4\pi}{3}\right)-\sin\left(\frac{2\pi}{3}\right)\right] = \sqrt{3}ia\left(\frac{1}{2}\sqrt{3}-\frac{1}{2}\sqrt{3}\right) = 0. \end{aligned}$$

Such that

$$q_i\partial_{k_i}h|_{\mathbf{K}} = 0.$$

The third and last term in the expansion $h\left(\mathbf{K}+\mathbf{q}\right)$

$$\frac{1}{2!}q_iq_j\partial_{k_i}\partial_{k_j}h\Big|_{\mathbf{K}}=\frac{1}{2}q_{\mathbf{x}}^2\partial_{k_{\mathbf{x}}}^2h\Big|_{\mathbf{K}}+\frac{1}{2}q_{\mathbf{y}}^2\partial_{k_{\mathbf{y}}}^2h\Big|_{\mathbf{K}}+q_{\mathbf{x}}q_{\mathbf{y}}\partial_{k_{\mathbf{x}}}\partial_{k_{\mathbf{y}}}h\big|_{\mathbf{K}}=\mathrm{III_h}+\mathrm{IV_h}+\mathrm{V_h},$$

where

$$\mathrm{III_h}\equiv\frac{1}{2}q_{\mathbf{x}}^2\partial_{k_{\mathbf{x}}}^2h\Big|_{\mathbf{K}},\qquad\mathrm{IV_h}\equiv\frac{1}{2}q_{\mathbf{y}}^2\partial_{k_{\mathbf{y}}}^2h\Big|_{\mathbf{K}},\qquad\mathrm{V_h}\equiv q_{\mathbf{x}}q_{\mathbf{y}}\partial_{k_{\mathbf{x}}}\partial_{k_{\mathbf{y}}}h\big|_{\mathbf{K}}.$$

The first term in the expansion yields

$$\begin{aligned}
\mathrm{III_h}&=\frac{1}{2}q_{\mathbf{x}}^2\partial_{k_{\mathbf{x}}}^2h\Big|_{\mathbf{K}}=\frac{1}{2}q_{\mathbf{x}}^2\partial_{k_{\mathbf{x}}}^2\left(-t'\sum_{\substack{\boldsymbol{\delta}_\alpha,\boldsymbol{\delta}_\beta\\ \alpha\neq\beta}}\mathrm{e}^{i\mathbf{k}\cdot\left(\boldsymbol{\delta}_\alpha-\boldsymbol{\delta}_\beta\right)}\right)\Bigg|_{\mathbf{K}}\\
&=\frac{t'}{2}q_{\mathbf{x}}^2\left[\left(\delta_1-\delta_2\right)_{\mathbf{x}}^2\left(\mathrm{e}^{i\mathbf{K}\cdot\left(\boldsymbol{\delta}_1-\boldsymbol{\delta}_2\right)}+\mathrm{e}^{-i\mathbf{K}\cdot\left(\boldsymbol{\delta}_1-\boldsymbol{\delta}_2\right)}\right)+\left(\delta_1-\delta_3\right)_{\mathbf{x}}^2\left(\mathrm{e}^{i\mathbf{K}\cdot\left(\boldsymbol{\delta}_1-\boldsymbol{\delta}_3\right)}+\mathrm{e}^{-i\mathbf{K}\cdot\left(\boldsymbol{\delta}_1-\boldsymbol{\delta}_3\right)}\right)\right.\\
&\left.+\left(\delta_2-\delta_3\right)_{\mathbf{x}}^2\left(\mathrm{e}^{i\mathbf{K}\cdot\left(\boldsymbol{\delta}_2-\boldsymbol{\delta}_3\right)}+\mathrm{e}^{-i\mathbf{K}\cdot\left(\boldsymbol{\delta}_2-\boldsymbol{\delta}_3\right)}\right)\right]\\
&=t'q_{\mathbf{x}}^2\left\{\left(\frac{a}{2}-\frac{a}{2}\right)^2\cos\left[\mathbf{K}\cdot\left(\boldsymbol{\delta}_1-\boldsymbol{\delta}_2\right)\right]+\left(\frac{a}{2}+a\right)^2\cos\left[\mathbf{K}\cdot\left(\boldsymbol{\delta}_1-\boldsymbol{\delta}_3\right)\right]+\left(\frac{a}{2}+a\right)^2\cos\left[\mathbf{K}\cdot\left(\boldsymbol{\delta}_2-\boldsymbol{\delta}_3\right)\right]\right\}\\
&=\frac{9t'}{4}q_{\mathbf{x}}^2a^2\left[\cos\left(\frac{4\pi}{3}\right)+\cos\left(\frac{2\pi}{3}\right)\right]=\frac{9t'}{4}q_{\mathbf{x}}^2a^2\left(-\frac{1}{2}-\frac{1}{2}\right)=-\frac{9t'}{4}q_{\mathbf{x}}^2a^2.
\end{aligned}$$

$\mathrm{IV_h}$ leads to

$$\begin{aligned}
\mathrm{IV_h}&=\frac{1}{2}q_{\mathbf{y}}^2\partial_{k_{\mathbf{y}}}^2h\Big|_{\mathbf{K}}=\frac{1}{2}q_y^2\partial_{k_y}^2\left(-t'\sum_{\substack{\boldsymbol{\delta}_\alpha,\boldsymbol{\delta}_\beta\\ \alpha\neq\beta}}\mathrm{e}^{i\mathbf{k}\cdot\left(\boldsymbol{\delta}_\alpha-\boldsymbol{\delta}_\beta\right)}\right)\Bigg|_{\mathbf{K}}\\
&=\frac{t'}{2}q_{\mathbf{y}}^2\left[\left(\delta_1-\delta_2\right)_{\mathbf{y}}^2\left(\mathrm{e}^{i\mathbf{K}\cdot\left(\boldsymbol{\delta}_1-\boldsymbol{\delta}_2\right)}+\mathrm{e}^{-i\mathbf{K}\cdot\left(\boldsymbol{\delta}_1-\boldsymbol{\delta}_2\right)}\right)+\left(\delta_1-\delta_3\right)_{\mathbf{y}}^2\left(\mathrm{e}^{i\mathbf{K}\cdot\left(\boldsymbol{\delta}_1-\boldsymbol{\delta}_3\right)}+\mathrm{e}^{-i\mathbf{K}\cdot\left(\boldsymbol{\delta}_1-\boldsymbol{\delta}_3\right)}\right)\right.\\
&\left.+\left(\delta_2-\delta_3\right)_{\mathbf{y}}^2\left(\mathrm{e}^{i\mathbf{K}\cdot\left(\boldsymbol{\delta}_2-\boldsymbol{\delta}_3\right)}+\mathrm{e}^{-i\mathbf{K}\cdot\left(\boldsymbol{\delta}_2-\boldsymbol{\delta}_3\right)}\right)\right]\\
&=t'q_{\mathbf{y}}^2\left\{\left(\frac{\sqrt{3}a}{2}+\frac{\sqrt{3}a}{2}\right)^2\cos\left[\mathbf{K}\cdot\left(\boldsymbol{\delta}_1-\boldsymbol{\delta}_2\right)\right]+\left(\frac{\sqrt{3}a}{2}\right)^2\cos\left[\mathbf{K}\cdot\left(\boldsymbol{\delta}_1-\boldsymbol{\delta}_3\right)\right]\right.\\
&\left.+\left(-\frac{\sqrt{3}a}{2}\right)^2\cos\left[\mathbf{K}\cdot\left(\boldsymbol{\delta}_2-\boldsymbol{\delta}_3\right)\right]\right\}=t'q_{\mathbf{y}}^2a^2\left[3\cos\left(\frac{2\pi}{3}\right)+\frac{3}{4}\cos\left(\frac{4\pi}{3}\right)+\frac{3}{4}\cos\left(\frac{2\pi}{3}\right)\right]\\
&=3t'q_{\mathbf{y}}^2a^2\left(-\frac{1}{2}-\frac{1}{8}-\frac{1}{8}\right)=-\frac{9t'}{4}q_{\mathbf{y}}^2a^2.
\end{aligned}$$

Lastly,

$$
\begin{aligned}
\mathrm{V_h} &= q_{\mathbf{x}} q_{\mathbf{y}} \partial_{k_{\mathbf{x}}} \partial_{k_{\mathbf{y}}} h\big|_{\mathbf{K}} = q_{\mathbf{x}} q_{\mathbf{y}} \partial_{k_{\mathbf{x}}} \partial_{k_{\mathbf{y}}} \left(-t' \sum_{\substack{\boldsymbol{\delta}_\alpha, \boldsymbol{\delta}_\beta \\ \alpha \neq \beta}} \mathrm{e}^{i\mathbf{k}\cdot\left(\boldsymbol{\delta}_\alpha - \boldsymbol{\delta}_\beta\right)} \right) \Bigg|_{\mathbf{K}} \\
&= t' q_{\mathbf{x}} q_{\mathbf{y}} \Big[\left(\delta_1 - \delta_2\right)_{\mathbf{x}} \left(\delta_1 - \delta_2\right)_{\mathbf{y}} \left(\mathrm{e}^{i\mathbf{K}\cdot\left(\boldsymbol{\delta}_1 - \boldsymbol{\delta}_2\right)} + \mathrm{e}^{-i\mathbf{K}\cdot\left(\boldsymbol{\delta}_1 - \boldsymbol{\delta}_2\right)} \right) \\
&+ \left(\delta_1 - \delta_3\right)_{\mathbf{x}} \left(\delta_1 - \delta_3\right)_{\mathbf{y}} \left(\mathrm{e}^{i\mathbf{K}\cdot\left(\boldsymbol{\delta}_1 - \boldsymbol{\delta}_3\right)} + \mathrm{e}^{-i\mathbf{K}\cdot\left(\boldsymbol{\delta}_1 - \boldsymbol{\delta}_3\right)} \right) \\
&+ \left(\delta_2 - \delta_3\right)_{\mathbf{x}} \left(\delta_2 - \delta_3\right)_{\mathbf{y}} \left(\mathrm{e}^{i\mathbf{K}\cdot\left(\boldsymbol{\delta}_2 - \boldsymbol{\delta}_3\right)} + \mathrm{e}^{-i\mathbf{K}\cdot\left(\boldsymbol{\delta}_2 - \boldsymbol{\delta}_3\right)} \right) \Big] \\
&= 2t' q_{\mathbf{x}} q_{\mathbf{y}} \left[\left(\frac{3a}{2}\right) \left(\frac{\sqrt{3}a}{2}\right) \cos\left(\frac{4\pi}{3}\right) + \left(\frac{3a}{2}\right) \left(-\frac{\sqrt{3}a}{2}\right) \cos\left(\frac{2\pi}{3}\right) \right] \\
&= 2t' q_{\mathbf{x}} q_{\mathbf{y}} a^2 \left(-\frac{3\sqrt{3}}{4} + \frac{3\sqrt{3}}{4} \right) = 0.
\end{aligned}
$$

This leads to the following

$$
\frac{1}{2!} q_i q_j \partial_{k_i} \partial_{k_j} h \Big|_{\mathbf{K}} = -\frac{9t'a^2}{4} |\mathbf{q}|^2.
$$

Therefore, $h(\mathbf{K}+\mathbf{q})$ has the following solution

$$
h(\mathbf{K}+\mathbf{q}) = 3t' - \frac{9t'a^2}{4} |\mathbf{q}|^2 = h^*(\mathbf{K}+\mathbf{q}),
$$

such that

$$
\frac{1}{2} \left[h(\mathbf{K}+\mathbf{q}) + h^*(\mathbf{K}+\mathbf{q}) \right] = 3t' - \frac{9t'a^2}{4} |\mathbf{q}|^2. \tag{6.53}
$$

Combining the results leads to the final answer for $E(\mathbf{q}+\mathbf{K})$ to $\mathcal{O}(\mathbf{q}^2/\mathbf{K}^2)$

$$
E(\mathbf{q}+\mathbf{K}) = 3t' \pm v_F |\mathbf{q}| - \left[\frac{9t'a^2}{4} \pm \frac{3ta^2}{8} \sin(3\theta_{\mathbf{q}}) \right] |\mathbf{q}|^2 + \mathcal{O}\left[(\mathbf{q}/\mathbf{K})^3 \right]. \tag{6.54}
$$

6.2.5 Density of States

For $t' = 0$, it is possible to derive an analytical expression for the density of states near the Dirac point K. First, the Hamiltonian will be written in terms of $\boldsymbol{\sigma}$ and $g(\mathbf{k})$ as defined in Eq. (6.36)

$$
H_{nn} = \sum_{\sigma,\mathbf{k}} \begin{pmatrix} a^\dagger_{\sigma,\mathbf{k}} & b^\dagger_{\sigma,\mathbf{k}} \end{pmatrix} \begin{pmatrix} 0 & g(\mathbf{k}) \\ g^*(\mathbf{k}) & 0 \end{pmatrix} \begin{pmatrix} a_{\sigma,\mathbf{k}} \\ b_{\sigma,\mathbf{k}} \end{pmatrix} = \sum_{\sigma,\mathbf{k}} \begin{pmatrix} a^\dagger_{\sigma,\mathbf{k}} & b^\dagger_{\sigma,\mathbf{k}} \end{pmatrix} \hat{H}(\mathbf{k}) \begin{pmatrix} a_{\sigma,\mathbf{k}} \\ b_{\sigma,\mathbf{k}} \end{pmatrix},
$$

where $\hat{H}(\mathbf{k}) = \boldsymbol{\sigma} \cdot d(\mathbf{k})$ where σ_i are the Pauli matrices, $d(\mathbf{k}) = [d(\mathbf{x}), d(\mathbf{y})]$ with $d(\mathbf{x}) = \mathrm{Re}[g(\mathbf{k})]$ and $d(\mathbf{y}) = -\mathrm{Im}[g(\mathbf{k})]$. To verify the validity this relation, $\hat{H}(\mathbf{k})$ will be computed. This leads to

$$
\mathrm{Re}[g(\mathbf{k})] = -t \sum_{\boldsymbol{\delta}_\alpha} \cos\left(\mathbf{k} \cdot \boldsymbol{\delta}_\alpha\right), \qquad \mathrm{Im}[g(\mathbf{k})] = -t \sum_{\boldsymbol{\delta}_\alpha} \sin\left(\mathbf{k} \cdot \boldsymbol{\delta}_\alpha\right),
$$

yielding

$$\hat{H}(\mathbf{k}) = \boldsymbol{\sigma} \cdot d(\mathbf{k}) = \sigma_{\mathbf{x}} d(\mathbf{x}) + \sigma_{\mathbf{y}} d(\mathbf{y}) = \begin{pmatrix} 0 & 1 \\ 1 & 0 \end{pmatrix} \mathrm{Re}[g(\mathbf{k})] - \begin{pmatrix} 0 & -i \\ i & 0 \end{pmatrix} \mathrm{Im}[g(\mathbf{k})]$$
$$= \begin{pmatrix} 0 & \mathrm{Re}[g(\mathbf{k})] + i\,\mathrm{Im}[g(\mathbf{k})] \\ \mathrm{Re}[g(\mathbf{k})] - i\,\mathrm{Im}[g(\mathbf{k})] & 0 \end{pmatrix}$$
$$= -t \sum_{\boldsymbol{\delta}_\alpha} \begin{pmatrix} 0 & \cos(\mathbf{k}\cdot\boldsymbol{\delta}_\alpha) + i\sin(\mathbf{k}\cdot\boldsymbol{\delta}_\alpha) \\ \cos(\mathbf{k}\cdot\boldsymbol{\delta}_\alpha) - i\sin(\mathbf{k}\cdot\boldsymbol{\delta}_\alpha) & 0 \end{pmatrix} = \begin{pmatrix} 0 & g(\mathbf{k}) \\ g^*(\mathbf{k}) & 0 \end{pmatrix}.$$

Such that indeed $\hat{H}(\mathbf{k}) = \boldsymbol{\sigma} \cdot d(\mathbf{k})$.

The density of states ρ is defined as

$$\rho(E) = -\frac{1}{\pi} \mathrm{Im}\,\mathrm{Tr}\left(E - \hat{H}(\mathbf{k}) + i\delta\right)^{-1},$$

where $\delta > 0$ to make sure the Green's function is retarded. Absorbing $i\delta$ in the energy as $E' = E + i\delta$ leads to

$$\left(E' - \hat{H}(\mathbf{k})\right)^{-1} = \frac{1}{E' - \boldsymbol{\sigma}\cdot d(\mathbf{k})} = \frac{E' + \boldsymbol{\sigma}\cdot d(\mathbf{k})}{E'^2 - d(\mathbf{k})^2}$$
$$= \frac{E' + \boldsymbol{\sigma}\cdot d(\mathbf{k})}{2E'} \left(\frac{1}{E' - d(\mathbf{k})} + \frac{1}{E' + d(\mathbf{k})}\right).$$

The first term of this equation is the interesting part because $d(\mathbf{k}) > 0$ and $E > 0$ is the energy band considered here. This leads to the following relation for the density of states

$$\rho(E) = -\frac{1}{\pi} \mathrm{Im}\,\mathrm{Tr}\left[\frac{E' + \boldsymbol{\sigma}\cdot d(\mathbf{k})}{2E'} \frac{1}{E' - d(\mathbf{k})}\right] = -\frac{1}{\pi} \mathrm{Im}\,\mathrm{Tr}\left[\frac{1}{2E'} \begin{pmatrix} E' & f(\mathbf{k}) \\ f^*(\mathbf{k}) & E' \end{pmatrix} \frac{1}{E' - d(\mathbf{k})}\right]$$
$$= -\frac{N_s}{\pi} \frac{2E'}{2E'} \int \mathrm{d}k\, \mathrm{Im}\left[\frac{1}{E' - d(\mathbf{k})}\right] = -\frac{N_s}{\pi} \int \mathrm{d}k\, \mathrm{Im}\left[\frac{1}{E - d(\mathbf{k}) + i\delta}\right],$$

where $\mathrm{d}k = \mathrm{d}^2k/(2\pi)^2$. The following identity is used

$$\mathrm{Im}\left(\frac{1}{x + i\delta}\right) = -\pi\delta(x)$$

to find

$$\rho(E) = -\frac{N_s}{\pi} \int \mathrm{d}k \cdot -\pi\delta(E - d(\mathbf{k})) = N_s \int \mathrm{d}k\, \delta(E - d(\mathbf{k})).$$

So far the derivation of the density of states has been general. Now, the expansion around the K point will be used. First of all, this means that $N_s = 4$ with a factor of 2 coming from the spin degree of freedom and the another factor of 2 coming from the valley degree of freedom. Next, $d(\mathbf{k})$ needs to be computed

$$d(\mathbf{k}) = \sqrt{d(\mathbf{x})^2 + d(\mathbf{y})^2}. \tag{6.55}$$

In App. 6.2.3 the following was obtained

$$g(\mathbf{K} + \mathbf{k}) = -\frac{3at}{4}\left[-\left(\sqrt{3}k_{\mathbf{x}} + k_{\mathbf{y}}\right) + i\left(k_{\mathbf{x}} - \sqrt{3}k_{\mathbf{y}}\right)\right],$$

such that

$$\begin{aligned} d(\mathbf{x}) &= \mathrm{Re}[g(\mathbf{K}+\mathbf{k})] = \frac{3at}{4}\left(\sqrt{3}k_{\mathbf{x}} + k_{\mathbf{y}}\right), \\ d(\mathbf{y}) &= -\mathrm{Im}[g(\mathbf{K}+\mathbf{k})] = \frac{3at}{4}\left(k_{\mathbf{x}} - \sqrt{3}k_{\mathbf{y}}\right). \end{aligned}$$

This then yields

$$\begin{aligned} d(\mathbf{k}) &= \sqrt{d(\mathbf{x})^2 + d(\mathbf{y})^2} = \pm\frac{3at}{4}\sqrt{3k_{\mathbf{x}}^2 + k_{\mathbf{y}}^2 + 2\sqrt{3}k_{\mathbf{x}}k_{\mathbf{y}} + k_{\mathbf{x}}^2 + 3k_{\mathbf{y}}^2 - 2\sqrt{3}k_{\mathbf{x}}k_{\mathbf{y}}} \\ &= \pm\frac{3at}{4}\sqrt{4k_{\mathbf{x}}^2 + 4k_{\mathbf{y}}^2} = \pm v_F|\mathbf{k}|, \end{aligned}$$

which coincides exactly with the result for $E_{nn}(\mathbf{q}+\mathbf{K})$ up to $\mathcal{O}(\mathbf{q}/\mathbf{K})$ in Eq. (6.49) as it should.

Remembering that $E > 0$ such that $d(\mathbf{k}) = v_F k$, the density of states is

$$\rho(E) = \frac{4}{(2\pi)^2}\int \mathrm{d}^2k\,\delta(E - v_F k) = \frac{4}{(2\pi)^2}\int_0^{2\pi}\mathrm{d}\theta\int \mathrm{d}k\,k\,\delta(E - v_F k).$$

Substituting according to $x = v_F k$ leads to the final result

$$\rho(E) = \frac{4}{2\pi}\int \frac{\mathrm{d}x}{v_F}\frac{x}{v_F}\,\delta(E - x) = \frac{2}{\pi}\frac{E}{v_F^2}.$$

The same result would have been found in the case of $E < 0$, therefore

$$\rho(E) = \frac{2}{\pi}\frac{|E|}{v_F^2}. \tag{6.56}$$

Next, the same procedure will be followed to find the density of states per unit cell for any momentum $\mathbf{k}$. As for the previous case, $d(\mathbf{k})$ coincides with the energy bands

$$d(\mathbf{k}) = \pm t\sqrt{3 + 2\cos\left(k_{\mathbf{y}}\sqrt{3}a\right) + 4\cos\left(k_{\mathbf{x}}\frac{3a}{2}\right)\cos\left(k_{\mathbf{y}}\frac{\sqrt{3}a}{2}\right)} = \pm t\sqrt{3 + f(\mathbf{k})}.$$

The density of states is

$$\rho(E) = \frac{N_s}{(2\pi)^2}\int \mathrm{d}^2k\,\delta(E - t\sqrt{3 + f(\mathbf{k})}) = \frac{N_s}{(2\pi)^2}\int \mathrm{d}k_{\mathbf{x}}\,\mathrm{d}k_{\mathbf{y}}\,\delta(h(\mathbf{k})),$$

where $h(\mathbf{k}) = E - t\sqrt{3 + f(\mathbf{k})}$. The following identity will be used to simplify the integral

$$\int_{-\infty}^{\infty}\mathrm{d}x\,\delta(f(x)) = \sum_i \frac{1}{f'(x_i)}, \qquad \text{where} \qquad f(x_i) = 0.$$

This leads to

$$\rho(E) = \frac{N_s}{(2\pi)^2}\int \mathrm{d}k_{\mathbf{y}}\ \left.\frac{1}{\partial_{k_{\mathbf{x}}}h(\mathbf{k})}\right|_{k_{\mathbf{x}}^*},$$

where $k_{\mathbf{x}}^*$ is the value for which $h(\mathbf{k}) = 0$. The derivative reads

$$\partial_{k_{\mathbf{x}}} h(\mathbf{k}) = \partial_{k_{\mathbf{x}}} \left(E - t\sqrt{3 + f(\mathbf{k})} \right) = -t \frac{\partial_{k_{\mathbf{x}}} f(\mathbf{k})}{2\sqrt{3 + f(\mathbf{k})}},$$

where

$$\partial_{k_{\mathbf{x}}} f(\mathbf{k}) = \partial_{k_{\mathbf{x}}} \left[2\cos\left(k_{\mathbf{y}}\sqrt{3}a\right) + 4\cos\left(k_{\mathbf{x}}\frac{3a}{2}\right)\cos\left(k_{\mathbf{y}}\frac{\sqrt{3}a}{2}\right) \right] = -6a\sin\left(k_{\mathbf{x}}\frac{3a}{2}\right)\cos\left(k_{\mathbf{y}}\frac{\sqrt{3}a}{2}\right),$$

such that

$$\partial_{k_{\mathbf{x}}} h(\mathbf{k}) = 6at\, \frac{\sin\left(k_{\mathbf{x}}\frac{3a}{2}\right)\cos\left(k_{\mathbf{y}}\frac{\sqrt{3}a}{2}\right)}{2\sqrt{3 + f(\mathbf{k})}}.$$

Using the delta function to rewrite this derivative yields

$$\delta(E - t\sqrt{3 + f(\mathbf{k})}) \neq 0, \qquad \text{such that} \qquad \sqrt{3 + f(\mathbf{k})} = \frac{E}{t},$$

which leads to

$$\partial_{k_{\mathbf{x}}} h(\mathbf{k}) = \frac{3at^2}{E} \sin\left(k_{\mathbf{x}}\frac{3a}{2}\right)\cos\left(k_{\mathbf{y}}\frac{\sqrt{3}a}{2}\right).$$

Plugging this back into the density of states yields

$$\rho(E) = \frac{N_s}{(2\pi)^2} \int \mathrm{d}k_{\mathbf{y}}\, \frac{E}{3at^2} \left[\sin\left(k_{\mathbf{x}}^*\frac{3a}{2}\right)\cos\left(k_{\mathbf{y}}\frac{\sqrt{3}a}{2}\right) \right]^{-1}.$$

Next, $\sin\left(k_{\mathbf{x}}^*\frac{3a}{2}\right)$ needs to be determined. The variable $k_{\mathbf{x}}^*$ is defined such that $h(\mathbf{k})|_{k_{\mathbf{x}}^*} = 0$

$$\begin{aligned}
E - t\sqrt{3 + f(\mathbf{k})}\Big|_{k_{\mathbf{x}}^*} &= 0 \\
t\sqrt{3 + 2\cos\left(k_{\mathbf{y}}\sqrt{3}a\right) + 4\cos\left(k_{\mathbf{x}}^*\frac{3a}{2}\right)\cos\left(k_{\mathbf{y}}\frac{\sqrt{3}a}{2}\right)} &= E \\
\frac{\frac{E^2}{t^2} - 3 - 2\cos\left(k_{\mathbf{y}}\sqrt{3}a\right)}{4\cos\left(k_{\mathbf{y}}\frac{\sqrt{3}a}{2}\right)} &= \cos\left(k_{\mathbf{x}}^*\frac{3a}{2}\right). \qquad (6.57)
\end{aligned}$$

Using the identity $\sin(x) = \sqrt{1 - \cos^2(x)}$

$$\begin{aligned}
\rho(E) = \frac{N_s}{(2\pi)^2}\frac{E}{3at^2} \int \mathrm{d}k_{\mathbf{y}} \Bigg[&\cos^2\left(k_{\mathbf{y}}\frac{\sqrt{3}a}{2}\right) - \frac{1}{16}\frac{E^4}{t^4} - \frac{9}{16} - \frac{1}{4}\cos^2\left(\sqrt{3}ak_{\mathbf{y}}\right) \\
&+ \frac{3}{8}\frac{E^2}{t^2} + \frac{1}{4}\frac{E^2}{t^2}\cos\left(\sqrt{3}ak_{\mathbf{y}}\right) - \frac{3}{8}\cos\left(\sqrt{3}ak_y\right) \Bigg]^{-1/2}.
\end{aligned}$$

This can be rewritten to find

$$\rho(E) = \frac{4}{\pi^2}\frac{|E|}{t^2}\frac{1}{\sqrt{Z_0}}\mathbf{F}\left(\frac{\pi}{2}, \sqrt{\frac{Z_1}{Z_0}}\right), \tag{6.58}$$

with at $-t \leq E \leq t$

$$Z_0 = \left(1 + \left|\frac{E}{t}\right|\right)^2 - \frac{[(E/t)^2 - 1]^2}{4}, \tag{6.59}$$

$$Z_1 = 4\left|\frac{E}{t}\right|, \tag{6.60}$$

and at $-3t \leq E \leq -t \vee t \leq E \leq 3t$

$$Z_0 = 4\left|\frac{E}{t}\right|, \tag{6.61}$$

$$Z_1 = \left(1 + \left|\frac{E}{t}\right|\right)^2 - \frac{[(E/t)^2 - 1]^2}{4}, \tag{6.62}$$

where $\mathbf{F}\left(\frac{\pi}{2}, \sqrt{\frac{Z_1}{Z_0}}\right)$ is the complete elliptical integral of the first kind.

6.3 Appendix to Chapter 4

6.3.1 Integrating out Phonons

As mentioned in Section. 4.2, the operators are replaced by fields using the following transformations

$$\begin{aligned}
a_{\mathbf{k},\sigma} &\rightarrow \psi_{A,\mathbf{k},\sigma}(\tau) = \frac{1}{\sqrt{\hbar\beta}}\sum_n \psi_{A,\mathbf{k},\sigma,n}\mathrm{e}^{-i\omega_n\tau}, \\
b_{\mathbf{k},\sigma} &\rightarrow \psi_{B,\mathbf{k},\sigma}(\tau) = \frac{1}{\sqrt{\hbar\beta}}\sum_n \psi_{B,\mathbf{k},\sigma n}\mathrm{e}^{-i\omega_n\tau}, \\
c_{A,\mathbf{q}} &\rightarrow \phi_{A,\mathbf{q}}(\tau) = \frac{1}{\sqrt{\hbar\beta}}\sum_n \phi_{A,\mathbf{q},n}\mathrm{e}^{-i\hat{\omega}_n\tau}, \\
c_{B,\mathbf{q}} &\rightarrow \phi_{B,\mathbf{q}}(\tau) = \frac{1}{\sqrt{\hbar\beta}}\sum_n \phi_{B,\mathbf{q},n}\mathrm{e}^{-i\hat{\omega}_n\tau},
\end{aligned}$$

where $\omega_n = (2n+1)\pi/(\hbar\beta)$ and $\hat{\omega}_n = 2n\pi/(\hbar\beta)$ for $n \in \mathbb{Z}$ are the Matsubara frequencies for fermions and bosons, respectively, and ϕ (ψ) obey the boson (fermion) (anti)commutation relations. The following definition is used to determine the action

$$S\left[\psi^\dagger, \psi\right] = \int_0^{\hbar\beta} \mathrm{d}\tau \left[\psi^\dagger(\tau)\partial_\tau\psi(\tau) + H\left(\psi^\dagger, \psi\right)\right].$$

The phonon action for the phonon on sublattice A is

$$
\begin{aligned}
&S_{\mathrm{ph},A}\left[\phi_A^\dagger,\phi_A\right]=\int_0^{\hbar\beta}\mathrm{d}\tau\sum_{\mathbf{q}}\left[\phi_{A,\mathbf{q}}^\dagger(\tau)\partial_\tau\phi_{A,\mathbf{q}}(\tau)+\hbar\omega_E\,\phi_{A,\mathbf{q}}^\dagger(\tau)\phi_{A,\mathbf{q}}(\tau)\right]\\
&=\frac{1}{\hbar\beta}\int_0^{\hbar\beta}\mathrm{d}\tau\sum_{\mathbf{q}}\sum_{n,n'}\left[\phi_{A,\mathbf{q},n}^\dagger\mathrm{e}^{i\hat{\omega}_n\tau}\partial_\tau\phi_{A,\mathbf{q},n'}\mathrm{e}^{-i\hat{\omega}_{n'}\tau}+\hbar\omega_E\,\phi_{A,\mathbf{q},n}^\dagger\mathrm{e}^{i\hat{\omega}_n\tau}\phi_{A,\mathbf{q},n'}\mathrm{e}^{-i\hat{\omega}_{n'}\tau}\right]\\
&=\frac{1}{\hbar\beta}\int_0^{\hbar\beta}\mathrm{d}\tau\sum_{\mathbf{q}}\sum_{n,n'}\mathrm{e}^{i(\hat{\omega}_n-\hat{\omega}_{n'})\tau}\left[\phi_{A,\mathbf{q},n}^\dagger\left(-i\hat{\omega}_{n'}\right)\phi_{A,\mathbf{q},n'}+\hbar\omega_E\,\phi_{A,\mathbf{q},n}^\dagger\phi_{A,\mathbf{q},n'}\right]\\
&=\frac{2\pi}{\hbar\beta}\sum_{\mathbf{q}}\sum_{n,n'}\delta\left(\hat{\omega}_n-\hat{\omega}_{n'}\right)[...]=\frac{2\pi}{\hbar\beta}\sum_{\mathbf{q}}\sum_{n,n'}\delta\left(\frac{2n\pi}{\hbar\beta}-\frac{2n'\pi}{\hbar\beta}\right)[...]\\
&=\frac{2\pi}{\hbar\beta}\frac{1}{\frac{2\pi}{\hbar\beta}}\sum_{\mathbf{q}}\sum_{n,n'}\delta\left(n-n'\right)[...]=\sum_{\mathbf{q},n}\left[\phi_{A,\mathbf{q},n}^\dagger\left(-i\hat{\omega}_n+\hbar\omega_{A,E}\right)\phi_{A,\mathbf{q},n}\right].
\end{aligned}
$$

The phonon action for the phonon on sublattice B is the same upon applying $A\to B$. The electron-phonon action $S_{A,\mathrm{el-ph}}\left[\psi_A^\dagger,\psi_A,\psi_B^\dagger,\psi_B,\phi_A^\dagger,\phi_A\right]$ for the phonon on sublattice A is

$$
\begin{aligned}
&S_{A,\mathrm{el-ph}}\left[\psi_A^\dagger,\psi_A,\psi_B^\dagger,\psi_B,\phi_A^\dagger,\phi_A\right]\\
&=\int_0^{\hbar\beta}\mathrm{d}\tau\sum_{\mathbf{k},\mathbf{q},\sigma}\left[\left(u_0\psi_{A,\mathbf{k}+\mathbf{q},\sigma}^\dagger(\tau)\psi_{A,\mathbf{k},\sigma}(\tau)+v(q)\psi_{B,\mathbf{k}+\mathbf{q},\sigma}^\dagger(\tau)\psi_{B,\mathbf{k},\sigma}(\tau)\right)\left(\phi_{A,-\mathbf{q}}^\dagger(\tau)+\phi_{A,\mathbf{q}}(\tau)\right)\right]\\
&=\frac{1}{\hbar\beta\sqrt{\hbar\beta}}\int_0^{\hbar\beta}\mathrm{d}\tau\sum_{\mathbf{k},\mathbf{q},\sigma}\sum_{n,n',n''}\left[\mathrm{e}^{i(\omega_n-\omega_{n'}+\hat{\omega}_{n''})\tau}\left(u_0\psi_{A,\mathbf{k}+\mathbf{q},\sigma,n}^\dagger\psi_{A,\mathbf{k},\sigma,n'}\right.\right.\\
&\left.+v(q)\psi_{B,\mathbf{k}+\mathbf{q},\sigma,n}^\dagger\psi_{B,\mathbf{k},\sigma,n'}\right)\phi_{A,-\mathbf{q},n''}^\dagger\\
&\left.+\mathrm{e}^{i(\omega_n-\omega_{n'}-\hat{\omega}_{n''})\tau}\left(g_0\psi_{A,\mathbf{k}+\mathbf{q},\sigma,n}^\dagger\psi_{A,\mathbf{k},\sigma,n'}+h(q)\psi_{B,\mathbf{k}+\mathbf{q},\sigma,n}^\dagger\psi_{B,\mathbf{k},\sigma,n'}\right)\phi_{A,\mathbf{q},n''}\right]\\
&=\frac{2\pi}{\hbar\beta\sqrt{\hbar\beta}}\sum_{\mathbf{k},\mathbf{q},\sigma}\sum_{n,n',n''}\left\{\delta\left(\omega_n-\omega_{n'}+\hat{\omega}_{n''}\right)[...]+\delta\left(\omega_n-\omega_{n'}-\hat{\omega}_{n''}\right)[...]\right\}\\
&=\frac{2\pi}{\hbar\beta\sqrt{\hbar\beta}}\sum_{\mathbf{k},\mathbf{q},\sigma}\sum_{n,n',n''}\left\{\delta\left(\frac{(2n+1)\pi}{\hbar\beta}-\frac{(2n'+1)\pi}{\hbar\beta}+\frac{2n''\pi}{\hbar\beta}\right)[...]\right.\\
&\left.+\delta\left(\frac{(2n+1)\pi}{\hbar\beta}-\frac{(2n'+1)\pi}{\hbar\beta}-\frac{2n''\pi}{\hbar\beta}\right)[...]\right\}\\
&=\frac{2\pi}{\hbar\beta\sqrt{\hbar\beta}}\frac{1}{\frac{2\pi}{\hbar\beta}}\sum_{\mathbf{k},\mathbf{q},\sigma}\sum_{n,n',n''}\left\{\delta\left(n-n'+n''\right)[...]+\delta\left(n-n'-n''\right)[...]\right\}\\
&=\frac{1}{\sqrt{\hbar\beta}}\sum_{\mathbf{k},\mathbf{q},\sigma}\sum_{m,n}\left[\left(u_0\psi_{A,\mathbf{k}+\mathbf{q},\sigma,m}^\dagger\psi_{A,\mathbf{k},\sigma,m-n}+v(q)\psi_{B,\mathbf{k}+\mathbf{q},\sigma,m}^\dagger\psi_{B,\mathbf{k},\sigma,m-n}\right)\phi_{A,-\mathbf{q},-n}^\dagger\right.\\
&\left.+\left(u_0\psi_{A,\mathbf{k}+\mathbf{q},\sigma,m}^\dagger\psi_{A,\mathbf{k},\sigma,m-n}+v(q)\psi_{B,\mathbf{k}+\mathbf{q},\sigma,m}^\dagger\psi_{B,\mathbf{k},\sigma,m-n}\right)\phi_{A,\mathbf{q},n}\right].
\end{aligned}
$$

Using the following definition for the density of electrons on sublattice A

$$\rho_{A,\mathbf{q},\sigma,n} \equiv \sum_{\mathbf{k},m} \psi^\dagger_{A,\mathbf{k}+\mathbf{q},\sigma,m+n}\psi_{A,\mathbf{k},\sigma,m} = \sum_{\mathbf{k},m} \psi^\dagger_{A,\mathbf{k}+\mathbf{q},\sigma,m}\psi_{A,\mathbf{k},\sigma m-n}$$

yields

$$\begin{aligned}
&S_{A,\mathrm{el-ph}}\left[\psi^\dagger_A,\psi_A,\psi^\dagger_B,\psi_B,\phi^\dagger_A,\phi_A\right] \\
&= \frac{1}{\sqrt{\hbar\beta}}\sum_{\mathbf{q},\sigma,n}\left[\left(u_0\rho_{A,\mathbf{q},\sigma,n}+v(q)\rho_{B,\mathbf{q},\sigma,n}\right)\phi^\dagger_{A,-\mathbf{q},-n}+\left(u_0\rho_{A,\mathbf{q},\sigma,n}+v(q)\rho_{B,\mathbf{q},\sigma,n}\right)\phi_{A,\mathbf{q},n}\right].
\end{aligned}$$

The total action $S_A\left[\psi^\dagger_A,\psi_A,\psi^\dagger_B,\psi_B,\phi^\dagger_A,\phi_A\right]$ for the phonon on sublattice A reads

$$\begin{aligned}
&S_A\left[\psi^\dagger_A,\psi_A,\psi^\dagger_B,\psi_B,\phi^\dagger_A,\phi_A\right] \\
&= \sum_{\mathbf{q},\sigma,n}\left[\phi^\dagger_{A,\mathbf{q},n}\left(-i\hat{\omega}_n+\hbar\omega_E\right)\phi_{A,\mathbf{q},n}+\frac{1}{\sqrt{\hbar\beta}}\left(u_0\rho_{A,\mathbf{q},\sigma,n}+v(q)\rho_{B,\mathbf{q},\sigma,n}\right)\phi^\dagger_{A,-\mathbf{q},-n}\right. \\
&\left.+\frac{1}{\sqrt{\hbar\beta}}\left(u_0\rho_{A,\mathbf{q},\sigma,n}+v(q)\rho_{B,\mathbf{q},\sigma,n}\right)\phi_{A,\mathbf{q},n}\right] \\
&= \sum_{\mathbf{q},\sigma,n}\left[\phi^\dagger_{A,\mathbf{q},n}\left(-i\hat{\omega}_n+\hbar\omega_E\right)\phi_{A,\mathbf{q},n}+\frac{1}{\sqrt{\hbar\beta}}\left(u_0\rho_{A,-\mathbf{q},\sigma,-n}+v(-q)\rho_{B,-\mathbf{q},\sigma,-n}\right)\phi^\dagger_{A,\mathbf{q},n}\right. \\
&\left.+\frac{1}{\sqrt{\hbar\beta}}\left(u_0\rho_{A,\mathbf{q},\sigma,n}+v(q)\rho_{B,\mathbf{q},\sigma,n}\right)\phi_{A,\mathbf{q},n}\right].
\end{aligned}$$

To be able to integrate out the phonons, the square needs to be completed. This yields

$$\begin{aligned}
&S_A\left[\psi^\dagger_A,\psi_A,\psi^\dagger_B,\psi_B,\phi^\dagger_A,\phi_A\right] \\
&= \sum_{\mathbf{q},\sigma,\sigma',n}\left(-i\hat{\omega}_n+\hbar\omega_{A,E}\right)\left[\phi^\dagger_{A,\mathbf{q},n}+\frac{1}{\sqrt{\hbar\beta}}\frac{1}{-i\hat{\omega}_n+\hbar\omega_E}\left(u_0\rho_{A,\mathbf{q},\sigma,n}+v(q)\rho_{B,\mathbf{q},\sigma,n}\right)\right] \\
&\times\left[\phi_{A,\mathbf{q},n}+\frac{1}{\sqrt{\hbar\beta}}\frac{1}{-i\hat{\omega}_n+\hbar\omega_E}\left(u_0\rho_{A,-\mathbf{q},\sigma',-n}+v(-q)\rho_{B,-\mathbf{q},\sigma',-n}\right)\right] \\
&-\frac{1}{\hbar\beta}\sum_{\mathbf{q},\sigma,\sigma',n}\frac{1}{-i\hat{\omega}_n+\hbar\omega_E}\left(u_0\rho_{A,\mathbf{q},\sigma,n}+v(q)\rho_{B,\mathbf{q},\sigma,n}\right)\left(u_0\rho_{A,-\mathbf{q},\sigma',-n}+v(-q)\rho_{B,-\mathbf{q},\sigma',-n}\right).
\end{aligned}$$

The action for the phonon on sublattice B can be found by applying $A \leftrightarrow B$ to this last result and reads

$$\begin{aligned}
&S_B\left[\psi^\dagger_A,\psi_A,\psi^\dagger_B,\psi_B,\phi^\dagger_B,\phi_B\right] \\
&= \sum_{\mathbf{q},\sigma,\sigma',n}\left(-i\hat{\omega}_n+\hbar\omega_{B,E}\right)\left[\phi^\dagger_{B,\mathbf{q},n}+\frac{1}{\sqrt{\hbar\beta}}\frac{1}{-i\hat{\omega}_n+\hbar\omega_E}\left(u_0\rho_{B,\mathbf{q},\sigma,n}+v(q)\rho_{A,\mathbf{q},\sigma,n}\right)\right] \\
&\times\left[\phi_{B,\mathbf{q},n}+\frac{1}{\sqrt{\hbar\beta}}\frac{1}{-i\hat{\omega}_n+\hbar\omega_E}\left(u_0\rho_{B,-\mathbf{q},\sigma',-n}+v(-q)\rho_{A,-\mathbf{q},\sigma',-n}\right)\right] \\
&-\frac{1}{\hbar\beta}\sum_{\mathbf{q},\sigma,\sigma',n}\frac{1}{-i\hat{\omega}_n+\hbar\omega_E}\left(u_0\rho_{B,\mathbf{q},\sigma,n}+v(q)\rho_{A,\mathbf{q},\sigma,n}\right)\left(u_0\rho_{B,-\mathbf{q},\sigma',-n}+v(-q)\rho_{A,-\mathbf{q},\sigma',-n}\right).
\end{aligned}$$

Next, the phonons are integrated out to obtain the effective action. For that purpose, the partition function is used. This yields

$$
\begin{aligned}
\mathcal{Z} &= \int \mathcal{D}\left[\psi_A^\dagger, \psi_A\right] \int \mathcal{D}\left[\psi_B^\dagger, \psi_B\right] \int \mathcal{D}\left[\phi_A^\dagger, \phi_A\right] \int \mathcal{D}\left[\phi_B^\dagger, \phi_B\right] \exp\left[-\frac{1}{\hbar\beta}\left(S_{\mathrm{el}}\left[\psi_A^\dagger, \psi_A, \psi_B^\dagger, \psi_B\right]\right.\right. \\
&\left.\left. + S_A\left[\psi_A^\dagger, \psi_A, \psi_B^\dagger, \psi_B, \phi_A^\dagger, \phi_A\right] + S_B\left[\psi_A^\dagger, \psi_A, \psi_B^\dagger, \psi_B, \phi_B^\dagger, \phi_B\right]\right)\right] \\
&= \int \mathcal{D}\left[\psi_A^\dagger, \psi_A\right] \int \mathcal{D}\left[\psi_B^\dagger, \psi_B\right] \int \mathcal{D}\left[\phi_A^\dagger, \phi_A\right] \int \mathcal{D}\left[\phi_B^\dagger, \phi_B\right] \exp\left\{-\frac{1}{\hbar\beta}\left(S_{\mathrm{el}}\left[\psi_A^\dagger, \psi_A, \psi_B^\dagger, \psi_B\right]\right.\right. \\
&+ \sum_{\mathbf{q},\sigma,\sigma',n} \left(-i\hat{\omega}_n + \hbar\omega_E\right)\left[\phi_{A,\mathbf{q},n}^\dagger + \frac{1}{\sqrt{\hbar\beta}} \frac{1}{-i\hat{\omega}_n + \hbar\omega_E}\left(u_0\rho_{A,\mathbf{q},\sigma,n} + v(q)\rho_{B,\mathbf{q},\sigma,n}\right)\right] \\
&\times \left[\phi_{A,\mathbf{q},n} + \frac{1}{\sqrt{\hbar\beta}} \frac{1}{-i\hat{\omega}_n + \hbar\omega_E}\left(u_0\rho_{A,-\mathbf{q},\sigma',-n} + v(-q)\rho_{B,-\mathbf{q},\sigma',-n}\right)\right] \\
&- \frac{1}{\hbar\beta} \sum_{\mathbf{q},\sigma,\sigma',n} \frac{1}{-i\hat{\omega}_n + \hbar\omega_E}\left(u_0\rho_{A,\mathbf{q},\sigma,n} + v(q)\rho_{B,\mathbf{q},\sigma,n}\right)\left(u_0\rho_{A,-\mathbf{q},\sigma',-n} + v(-q)\rho_{B,-\mathbf{q},\sigma',-n}\right) \\
&+ \sum_{\mathbf{q},\sigma,\sigma',n} \left(-i\hat{\omega}_n + \hbar\omega_E\right)\left[\phi_{B,\mathbf{q},n}^\dagger + \frac{1}{\sqrt{\hbar\beta}} \frac{1}{-i\hat{\omega}_n + \hbar\omega_E}\left(u_0\rho_{B,\mathbf{q},\sigma,n} + v(q)\rho_{A,\mathbf{q},\sigma,n}\right)\right] \\
&\times \left[\phi_{B,\mathbf{q},n} + \frac{1}{\sqrt{\hbar\beta}} \frac{1}{-i\hat{\omega}_n + \hbar\omega_E}\left(u_0\rho_{B,-\mathbf{q},\sigma',-n} + v(-q)\rho_{A,-\mathbf{q},\sigma',-n}\right)\right] \\
&\left.\left.- \frac{1}{\hbar\beta} \sum_{\mathbf{q},\sigma,\sigma',n} \frac{1}{-i\hat{\omega}_n + \hbar\omega_E}\left(u_0\rho_{B,\mathbf{q},\sigma,n} + v(q)\rho_{A,\mathbf{q},\sigma,n}\right)\left(u_0\rho_{B,-\mathbf{q},\sigma',-n} + v(-q)\rho_{A,-\mathbf{q},\sigma',-n}\right)\right)\right\} \\
&= \int \mathcal{D}\left[\psi_A^\dagger, \psi_A\right] \int \mathcal{D}\left[\psi_B^\dagger, \psi_B\right] \exp\left[-\frac{1}{\hbar\beta}\left(S_{\mathrm{el}}\left[\psi_A^\dagger, \psi_A, \psi_B^\dagger, \psi_B\right]\right.\right. \\
&- \frac{1}{\hbar\beta} \sum_{\mathbf{q},\sigma,\sigma',n} \frac{1}{-i\hat{\omega}_n + \hbar\omega_E}\left(u_0\rho_{A,\mathbf{q},\sigma,n} + v(q)\rho_{B,\mathbf{q},\sigma,n}\right)\left(u_0\rho_{A,-\mathbf{q},\sigma',-n} + v(-q)\rho_{B,-\mathbf{q},\sigma',-n}\right) \\
&\left.\left.- \frac{1}{\hbar\beta} \sum_{\mathbf{q},\sigma,\sigma',n} \frac{1}{-i\hat{\omega}_n + \hbar\omega_E}\left(u_0\rho_{B,\mathbf{q},\sigma,n} + v(q)\rho_{A,\mathbf{q},\sigma,n}\right)\left(u_0\rho_{B,-\mathbf{q},\sigma',-n} + v(-q)\rho_{A,-\mathbf{q},\sigma',-n}\right)\right)\right].
\end{aligned}
$$

This leads to

$$
\begin{aligned}
S_{\mathrm{eff}}\left[\psi_A^\dagger, \psi_A, \psi_B^\dagger, \psi_B\right] &= S_{\mathrm{el}}\left[\psi_A^\dagger, \psi_A, \psi_B^\dagger, \psi_B\right] \\
&- \frac{1}{\hbar\beta} \sum_{\mathbf{q},\sigma,\sigma',n} \frac{1}{-i\hat{\omega}_n + \hbar\omega_E}\left(u_0\rho_{A,\mathbf{q},\sigma,n} + v(q)\rho_{B,\mathbf{q},\sigma,n}\right)\left(u_0\rho_{A,-\mathbf{q},\sigma',-n} + v(-q)\rho_{B,-\mathbf{q},\sigma',-n}\right) \\
&- \frac{1}{\hbar\beta} \sum_{\mathbf{q},\sigma,\sigma',n} \frac{1}{-i\hat{\omega}_n + \hbar\omega_E}\left(u_0\rho_{B,\mathbf{q},\sigma,n} + v(q)\rho_{A,\mathbf{q},\sigma,n}\right)\left(u_0\rho_{B,-\mathbf{q},\sigma',-n} + v(-q)\rho_{A,-\mathbf{q},\sigma',-n}\right).
\end{aligned}
$$

6.3.2 Deriving the Hubbard Action

Replacing the operators in Eq. (4.15) by fields leads to the following

$$S_{\mathrm{Hub},U,V}\left[\psi_A^\dagger,\psi_A,\psi_B^\dagger,\psi_B\right]=\frac{U}{N}\int_0^{\hbar\beta}\mathrm{d}\tau\sum_{\mathbf{k},\mathbf{k}',\mathbf{q}}\psi^\dagger_{A,\mathbf{k}-\mathbf{q},\uparrow}(\tau)\,\psi^\dagger_{A,\mathbf{k}'+\mathbf{q},\downarrow}(\tau)\,\psi_{A,\mathbf{k}',\downarrow}(\tau)\,\psi_{A,\mathbf{k},\uparrow}(\tau)+A\to B$$
$$+\frac{V}{N}\int_0^{\hbar\beta}\mathrm{d}\tau\sum_{\mathbf{k},\mathbf{k}',\mathbf{q}}\sum_{\sigma,\sigma'}\gamma_{\mathbf{q}}\psi^\dagger_{A,\mathbf{k}+\mathbf{q},\sigma}(\tau)\,\psi_{A,\mathbf{k},\sigma}(\tau)\,\psi^\dagger_{B,\mathbf{k}'-\mathbf{q},\sigma'}(\tau)\,\psi^\dagger_{B,\mathbf{k}',\sigma'}(\tau).$$

Expanding in terms of the Matsubara frequencies ω_n yields the following for the Hubbard U action for the electrons on sublattice A

$$\begin{aligned}
&S_U\left[\psi_A^\dagger,\psi_A\right]\\
&=\frac{1}{(\hbar\beta)^2}\frac{U}{N}\int_0^{\hbar\beta}\mathrm{d}\tau\sum_{\mathbf{k},\mathbf{k}',\mathbf{q}}\sum_{n,n',n'',n'''}\mathrm{e}^{i(\omega_n+\omega_{n'}-\omega_{n''}-\omega_{n'''})\tau}\left[\psi^\dagger_{A,\mathbf{k}-\mathbf{q},\uparrow,n}\psi^\dagger_{A,\mathbf{k}'+\mathbf{q},\downarrow,n'}psi_{A,\mathbf{k}',\downarrow,n''}\psi_{A,\mathbf{k},\uparrow,n'''}\right]\\
&=\frac{2\pi}{(\hbar\beta)^2}\frac{U}{N}\sum_{\mathbf{k},\mathbf{k}',\mathbf{q}}\sum_{n,n',n'',n'''}\delta\left(\omega_n+\omega_{n'}-\omega_{n''}-\omega_{n'''}\right)[...]\\
&=\frac{2\pi}{(\hbar\beta)^2}\frac{U}{N}\sum_{\mathbf{k},\mathbf{k}',\mathbf{q}}\sum_{n,n',n'',n'''}\delta\left(\frac{(2n+1)\,\pi}{\hbar\beta}+\frac{(2n'+1)\,\pi}{\hbar\beta}-\frac{(2n''+1)\,\pi}{\hbar\beta}-\frac{(2n'''+1)\,\pi}{\hbar\beta}\right)[...]\\
&=\frac{2\pi}{(\hbar\beta)^2}\frac{1}{\frac{2\pi}{\hbar\beta}}\frac{U}{N}\sum_{\mathbf{k},\mathbf{k}',\mathbf{q}}\sum_{n,n',n'',n'''}\delta\left(n+n'-n''-n'''\right)[...]\\
&=\frac{1}{\hbar\beta}\frac{U}{N}\sum_{\mathbf{k},\mathbf{k}',\mathbf{q}}\sum_{n,m,m'}\psi^\dagger_{A,\mathbf{k}-\mathbf{q},\uparrow,m-n}\psi^\dagger_{A,\mathbf{k}'+\mathbf{q},\downarrow,m'+n}\psi_{A,\mathbf{k}',\downarrow,m'}\psi_{A,\mathbf{k},\uparrow,m}=\frac{1}{\hbar\beta}\frac{U}{N}\sum_{\mathbf{q},n}\rho_{A,\mathbf{q},\downarrow,n}\rho_{A,-\mathbf{q},\uparrow,-n},
\end{aligned}$$

where the density of electrons $\rho_{A,\mathbf{q},\sigma,n}$ is defined in Eq. (4.11). The action for the Hubbard U on sublattice B can be found by applying $A\to B$. Replacing the operators by fields for the Hubbard V term leads to the following action Lastly, $S_V\left[\psi_A^\dagger,\psi_A,\psi_B^\dagger,\psi_B\right]$ yields

$$\begin{aligned}
&S_V\left[\psi_A^\dagger,\psi_A,\psi_B^\dagger,\psi_B\right]\\
&=\frac{1}{(\hbar\beta)^2}\frac{V}{N}\int_0^{\hbar\beta}\mathrm{d}\tau\sum_{\mathbf{k},\mathbf{k}',\mathbf{q}}\sum_{\sigma,\sigma'}\sum_{n,n',n'',n'''}\mathrm{e}^{i(\omega_n-\omega_{n'}+\omega_{n''}-\omega_{n'''})\tau}\left[\gamma_{\mathbf{q}}\psi^\dagger_{A,\mathbf{k}+\mathbf{q},\sigma,n}\psi_{A,\mathbf{k},\sigma,n'}\psi^\dagger_{B,\mathbf{k}'-\mathbf{q},\sigma',n''}\psi^\dagger_{B,\mathbf{k}',\sigma',n'''}\right]\\
&=\frac{2\pi}{(\hbar\beta)^2}\frac{V}{N}\sum_{\mathbf{k},\mathbf{k}',\mathbf{q}}\sum_{\sigma,\sigma'}\sum_{n,n',n'',n'''}\delta\left(\omega_n-\omega_{n'}+\omega_{n''}-\omega_{n'''}\right)[...]\\
&=\frac{2\pi}{(\hbar\beta)^2}\frac{1}{\frac{2\pi}{\hbar\beta}}\frac{V}{N}\sum_{\mathbf{k},\mathbf{k}',\mathbf{q}}\sum_{\sigma,\sigma'}\sum_{n,n',n'',n'''}\delta\left(n-n'+n''-n'''\right)[...]\\
&=\frac{1}{\hbar\beta}\frac{V}{N}\sum_{\mathbf{k},\mathbf{k}',\mathbf{q}}\sum_{\sigma,\sigma'}\sum_{n,m,m'}\gamma_{\mathbf{q}}\psi^\dagger_{A,\mathbf{k}+\mathbf{q},\sigma,m+n}\psi_{A,\mathbf{k},\sigma,m}\psi^\dagger_{B,\mathbf{k}'-\mathbf{q},\sigma',m'-n}\psi^\dagger_{B,\mathbf{k}',\sigma',m'}\\
&=\frac{1}{\hbar\beta}\frac{V}{N}\sum_{\mathbf{q},\sigma,\sigma',n}\gamma_{\mathbf{q}}\rho_{A,\mathbf{q},\sigma,n}\rho_{B,-\mathbf{q},\sigma',-n}.
\end{aligned}$$

6.3.3 Solving the Zero-Temperature Gap Equation for the Kekule Order

The zero-temperature gap equation for the Kekule order yields the following

$$\begin{aligned}
1 &= \frac{\tilde{V}}{3}\sum_{s=\pm}\int\frac{\mathrm{d}\mathbf{q}}{(2\pi)^2}\frac{1}{\sqrt{\left(v_F|q|+s\mu\right)^2+\tilde{V}^2m^2(0)}} \\
&= \frac{\tilde{V}}{3}\sum_{s=\pm}\int_0^{2\pi}\mathrm{d}\theta\int_0^{\Lambda}\frac{\mathrm{d}q}{(2\pi)^2}\frac{q}{\sqrt{\left(v_F|q|+s\mu\right)^2+\tilde{V}^2m^2(0)}} \\
&= \frac{\tilde{V}}{6\pi v_F}\sum_{s=\pm}\int_0^{\Lambda}\mathrm{d}q\frac{v_Fq+s\mu-s\mu}{\sqrt{\left(v_F|q|+s\mu\right)^2+\tilde{V}^2m^2(0)}} \\
&= \frac{\tilde{V}}{6\pi v_F}\sum_{s=\pm}\int_0^{\Lambda}\mathrm{d}q\left(\frac{v_Fq+s\mu}{\sqrt{\left(v_F|q|+s\mu\right)^2+\tilde{V}^2m^2(0)}}-\frac{s\mu}{\sqrt{\left(v_F|q|+s\mu\right)^2+\tilde{V}^2m^2(0)}}\right) \\
&= \frac{\tilde{V}}{6\pi v_F}\left[I_m+II_m\right],
\end{aligned}$$

where

$$\begin{aligned}
I_m &= \sum_{s=\pm}\int_0^{\Lambda}\mathrm{d}q\frac{v_Fq+s\mu}{\sqrt{\left(v_F|q|+s\mu\right)^2+\tilde{V}^2m^2(0)}}, \\
II_m &= -\sum_{s=\pm}\int_0^{\Lambda}\mathrm{d}q\frac{s\mu}{\sqrt{\left(v_F|q|+s\mu\right)^2+\tilde{V}^2m^2(0)}}.
\end{aligned}$$

I_m can be solved by substituting $u=v_Fq+s\mu$ such that

$$\begin{aligned}
I_m &= \sum_{s=\pm}\int_{s\mu}^{v_F\Lambda}\frac{\mathrm{d}u}{v_F}\frac{u}{\sqrt{u^2+\tilde{V}^2m^2(0)}}=\frac{1}{v_F}\sum_{s=\pm}\left[\sqrt{u^2+\tilde{V}^2m^2(0)}\right]_{s\mu}^{v_F\Lambda} \\
&= \frac{1}{v_F}\sum_{s=\pm}\left(v_F\Lambda-\sqrt{\mu^2+\tilde{V}^2m^2(0)}\right)=\frac{2}{v_F}\left(v_F\Lambda-\sqrt{\mu^2+\tilde{V}^2m^2(0)}\right),
\end{aligned}$$

where it is used that $\Lambda \gg m(0)$. To solve II_m, the substitution $u = (v_F q + s\mu)/\tilde{V}m(0)$ is used

$$\begin{aligned}
II_m &= -\sum_{s=\pm}\frac{s\mu}{v_F}\int_{\frac{s\mu}{\tilde{V}m(0)}}^{\frac{v_F\Lambda}{\tilde{V}m(0)}} \mathrm{d}u \frac{\tilde{V}m(0)}{\tilde{V}m(0)\sqrt{u^2+1}} = -\sum_{s=\pm}\frac{s\mu}{v_F}\left[\ln\left|u+\sqrt{u^2+1}\right|\right]_{\frac{s\mu}{\tilde{V}m(0)}}^{\frac{v_F\Lambda}{\tilde{V}m(0)}} \\
&= -\sum_{s=\pm}\frac{s\mu}{v_F}\left[\ln\left|\frac{v_F\Lambda}{\tilde{V}m(0)}+\sqrt{\left(\frac{v_F\Lambda}{\tilde{V}m(0)}\right)^2+1}\right| - \ln\left|\frac{s\mu}{\tilde{V}m(0)}+\sqrt{\left(\frac{s\mu}{\tilde{V}m(0)}\right)^2+1}\right|\right] \\
&= -\sum_{s=\pm}\frac{s\mu}{v_F}\left[\ln\left|\frac{v_F\Lambda}{\tilde{V}m(0)}+\frac{1}{\tilde{V}m(0)}\sqrt{v_F^2\Lambda^2+\tilde{V}^2m^2(0)}\right| - \ln\left|\frac{s\mu}{\tilde{V}m(0)}+\frac{1}{\tilde{V}m(0)}\sqrt{\mu^2+\tilde{V}^2m^2(0)}\right|\right] \\
&= -\frac{\mu}{v_F}\left[\ln\left|v_F\Lambda+\sqrt{v_F^2\Lambda^2+\tilde{V}^2m^2(0)}\right| - \ln\left|\mu+\sqrt{\mu^2+\tilde{V}^2m^2(0)}\right|\right] \\
&\quad +\frac{\mu}{v_F}\left[\ln\left|v_F\Lambda+\sqrt{v_F^2\Lambda^2+\tilde{V}^2m^2(0)}\right| - \ln\left|-\mu+\sqrt{\mu^2+\tilde{V}^2m^2(0)}\right|\right] \\
&= \frac{\mu}{v_F}\ln\left[\frac{\mu+\sqrt{\mu^2+\tilde{V}^2m^2(0)}}{-\mu+\sqrt{\mu^2+\tilde{V}^2m^2(0)}}\right].
\end{aligned}$$

Therefore, the following result is obtained

$$1 = \frac{\tilde{V}}{6\pi v_F^2}\left[2\left(v_F\Lambda-\sqrt{\mu^2+\tilde{V}^2m^2(0)}\right)+\mu\ln\left(\frac{\mu+\sqrt{\mu^2+\tilde{V}^2m^2(0)}}{-\mu+\sqrt{\mu^2+\tilde{V}^2m^2(0)}}\right)\right],$$

which corresponds to the result in Ref. [40].

6.3.4 Strong-Coupling Limit in Natural Logarithm

The following limit has to be solved

$$\ln\left(\frac{\sqrt{1+x^2}+1}{\sqrt{1+x^2}-1}\right)\bigg|_{x\to\infty}.$$

To be able to take the limit, the natural logarithm is rewritten according to

$$\ln\left(\frac{\sqrt{1+x^2}+1}{\sqrt{1+x^2}-1}\right) = \ln\left(\frac{\sqrt{\frac{1}{x^2}+1}+\frac{1}{x}}{\sqrt{\frac{1}{x^2}+1}-\frac{1}{x}}\right) \equiv \ln\left(\frac{\sqrt{y^2+1}+y}{\sqrt{y^2+1}-y}\right),$$

where $y \equiv 1/x$ such that in the limit $x \to \infty$, $y \to 0$. This leads to

$$\ln\left(\frac{\sqrt{y^2+1}+y}{\sqrt{y^2+1}-y}\right) \xrightarrow{y\to 0} \ln\left(\frac{\sqrt{y^2+1}+y}{\sqrt{y^2+1}-y}\right)\bigg|_{y\to0} + y\left[\frac{\mathrm{d}}{\mathrm{d}y}\ln\left(\frac{\sqrt{y^2+1}+y}{\sqrt{y^2+1}-y}\right)\right]\bigg|_{y\to0}.$$

The first term is clearly zero, i.e.

$$\ln\left(\frac{\sqrt{y^2+1}+y}{\sqrt{y^2+1}-y}\right)\bigg|_{y\to0} = \ln\left(\frac{1}{1}\right) = 0.$$

The derivative in the second term yields

$$\begin{aligned}
&\frac{\mathrm{d}}{\mathrm{d}y}\ln\left(\frac{\sqrt{y^2+1}+y}{\sqrt{y^2+1}-y}\right) = \frac{\sqrt{y^2+1}-y}{\sqrt{y^2+1}+y}\frac{\mathrm{d}}{\mathrm{d}y}\left(\frac{\sqrt{y^2+1}+y}{\sqrt{y^2+1}-y}\right)\\
&= \frac{\sqrt{y^2+1}-y}{\sqrt{y^2+1}+y}\frac{1}{\left(\sqrt{y^2+1}-y\right)^2}\left[\left(\frac{y}{\sqrt{y^2+1}}+1\right)\left(\sqrt{y^2+1}-y\right)\right.\\
&\left.-\left(\sqrt{y^2+1}+y\right)\left(\frac{y}{\sqrt{y^2+1}}-1\right)\right]\\
&= \frac{1}{\left(\sqrt{y^2+1}+y\right)\left(\sqrt{y^2+1}-y\right)}\left[y+\sqrt{y^2+1}-\frac{y^2}{\sqrt{y^2+1}}-y-y+\sqrt{y^2+1}-\frac{y^2}{\sqrt{y^2+1}}+y\right]\\
&= \frac{1}{y^2+1-y^2}\left(2\sqrt{y^2+1}-\frac{2y^2}{\sqrt{y^2+1}}\right) = 2\left(\frac{y^2+1-y^2}{\sqrt{y^2+1}}\right) = \frac{2}{\sqrt{y^2+1}},
\end{aligned}$$

such that the following is obtained

$$\ln\left(\frac{\sqrt{y^2+1}+y}{\sqrt{y^2+1}-y}\right) \xrightarrow{y\to 0} = y\left.\frac{2}{\sqrt{y^2+1}}\right|_{y\to 0} = 2y = \frac{2}{x}.$$

Therefore, the result is

$$\ln\left(\frac{\sqrt{1+x^2}+1}{\sqrt{1+x^2}-1}\right)\Bigg|_{x\to\infty} = \frac{2}{x}. \tag{6.63}$$

6.3.5 Solving the Zero-Temperature Gap Equation for the Kekule Order

To be able to solve the zero-temperature gap equation for the hidden order, the denominator is rewritten according to

$$\begin{aligned}
&(v_F|q|+s\mu)^2 + v_F^2|q|^2\frac{\tilde{V}^2\left|\Delta'(0)\right|^2}{t^2} = v_F^2|q|^2\left(1+\frac{\tilde{V}^2\left|\Delta'(0)\right|^2}{t^2}\right) + 2s\,\mu\,v_F|q| + \mu^2\\
&= v_F^2\left(1+\frac{\tilde{V}^2\left|\Delta'(0)\right|^2}{t^2}\right)\left[|q|^2 + \frac{2s\,\mu}{v_F\left(1+\frac{\tilde{V}^2|\Delta'(0)|^2}{t^2}\right)}|q| + \frac{\mu^2}{v_F^2\left(1+\frac{\tilde{V}^2|\Delta'(0)|^2}{t^2}\right)}\right]\\
&= v_F^2\left(1+\frac{\tilde{V}^2\left|\Delta'(0)\right|^2}{t^2}\right)\left\{\left[|q| + \frac{s\,\mu}{v_F\left(1+\frac{\tilde{V}^2|\Delta'(0)|^2}{t^2}\right)}\right]^2 + \frac{\mu^2}{v_F^2\left(1+\frac{\tilde{V}^2|\Delta'(0)|^2}{t^2}\right)} - \frac{\mu^2}{v_F^2\left(1+\frac{\tilde{V}^2|\Delta'(0)|^2}{t^2}\right)^2}\right\}\\
&= v_F^2\delta\left[\left(|q|+\frac{s\,\mu}{v_F\delta}\right)^2 + \frac{\mu^2}{v_F^2\delta} - \frac{\mu^2}{v_F^2\delta^2}\right],
\end{aligned}$$

where $1+\frac{\tilde{V}^2|\Delta'(0)|^2}{t^2}\equiv\delta$. This yields the following for Eq. (4.58)

$$\begin{aligned}1 &= \frac{\tilde{V}}{6}\frac{v_F^2}{t^2}\sum_{s=\pm}\int\frac{\mathrm{d}\mathbf{q}}{(2\pi)^2}\frac{q^2}{\sqrt{v_F^2\delta\left[\left(|q|+\frac{s\,\mu}{v_F\delta}\right)^2+\frac{\mu^2}{v_F^2\delta}-\frac{\mu^2}{v_F^2\delta^2}\right]}}\\ &= \frac{\tilde{V}}{6}\frac{v_F^2}{t^2}\frac{1}{v_F\sqrt{\delta}}\sum_{s=\pm}\int_0^{2\pi}\mathrm{d}\theta\int_0^{\Lambda}\frac{\mathrm{d}q}{(2\pi)^2}\frac{q^3}{\sqrt{\left(|q|+\frac{s\,\mu}{v_F\delta}\right)^2+\frac{\mu^2}{v_F^2\delta}-\frac{\mu^2}{v_F^2\delta^2}}}.\end{aligned}$$

Substituting with $u=|q|+\frac{s\,\mu}{v_F\delta}$ leads to

$$1=\frac{\tilde{V}}{6}\frac{v_F}{t^2\sqrt{\delta}}\frac{1}{2\pi}\sum_{s=\pm}\int_{\frac{s\mu}{v_F\delta}}^{\Lambda}\mathrm{d}u\frac{\left(u-\frac{s\mu}{v_F\delta}\right)^3}{\sqrt{u^2+\frac{\mu^2}{v_F^2}\left(\frac{1}{\delta}-\frac{1}{\delta^2}\right)}}.$$

Expanding $\left(u-\frac{s\mu}{v_F\delta}\right)^3$ yields

$$\left(u-\frac{s\mu}{v_F\delta}\right)^3=\left(u^2+\frac{\mu^2}{v_F^2\delta^2}-2\frac{s\mu}{v_F\delta}u\right)\left(u-\frac{s\mu}{v_F\delta}\right)=u^3-3\frac{s\mu}{v_F\delta}u^2+3\frac{\mu^2}{v_F^2\delta^2}u-\frac{s\mu^3}{v_F^3\delta^3},$$

such that

$$\begin{aligned}1 &= \frac{\tilde{V}}{6}\frac{v_F}{t^2\sqrt{\delta}}\frac{1}{2\pi}\sum_{s=\pm}\int_{\frac{s\mu}{v_F\delta}}^{\Lambda}\mathrm{d}u\frac{\left(u^3+3\frac{\mu^2}{v_F^2\delta^2}u\right)-\frac{s\mu}{v_F\delta}\left(3u^2+\frac{\mu^2}{v_F^2\delta^2}\right)}{\sqrt{u^2+\frac{\mu^2}{v_F^2}\left(\frac{1}{\delta}-\frac{1}{\delta^2}\right)}}\\ &= \frac{\tilde{V}}{6}\frac{v_F}{t^2\sqrt{\delta}}\frac{1}{2\pi}\left[I_{\Delta'}+II_{\Delta'}\right],\end{aligned}$$

where

$$\begin{aligned}I_{\Delta'} &= \sum_{s=\pm}\int_{\frac{s\mu}{v_F\delta}}^{\Lambda}\mathrm{d}u\frac{u^3+3\frac{\mu^2}{v_F^2\delta^2}u}{\sqrt{u^2+\frac{\mu^2}{v_F^2}\left(\frac{1}{\delta}-\frac{1}{\delta^2}\right)}},\\ II_{\Delta'} &= -\sum_{s=\pm}\int_{\frac{s\mu}{v_F\delta}}^{\Lambda}\mathrm{d}u\frac{s\mu}{v_F\delta}\frac{3u^2+\frac{\mu^2}{v_F^2\delta^2}}{\sqrt{u^2+\frac{\mu^2}{v_F^2}\left(\frac{1}{\delta}-\frac{1}{\delta^2}\right)}}.\end{aligned}$$

Solving $I_{\Delta'}$ leads to

$$I_{\Delta'}=\int_{\frac{\mu}{v_F\delta}}^{\Lambda}\mathrm{d}u\frac{u^3+3\frac{\mu^2}{v_F^2\delta^2}u}{\sqrt{u^2+\frac{\mu^2}{v_F^2}\left(\frac{1}{\delta}-\frac{1}{\delta^2}\right)}}+\int_{-\frac{\mu}{v_F\delta}}^{\Lambda}\mathrm{d}u\frac{u^3+3\frac{\mu^2}{v_F^2\delta^2}u}{\sqrt{u^2+\frac{\mu^2}{v_F^2}\left(\frac{1}{\delta}-\frac{1}{\delta^2}\right)}}.$$

Writing

$$\int_{-\frac{\mu}{v_F\delta}}^{\Lambda}\mathrm{d}u=\int_{-\frac{\mu}{v_F\delta}}^{\frac{\mu}{v_F\delta}}\mathrm{d}u+\int_{\frac{\mu}{v_F\delta}}^{\Lambda}\mathrm{d}u,$$

leads to

$$I_{\Delta'} = 2\int_{\frac{\mu}{v_F\delta}}^{\Lambda} \mathrm{d}u \frac{u^3 + 3\frac{\mu^2}{v_F^2\delta^2}u}{\sqrt{u^2 + \frac{\mu^2}{v_F^2}\left(\frac{1}{\delta} - \frac{1}{\delta^2}\right)}} + \int_{-\frac{\mu}{v_F\delta}}^{\frac{\mu}{v_F\delta}} \mathrm{d}u \frac{u^3 + 3\frac{\mu^2}{v_F^2\delta^2}u}{\sqrt{u^2 + \frac{\mu^2}{v_F^2}\left(\frac{1}{\delta} - \frac{1}{\delta^2}\right)}}.$$

The second integral equals zero because an odd function is integrated over a symmetric limit. Therefore,

$$I_{\Delta'} = 2\int_{\frac{\mu}{v_F\delta}}^{\Lambda} \mathrm{d}u \frac{u^3 + 3\frac{\mu^2}{v_F^2\delta^2}u}{\sqrt{u^2 + \frac{\mu^2}{v_F^2}\left(\frac{1}{\delta} - \frac{1}{\delta^2}\right)}} = I_{\Delta'}^{(1)} + I_{\Delta'}^{(2)},$$

where

$$\begin{aligned} I_{\Delta'}^{(1)} &= 2\int_{\frac{\mu}{v_F\delta}}^{\Lambda} \mathrm{d}u \frac{u^3}{\sqrt{u^2 + \frac{\mu^2}{v_F^2}\left(\frac{1}{\delta} - \frac{1}{\delta^2}\right)}}, \\ I_{\Delta'}^{(2)} &= \frac{6\mu^2}{v_F^2\delta^2}\int_{\frac{\mu}{v_F\delta}}^{\Lambda} \mathrm{d}u \frac{u}{\sqrt{u^2 + \frac{\mu^2}{v_F^2}\left(\frac{1}{\delta} - \frac{1}{\delta^2}\right)}}. \end{aligned}$$

$I_{\Delta'}^{(1)}$ is solved using the substitution $v = \sqrt{u^2 + \frac{\mu^2}{v_F^2}\left(\frac{1}{\delta} - \frac{1}{\delta^2}\right)}$. This leads to

$$\begin{aligned} I_{\Delta'}^{(1)} &= 2\int_{\frac{\mu}{v_F\sqrt{\delta}}}^{\Lambda} \mathrm{d}v\, v \frac{v^2 - \frac{\mu^2}{v_F^2}\left(\frac{1}{\delta} - \frac{1}{\delta^2}\right)}{v} = 2\int_{\frac{\mu}{v_F\sqrt{\delta}}}^{\Lambda} \mathrm{d}v \left[v^2 - \frac{\mu^2}{v_F^2}\left(\frac{1}{\delta} - \frac{1}{\delta^2}\right)\right] \\ &= 2\left[\frac{1}{3}v^3 - \frac{\mu^2}{v_F^2}\left(\frac{1}{\delta} - \frac{1}{\delta^2}\right)v\right]_{\frac{\mu}{v_F\sqrt{\delta}}}^{\Lambda} \\ &= \frac{2}{3}\Lambda^3 - 2\frac{\mu^2(\delta-1)}{v_F^2\delta^2}\Lambda + \frac{4}{3}\frac{\mu^3}{v_F^3\delta\sqrt{\delta}} - 2\frac{\mu^3}{v_F^3\delta^2\sqrt{\delta}}. \end{aligned}$$

Solving $I_{\Delta'}^{(2)}$ leads to

$$\begin{aligned} I_{\Delta'}^{(2)} &= \frac{6\mu^2}{v_F^2\delta^2}\left[\sqrt{u^2 + \frac{\mu^2}{v_F^2}\left(\frac{1}{\delta} - \frac{1}{\delta^2}\right)}\right]_{\frac{\mu}{v_F\delta}}^{\Lambda} = \frac{6\mu^2}{v_F^2\delta^2}\left[\Lambda - \sqrt{\frac{\mu^2}{v_F^2\delta^2} + \frac{\mu^2}{v_F^2}\left(\frac{1}{\delta} - \frac{1}{\delta^2}\right)}\right] \\ &= \frac{6\mu^2}{v_F^2\delta^2}\left(\Lambda - \frac{\mu}{v_F\sqrt{\delta}}\right) = \frac{6\mu^2}{v_F^2\delta^2}\Lambda - \frac{6\mu^3}{v_F^3\delta^2\sqrt{\delta}}. \end{aligned}$$

Therefore,

$$\begin{aligned} I_{\Delta'} &= \frac{2}{3}\Lambda^3 - 2\frac{\mu^2(\delta-1)}{v_F^2\delta^2}\Lambda + \frac{4}{3}\frac{\mu^3}{v_F^3\delta\sqrt{\delta}} - 2\frac{\mu^3}{v_F^3\delta^2\sqrt{\delta}} + \frac{6\mu^2}{v_F^2\delta^2}\Lambda - \frac{6\mu^3}{v_F^3\delta^2\sqrt{\delta}} \\ &= \frac{2}{3}\Lambda^3 - \frac{2\mu^2}{v_F^2\delta}\Lambda + \frac{8\mu^2}{v_F^2\delta^2}\Lambda + \frac{4}{3}\frac{\mu^3}{v_F^3\delta\sqrt{\delta}} - \frac{8\mu^3}{v_F^3\delta^2\sqrt{\delta}} \\ &= \frac{2}{3}\Lambda^3 - \frac{2\mu^2(\delta-4)}{v_F^2\delta^2}\Lambda + \frac{4\mu^3(\delta-6)}{3v_F^3\delta^2\sqrt{\delta}}. \end{aligned}$$

Solving $II_{\Delta'}$ leads to

$$\begin{aligned}
II_{\Delta'} &= -\int_{\frac{\mu}{v_F\delta}}^{\Lambda} \mathrm{d}u \frac{\mu}{v_F\delta} \frac{3u^2+\frac{\mu^2}{v_F^2\delta^2}}{\sqrt{u^2+\frac{\mu^2}{v_F^2}\left(\frac{1}{\delta}-\frac{1}{\delta^2}\right)}} + \int_{-\frac{\mu}{v_F\delta}}^{\Lambda} \mathrm{d}u \frac{\mu}{v_F\delta} \frac{3u^2+\frac{\mu^2}{v_F^2\delta^2}}{\sqrt{u^2+\frac{\mu^2}{v_F^2}\left(\frac{1}{\delta}-\frac{1}{\delta^2}\right)}} \\
&= \int_{\Lambda}^{\frac{\mu}{v_F\delta}} \mathrm{d}u \frac{\mu}{v_F\delta} \frac{3u^2+\frac{\mu^2}{v_F^2\delta^2}}{\sqrt{u^2+\frac{\mu^2}{v_F^2}\left(\frac{1}{\delta}-\frac{1}{\delta^2}\right)}} + \int_{-\frac{\mu}{v_F\delta}}^{\Lambda} \mathrm{d}u \frac{\mu}{v_F\delta} \frac{3u^2+\frac{\mu^2}{v_F^2\delta^2}}{\sqrt{u^2+\frac{\mu^2}{v_F^2}\left(\frac{1}{\delta}-\frac{1}{\delta^2}\right)}} \\
&= \int_{-\frac{\mu}{v_F\delta}}^{\frac{\mu}{v_F\delta}} \mathrm{d}u \frac{\mu}{v_F\delta} \frac{3u^2+\frac{\mu^2}{v_F^2\delta^2}}{\sqrt{u^2+\frac{\mu^2}{v_F^2}\left(\frac{1}{\delta}-\frac{1}{\delta^2}\right)}}.
\end{aligned}$$

Realizing that the integrant is an even function finally leads to

$$II_{\Delta'} = 2\int_0^{\frac{\mu}{v_F\delta}} \mathrm{d}u \frac{\mu}{v_F\delta} \frac{3u^2+\frac{\mu^2}{v_F^2\delta^2}}{\sqrt{u^2+\frac{\mu^2}{v_F^2}\left(\frac{1}{\delta}-\frac{1}{\delta^2}\right)}} = II_{\Delta'}^{(1)} + II_{\Delta'}^{(2)},$$

where

$$II_{\Delta'}^{(1)} = \frac{6\mu}{v_F\delta}\int_0^{\frac{\mu}{v_F\delta}} \mathrm{d}u \frac{u^2}{\sqrt{u^2+\frac{\mu^2}{v_F^2}\left(\frac{1}{\delta}-\frac{1}{\delta^2}\right)}}, \qquad II_{\Delta'}^{(2)} = \frac{2\mu^3}{v_F^3\delta^3}\int_0^{\frac{\mu}{v_F\delta}} \mathrm{d}u \frac{1}{\sqrt{u^2+\frac{\mu^2}{v_F^2}\left(\frac{1}{\delta}-\frac{1}{\delta^2}\right)}}.$$

$II_{\Delta'}^{(1)}$ is solved using the substitution $u = \frac{\mu}{v_F}\sqrt{\frac{1}{\delta}-\frac{1}{\delta^2}}\sinh(v)$. This leads to

$$\begin{aligned}
II_{\Delta'}^{(1)} &= \frac{6\mu}{v_F\delta}\int_0^{\sinh^{-1}\left(\sqrt{\delta-1}^{-1}\right)} \mathrm{d}v \frac{\mu}{v_F}\sqrt{\frac{1}{\delta}-\frac{1}{\delta^2}}\cosh(v) \frac{\frac{\mu^2}{v_F^2}\left(\frac{1}{\delta}-\frac{1}{\delta^2}\right)\sinh^2(v)}{\frac{\mu}{v_F}\sqrt{\frac{1}{\delta}-\frac{1}{\delta^2}}\sqrt{\sinh^2(v)+1}} \\
&= \frac{6\mu^3}{v_F^3\delta}\left(\frac{1}{\delta}-\frac{1}{\delta^2}\right)\int_0^{\sinh^{-1}\left(\sqrt{\delta-1}^{-1}\right)} \mathrm{d}v \frac{\cosh(v)\sinh^2(v)}{\cosh(v)} \\
&= \frac{6\mu^3}{v_F^3\delta}\left(\frac{\delta}{\delta^2}-\frac{1}{\delta^2}\right)\int_0^{\sinh^{-1}\left(\sqrt{\delta-1}^{-1}\right)} \mathrm{d}v \sinh^2(v) = \frac{3\mu^3}{v_F^3}\frac{\delta-1}{\delta^3}\int_0^{\sinh^{-1}\left(\sqrt{\delta-1}^{-1}\right)} \mathrm{d}v\ [\cosh(2v)-1] \\
&= \frac{3\mu^3}{v_F^3}\frac{\delta-1}{\delta^3}\left[\frac{1}{2}\sinh(2v)-v\right]_0^{\sinh^{-1}\left(\sqrt{\delta-1}^{-1}\right)} = \frac{3\mu^3}{v_F^3}\frac{\delta-1}{\delta^3}\left[\sinh(v)\cosh(v)-v\right]_0^{\sinh^{-1}\left(\sqrt{\delta-1}^{-1}\right)} \\
&= \frac{3\mu^3}{v_F^3}\frac{\delta-1}{\delta^3}\left\{\frac{1}{\sqrt{\delta-1}}\cosh\left[\sinh^{-1}\left(\sqrt{\delta-1}^{-1}\right)\right]-\sinh^{-1}\left(\sqrt{\delta-1}^{-1}\right)\right\} \\
&= \frac{3\mu^3}{v_F^3}\frac{\delta-1}{\delta^3}\left[\frac{1}{\sqrt{\delta-1}}\sqrt{1+\left(\frac{1}{\sqrt{\delta-1}}\right)^2}-\ln\left(\frac{1}{\sqrt{\delta-1}}+\sqrt{\left(\frac{1}{\sqrt{\delta-1}}\right)^2+1}\right)\right] \\
&= \frac{3\mu^3}{v_F^3}\frac{\delta-1}{\delta^3}\left[\frac{1}{\sqrt{\delta-1}}\sqrt{\frac{\delta-1}{\delta-1}+\frac{1}{\delta-1}}-\ln\left(\frac{1}{\sqrt{\delta-1}}+\sqrt{\frac{1}{\delta-1}+\frac{\delta-1}{\delta-1}}\right)\right] \\
&= \frac{3\mu^3}{v_F^3}\frac{\delta-1}{\delta^3}\left[\frac{\sqrt{\delta}}{\delta-1}-\ln\left(\frac{\sqrt{\delta}+1}{\sqrt{\delta-1}}\right)\right] = \frac{3\mu^3}{v_F^3}\left[\frac{1}{\delta^2\sqrt{\delta}}-\frac{\delta-1}{\delta^3}\ln\left(\frac{\sqrt{\delta}+1}{\sqrt{\delta-1}}\right)\right].
\end{aligned}$$

$II^{(2)}_{\Delta'}$ is solved using the substitution $u = \frac{\mu}{v_F}\sqrt{\frac{1}{\delta}-\frac{1}{\delta^2}}\sinh(w)$. This leads to

$$\begin{aligned}
II^{(2)}_{\Delta'} &= \frac{2\mu^3}{v_F^3\delta^3}\int_0^{\sinh^{-1}\left(\sqrt{\delta-1}^{-1}\right)} \mathrm{d}w\, \frac{\mu}{v_F}\sqrt{\frac{1}{\delta}-\frac{1}{\delta^2}}\frac{\cosh(w)}{\frac{\mu}{v_F}\sqrt{\frac{1}{\delta}-\frac{1}{\delta^2}}\sqrt{\sinh^2(w)+1}} \\
&= \frac{2\mu^3}{v_F^3\delta^3}\int_0^{\sinh^{-1}\left(\sqrt{\delta-1}^{-1}\right)} \mathrm{d}w\frac{\cosh(w)}{\cosh(w)} = \frac{2\mu^3}{v_F^3\delta^3}\int_0^{\sinh^{-1}\left(\sqrt{\delta-1}^{-1}\right)} \mathrm{d}w \\
&= \frac{2\mu^3}{v_F^3\delta^3}\left[w\right]_0^{\sinh^{-1}\left(\sqrt{\delta-1}^{-1}\right)} = \frac{2\mu^3}{v_F^3\delta^3}\sinh^{-1}\left(\sqrt{\delta-1}^{-1}\right) \\
&= \frac{2\mu^3}{v_F^3\delta^3}\ln\left(\sqrt{\delta-1}^{-1}+\sqrt{(\delta-1)^{-1}+1}\right) = \frac{2\mu^3}{v_F^3\delta^3}\ln\left(\frac{\sqrt{\delta}+1}{\sqrt{\delta-1}}\right) \qquad (6.64)
\end{aligned}$$

Therefore,

$$\begin{aligned}
II_{\Delta'} &= \frac{3\mu^3}{v_F^3}\left[\frac{1}{\delta^2\sqrt{\delta}}-\frac{\delta-1}{\delta^3}\ln\left(\frac{\sqrt{\delta}+1}{\sqrt{\delta-1}}\right)\right]+\frac{2\mu^3}{v_F^3\delta^3}\ln\left(\frac{\sqrt{\delta}+1}{\sqrt{\delta-1}}\right) \\
&= \frac{\mu^3}{v_F^3\delta^2}\left[\frac{3}{\sqrt{\delta}}+\ln\left(\frac{\sqrt{\delta}+1}{\sqrt{\delta-1}}\right)\left(\frac{5}{\delta}-3\right)\right].
\end{aligned}$$

Therefore,

$$\begin{aligned}
1 &= \frac{\tilde{V}}{6}\frac{v_F}{t^2\sqrt{\delta}}\frac{1}{2\pi}\left[\frac{2}{3}\Lambda^3-\frac{2\mu^2(\delta-4)}{v_F^2\delta^2}\Lambda+\frac{4\mu^3(\delta-6)}{3v_F^3\delta^2\sqrt{\delta}}+\frac{3\mu^3}{v_F^3\delta^2\sqrt{\delta}}\right. \\
&\quad \left.+\frac{\mu^3}{v_F^3\delta^2}\ln\left(\frac{\sqrt{\delta}+1}{\sqrt{\delta-1}}\right)\left(\frac{5}{\delta}-3\right)\right] \\
&= \frac{\tilde{V}}{6}\frac{v_F}{t^2}\frac{1}{2\pi}\left[\frac{2\Lambda^3}{3\sqrt{\delta}}-\frac{2\mu^2(\delta-4)}{v_F^2\delta^2\sqrt{\delta}}\Lambda+\frac{\mu^3\left(\frac{4\delta}{3}-5\right)}{3v_F^3\delta^3}+\frac{\mu^3}{v_F^3\delta^2\sqrt{\delta}}\ln\left(\frac{\sqrt{\delta}+1}{\sqrt{\delta-1}}\right)\left(\frac{5}{\delta}-3\right)\right].
\end{aligned}$$

Plugging $\delta = 1+\frac{\tilde{V}^2|\Delta'(0)|^2}{t^2} \equiv 1+\alpha^2$ where $\alpha = \frac{\tilde{V}|\Delta'(0)|}{t}$, back in leads to the final result

$$\begin{aligned}
1 &= \frac{\tilde{V}}{6}\frac{v_F}{t^2}\frac{1}{2\pi}\left\{2\Lambda\left[\frac{\Lambda^2}{3\sqrt{1+\alpha^2}}+\frac{\mu^2}{v_F^2}\left(\frac{4-1-\alpha^2}{(1+\alpha^2)^{5/2}}\right)\right]\right. \\
&\quad \left.+\frac{\mu^3}{v_F^3}\left[\frac{4(1+\alpha^2)-15}{9(1+\alpha^2)^3}+\ln\left(\frac{\sqrt{1+\alpha^2}+1}{\sqrt{1+\alpha^2-1}}\right)\left(\frac{5-3(1+\alpha^2)}{(1+\alpha^2)^{7/2}}\right)\right]\right\} \\
&= \frac{\tilde{V}}{6}\frac{v_F}{t^2}\frac{1}{2\pi}\left\{2\Lambda\left[\frac{\Lambda^2}{3\sqrt{1+\alpha^2}}+\frac{\mu^2}{v_F^2}\left(\frac{3-\alpha^2}{(1+\alpha^2)^{5/2}}\right)\right]\right. \\
&\quad \left.+\frac{\mu^3}{v_F^3}\left[\frac{4\alpha^2-11}{9(1+\alpha^2)^3}+\ln\left(\frac{\sqrt{1+\alpha^2}+1}{\alpha}\right)\left(\frac{2-3\alpha^2}{(1+\alpha^2)^{7/2}}\right)\right]\right\}.
\end{aligned}$$

6.3.6 Solving the Finite-Temperature Gap Equation for the Kekule Order at Critical Temperature

Solving Eq. (4.73) at the critical temperature leads to the following

$$\begin{aligned}
1 &= \frac{\tilde{V}}{3}\sum_{s=\pm}\int\frac{\mathrm{d}\mathbf{q}}{(2\pi)^2}\frac{1}{v_F|q|+s\mu}\tanh\left(\frac{\beta_c\left(v_F|q|+s\mu\right)}{2}\right)\\
&= \frac{\tilde{V}}{3}\sum_{s=\pm}\int_0^{2\pi}\mathrm{d}\theta\int_0^{\Lambda}\frac{\mathrm{d}q}{(2\pi)^2}\frac{q}{v_F|q|+s\mu}\tanh\left(\frac{\beta_c\left(v_F|q|+s\mu\right)}{2}\right)\\
&= \frac{\tilde{V}}{3v_F}\sum_{s=\pm}\int_0^{2\pi}\mathrm{d}\theta\int_0^{\Lambda}\frac{\mathrm{d}q}{(2\pi)^2}\frac{v_Fq+s\mu-s\mu}{v_F|q|+s\mu}\tanh\left(\frac{\beta_c\left(v_F|q|+s\mu\right)}{2}\right)\\
&= \frac{\tilde{V}}{3v_F}\sum_{s=\pm}\int_0^{2\pi}\mathrm{d}\theta\int_0^{\Lambda}\frac{\mathrm{d}q}{(2\pi)^2}\left[\tanh\left(\frac{\beta_c\left(v_F|q|+s\mu\right)}{2}\right)-\frac{s\mu}{v_F|q|+s\mu}\tanh\left(\frac{\beta_c\left(v_F|q|+s\mu\right)}{2}\right)\right]\\
&= \frac{\tilde{V}}{6\pi v_F}\left[I'_m+II'_m\right],
\end{aligned}$$

where

$$\begin{aligned}
I'_m &\equiv \sum_{s=\pm}\int_0^{\Lambda}\mathrm{d}q\tanh\left(\frac{\beta_c\left(v_F|q|+s\mu\right)}{2}\right),\\
II'_m &\equiv -\sum_{s=\pm}\int_0^{\Lambda}\mathrm{d}q\,\frac{s\mu}{v_F|q|+s\mu}\tanh\left(\frac{\beta_c\left(v_F|q|+s\mu\right)}{2}\right).
\end{aligned}$$

Solving I'_m using the substitution $u=\frac{\beta_c}{2}\left(v_F|q|+s\mu\right)$ leads to

$$\begin{aligned}
I'_m &= \frac{2}{\beta_cv_F}\sum_{s=\pm}\int_{\frac{\beta_c}{2}s\mu}^{\frac{\beta_c}{2}v_F\Lambda}\mathrm{d}u\tanh(u)=\frac{2}{\beta_cv_F}\sum_{s=\pm}\left[\ln\left(\cosh(u)\right)\right]_{\frac{\beta_c}{2}s\mu}^{\frac{\beta_c}{2}v_F\Lambda}\\
&= \frac{2}{\beta_cv_F}\sum_{s=\pm}\ln\left[\frac{\cosh(\frac{\beta_c}{2}v_F\Lambda)}{\cosh(\frac{\beta_c}{2}s\mu)}\right].
\end{aligned}$$

Using that $\cosh(-x)=\cosh(x)$ then yields

$$I'_m=\frac{4}{\beta_cv_F}\ln\left[\frac{\cosh(\frac{\beta_c}{2}v_F\Lambda)}{\cosh(\frac{\beta_c}{2}\mu)}\right].$$

Rewriting II'_m leads to

$$\begin{aligned}
II'_m &= -\sum_{s=\pm}s\mu\int_0^{\Lambda}\mathrm{d}q\,\frac{1}{v_F|q|+s\mu}\tanh\left(\frac{\beta_c\left(v_F|q|+s\mu\right)}{2}\right)\\
&= -\sum_{s=\pm}s\mu\frac{\beta_c}{2}\int_0^{\Lambda}\mathrm{d}q\,\frac{2}{\beta_c\left(v_F|q|+s\mu\right)}\tanh\left(\frac{\beta_c\left(v_F|q|+s\mu\right)}{2}\right).
\end{aligned}$$

Again substituting with $u = \frac{\beta_c}{2}\left(v_F|q| + s\mu\right)$ leads to

$$II'_m = -\sum_{s=\pm} s\mu \frac{\beta_c}{2} \int_{\frac{\beta_c}{2}s\mu}^{\frac{\beta_c}{2}v_F\Lambda} \frac{2}{\beta_c v_F} \mathrm{d}u \, \frac{1}{u} \tanh(u) = -\sum_{s=\pm} \frac{s\mu}{v_F} \int_{\frac{\beta_c}{2}s\mu}^{\frac{\beta_c}{2}v_F\Lambda} \mathrm{d}u \, \frac{\tanh(u)}{u}.$$

Performing the sum over s and realizing that $\tanh(u)/u$ is an even function yields

$$\begin{aligned} II'_m &= -\frac{\mu}{v_F} \int_{\frac{\beta_c}{2}\mu}^{\frac{\beta_c}{2}v_F\Lambda} \mathrm{d}u \, \frac{\tanh(u)}{u} + \frac{\mu}{v_F} \int_{-\frac{\beta_c}{2}\mu}^{\frac{\beta_c}{2}v_F\Lambda} \mathrm{d}u \, \frac{\tanh(u)}{u} \\ &= \frac{\mu}{v_F} \int_{\frac{\beta_c}{2}v_F\Lambda}^{\frac{\beta_c}{2}\mu} \mathrm{d}u \, \frac{\tanh(u)}{u} + \frac{\mu}{v_F} \int_{-\frac{\beta_c}{2}\mu}^{\frac{\beta_c}{2}v_F\Lambda} \mathrm{d}u \, \frac{\tanh(u)}{u} \\ &= \frac{\mu}{v_F} \int_{-\frac{\beta_c}{2}\mu}^{\frac{\beta_c}{2}\mu} \mathrm{d}u \, \frac{\tanh(u)}{u} = \frac{2\mu}{v_F} \int_0^{\frac{\beta_c}{2}\mu} \mathrm{d}u \, \frac{\tanh(u)}{u}. \end{aligned}$$

Therefore, the following is obtained

$$1 = \frac{\tilde{V}}{6\pi v_F} \left\{ \frac{4}{\beta_c v_F} \ln\left[\frac{\cosh(\frac{\beta_c}{2}v_F\Lambda)}{\cosh(\frac{\beta_c}{2}\mu)} \right] + \frac{2\mu}{v_F} \int_0^{\frac{\beta_c}{2}\mu} \mathrm{d}u \, \frac{\tanh(u)}{u} \right\}.$$

6.3.7 Solving the Finite-Temperature Gap Equation for the Hidden Order at Critical Temperature

Solving Eq. (4.76) at the critical temperature leads to the following

$$\begin{aligned} 1 &= \frac{\tilde{V}}{6}\frac{v_F^2}{t^2} \sum_{s=\pm} \int \frac{\mathrm{d}\mathbf{q}}{(2\pi)^2} \frac{|q|^2}{v_F|q| + s\mu} \tanh\left(\frac{\beta\left(v_F|q| + s\mu\right)}{2} \right) \\ &= \frac{\tilde{V}}{6}\frac{v_F^2}{t^2} \sum_{s=\pm} \int_0^{2\pi} \mathrm{d}\theta \int_0^{\Lambda} \frac{\mathrm{d}q}{(2\pi)^2} \frac{q^3}{(v_F|q| + s\mu)} \tanh\left(\frac{\beta_c\left(v_F|q| + s\mu\right)}{2} \right) \\ &= \frac{\tilde{V}}{6}\frac{v_F^2}{t^2}\frac{1}{2\pi} \sum_{s=\pm} \int_0^{\Lambda} \mathrm{d}q \frac{q^3}{(v_F|q| + s\mu)} \tanh\left(\frac{\beta_c\left(v_F|q| + s\mu\right)}{2} \right). \end{aligned}$$

Substituting according to $u = v_F q + s\mu$ leads to

$$\begin{aligned} 1 &= \frac{\tilde{V}}{6}\frac{v_F^2}{t^2}\frac{1}{2\pi} \sum_{s=\pm} \int_{s\mu}^{v_F\Lambda} \frac{\mathrm{d}u}{v_F} \frac{\left(u - s\mu\right)^3}{v_F^3} \frac{1}{u} \tanh\left(\frac{\beta_c u}{2} \right) \\ &= \frac{\tilde{V}}{6}\frac{1}{t^2 v_F^2}\frac{1}{2\pi} \sum_{s=\pm} \int_{s\mu}^{v_F\Lambda} \mathrm{d}u \frac{\left(u - s\mu\right)^3}{u} \tanh\left(\frac{\beta_c u}{2} \right). \end{aligned}$$

Expanding $\left(u - s\mu\right)^3$ yields

$$\left(u - s\mu\right)^3 = \left(u^2 + \mu^2 - 2s\mu u\right)\left(u - s\mu\right) = u^3 - 3s\mu u^2 + 3\mu^2 u - s\mu^3,$$

such that

$$\begin{aligned}
1 &= \frac{\tilde{V}}{6}\frac{1}{t^2 v_F^2}\frac{1}{2\pi}\sum_{s=\pm}\int_{s\mu}^{v_F\Lambda}\frac{\mathrm{d}u}{u}\left[\left(u^3+3\mu^2 u\right)-s\left(3\mu u^2+\mu^3\right)\right]\tanh\left(\frac{\beta_c u}{2}\right)\\
&= \frac{\tilde{V}}{6}\frac{1}{t^2 v_F^2}\frac{1}{2\pi}\sum_{s=\pm}\int_{s\mu}^{v_F\Lambda}\mathrm{d}u\left[\left(u^2+3\mu^2\right)-s\mu\frac{\left(3u^2+\mu^2\right)}{u}\right]\tanh\left(\frac{\beta_c u}{2}\right)\\
&= \frac{\tilde{V}}{6}\frac{1}{t^2 v_F^2}\frac{1}{2\pi}\left[I'_{\Delta'}+II'_{\Delta'}\right],
\end{aligned}$$

where

$$\begin{aligned}
I'_{\Delta'} &\equiv \sum_{s=\pm}\int_{s\mu}^{v_F\Lambda}\mathrm{d}u\left(u^2+3\mu^2\right)\tanh\left(\frac{\beta_c u}{2}\right),\\
II'_{\Delta'} &\equiv -\sum_{s=\pm}\int_{s\mu}^{v_F\Lambda}\frac{\mathrm{d}u}{u}s\mu\left(3u^2+\mu^2\right)\tanh\left(\frac{\beta_c u}{2}\right).
\end{aligned}$$

Solving $I'_{\Delta'}$ leads to

$$I'_{\Delta'}=\int_{\mu}^{v_F\Lambda}\mathrm{d}u\left(u^2+3\mu^2\right)\tanh\left(\frac{\beta_c u}{2}\right)+\int_{-\mu}^{v_F\Lambda}\mathrm{d}u\left(u^2+3\mu^2\right)\tanh\left(\frac{\beta_c u}{2}\right).$$

Writing

$$\int_{-\mu}^{v_F\Lambda}\mathrm{d}u=\int_{-\mu}^{\mu}\mathrm{d}u+\int_{\mu}^{v_F\Lambda}\mathrm{d}u,$$

leads to

$$I'_{\Delta'}=2\int_{\mu}^{v_F\Lambda}\mathrm{d}u\left(u^2+3\mu^2\right)\tanh\left(\frac{\beta_c u}{2}\right)+\int_{-\mu}^{\mu}\mathrm{d}u\left(u^2+3\mu^2\right)\tanh\left(\frac{\beta_c u}{2}\right).$$

The second integral equals zero because an odd function is integrated over a symmetric limit. Therefore,

$$I'_{\Delta'}=2\int_{\mu}^{v_F\Lambda}\mathrm{d}u\left(u^2+3\mu^2\right)\tanh\left(\frac{\beta_c u}{2}\right).$$

Substituting $v=(\beta_c u)/2$ leads to

$$\begin{aligned}
I'_{\Delta'} &= 2\int_{\frac{\beta_c}{2}\mu}^{\frac{\beta_c}{2}v_F\Lambda}\frac{2\mathrm{d}v}{\beta_c}\left(\left(\frac{2v}{\beta_c}\right)^2+3\mu^2\right)\tanh\left(v\right)\\
&= \frac{4}{\beta_c^3}\int_{\frac{\beta_c}{2}\mu}^{\frac{\beta_c}{2}v_F\Lambda}\mathrm{d}v\left(4v^2+3\beta_c^2\mu^2\right)\tanh\left(v\right).
\end{aligned}$$

Solving $II'_{\Delta'}$ leads to

$$\begin{aligned}
II'_{\Delta'} &= -\int_{\mu}^{v_F\Lambda}\frac{\mathrm{d}u}{u}\mu\left(3u^2+\mu^2\right)\tanh\left(\frac{\beta_c u}{2}\right)+\int_{-\mu}^{v_F\Lambda}\frac{\mathrm{d}u}{u}\mu\left(3u^2+\mu^2\right)\tanh\left(\frac{\beta_c u}{2}\right)\\
&= \int_{v_F\Lambda}^{\mu}\frac{\mathrm{d}u}{u}\mu\left(3u^2+\mu^2\right)\tanh\left(\frac{\beta_c u}{2}\right)+\int_{-\mu}^{v_F\Lambda}\frac{\mathrm{d}u}{u}\mu\left(3u^2+\mu^2\right)\tanh\left(\frac{\beta_c u}{2}\right)\\
&= \int_{-\mu}^{\mu}\frac{\mathrm{d}u}{u}\mu\left(3u^2+\mu^2\right)\tanh\left(\frac{\beta_c u}{2}\right).
\end{aligned}$$

Substituting $v = (\beta_c u)/2$ leads to

$$\begin{aligned} II'_{\Delta'} &= \int_{-\frac{\beta_c}{2}\mu}^{\frac{\beta_c}{2}\mu} \frac{2\mathrm{d}v}{\beta_c} \frac{\beta_c}{2v}\mu \left(3\left(\frac{2v}{\beta_c}\right)^2 + \mu^2\right) \tanh(v) \\ &= \frac{1}{\beta_c^2} \int_{-\frac{\beta_c}{2}\mu}^{\frac{\beta_c}{2}\mu} \frac{\mathrm{d}v}{v}\mu \left(12v^2 + \beta_c^2\mu^2\right) \tanh(v). \end{aligned}$$

Realizing that the integrant is an even function finally leads to

$$II'_{\Delta'} = \frac{2}{\beta_c^2} \int_0^{\frac{\beta_c}{2}\mu} \frac{\mathrm{d}v}{v}\mu \left(12v^2 + \beta_c^2\mu^2\right) \tanh(v).$$

Therefore,

$$1 = \frac{\tilde{V}}{6} \frac{1}{t^2 v_F^2} \frac{1}{\pi} \frac{1}{\beta_c^3} \left[2\int_{\frac{\beta_c}{2}\mu}^{\frac{\beta_c}{2}v_F\Lambda} \mathrm{d}v \left(4v^2 + 3\beta_c^2\mu^2\right) \tanh(v) + \beta_c\mu \int_0^{\frac{\beta_c}{2}\mu} \frac{\mathrm{d}v}{v} \left(12v^2 + \beta_c^2\mu^2\right) \tanh(v) \right].$$

6.3.8 *s*-Wave Superconductor

In this Appendix, *s*-wave superconducting state is reviewed to show that it is preferred over the Kekule order, as one would expect. It will be seen that the *s*-wave order behaves in a similar fashion as the Kekule order, which makes sense because they both open a superconducting gap in the system. This means that the results such as the gap equations for the *s*-wave will correspond to those of the Kekule order up to a prefactor. It will be shown that the *s*-wave is preferred over the Kekule and hidden order. First, the ground-state energy is computed. This will be followed by deriving the zero-temperature gap equation, critical coupling, zero-temperature gap, finite-temperature gap and the critical temperature for the *s*-wave from the results found for the *s*-Kekule order.

Ground-State Energy

To find the energy, the following is used

$$\sum_{\mathbf{q}} \left(E_{0,\Delta_0} + M_t + M_\mu + M_{\Delta_0}\right) \psi = E_{\Delta_0}\psi,$$

where

$$E_{0,\Delta_0} = 4N\tilde{U} \left|\Delta_0\right|^2.$$

Squaring $M_t + M_\mu + M_{\Delta_0}$ leads to

$$\left(M_t + M_\mu + M_{\Delta_0}\right)^2 = M_t^2 + M_\mu + M_{\Delta_0}^2 + 2M_tM_\mu,$$

where it is used that $\{M_t\,,\, M_\mu\} = 2M_tM_\mu$ and $\{M_t + M_\mu\,,\, M_{\Delta_0}\} = 0$, and where M_t^2, M_μ^2 and $2M_tM_\mu$ were computed before and

$$M_{\Delta_0}^2 = \tilde{U}^2 \left|\Delta_0\right|^2 (\tau_0 \otimes \sigma_0 \otimes \mathbb{I}).$$

Therefore, the result is

$$\begin{aligned}(M_t + M_\mu + M_{\Delta_0})^2 &= \left(\mu^2 + v_F^2|q|^2 + \tilde{U}^2\,|\Delta_0|^2\right)(\tau_0 \otimes \sigma_0 \otimes \mathbb{I}) \\ &\quad -2\mu\, v_F\, \tau_3 \otimes \sigma_0 \otimes (i\gamma_0\gamma_1 q_y - i\gamma_0\gamma_2 q_x)\,.\end{aligned}$$

Diagonalizing this term leads to the dispersion

$$(\omega_{\Delta_0,s})^2 = (v_F|q| + s\mu)^2 + \tilde{U}^2\,|\Delta_0|^2\,,$$

where $s = \pm$. Now the energy is given by

$$E_{\Delta_0} = E_{0,\Delta_0} + \sum_{\mathbf{q},s=\pm} \sqrt{(\omega_{\Delta_0,s})^2} = E_{0,\Delta_0} \pm \sum_{\mathbf{q},s=\pm} \omega_{\Delta_0,s},$$

such that the ground-state energy reads

$$\begin{aligned}E_{\text{g.s.},\Delta_0} &= E_{0,\Delta_0} - \sum_{\mathbf{q},s=\pm} \omega_{\Delta_0,s} \\ &= 4N\tilde{U}\,|\Delta_0|^2 - 4N\sum_{s=\pm}\int \frac{\mathrm{d}\mathbf{q}}{(2\pi)^2}\sqrt{(v_F|q| + s\mu)^2 + \tilde{U}^2\,|\Delta_0|^2},\end{aligned}$$

where $\sum_{\mathbf{q}} \to 4N\int \mathrm{d}\mathbf{q}/(2\pi)^2$ with the extra factor of 2 coming from the spin degree of freedom and where s represents the particle-hole degree of freedom. This leads to the final result for the ground-state energy per site of honeycomb lattice

$$\frac{E_{\text{g.s.},\Delta_0}}{4N} = \tilde{U}\,|\Delta_0|^2 - \sum_{s=\pm}\int \frac{\mathrm{d}\mathbf{q}}{(2\pi)^2}\sqrt{(v_F|q| + s\mu)^2 + \tilde{U}^2\,|\Delta_0|^2}. \tag{6.65}$$

Zero Temperature

Minimizing the ground-state energy over the s-wave order parameter leads to the zero-temperature gap equation

$$1 = \frac{\tilde{U}}{2}\sum_{s=\pm}\int \frac{\mathrm{d}\mathbf{q}}{(2\pi)^2}\frac{1}{\sqrt{(v_F|q| + s\mu)^2 + \tilde{U}^2\,|\Delta_0(0)|^2}}. \tag{6.66}$$

One can see immediatly that this gap equation looks the same as the one for the Kekule order in Eq. (4.57) up to a prefactor. Therefore, the critical coupling and the zero-temperature gap derived from this equation will also be the same up to a prefactor. This leads to the following results for the critical coupling

$$\tilde{U}_c = \frac{2\pi v_F}{\Lambda}, \tag{6.67}$$

and for the zero-temperature gap at zero chemical potential

$$|\Delta_0\,(0, \mu = 0)| = \frac{2\pi v_F^2}{\tilde{U}_c\tilde{U}}\left(1 - \frac{\tilde{U}_c}{\tilde{U}}\right), \tag{6.68}$$

and at finite chemical potential in the weak and strong-coupling limit, respectively,

$$|\Delta_0(0,\mu)| \to \begin{cases} \frac{|\Delta_0(0,\mu=0)|}{2}\left[1+\sqrt{1+\frac{4\mu^2}{\tilde{U}^2|\Delta_0|^2}}\right], & |\tilde{U}| > |\tilde{U}_c|,\ |\Delta_0(0)|/\mu \gg 1, \\ \frac{2\mu}{\tilde{U}} \mathrm{e}^{\frac{\tilde{U}}{\mu}|\Delta_0(0,\mu=0)|-1}, & |\tilde{U}| < |\tilde{U}_c|,\ |\Delta_0(0)|/\mu \ll 1. \end{cases}$$

The critical coupling for the s-wave order parameter $\tilde{U}_c$ is smaller than the critical coupling for the Kekule order parameter $\tilde{V}_c$, which means that as predicted the s-wave order is preferred over the Kekule order and subsequently, also over the hidden order.

Finite-Temperature Gap Equation

The thermodynamical potential for this system reads

$$\Omega_{\Delta_0} = 4N\tilde{U}\left|\Delta_0\right|^2 - \frac{1}{\beta}\sum_{\mathbf{q};s,s'=\pm} \ln\left[1+\exp\left(-\beta s\sqrt{\left(v_F|q|+s'\mu\right)^2+\tilde{U}^2\left|\Delta_0\right|^2}\right)\right].$$

Minimizing with respect to the s-wave gap Δ_0 following the same steps as for the Kekule order leads to the following finite-temperature gap equation

$$1 = \frac{\tilde{U}}{2}\int \frac{\mathrm{d}\mathbf{q}}{(2\pi)^2}\sum_{s=\pm}\frac{1}{\tilde{\omega}_{\Delta_0;s}}\tanh\left(\frac{\beta\tilde{\omega}_{\Delta_0;s}}{2}\right), \tag{6.69}$$

where

$$\tilde{\omega}_{\Delta_0;s} = \sqrt{\left(v_F|q|+s\mu\right)^2+\tilde{U}^2\left|\Delta_0\right|^2}. \tag{6.70}$$

The finite-temperature gap equation corresponds to the one for the Kekule order up to a prefactor.

Critical Temperature

The critical temperature for the s-wave order parameter is found in a similar fashion as for the Kekule order. The result reads for the strong and weak-coupling limit, respectively,

$$T_c'' \to \begin{cases} \frac{1}{2\ln(2)k_B}\left[\frac{\tilde{U}^2|\Delta_0(0,\mu)|^2}{\mu+\tilde{U}^2|\Delta_0(0,\mu)|}+\mu\right], & |\tilde{U}| > |\tilde{U}_c|,\ \beta_c\mu \ll 1, \\ \frac{e^\gamma}{k_B\pi}\tilde{U}\left|\Delta_0(0,\mu)\right|, & |\tilde{U}| < |\tilde{U}_c|,\ \beta_c\mu \gg 1. \end{cases}$$

Acknowledgments

I would like to thank both my supervisors, Prof. Dr. Cristiane Morais Smith and Dr. Vladimir Juričić, for their great enthusiasm while supervising my Thesis and taking up the role of mentors. I would like to thank Prof. Dr. Cristiane Morais Smith for welcoming me in her group from the start and making me feel like a valued addition. She always relates physics with a spark in her eyes. She is a true inspiration to me and has shown me to always believe in myself. I would like to thank Dr. Vladimir Juričić, who has spend many hours with me looking at equations and discussing physical concepts and who took the trouble to help me with presentations and conceptual questions even when we were far apart in distance. I have greatly benefited from his extensive knowledge. Both my supervisors contributed to the great experience I have had working on this project and they have inspired me to pursue a PhD. I hope we will stay in touch and perhaps collaborate again in the future.

Bibliography

[1] A.H. Castro Neto, F. Guinea, N.M.R. Peres, K.S. Novoselov, and A.K. Geim, Rev. Mod. Phys. **81**, 109 (2009).

[2] J.D. Bjorken, and S.D. Drell, *Relativistic Quantum Mechanics*. McGraw-Hill, 1964.

[3] C. W. J. Beenakker, Phys. Rev. Lett. **97**, 067007 (2006).

[4] B. Uchoa, and A.H. Castro Neto, Phys. Rev. Lett. **98**, 146801 (2007).

[5] B. Roy, and I. F. Herbut, Phys. Rev. B **82**, 035429 (2010).

[6] G. Wang, M. O. Goerbig, C. Miniatura, B. Grémaud, Europhys. Lett. **95**, 47013 (2011).

[7] R. Nandkishore, L.S. Levitov, and A.V. Chubukov, Nat. Phys. **8**, 158 (2012).

[8] M.L. Kiesel, C. Platt, W. Hanke, D.A. Abanin, and R. Thomale, Phys. Rev. B **86**, 020507 (2012).

[9] A.M. Black-Schaffer, W. Wu, and K. Le Hur, Phys. Rev. B **90**, 054521 (2014).

[10] B. Roy, V. Juričić, and I.F. Herbut, Phys. Rev. B **87**, 041401 (2013).

[11] B. Roy, and V. Juričić, Phys. Rev. B **90**, 041413 (2014).

[12] L.-K. Lim, A. Lazarides, A. Hemmerich, and C. Morais Smith, Europhys. Lett. **88**, 36001 (2009).

[13] L.-K. Lim, A. Lazarides, A. Hemmerich, and C. Morais Smith, Phys. Rev. A **82**, 013616 (2010).

[14] A. Altland, and B. Simons, *Condensed Matter Field Theory*. Second Edition, Cambridge University Press, 2010.

[15] H.B. Heersche, P. Jarillo-Herrero, J.B. Oostinga, L.M.K. Vandersypen, and A.F. Morpurgo, Nat. Lett. **446**, 56 (2007).

[16] C. Tonnoir, A. Kimouche, J. Coraux, L. Magaud, B. Delsol, B. Gilles, and C. Chapelier, Phys. Rev. Lett. **111**, 246805 (2013).

[17] G. Profeta, M. Calandra, and F. Mauri, Nat. Phys. **8**, 131 (2012).

[18] M. P. Boneschanscher, W. H. Evers, J. J. Geuchies, T. Altantzis, B. Goris, F. T. Rabouw, S. A. P. van Rossum, H. S. J. van der Zant, L. D. A. Siebbeles, G. Van Tendeloo, I. Swart, J. Hilhorst, A. V. Petukhov, S. Balls, and D. Vanmaekelbergh, Science, **344**, 1377 (2014).

[19] E. Kalesaki, C. Delerue, C. Morais Smith, W. Beugeling, A. Allan, and D. Vanmaekelbergh, Phys. Rev. X **4**, 011010 (2014).

[20] W. Beugeling, E. Kalesaki, C. Delerue, Y. M. Niquet, D. Vanmaekelbergh, and C. Morais Smith, Nat. Commun. **6**, 6316 (2015).

[21] Z. Sun, I. Swart, C. Delerue, D. Vanmaekelbergh, and P. Liljeroth, Phys. Rev. Lett. **102**, 196401 (2009).

[22] J. Bardeen, L.N. Cooper, and J.R. Schrieffer, Phys. Rev. **108**, 1157 (1957).

[23] L.N. Cooper, Phys. Rev. **104**, 1189 (1956).

[24] M. Tinkham, *Introduction to Superconductivity*. Second Edition, McGraw-Hill Inc., 1996, pp. 2,3, 10–12.

[25] W. Meissner and R. Ochsenfeld, Naturwissenschaften. **21**, 787, (1933).

[26] V.L. Ginzburg, and L.D. Landau, Zh. Eksp. Teor. Fiz. **20**, 1064, (1950). English translation: D. ter Haar, *L.D. Landau, Collected papers*, Oxford: Pergamon Press, 1965.

[27] J. Chalker, *Quantum Theory of Condensed Matter*. Lecture Notes, Physics Department, Oxford University, 2013, pp. 2, 27.

[28] C. Morais Smith, *Microscopic Theory: BCS Theory*. Lecture Notes for the course Statistical Field Theory, Institute for Theoretical Physics, Utrecht University.

[29] C. Morais Smith *Chapter 2 - Second quantization, electrons and phonons*. Lecture Notes for the course Statistical Field Theory, Institute for Theoretical Physics, Utrecht University.

[30] R. Peace, "Graphene: Band and flex for mobile phones," BBC: Future, March 7, 2013, accessed June 24, 2014, http://www.bbc.com/future/story/20130306-bend-and-flex-for-mobile-phones

[31] P.R. Wallace, Phys. Rev. **71**, 622 (1947).

[32] A.H. Castro Neto, F. Guinea, N.M.R. Peres, K.S. Novoselov, and A.K. Geim, Rev. of Mod. Phys. **81**, 109 (2009).

[33] J.M. Ziman, *Principles of the Theory of Solids, Second Edition*, Cambridge University Press, 1964.

[34] D. Larsen, *Physical Chemistry, Quantum Mechanics, 9: The Hydrogen Atom, Atomic Theory, Electrons in Atoms, Electronic Orbitals.* Digital image. UC Davin ChemWiki. UC Davis, n.d. Web. 26 March 2015. <http://chemwiki.ucdavis.edu/Physical Chemistry/Quantum Mechanics/09. The Hydrogen Atom/Atomic Theory/Electrons in Atoms/Electronic Orbitals>

[35] M.O. Goerbig, Rev. of Mod. Phys, **83**, 1193 (2011).

[36] N.W. Ashcroft and D.N. Mermin, *Solid State Physics*, (Hartcourt College Publishers) 1976.

[37] E. Kalesaki, W.H. Evers, G. Allan, D. Vanmaekelbergh, and C. Delerue, Phys. Rev. B **88**, 115431 (2013).

[38] M. Schluter, M. Lannoo, M. Needels, G. A. Baraff, and D. Tomanék, Phys. Rev. Lett. **68**, 526 (1992).

[39] F. D. Klironomos, and S.-W. Trai, Phys. Rev. B **74**, 205109 (2006).

[40] B. Uchoa, G. G. Cabrera, and A. H. Castro Neto Phys. Rev. B **71**, 184509 (2005).